

Cytogenetic and epigenetic analysis of human gametes and preimplantation embryos

Dhruti Ashokbhai Babariya

Christ Church College

University of Oxford

Supervised by:

Prof Dagan Wells

Nuffield Department of Obstetrics and Gynaecology

A thesis submitted for the degree of

Doctor of Philosophy

Michaelmas 2017-18

Dedicated to the struggles of my parents,

unwavering perseverance of my mother and dreams of my late father; this is the answer to all your sacrifices and struggles for me.

Acknowledgements

First and foremost, I would like to offer my sincere gratitude to my supervisor Prof Dagan Wells, who not only provided me with the opportunity to do a PhD with him but inadvertently also enabled the beginning of my life-changing journey in the magical city of spires, Oxford. His scientific acumen, calm persona and easy-going personality has made this PhD a fruitful and pleasant experience.

I would also like to acknowledge and thank my past and present colleagues at Reprogenetics UK for their help and support during the course of my PhD. To Elpida, I am thankful for advice, critical feedback and guidance. To Samer, Zeynep, Tishy, Megan and Georgina I am grateful for making the lab an enjoyable place to work in. To my previous PGD dream team; Araz, Kethan and Arie, I am thankful to them for being great colleagues through thick and thin. To Nada, I am thankful for being a good friend, great co-trouble shooter for NGS woes and an amazing company to hang out with.

Apart from being an academically enriching experience, Oxford has provided me with opportunities which have critically shaped my opinions and enabled personal growth, for which I will forever be grateful. I have crossed paths with some incredible people at Oxford who have come to be an integral part of my life. I am greatly indebted to Katharina and Nadhirah, my two pillars in Oxford. Through the tears and laughter, they have always been there for me and the PhD journey in Oxford without them almost seems inconceivable. I am also grateful to have met Max, whose love and support has deeply helped me during the last phase of my PhD.

I am greatly thankful to Siddharth, a good friend and an even better Bioinformatician who has always readily helped me at short notice. I would also like to thank Celine and Kevin for always looking out for me.

Lastly, this thesis wouldn't have been possible without support in all shapes and forms from my close friends in Oxford and my family in India. Karan and Jaydeep, thank you for your help during the final leg of my PhD. Lastly, I would like to thank my mother for always believing in me, I wouldn't have accomplished anything in life without her sacrifices and love.

Abstract

Name: Dhruti Babariya **Degree:** DPhil in Obstetrics and Gynaecology

Department: Nuffield Department of Obstetrics and Gynaecology

College: Christ Church **Term of thesis submission:** Michaelmas 2017-18

Despite major advances in the assisted reproductive treatments, it remains the case that most embryos transferred to the uterus fail to implant or are lost shortly after. Chromosome aneuploidy has been characterised as one of the major factors impacting embryo viability.

While the incidence of whole chromosome aneuploidies has been well characterised, little is known about segmental aneuploidy affecting fragments of chromosomes. One of the aims of this study was to investigate the frequency, origin and clinical relevance of segmental aneuploidy in human oocytes and preimplantation embryos. The incidence of segmental aneuploidy significantly increased following fertilisation, peaking at the cleavage stage and declined during the transition to the blastocyst stage. Unlike whole chromosomal aneuploidy, occurrence of segmental aneuploidy was not correlated with advancing female age. Interestingly, IVF culture conditions such as media systems and gas composition were found to significantly influence the incidence of segmental aneuploidy. In addition, the study found that embryos generated by patients suffering from recurrent implantation failure had a higher proportion of segmental aneuploidies than those generated by patients undergoing IVF treatment for advanced maternal age or recurrent miscarriage, suggesting an underlying patient factor.

Preimplantation genetic testing for aneuploidy (PGT-A), using embryo biopsies, is routinely employed during *in vitro* fertilisation to select against aneuploid embryos. However, it is speculated that the invasive nature of the embryo biopsy procedures can adversely impact embryo viability. Therefore, non-invasive sources of embryonic DNA, including blastocoel fluid and spent culture media, were explored during the course of this study and a non-invasive PGT-A method was successfully developed. Promising results were obtained following the application of the developed non-invasive assay to spent culture media samples, showcasing its potential for future clinical application.

Although not as well characterised as aneuploidy, epigenetics is a key emerging factor impacting embryo development. Of particular interest to the IVF community is the epigenetic phenomenon of genomic imprinting wherein a gene is monoallelically expressed in a parent of origin fashion. A few studies have shown a significantly higher rate of imprinting disorders such as Beckwith Wiedemann syndrome in children born after ART as compared to those conceived naturally. Hence, the last part of this study aimed to investigate the imprinting landscape in preimplantation human embryos. A multiplex PCR based bisulfite sequencing approach was successfully developed which was further utilised to study imprinting patterns of 23 imprinted genes simultaneously in trophectoderm and inner cell mass biopsies from euploid human blastocysts. To our knowledge, this is the first study to successfully analyse the methylation patterns of a large number of imprinted genes simultaneously in human blastocysts.

Table of Contents

List of abbreviations 1
Chapter 1: Introduction 2
1.2. Problem definition 4
1.3. Aims and outline of the thesis 7
Chapter 2: Background 9
2.1. Infertility and assisted reproduction 10
2.2. Assisted Reproductive Techniques 12
2.2.1. Ovarian stimulation and oocyte retrieval 13
2.2.2. Fertilisation 13
2.2.3. Embryo culture 15
2.2.4. Genetic screening and selection of embryos 16
2.3. Factors affecting human embryo viability 23
2.3.1 Chromosomal aneuploidy 25
2.3.2. Mitochondrial dysfunction 33
2.3.3. Messenger RNA (mRNA) from oocyte 34
2.3.4. Genetic factors 34
2.3.5. Epigenetic factors 35
Chapter 3: General Materials and Methods 38
3.1. Biological sample preparation 40
3.1.1. Culture of cell lines 40
3.1.2. Collection of buccal cells and lymphocytes 40
3.1.3. DNA extraction 41
3.1.4. Cell isolation 42
3.2. DNA amplification 44
3.2.1. Conventional PCR 45
3.2.3. Multiplex PCR 46
3.2.4. Whole genome amplification (WGA) 47
3.3. Downstream DNA processes 50
3.3.1. Measurement of DNA concentration 50
3.3.2. Visualisation of DNA 50
3.3.3. Gel extraction 52
3.3.4. Next Generation Sequencing (NGS) 53
3.4. Bioinformatics 54
3.4.1. Selection of the DNA sequence 54

3.4.2. Primer design 54
3.4.3. Checking primer parameters 55
Chapter 4: A detailed cytogenetic analysis of the incidence of segmental aneuploidies in human oocytes and preimplantation embryos 57
4.1. Introduction 58
4.2. Study Aims 65
4.2. Materials and Methods 67
4.2.1. Sample details 67
4.2.2. Sample preparation and WGA 68
4.2.3. Validation of aCGH and NGS for the detection of whole chromosomal and mosaic aneuploidy 72
4.2.5. Statistical analysis 75
4.3. Results 77
4.3.1. Validation of CCS methods for detection of whole chromosomal and segmental aneuploidy 77
4.3.2. Detailed cytogenetic investigation of segmental aneuploidy using aCGH 80
4.3.3. Investigation of the origin of segmental aneuploidy 89
4.3.4. Investigation of clinical factors affecting rate of segmental aneuploidy 93
4.4 DISCUSSION 100
4.4.1. Frequency of segmental aneuploidy in human oocytes and preimplantation embryos 100
4.4.2. Origin of segmental aneuploidy in preimplantation embryos 107
4.4.3. Factors affecting frequency of segmental aneuploidy 111
4.4.4. Summary 114
Chapter 5: Exploring blastocoel fluid and spent culture media as non-invasive sources of embryonic DNA 116
5.1. Introduction 117
5.1.1. Spent culture media 118
5.1.2. Blastocoel fluid 120
5.1.3. Study aims 122
5.2. Materials and methods 123
5.2.1. Sample characteristics 123
5.2.2. Sample collection 123
5.2.3. Development of Y chromosome assay 124
5.2.4. Development of amplification protocols for non-invasive genetic approaches 125
5.2.5. Next generation sequencing 132
5.2.6. Chromosomal copy number analysis 133
5.2.7. Sensitivity and Specificity calculation 134

5.3. Results 137
5.3.1. Development and validation of Y-chromosome assay 137
5.3.2. Testing the hypothesis 139
5.3.3. Development and optimisation of amplification methodology 140
5.3.7. Experimental Validation of Method C 150
5.3.8. Clinical validation of Method C 154
5.4. Discussion 167
5.4.1. Development of WGA method for minute quantities of fragmented DNA 168
5.4.2. Experimental validation of modified MDA method 174
5.4.2. Clinical validation of modified MDA method on blastocoel fluid and spent media samples 176
5.4.3. Analysis of nature of DNA fragments in blastocoel fluid and spent media samples 179
5.4.5. Summary 182
Chapter 6: Investigating imprinting landscape of preimplantation embryos 184
6.1. Introduction 185
6.1.1. Elements of imprinted genes 185
6.1.2. Genomic imprinting life cycle 186
6.1.3. Assisted reproductive techniques and epigenetics 187
6.1.4. Aims 188
6.2. Materials and Methods 189
6.2.1. Bioinformatics 189
6.2.2. Experimental methodologies 193
6.3. Results 198
6.3.1. Development of imprinted genes panel 198
6.3.2. Overall methylation level analysis: trophectoderm and inner cell mass specific 200
6.3.2. Overall methylation level analysis: Imprinted genes specific 201
6.3.3. Imprinting landscape for 20 imprinted genes in TE and ICM from euploid blastocysts 203
6.3.4. CpG site specific methylation levels 205
6.4. Discussion 215
6.4.1. Need for detection of imprinting perturbations 215
6.4.2. Imprinting patterns in TE and ICM samples 217
6.4.3. CpG site specific methylation patterns for ICM and TE samples 219
6.4.4. Study limitations 221
6.5.5. Summary 223
Chapter 7: Final conclusion 224
7.1. Synopsis of thesis: 225

7.2 Study Limitations 229
7.3. Future research 230
References 232
Appendices 252

List of abbreviations

Abbreviation	Full form
ART	Assisted reproductive techniques
IVF	*In vitro* fertilisation
ICSI	Intracytoplasmic sperm injection
PGD	Preimplantation genetic diagnosis
PGT-A	Preimplantation genetic testing for aneuploidy
PVA	Polyvinyl alcohol
PBS	Phosphate-buffered saline
PCR	Polymerase chain reaction
WGA	Whole genome amplification
dNTPs	Deoxyribonucleotide triphosphate
NGS	Next generation sequencing
aCGH	Array comparative genomic hybridisation
qRT-PCR	Quantitative real time polymerase chain reaction
SNP	Single nucleotide polymorphism
MDA	Multiple displacement amplification
DNA	Deoxyribonucleic acid
dsDNA	Double stranded deoxyribonucleic acid
ssDNA	Single stranded deoxyribonucleic acid
SPRI	Solid Phase Reversible Immobilization
DTT	Dithiothreitol
mRNA	Messenger ribonucleotide acid
CpG	Cytosine phosphate guanine
TE	Trophectoderm
ICM	Inner cell mass
RIF	Recurrent implantation failure
RPL	Recurrent pregnancy loss
AMA	Advanced maternal age
ICR	Imprinting control region
NC	Negative control
PC	Positive control
LS	Linker sequence
FISH	Fluorescent *in situ* hybridisation
CCS	Comprehensive chromosomal screening
MI	Meiosis one
MII	Meiosis two

Chapter 1: Introduction

This chapter aims to introduce various aspects of this thesis including a synopsis of literature, problem definition, the aim and scope of the planned research in the field of reproductive genetics as well as providing an outline of the thesis structure.

The first detailed characterisation of human preimplantation embryos was performed by Hertig and Rock, studying naturally conceived embryos derived from volunteers undergoing elective hysterectomy (Hertig et al., 1954). The earliest embryos obtained were at 2-cell stage of development and the oldest were undergoing gastrulation. Crucial advancements were achieved in the field of embryo biology and assisted reproduction around the same time with development of superovulation in mice by Edwards and Fowler in 1957 (Fowler and Edwards, 1957), followed shortly after by the first successful live births using *in vitro* fertilisation of rabbit oocytes in 1959 by Chang (Chang, 1959). These studies helped to provide the foundations for *in vitro* fertilisation (IVF) treatment in humans, ultimately culminating with the birth of first IVF baby, Louise Brown, in 1978 (Steptoe and Edwards, 1992a). Since then, access to gametes and preimplantation embryos, produced during the course of routine IVF treatment and donated for research purposes, has greatly enhanced the understanding of the early human embryo.

Human development begins with the cells of the embryo in a relatively transcriptionally silent state. The transition from quiescent oocyte to transcriptionally active embryo is accomplished in approximately three days, involving fertilisation of the egg by a single sperm, followed by fusion of the male and female pronuclei and completed with genetic and epigenetic reprogramming and the onset of gene expression between the 4- and 8-cell cell stage (Braude et al., 1988, Assou et al., 2011; Fulka et al., 2004). This dynamic period is perhaps the most vulnerable phase in mammalian development as the embryo needs to successfully navigate a complex sequence of critical cellular, molecular and epigenetic changes. These changes subsequently lead to lineage segregation of blastomeres inside the developing blastocyst (reviewed by de Paepe et al., 2014).

The goal of assisted reproduction treatment in humans is to deliver a healthy baby through transfer of a viable embryo to the uterus. Many of the interventions required for IVF treatment occur at the same time as the key developmental transitions described above. For IVF to be successful, and for the long-term health of the children produced, it is important that IVF treatment does not interfere with these vital processes. With the development of sensitive molecular cytogenetic methods, rapid advancements in the field of genetic screening of the embryos have been achieved, assisting with the selection of the most viable embryo for transfer (Vermeesch et al., 2016). Relationships between viability of the embryo and its chromosomal status, kinetics of development, proteome and metabolome have been proposed (Gardner et al., 2015; Roberts et al., 2016). It is likely that a better understanding of human embryo physiology, genetics and developmental kinetics will further improve identification of embryos most likely to result in a healthy pregnancy. The preferential transfer of such embryos is expected to enhance the efficiency of IVF treatment, reducing the number of transfers that fail to yield a viable pregnancy, thus reducing costs and the amount of time required to achieve a live birth.

1.2. Problem definition

Human embryo viability and development is governed by an intrinsic network of genomic, epigenomic and metabolomics factors. Despite over six decades of studying the early human embryo, much remains unknown about this critical stage of human development. Moreover, understanding the human preimplantation development has implications for the field of assisted reproduction.

The field of assisted reproduction has gained an impetus since the advent of sophisticated medical and molecular technologies. An estimated 48.5 million couples

worldwide are infertile, a majority of these belonging to developing countries (Mascarenhas et al., 2012), yet many advanced treatments, especially those involving molecular genetic analysis of IVF embryos, remain unavailable to patients in less affluent countries. The main limiting factors rendering such treatments inaccessible are the high costs, expensive equipment and lack of skilled personnel to perform the sophisticated techniques. One such technique is genetic testing of preimplantation embryos for either hereditary disorders (known as preimplantation genetic diagnosis, PGD) or for spontaneously occurring chromosomal aneuploidy (preimplantation genetics testing for aneuploidy, PGT-A). Collectively, PGD and PGT-A have aided tens of thousands of couples to conceive a healthy baby. In order to achieve PGD or PGT-A, techniques typically involve laser guided biopsy of embryos produced during the course of an IVF cycle, followed by sensitive molecular methodologies for genetic analysis of the small number of cells sampled. One aspect of this project was to develop a non-invasive genetic diagnostic tool which circumvents the need to perform embryo biopsies for genetic testing purposes. The method would make sophisticated genetic investigations, used in conjunction with ART, more accessible to patients from developing countries by reducing costs of equipment and the skill level required, two of the most important barriers to the provision of such tests.

The development of selection schemes for the identification of the most competent embryo has been of great interest since the first introduction of IVF, as the quantity of embryos produced in a given treatment cycle typically exceeds the number that would ideally be transferred (single embryo transfer is recommended in order to avoid the risk of multiple gestations and associated medical complications). Until recently, morphological characteristics of the gametes and embryos were the primary determinant of their competence, assessed in all IVF clinics worldwide to guide embryo selection. Screening for

aneuploidy was the first genetic approach proposed for extending embryo assessment beyond morphological evaluation (Munne et al., 1993). More recently, proteome and metabolome profiling of gametes and embryos have also been explored in terms of competence assessment, although thus far these approaches have seldom been applied in a clinical context (Katz-Jaffe et al., 2006; Sultan et al., 2008; Gardner & Wale, 2013). Understanding the etiologies of abnormalities in gametogenesis, fertilisation and embryonic development is not just a matter of academic curiosity but has great implications in the field of assisted reproduction. Despite over four decades of experience with IVF, its success rate remains fairly low (Roque *et al.*, 2013). This is in part due to the paucity of research in identifying all the essential biomarkers for embryo viability. Although immense progress has been made in this area in past decades, much remains unknown about the cellular and molecular mechanisms regulating the early stages of preimplantation development, thereby limiting the predictive values of embryo competence by existing methodologies. This thesis broadly aims to investigate, or create tools for the analysis of, two such factors, cytogenetic and epigenetic, of relevance to human embryo viability.

1.3. Aims and outline of the thesis

The overarching aim of this study was to investigate certain underexplored cytogenetic and epigenetic factors underlying human embryo viability. A combination of detailed observational studies and development of novel molecular methodologies was utilised to achieve this aim and the details of each sub-aim is described in the outline of the thesis below:

- **Chapter 2 - General Introduction**: The first section gives the background of the field of infertility and reproductive genetics, laying down the theoretical dimensions of the research undertaken during the course of this thesis.
- **Chapter 3 - General Materials and Methods**: The second chapter outlines the general materials and methodologies employed for various experiments during the course of the study.

  There are three results chapters (Chapter 4, 5 and 6); each including an introduction, materials and methods, results and discussion section; specific to the individual chapter.
- **Chapter 4 - Segmental Aneuploidy**: This chapter establishes the frequency, origin and potential clinical relevance of segmental aneuploidy in human oocytes and preimplantation embryos. Additionally, a cytogenetic map detailing the chromosomal breakage sites (resulting in segmental aneuploidies during gametogenesis and embryogenesis) across the entire genome was also created.
- **Chapter 5 – Development of non-invasive methods for analysis of embryonic DNA**: Novel molecular approaches to investigate the minute quantities of embryonic DNA present in spent culture media as well as blastocoel fluid from blastocyst stage embryos were developed and validated.

- **Chapter 6 – Investigating imprinting landscape of preimplantation embryos**: Genomic imprinting, an important class of epigenetic regulation, was investigated in preimplantation embryos with the aim of establishing an imprinting landscape in early human embryos for 20 developmentally important imprinted genes.
- **Chapter 7 – Final conclusions**: The purpose of the final chapter is to reflect and discuss on the extent to which this study has addressed some of the key factors underlying human embryo viability.

Chapter 2: Background

This chapter provides the background for the thesis along with relevant literature review. The chapter is divided into three distinct parts. The first section of this chapter provides an overview of assisted reproduction in the context of infertility. The second section deals with an in-depth background of assisted reproductive techniques and the final section discusses the cytogenetic, epigenetic and molecular factors underlying human embryo viability.

2.1. Infertility and assisted reproduction

Natural conception is a complex process with several factors determining its success including the capability to produce competent sperm and oocytes, unblocked fallopian tubes, the ability of sperm to fertilise the oocyte, the implantation potential of the embryo and a uterine environment suitable for embryo implantation and the establishment of a pregnancy (Bedford, 1970). Hindrance to any of the aforementioned reproductive processes may lead to infertility, which affects approximately 10% of reproductive aged couples (Boivin et al., 2007). Medically, WHO defines infertility as a disease of the reproductive system leading to a failure to conceive after one year of unprotected intercourse (Zegers-Hochschild et al., 2009). A wide variety of male and female reproductive factors can cause infertility such as sperm dysfunction, ovulation disorder and fallopian tube damage. To circumvent some of the issues contributing to infertility, couples have increasingly been seeking treatments in form of assisted reproductive techniques (ART). Assisted reproductive treatments can be availed by infertile couples, couples having a known history of genetic disorder in the family and wishing to avoid an affected pregnancy (via preimplantation genetic diagnosis), same sex couples or by people seeking fertility preservation, either for social reasons (e.g. oocyte cryopreservation) or due to planned chemotherapeutic treatments damaging to future fertility.

Human embryonic development begins at fertilisation with the fusion of haploid male and female pronuclei in the zygote. The subsequent replication of maternal and paternal chromosomes followed by mitotic cell divisions continues until the fourth day after fertilisation, when embryo compaction starts leading to formation of a morula. The embryo then starts differentiating, forming a blastocyst composed of two distinct cellular lineages - an outer trophectoderm layer, which will ultimately form the extra-embryonic tissues (e.g.

placenta), and an inner cell mass, which will go on to form the embryo itself. The development of the preimplantation embryo from zygote to blastocyst takes place in the fallopian tube *in vivo* (Grobstein, 1985), while in the context of *in vitro* fertilisation (IVF) sperm and oocytes are bought together outside the body and the resulting embryos are cultured, typically for three to five days before transfer to the mother's uterus or cryopreservation for future use.

Since the birth of the first 'test tube' baby after IVF in 1978, fertility treatments have revolutionised the field of infertility management with ~2% of babies in the UK born through such treatments (HFEA report, 2014). However, the success rate of IVF remains fairly low with only ~25% of embryos transferred resulting in a live birth. In most IVF treatment cycles several embryos are produced, but their capacities for producing a viable pregnancy can differ dramatically. Consequently, one of the major challenges for fertility treatments is the identification and transfer of the embryo(s) most likely to result in a healthy pregnancy. Over the last couple of decades it has become apparent that chromosomal aneuploidy is one of the major causes of a negative IVF outcome leading to miscarriage or birth of children with genetic disorders (such as Down's syndrome) (Delhanty et al., 1997; Munne & Cohen, 1998; Scott et al., 2012; Wells et al., 1999). Hence, the clinical analysis of chromosomes in IVF derived embryos, known as preimplantation genetic screening (PGS) also known as preimplantation genetic testing of aneuploidy (PGT-A), has gained impetus in the past decade (reviewed by Gleicher et al., 2014; Thornhill et al., 2005). Studies have demonstrated that various factors such as mitochondrial dysfunction and epigenetic defects may also have negative effect on the embryo viability (Olson et al., 2005; Schatten et al., 2014; Fragouli et al., 2015; Ravichandran et al., 2017). Therefore, it is pertinent to develop new methods to identify the underlying molecular mechanisms contributing to a negative IVF outcome.

The most widely used method for the evaluation of embryo implantation potential, employed in virtually all IVF clinics worldwide, involves the morphological evaluation of embryos at various stages of preimplantation development. However, this form of assessment is subjective and is not fully reflective of embryo potential (Machtinger & Racowsky, 2012). To enhance the identification of the most viable embryos, PGT-A has been widely employed to screen for the chromosomal copy number in oocytes and preimplantation embryos. However, even when euploid embryos of excellent morphology are transferred to the uterus, implantation rates rarely exceed ~70%. Hence, the identification of new and reliable biomarkers predictive of embryo viability are needed in order to further enhance the success rates if IVF treatments.

Moreover, there is a huge drive towards the policy of single embryo transfer (sET) in order to minimise the rate of multiple pregnancy due to increased complications and risks to maternal and fetal health during multiple gestations (Penzias *et al.*, 2017). In order to minimise such risks, the sET policies are increasingly being adopted by large numbers of IVF clinics. In the light of such a policy, it becomes yet more pertinent that the embryo selected for transfer is the one with the highest viability potential which will most likely lead to a successful pregnancy and the subsequent birth of a healthy child.

2.2. Assisted Reproductive Techniques

The past forty years have seen increasingly rapid advances in the field of assisted reproduction. With the development of sophisticated molecular technologies and advancement in embryo culture methods, usage of ARTs has seen an unprecedented surge with over 6 million babies born worldwide through ARTs since the first IVF birth in 1978 (Kushnir et al., 2017). This section describes the commonly employed methods during ART.

2.2.1. Ovarian stimulation and oocyte retrieval

Ovarian stimulation is utilised to produce multiple dominant follicles and to mature them into numerous oocytes during the same cycle in order to increase the chances of conception either *in vivo* (with or without intrauterine insemination) or *in vitro* (with IVF or ICSI) (Oehninger and Hodgen, 1990). Post ovarian stimulation, numerous cumulus-oocyte complexes can be collected from follicles by transvaginal oocyte retrieval procedure. Different types of protocols are used to carry out ovarian stimulation, with exogenous gonadotrophin hormones based methods most commonly being used (Griesinger et al., 2005). The multitude of oocytes generated during the same cycle facilitates the next steps in assisted reproduction namely, fertilisation, embryo culture, embryo selection and uterine transfer (Fauser *et al.*, 1999).

2.2.2. Fertilisation

Post oocyte retrieval, the eggs are fertilised with pre-prepared sperm samples by either a) conventional *in vitro* fertilisation (IVF), which involves mixing of eggs and sperm in a petri dish or b) intracytoplasmic sperm injection (ICSI) wherein a single sperm is injected into an egg using a micromanipulator. The development of IVF proved to be an efficient way to alleviate some of the most important forms of female factor infertility, in particular tubal infertility (Evers, 2002). However, over the years it became apparent that IVF was not the ideal fertility intervention for certain male factor infertility, in particular with semen characteristics below the WHO reference values concerning concentration, morphology and motility (Cooper et al., 2009). The percentage of oocytes fertilised by such sperm were much lower, in turn affecting the number of embryos generated during an IVF cycle (Tournaye et al., 1992). To address the issue of male factor infertility, at the end of 1980s several new

procedures for ART were developed to facilitate the fertilisation of oocyte. In the chronological order, these included-a) partial zona dissection (PZD), wherein an opening was made in zona pellucida allowing the sperm to access the oolema; b) subzonal insemination (SUZI) which involved the injection of few motile sperm through the zona pellucida and into the perivitelline space and lastly, c) intracytoplasmic sperm injection (ICSI), in which a single spermatozoon is microinjected into an oocyte's cytoplasm directly. The experience with PZD and SUZI was not very encouraging as the fertilisation rates remained low and hence these were not suitable to be applied in routine clinical practice. However, in 1992, Palermo and colleagues published the first report of pregnancies and deliveries after replacement of embryos generated by ICSI (Palermo et al., 1992). Shortly after, several studies demonstrated that fertilisation rates were better with ICSI as compared to PZD and SUZI (Tournaye et al., 1994; Van Steirteghem et al., 1993a; Van Steirteghem et al., 1993b). Currently, ICSI is widely used by IVF clinics for a significant proportion of routine fertilisations and not just restricted to severe male factor infertility. In addition, for embryos undergoing genetic testing, ICSI is the preferred fertilisation method over conventional IVF in order to avoid maternal DNA contamination originating from cumulus cells (which are removed prior to sperm injection) or paternal DNA contamination associated with surplus sperm attached to the zona pellucida. However, some concerns have been raised about ICSI practices, with studies reporting link between children born after ICSI and increased risk of imprinting disorders (Cox et al., 2002; DeBaun et al., 2003) and an increase in *de novo* sex and autosomal chromosome aberrations (Bonduelle et al., 2002). However, the sample sizes were relatively small for these studies and their findings need to be confirmed in bigger population.

2.2.3. Embryo culture

Historically, embryo culture media were synthesised to physiologically mimic the female reproductive tract in order to culture gametes and embryos *in vitro* and ultimately to increase the chance of a healthy pregnancy (as reviewed by Biggers, 2002). Presently, there are two main types of culture media systems widely used; continuous and sequential. The sequential media attempts to mimic the changing needs of the developing embryo at different stages of growth and involves transferring the embryo at cleavage stage to a different media formulation for the blastocyst development (Gardner & Lane, 1998). In contrast, continuous culture entails the embryo development in the same media from fertilisation till blastocyst stage, without any change in media formulations throughout the culture (Summers and Biggers, 2003). Several comparative studies between continuous and sequential media have been performed but contradictory results have been reported on the superiority of their performance (Aoki et al., 2005; Paternot, Debrock et al., 2010; Werner et al., 2016).

The growth of ART embryos is inferior to those of *in vivo* embryos, suggesting that ART procedures might invoke cellular and metabolic stress which might ultimately prove detrimental for the embryo (**Figure 1**). Culture media is an integral part of the ART procedure as the *in vitro* interactions of the developing embryo with its environment are necessary for embryo's successful development. Also, studies have shown that culture media can influence the epigenetic reprogramming during early development (reviewed by Uyar & Seli, 2014). Hence, it is important that further investigations are carried out to optimize environmental conditions in which the preimplantation embryo can evolve.

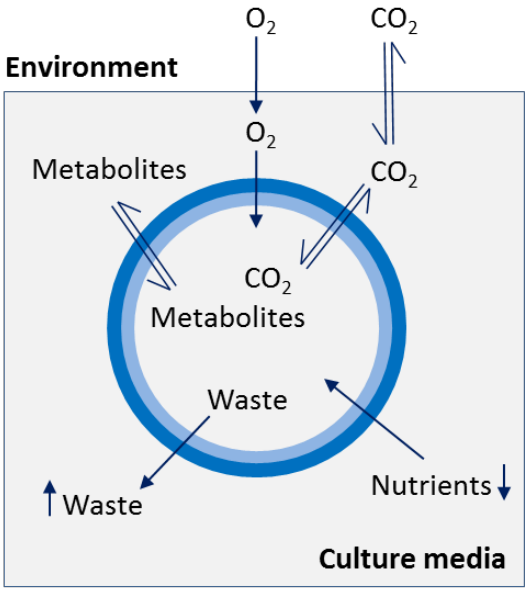


Figure 1. Stress induced during embryo culture. The physiology of embryo interaction *in vivo* is very different from that of *in vitro* culture. The embryo may experience culture conditions induced stress due to depleting nutrients, increasing waste or pH imbalance.

2.2.4. Genetic screening and selection of embryos

In 1990, Handyside and colleagues reported the first successful pregnancies following the transfer of female embryos after embryo biopsy and sex determination, in order to avoid an X-linked genetic disorder. This was the culmination of the development of revolutionary techniques which later came to be known as preimplantation genetic diagnosis (PGD). Initially, only DNA amplification based methods were used for PGD but shortly after, fluorescence *in situ* hybridisation (FISH) techniques were introduced, which enabled the detection of abnormal numbers of copies of chromosomes or chromosomal segments too (Delhanty et al., 1993; Griffin et al., 1992).

The process of IVF generates a considerable number of embryos; depending on the age and ovarian reserve of the female patient. However, only one or two embryos are transferred to the uterus in a single cycle in order to reduce the risk of complications associated with multiple gestations. Traditionally, morphological evaluation of the embryos is used to grade them with a view to identifying the most viable embryo for transfer to the

uterus. However, several studies have demonstrated that the correlation between morphology and chromosomal status is weak (Alfarawati et al., 2011; Munné et al., 2007). Therefore, embryos harbouring lethal aneuploidy will sometimes have superior morphology to sibling embryos with a normal number of chromosomes. With further development of FISH methods to screen multiple chromosomes simultaneously (Munné et al., 1993), the first deliveries after screening of embryos for spontaneously arising aneuploidies were reported in 1995 by Verlinsky and colleagues. This method for aneuploidy screening is widely referred to as preimplantation genetic screening (PGS), but is more appropriately termed preimplantation genetic testing for aneuploidy (PGT-A) (Zegers-Hochschild et al., 2017).The rationale was to identify and choose for transfer chromosomally normal embryos in order to increase the implantation and pregnancy rates (Wilton, 2002). Thus, two very powerful techniques, one for diagnosis of genetic disorders (PGD) and the other for screening of chromosomal copy number in embryos (PGT-A), emerged in the field of preimplantation reproductive genetics. Genetic material from cell(s) of embryos is required for both methods, which is facilitated by oocyte or embryo biopsy described in detail in the next section (2.2.4.1).

2.2.4.1. Biopsy of polar bodies and embryos

In order to assess certain aspects of the genetic quality of oocytes and embryos, the genetic/chromosomal constituents of polar bodies and cell(s) from embryos can be examined. This typically involves polar body or embryo biopsy, a two-step procedure wherein the zona pellucida is penetrated followed by removal of one or more cells for chromosomal or genetic analysis. The breaching of zona was originally performed by using Tyrode's acid solution to dissolve a hole but is nowadays more often performed by laser ablation. Thereafter, specialised micropipettes are used to remove the cell(s) needed for further analysis. The

biopsies can be carried out at any developmental stage from mature (MII) oocyte to blastocyst stage. For clinical usage, biopsies are performed at any of the three developmental stages, a) fertilised oocytes (removal of one or both polar bodies); b) cleavage stage (removal of one or occasionally two cells); and c) blastocyst stage (removal of a ~5 cells from outer trophectoderm layer) (**Figure 2**).

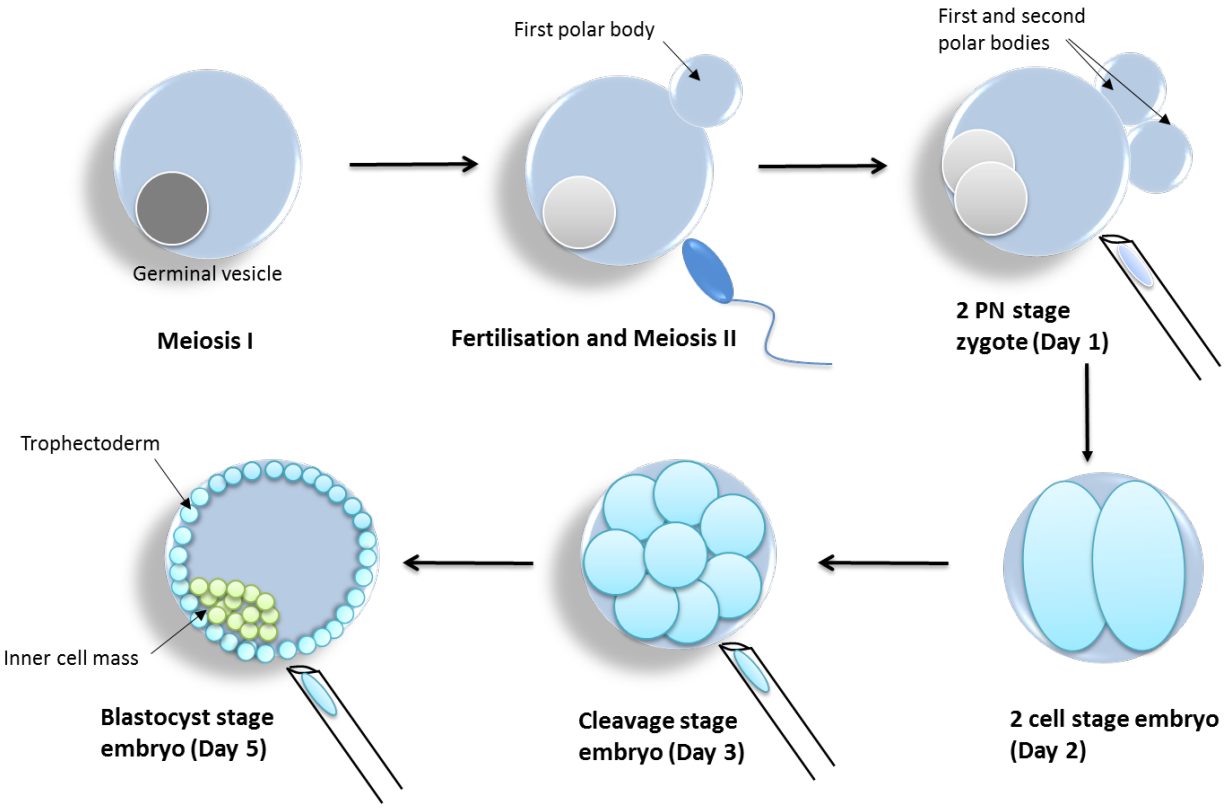


Figure 2. Embryo biopsies. The biopsies can be performed at either a) fertilised oocyte stage, b) cleavage stage or c) blastocyst stage of development.

2.2.4.2. Preimplantation genetic testing for aneuploidy (PGT-A)

Since its first usage in the early 1990s, the clinical application of PGT-A for routine chromosomal screening of embryos has shown almost continuous growth. A determination of the chromosomal constitution of biopsied cells provides a means of inferring the chromosomal status of the corresponding egg or embryo and hence facilitates choosing those

that are euploid and are likely to have the greatest likelihood of normal development. The rationale behind PGT-A stems from a) the frequent observation of aneuploidies in miscarriages, b) observation of a high frequency of aneuploidies in embryos generated after IVF and c) the incompatibility of these aneuploidies with life (Sullivan et al., 2004; Hassold & Hunt, 2001). PGT-A can be considered as an adjunct to IVF and the indications for it include advanced maternal age (>35 years), previous miscarriages, repeated IVF failure and severe male factor infertility (Harper et al., 2010).

Traditionally, FISH was utilised to perform PGT-A, interrogating between 5 and 12 chromosomes on biopsy specimens composed of one or two cells from cleavage stage embryos (three days post fertilisation) (Colls et al., 2009). The embryos deemed 'euploid' by testing of the select few chromosomes were subsequently transferred and the 'aneuploid' embryos discarded. However, this was based on the theoretical premise of PGT-A, without evidence of efficacy from randomized controlled trials (RCTs). Later on, multiple RCTs showed that PGT-A using FISH did not improve the pregnancy and delivery rates (e.g. Blockeel et al., 2008; Debrock et al., 2010; Hardarson et al., 2008; Mastenbroek et al., 2007; Staessen et al., 2004).

One of the major drawbacks of FISH was the limited number of probes labelled with different fluorochromes, restricting the number of chromosomes that could be analysed in a single interphase nucleus. Moreover, the analysed blastomere may not always be representative of the entire embryo due to chromosomal mosaicism (Fragouli & Wells, 2011; Vanneste et al., 2009). Hence, the European Society of Human Reproduction and Embryology (ESHRE) issued a position statement in 2010 that FISH is not advised for PGT-A on cleavage stage embryos (Harper et al., 2010). These limitations of FISH led to a shift towards superior

platforms which can screen all the chromosomes simultaneously (comprehensive chromosomal screening; CCS).

The most widely used CCS techniques currently being used include microarray competitive genomic hybridisation (aCGH), single nucleotide polymorphisms (SNP) microarrays, quantitative real time PCR (qPCR) and next generation sequencing (NGS) (Brezina et al., 2016) (**Figure 3**). The aCGH and SNP array approaches utilise a whole genome amplification step (WGA) wherein the biopsied samples are amplified and subsequently fluorescently labelled and hybridised to thousands of genome wide probes on a microarray. In the case of aCGH, the chromosomal copy numbers are then determined by comparing the fluorescent signals attributable to DNA from the embryo sample with that of a chromosomally normal 'reference' DNA sample, labelled with a different colour. Aneuploidy is indicated when all of the probes mapping to a single chromosomes show the same deviations in the fluorescence ratio of sample DNA to reference DNA (Gutiérrez-Mateo et al., 2011).

For SNP arrays, the total amount of fluorescence detected on probes derived from individual chromosomes can reveal losses or duplications of chromosomal material. Additionally, if the parental DNA samples are available, the parental origin of aneuploidy can sometimes be inferred by tracing the inheritance of parental haplotypes (Johnson et al., 2010). The most widely used platform for NGS currently requires a WGA step followed by low pass sequencing of the resulting products (i.e. <0.1% of the genome is sequenced). The short reads are then aligned to a reference genome to determine the chromosomal imbalances by specialised algorithms (Fiorentino et al., 2014, Wells et al., 2014). However, recently a targeted NGS approach for CCS has been described which does not require a WGA step and utilises primers to target specific loci across the genome (Martin et al., 2017). The qPCR

approach is based on the principle of relative quantification of the fluorescence emitted by probes hybridised to specific regions across the genome and unlike other CCS methods, does not require WGA (Treff *et al.*, 2012). Different CCS platforms have their respective advantages and disadvantages related to cost, turnaround time and resolution (Handyside, 2013).

2.2.4.3. Preimplantation genetic diagnosis (PGD)

Preimplantation genetic diagnosis (PGD) aims to characterise the genetic status of an early human embryo, which is at risk of inheriting a genetic disorder from either one or both of its parents. The first successful PGD analysis in human embryos was reported in 1990 and was performed for an X-linked recessive disorder (Handyside et al., 1990). Following IVF, the PGD analysis was performed by PCR amplification of Y-chromosome specific sequences which enabled sex selection of the female embryos which are at a lower risk of inheriting the X-linked recessive disorder as compared to the males. Since then, PGD has been offered to numerous couples carrying recessive/ dominant, autosomal/ X-linked disorders, chromosomal rearrangements or mitochondrial disorders (Vermeesch, Voet and Devriendt, 2016). Additionally, PGD has also been used for HLA matching in order to 'create' an offspring that can serve as a tissue-matched stem cell donor in families having children affected with severe blood disorders (Tur-Kaspa and Jeelani, 2015). Traditionally, PGD is performed using a multiplex PCR based approach wherein primers are used to amplify a sequence containing the mutation of interest as well as several polymorphic short repeats flanking the mutation (Wells & Delhanty, 2001). These products are subsequently detected by any of several alternative methods, depending on whether it is necessary to determine their length (in the case of highly polymorphic short tandem repeats [STRs] used for linkage analysis) or evaluate their actual DNA sequence.

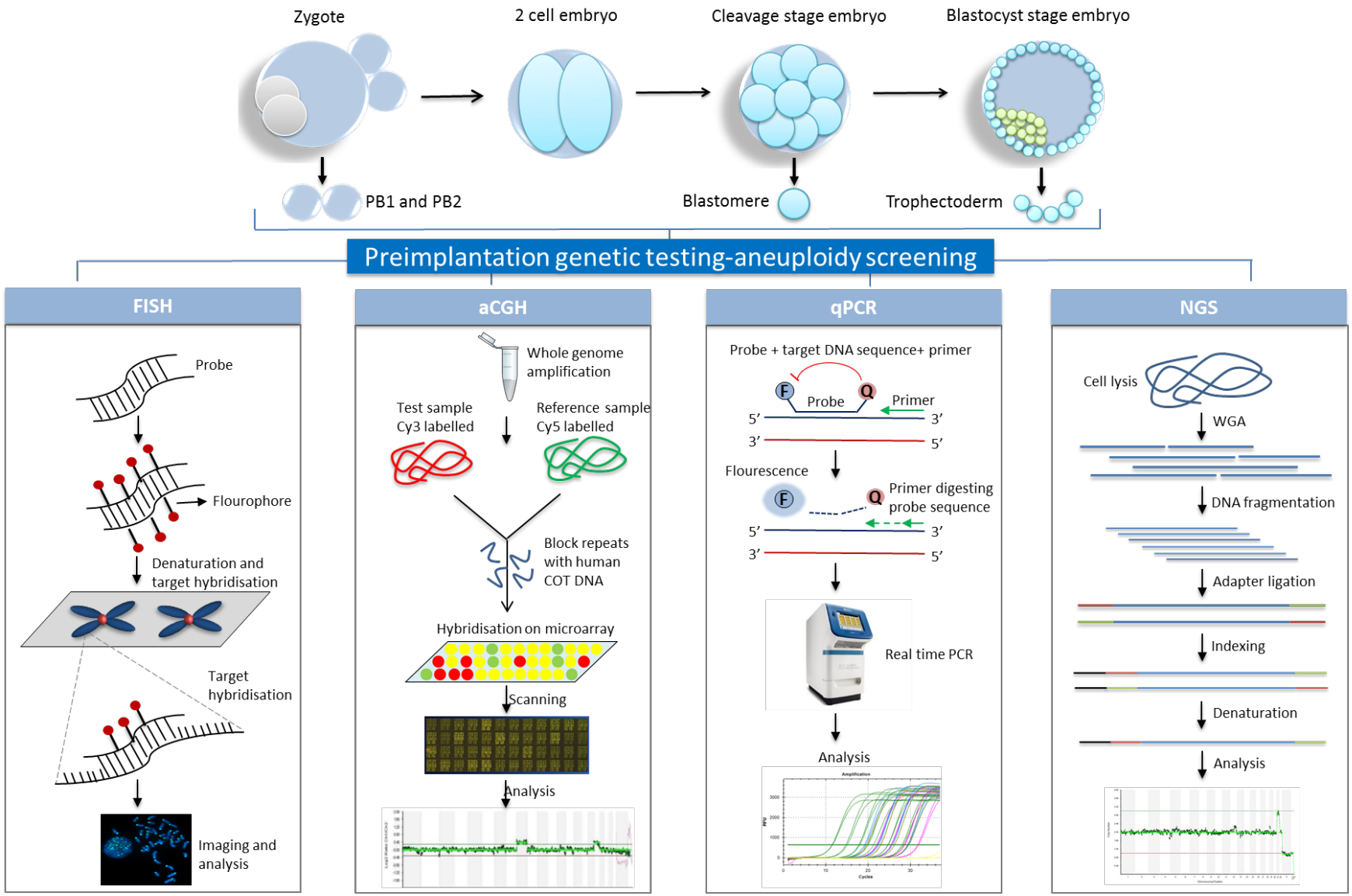


Figure 3. Techniques used for PGT-A. Traditionally, FISH was used for chromosome screening. More recently advanced molecular methodologies such as array comparative genomic hybridisation (aCGH), quantitative real time PCR (qPCR) and next generation sequencing (NGS) have been employed for CCS.

The combination of linkage analysis and direct mutation detection that this sort of strategy affords allows the identification of inherited mutant alleles and reduces the risk of error due to allele drop out events (failure of amplification of one of the alleles) affecting the PCR fragment encompassing the mutation, hence increasing the accuracy of PGD. However, this approach requires developing family-specific markers to ascertain inheritance of mutant parental allele(s) and it can be challenging to identify an adequate number of 'informative' (having different number of nucleic repeats for each of the four parental chromosomes) markers. To circumvent this issue, more recently a comprehensive linkage-based test, involving SNP genotyping of the parents, a close relative of known disease state, and the embryo cell(s) was proposed (Handyside et al., 2010). The method is known as karyomapping and utilises over 300,000 SNPs dispersed across the human genome, enabling the inheritance of individual parental chromosomes to be tracked from the mother and father to their embryos, revealing instances when chromosome(s) carrying specific mutations have been transmitted, as well as instances of aneuploidy (Natesan *et al.*, 2014).

2.3. Factors affecting human embryo viability

Human preimplantation embryonic development is characterised by fusion of male and female pronuclei, epigenetic reprogramming, and degradation of maternal transcripts followed by embryonic genome activation (EGA) (**Figure 4**). It is crucial to understand the cellular and molecular dynamics during early embryo development as well as establish the correlation between these mechanisms during normal and abnormal embryonic development. This will further aid in gaining an insight into the physiology of the preimplantation embryo and factors affecting its survival. This section discusses various factors underlying human embryo viability as depicted in **Figure 5.**

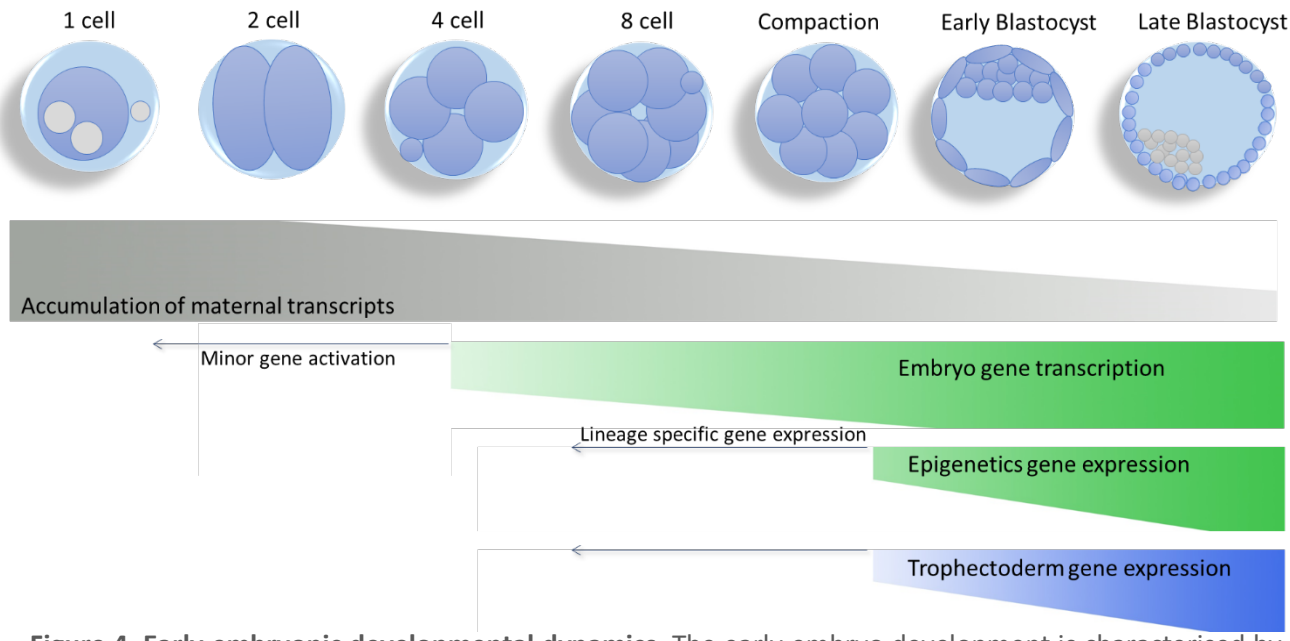


Figure 4. Early embryonic developmental dynamics. The early embryo development is characterised by several vital cellular and molecular processes. As the embryo develops, the maternal transcripts are degraded, the embryonic genome activates at Day-3 post fertilisation and the embryo undergoes epigenome reprogramming leading to cell lineage differentiation. All the aforementioned processes are of vital importance for normal embryonic development.

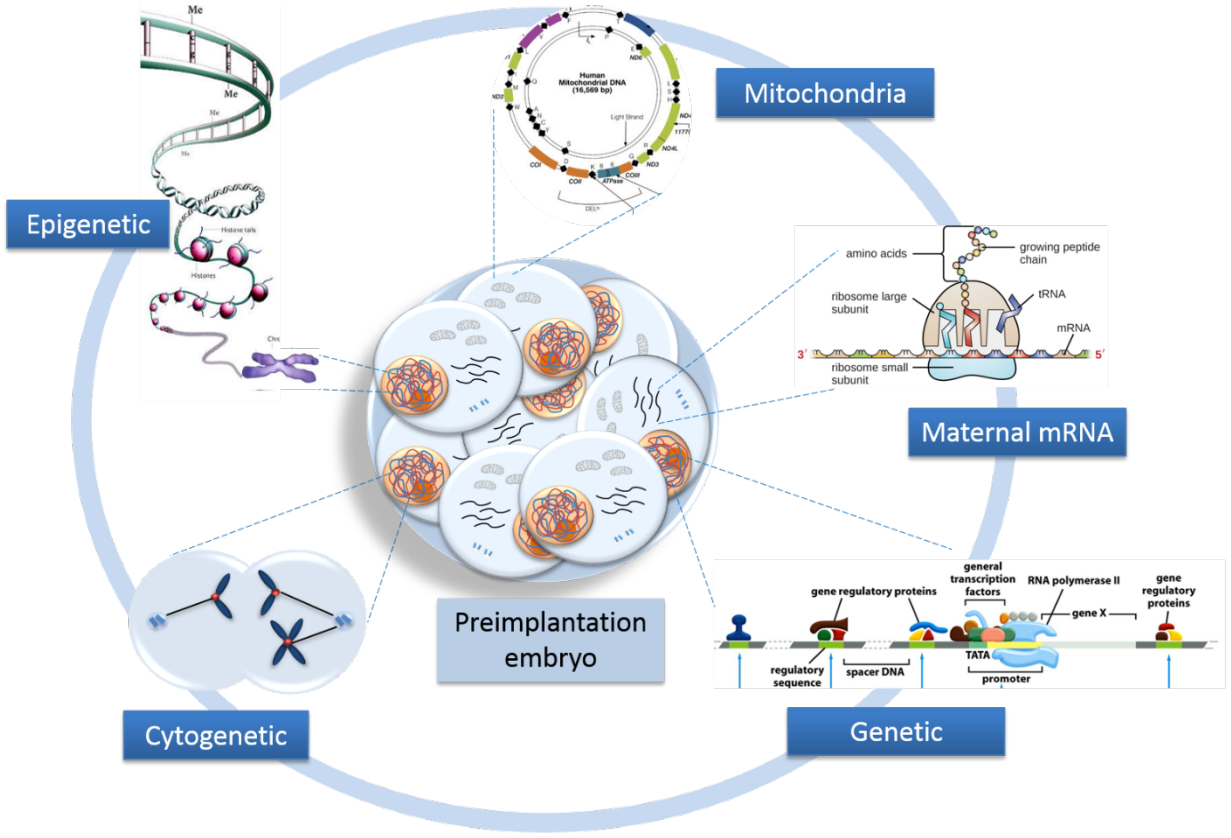


Figure 5. Factors affecting human embryo viability. The preimplantation embryo relies on numerous factors for normal development including maternal mRNA and transcripts, mitochondria, cytogenetic stability, epigenetic reprogramming and genetic fidelity. Each of these has been discussed in detail in section 2.3.

2.3.1 Chromosomal aneuploidy

The incidence of chromosomal aneuploidy varies vastly depending upon the developmental stage of evaluation. It is estimated that approximately 0.3% of liveborns are aneuploid with the frequency increasing to ~4% in stillbirths and ~65% amongst clinically recognised spontaneous abortions (Hassold et al., 1996, Menasha et al., 2005). Early human embryo development is prone to chromosomal errors which may arise during the critical stages of meiosis, fertilisation and/or the first few mitotic divisions post fertilisation (Delhanty et al., 1993; Munné et al., 1993; Wilton, 2002). Aneuploidy is described as an extra or missing copy of a chromosome in a cell. The advent of ART has made the analysis of chromosomal aneuploidies feasible in human gametes and preimplantation embryos, since it provides access to such material, which was previously extremely limited. As compared to other species, human gametogenesis and embryogenesis appear to be particularly error prone processes with approximately 10-30% of fertilised oocytes being chromosomally aneuploid and ~50% of embryos generated by IVF being chromosomally abnormal (Dailey et al., 1996; Wells & Delhanty, 2000). Aneuploidy mostly leads to implantation failure or miscarriage, with less common outcomes including stillbirth or children born with developmental abnormalities associated with conditions such as Down's syndrome (trisomy 21), Klinefelter (XXY) syndrome and Patau syndrome (trisomy 13) (Hassold, & Hunt, 2012). Moreover, studies have shown that human embryos have a higher frequency of chromosomal abnormalities as compared to those observed during miscarriages and postnatal life, indicating a strong selection pressure against abnormal embryos (Hook, Cross and Schreinemachers, 1983; Goddijn and Leschot, 2000; Morales *et al.*, 2008). This negative selection most likely occurs during preimplantation development, leading to developmental arrest of the abnormal embryo (Rubio *et al.*, 2003).

Hence, it is crucial to investigate and understand the origin of chromosomal aneuploidies for better clinical management of IVF generated embryos.

2.3.1.1. Origin of aneuploidy

Chromosomal aneuploidies can be broadly classified into two categories based on their origin, namely meiotic and mitotic. Meiotic chromosomal aneuploidies are introduced in the embryo by either the sperm or the oocyte, whereas the mitotic ones arise during the subsequent cell divisions following fertilisation (**Figure 6** and **Figure 7**).

2.3.1.2. Meiotic segregation errors

Meiosis is a specialised process which generates haploid gametes through a particular cell division process consisting of one round of DNA replication followed by two cell divisions. The first division (meiosis I, MI) involves the separation of homologous chromosomes whereas the second division (meiosis II, MII) leads to the segregation of sister chromatids, giving rise to haploid daughter cells (reviewed by Cooper, 2000). The process of meiosis is a prerequisite for sexual reproduction and involves the unique process of recombination wherein genetic material is exchanged between homologous chromosomes (Dressler and Potter, 1982). Errors of chromosome segregation during MI and MII divisions in gametes lead to 'uniform' aneuploidy in the resulting embryos with all the daughter cells carrying the same anomaly (Hassold & Hunt, 2001).

Even though the basic purpose of meiotic divisions for the male and female gametes is similar, there is a vast difference in the actual manifestation of the mechanism. The replication of DNA at the start of MI is followed by prophase I, wherein the homologous chromosomes synapse and recombine. These homologous chromosomes segregate at the end of MI whereas the sister chromatids separate at the end of MII (**Figure 6**). In males,

meiosis takes place throughout life after puberty. Whereas in females, meiosis initiates during fetal development, arrests at prophase I before birth and resumes only prior to ovulation during adulthood, which could be as much as five decades later. The second major difference between male and female meiosis is in the number of daughter cells generated at the end of both meiotic divisions. In females, two unequal meiotic divisions result in the production of one functional, haploid oocyte and two smaller, non-functional products known as polar bodies which contain mirror image of the chromosome complement of the oocyte. Once extruded, the polar bodies take no part in further development and can be used to indirectly infer the karyotype of the oocyte (**Figure 6**). In contrast, male meiosis results in the production of four equal, functional and haploid sperm cells. These differences between the meiotic divisions of sperm and oocyte may explain why most human aneuploidies found in the embryos originate from the egg and not sperm (Dailey et al., 1996b; Rabinowitz et al., 2012). It is speculated that the long time-interval between meiotic arrest during fetal development and monthly ovulation cycle in adult females leads to a maternal age effect, impacting the incidence of aneuploidy. Moreover, numerous studies have reported a significantly higher incidence of chromosomal aneuploidy in the oocytes, embryos and pregnancies of women of advanced reproductive age as compared to their younger counterparts (Munné et al., 1995; Battaglia et al., 1996; Franasiak et al., 2014). A number of studies have postulated that most aneuploid chromosomes originate from segregation errors during meiosis I in oocytes and increase with advancing maternal age (Hassold & Sherman, 2000; Jones & Lane, 2013; Nagaoka et al., 2012).

Traditionally, non-disjunction of whole chromosomes (during MI) or of sister chromatids (during MII division) was considered as the main cause of aneuploidy arising during female meiosis (Dailey et al., 1996; Licznerski & Lindsten, 2009). However, several

studies later demonstrated that meiotic errors occur at a higher frequency by premature separation of sister chromatids (PSSC), in oocytes of women with advanced maternal age undergoing IVF (Angell, 1997; Gabriel et al., 2011; Pellestor et al., 2002) (**Figure 6**). A few studies have also suggested that the IVF procedures used for ovulation induction may increase the frequency of meiotic errors in oocytes thereby secondarily increasing chromosomal aneuploidies in the resulting the embryos (Baart et al., 2007; Handyside et al., 2012).

Unlike oogenesis, male meiosis results in four equivalent, functional spermatozoa. The presence of millions of sperm per ejaculate renders the analysis of sperm relatively straightforward as compared to that of oocytes. However, currently it is not possible to test a sperm without destroying it, unlike oocytes where the extruded polar bodies can be studied without damaging the oocyte. The overall incidence of aneuploidy in sperm nuclei is predicted to be approximately 4.5% (reviewed by Templado et al.,2005; Templado et al., 2011) with a sharp increase, up to 14%, observed in certain infertile males (Calogero et al., 2003; Chatziparasidou et al., 2015; Gianaroli et al., 2005). Nevertheless, the maternal contribution to aneuploidy in the resultant embryos is significantly higher than that of paternal origin (McCoy et al., 2015).

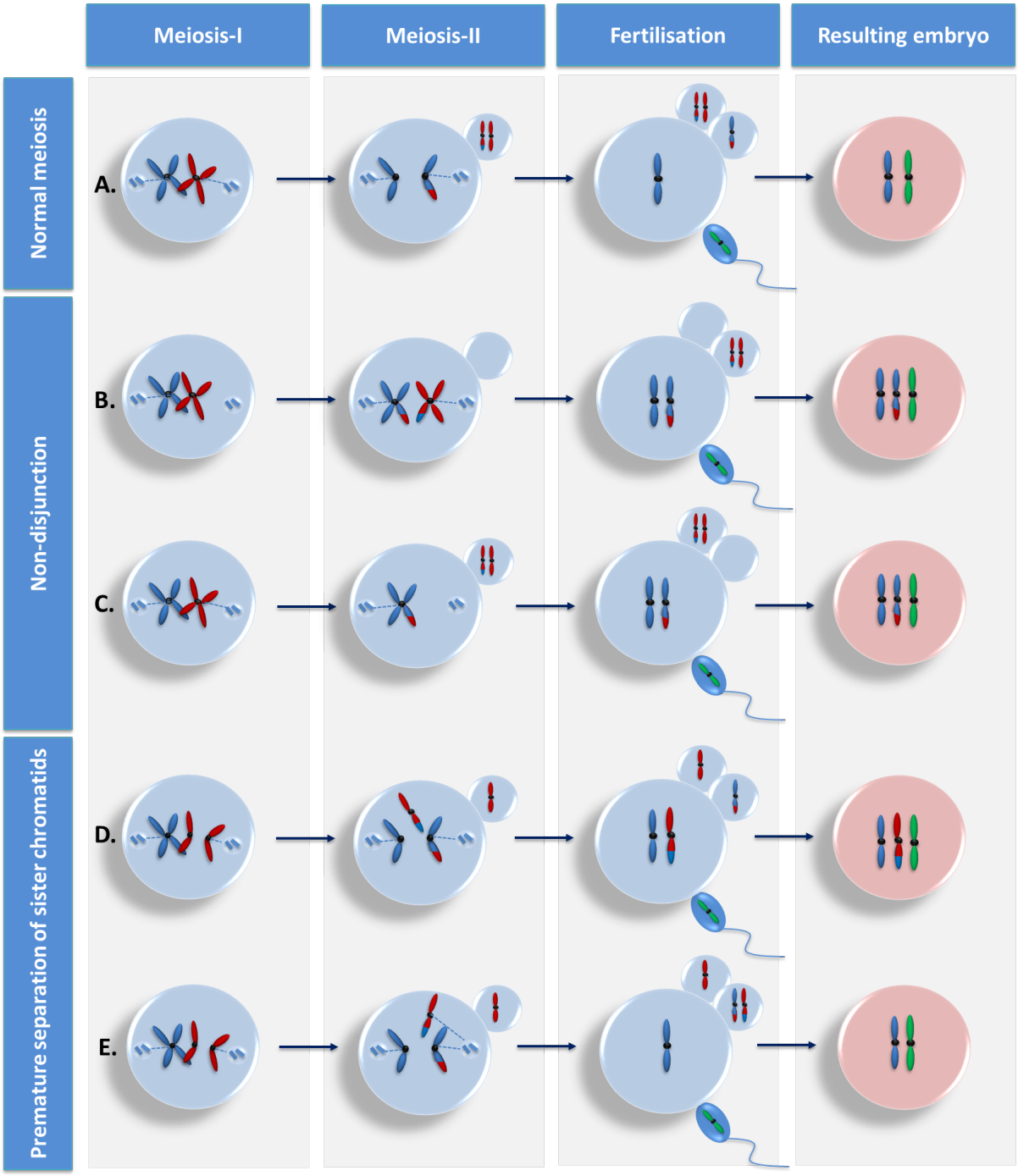


Figure 6. Origin of meiotic aneuploidy in human oocytes. A. Normal meiosis results in a haploid oocyte which after fertilisation leads to development of a diploid embryo. Non-disjunction during meiosis I **(B)** or meiosis II **(C)** leads to aneuploidy in the oocyte and resulting embryo. Similarly, premature separation of sister chromatids during meiosis I can lead to aneuploidy in the resultant embryo **(D)**.

Overall, the numerical chromosomal aneuploidies arising from meiotic errors is influenced by two factors; chromosome segregation errors and malfunction of meiotic cell cycle checkpoints (Polanski, 2013). Some studies have suggested that the high incidence of meiotic errors in oocytes is not due to chromosome segregation errors but rather because of less effective cell cycle checkpoints during oogenesis than in spermatogenesis (Sandalinas et al., 2000; Uroz et al., 2011). This emphasises the importance of assessing IVF related factors such as ovarian stimulation, micromanipulation during ICSI and culture media conditions which might inadvertently disrupt crucial cellular processes during oogenesis.

2.3.1.3. Mitotic errors

It has been well documented in literature that the majority of chromosomal aneuploidies occurring in human preimplantation embryos arise during the first few mitotic divisions following fertilisation (Munné, et al., 1993; Mantikou et al., 2012; Fragouli et al., 2013). Data from several studies suggest that mitotic aneuploidies affect developmental potential of embryos, leading to developmental arrest, implantation failure or in cases of implantation, results in fetal or placental mosaicism (Katz-Jaffe, Trounson, & Cram, 2004; Robinson et al., 1997; Wilkins-Haug et al., 2006). Moreover, it can also cause complications in liveborns such as intrauterine growth delay, mental retardation, uniparental disomy and congenital malformations (Iourov et al., 2010; Moore & Best, 2001).

Mitotic errors lead to chromosomal mosaicism in embryos whereby karyotypically distinct cell lines are present within the same embryo (Munné et al., 1994). Chromosomal mosaicism in human preimplantation embryos produced using IVF techniques was reported by Delhanty and colleagues in 1993. Since then, immense progress has been made in elucidating the frequency and mechanisms of mosaic aneuploidies, especially with the advent

of sophisticated next generation sequencing (NGS) technologies. Although a high proportion of embryos generated during IVF are chromosomally mosaic, the degree of mosaicism varies vastly depending upon the embryonic stage being investigated (McCoy, 2017).

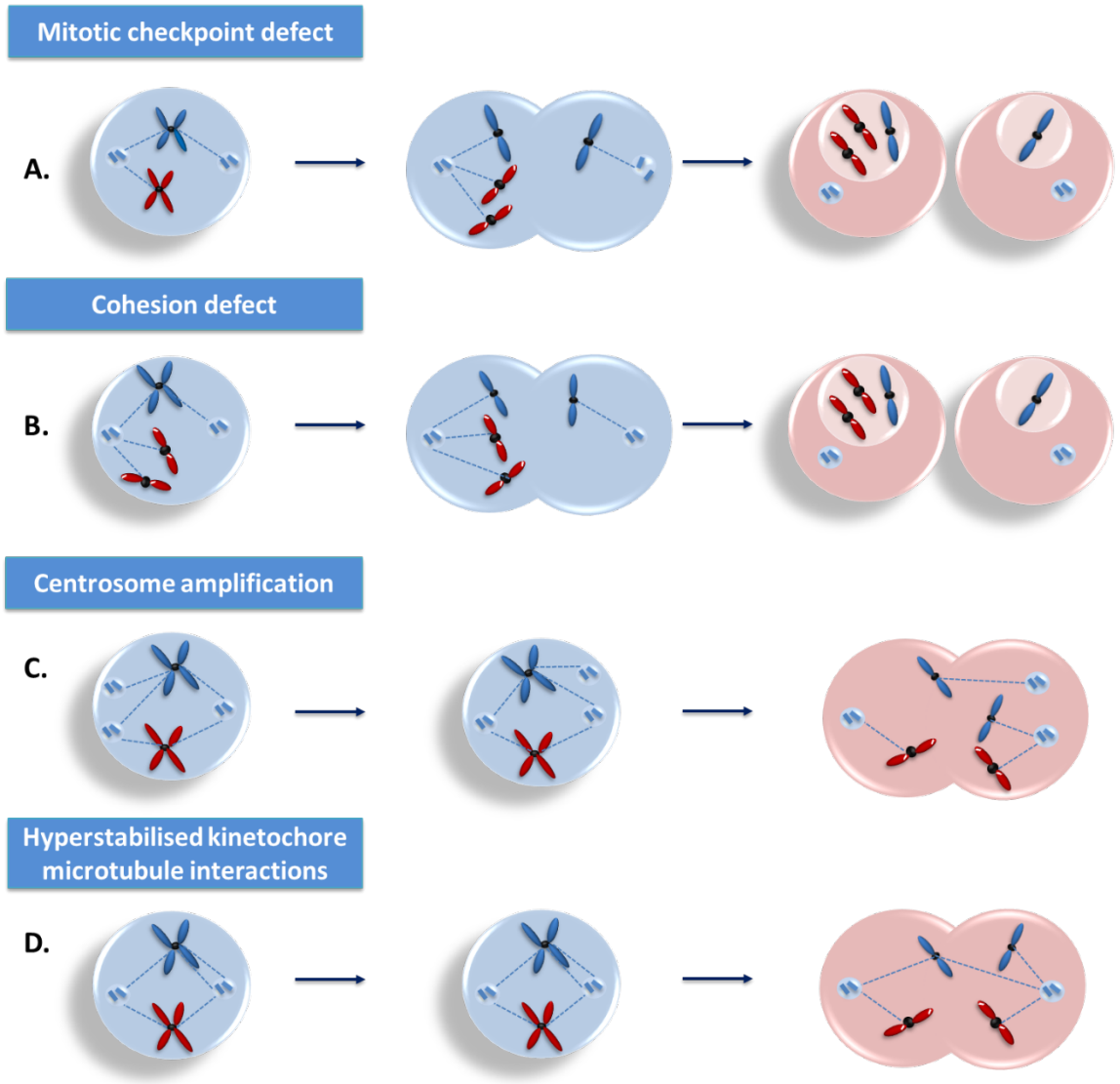


Figure 7. Origin of mitotic aneuploidy. The figure shows different pathways leading to mitotic aneuploidy in developing preimplantation embryos.

Currently, little is known about the exact origin of mitotic aneuploidies but it is likely that a combination of various mechanisms lead to the observed high frequency in human embryos. The initial cleavage divisions take place utilising the maternal RNAs and proteins as the embryonic genome is largely inactive until the 4-8-cell stage (Braude et al., 1988). Recent single cell gene expression studies showed that maternal effect genes were differentially

expressed in aneuploid/ euploid and arresting/normally developing embryos (Vera-Rodriguez et al., 2015). Also, relaxed mitotic cell cycle check points in cleavage stage embryos are implicated in the high incidence of chromosomal abnormalities during the first few mitotic divisions (Harrison et al., 2000; Lee & Kiessling, 2017). Also, the G1 and G2 checkpoint proteins are shown to be absent in 8-cell embryos (Kiessling *et al.*, 2009). The weakening of these checkpoints may lead to the cell cycle to proceed to M-phase before the chromosomes are fully replicated, appropriately aligned on the mitotic spindle or cleared of DNA damage. Without the proper correction of replication errors and completion of each phase of the cell cycle in an ordered and timely fashion, embryos are likely to be at increased risk of anaphase lag, whereby cytokinesis occurs before all of the chromosomes have aligned on the spindle and/or have completed their migrations to the spindle poles, leading to the exclusion of one or more chromosomes from the reforming nucleus (Chavez *et al.*, 2012).

Recently, Jacobs and colleagues demonstrated that the activation of spindle assembly checkpoint (SAC) in cleavage stage human embryos does not induce apoptosis in aberrant cells until the blastocyst stage, thereby accumulating chromosomal aneuploidies during the ensuing cleavage divisions (Jacobs et al., 2017). The centrosome acts as the microtubule organising center (MTOC), which coordinates the bipolar spindle formation. A growing body of evidence suggests that aberrations to the centrosome can lead to anaphase lag, micronucleus formation and multipolar mitosis, thereby leading to chromosomal errors in cleavage stage embryos (Holubcová et al., 2015; Manandhar et al., 2005) (**Figure 7**).

As mitotic aneuploidies and chromosomal mosaicism are increasingly recognised as pervasive features of preimplantation development, attention needs to be paid to their underlying molecular pathways and developmental consequences.

2.3.2. Mitochondrial dysfunction

Mitochondria play a crucial role in several essential cellular processes such as amino acid synthesis, calcium homeostasis and generation of energy by producing ATP via the process of oxidative phosphorylation (OXPHOS) (Dumollard et al., 2009; John et al., 2010). Compared to our knowledge about mitochondrial function in somatic cells, relatively little is known about their role in oocytes and embryos. However, data from several studies have associated mitochondrial dysfunction in murine oocytes and embryos with infertility, especially in females affected by diabetes and obesity (Moley et al., 1998; Wang et al., 2009; Zhang et al., 2013). Mitochondria are important in the formation of meiotic spindles in oocytes as well as for the maintenance of MII spindle before fertilisation (Eichenlaub-Ritter et al., 2004). Irregularities in meiotic spindle functions may lead to chromosomal segregation errors giving rise to aneuploidy.

Several recent studies have indicated that the mitochondrial DNA (mtDNA) levels are elevated in embryos from older women as well as in euploid embryos with lower implantation potential (Diez-Juan et al., 2015; Fragouli et al., 2015; Ravichandran et al., 2017). Although there is conflicting data about the relationship between relative mtDNA quantities and implantation potential of an embryo, discerning mitochondrial function during oogenesis and embryogenesis remains of much interest (Owen *et al.*, 2016; Treff *et al.*, 2017; Victor *et al.*, 2017).

2.3.3. Messenger RNA (mRNA) from oocyte

As discussed earlier, prior to EGA, the embryo is reliant on the maternal pool of RNA and proteins for the first three days of development (Telford et al., 1990). The gene expression in mammalian oocytes is variable throughout oogenesis (Pan et al.,2005). A decay of approximately 30-50% of RNA transcripts occurs during the final transition from germinal vesicle (GV) to metaphase II oocyte (Biase et al., 2008) (**Figure 4**). However, there is an upregulation of certain genes during the final stage of oocyte maturation and these maternal gene products are stored to sustain the embryo development until the genome of embryo activates at cleavage stage (Katz-Jaffe et al.,2009). Several groups have shown that early embryo development is influenced by the quality of oocyte (Lonergan et al., 2000; Patel et al., 2007; Caixeta et al., 2009; Romar et al., 2011). Moreover, the mRNA stores in oocytes seem to decrease with advancing maternal age, potentially reducing the efficiency of critical cellular processes such as DNA repair, due to a reduction in mRNAs necessary for the production of essential proteins involved in the pathways (Hamatani *et al.*, 2004). This may conceivably lead to chromosomal aneuploidies in the resultant embryo.

2.3.4. Genetic factors

Post EGA, the genes are expressed in a stage-specific and time dependent fashion (Hamatani *et al.*, 2006). The genes associated with developmental competence are involved in the regulation of multiple crucial cellular functions including transcription and translation, posttranslational modifications, cell cycle regulation, cell signalling and metabolism (Wrenzycki *et al.*, 2005). In a ground-breaking paper in 2016, Petropoulos and colleagues described a comprehensive transcriptional map of early human embryo thereby giving an insight into the complex array of genes driving the initial stages of embryo development

(Petropoulos *et al.*, 2016). Understanding the gene expression profiles during embryo development is vital as studies have shown that variations in parents' genomes may compromise the normal development of the resulting embryos (McCoy et al., 2015). Moreover, the gene expression is influenced by fluctuating environmental conditions, altered nutritional requirements and stress (Hansis et al., 2001; Spanos et al., 2002). Therefore, studying the gene expression not only provides an understanding of the dynamics of early human embryo but is likely to have clinical implications particularly in the field of assisted reproduction. This has led to a drive for non-invasive screening of embryos by identifying biomarkers for embryo viability. Most of these biomarkers are derived from the downstream products of the gene expression including mRNA transcripts and proteins. Together, the field of omics has gained an impetus for identification of novel embryo viability markers (Katz-Jaffe, McReynolds et al., 2009; Seli et al., 2010; Wang & Bodovitz, 2010).

2.3.5. Epigenetic factors

The central dogma of molecular biology, proposed by Francis Crick in 1958, formed the foundation for modern understanding of the flow of genetic information and gene expression in living organisms (Crick, 1970). Moreover, extensive experiments conducted during 1960s established the concept of the 'genetic code', whereby, the information in the genes is read in form of codons which are ultimately translated into proteins (Crick, 1968; Root-Bernstein, 1982). Hence, the string of nucleotides that make up DNA, which stores hereditary information, serves as the functional unit of gene expression. However, gene expression and inheritable changes are not only controlled by the fundamental DNA sequences, but also by something which literally means above genetics - epigenetics.

The term ‘epigenetics’ was coined by Conrad Waddington in 1942 in order to define events contributing towards phenotypic development that could not be explained by conventional genetics.

Today, epigenetics is understood as the mitotically and meiotically heritable changes in gene function and subsequent cellular phenotype which do not entail a change in the underlying DNA sequence (DuPont et al. 2009). Epigenetics plays a crucial role in attributing cell fate in various differentiated cell types and asserting barriers against reversal to the preceding cellular state (Reik, 2007). Therefore, the genome distinguishes one individual from another while the epigenome differentiates one cell type from another (Gosden and Feinberg, 2007). The fusion of haploid male and female gamete during fertilization leads to the formation of a diploid zygote in mammals. The totipotent zygote gives rise to various differentiated cell types during embryonic development. The difference in potency of the zygote and differentiated cell types is attributed to the epigenetic modifications such as DNA methylation, histone

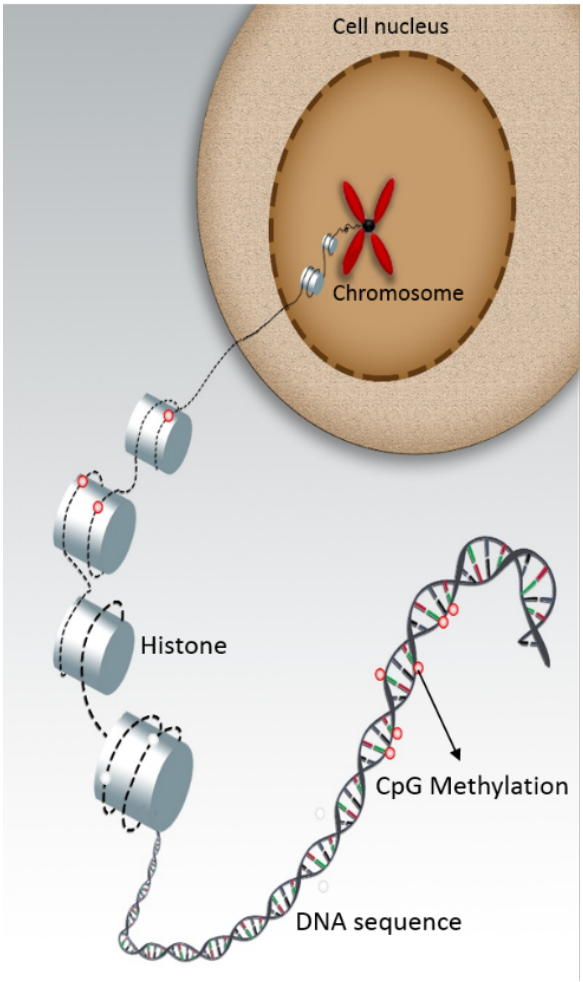


Figure 8. DNA methylation and histone tail modifications- the crucial markers of epigenetic modifications. DNA methylation at CpG dinucleotide is an important epigenetic mark which is mostly leads to transcriptional inactivation of a gene. Histones are a class of proteins around which the DNA is packaged. Modifications in the histone residues are associated with either transcriptional activation or silencing by altering the availability of the DNA coiled around the histones.

modifications, chromatin remodelling and non-coding RNA (Hemberger et al. 2009) (**Figure 8**).

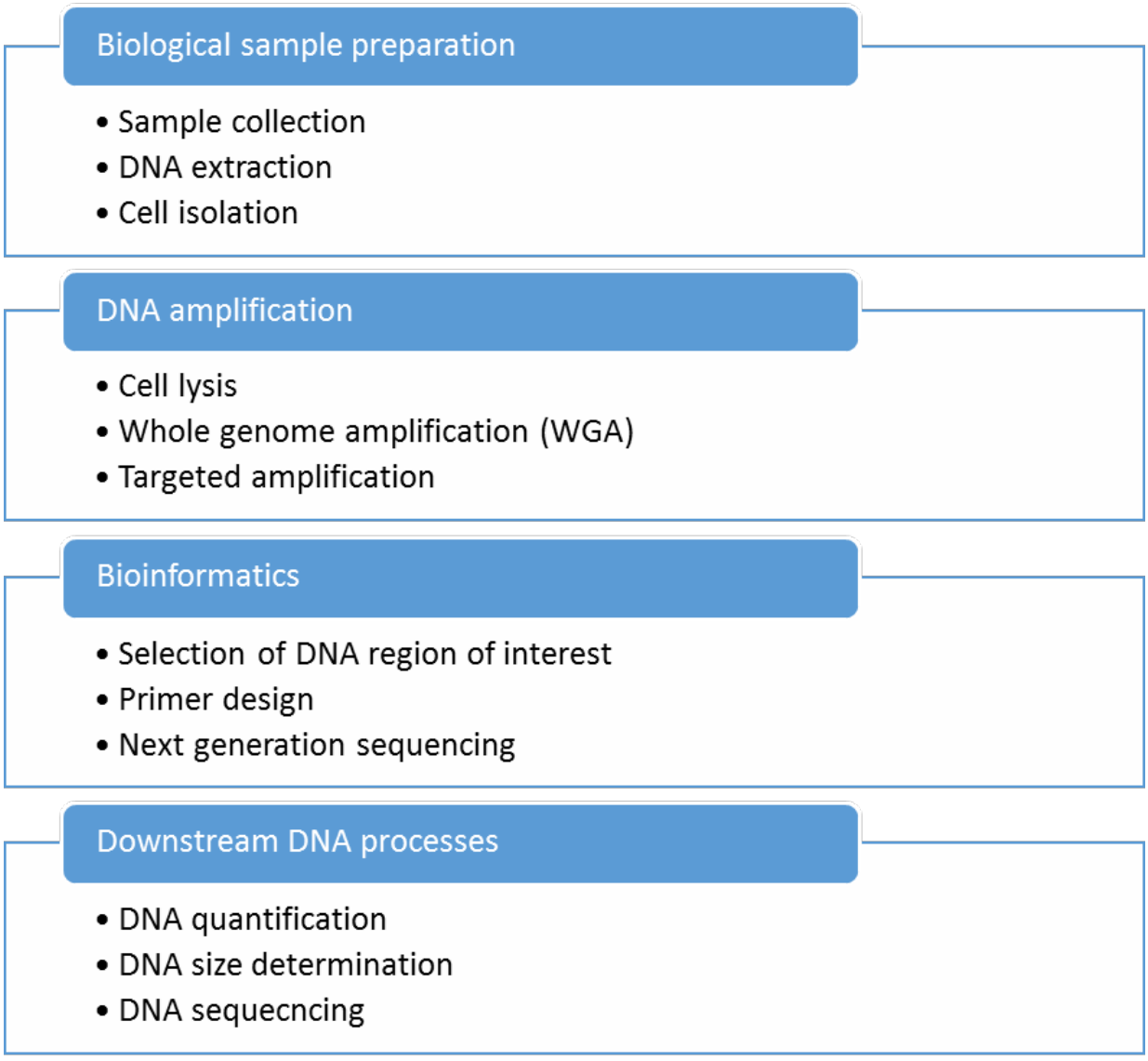
The period during which ART is performed coincides with the epigenetic reprogramming in mammalian gametes and preimplantation embryos. The process of ART involves ovarian stimulation, gamete manipulation and embryo culture *in vitro*. Furthermore, studies have reported that the incidence of epigenetic disorders such as Beckwith-Wiedeman and Angelmann syndrome have been found to be significantly higher in children born after ART compared to those conceived naturally (Amor and Halliday, 2008). Hence it is important to study the impact of ART on the dynamic process of epigenetics during the *in vitro* culture of embryos. A more in-depth discussion on epigenetic mechanisms is described in **Chapter 6**.

Chapter 3: General Materials and Methods

The previous chapters establish the motivation for this research along with study aims and objectives, and relevant literature. This chapter contains a detailed description of the general Methods and Materials used for the next results chapters to achieve these objectives. Additional details unique to each study can be found directly in the specific sections.

This chapter describes all the common materials and methods utilised for various experiments during the course of the project. **Table 1** shows the 4 main sections of this chapter including a) biological sample preparation, b) DNA amplification methodologies, c) bioinformatics and d) general downstream processing of the samples. Individual results chapters contain a separate materials and methods section, each describing the specific methods used for the particular results chapter.

Table 1. Flowchart showing structure of Materials and Methods chapter



3.1. Biological sample preparation

The biological samples used during the course of the entire project consisted of human cell lines, isolated lymphocytes and buccal cells, DNA extracted from blood, buccal samples and preimplantation human embryos. This section describes the collection and preparation of the aforementioned samples for further downstream analyses.

3.1.1. Culture of cell lines

The human cell lines were purchased from the Coriell Institute of Medical Research (New Jersey, USA). The cell lines were maintained, cultured and stored by Ms Katharina Spath. All the procedures for handling cell lines were performed in sterile, cell culture hoods. In brief, the cells were incubated in a humidified incubator at 37°C, 5% carbon dioxide (CO_2), 5% oxygen and 90% nitrogen. The sub-culture of cells was performed in Chang Medium C (Irvine Scientific), prepared according to the manufacturer' protocol. The culture of adherent cell lines cell culture flasks with filter caps. The inspection of cell growth was performed under an inverted microscope (Olympus, UK). For sub-culture, the cell suspension was transferred to 15ml conical tube and centrifuged at 200 x g for 10 minutes to obtain a cell pellet. The pellet was resuspended in fresh culture media and transferred to a new culture flask. Cells were sub-cultured for 3-5 days until confluent. The sub-cultured cells were either stored long term by cryopreservation or isolated for experiments as described in **Section 3.1.4**.

3.1.2. Collection of buccal cells and lymphocytes

For the validation of methodologies developed for a) imprinted genes analysis and b) exploring blastocoel fluid and spent culture media for embryonic genomic DNA; buccal and lymphocyte cells were collected from chromosomally normal, healthy male and female volunteers.

For the collection of buccal cells, either of the two kits, Isohelix SK-2S Buccal swabs (Isohelix Ltd, UK) or Catch All sample collection swabs (Epicentre) was used. Isohelix kit was utilized if DNA extraction was to be performed later and for the purpose of buccal cell isolation, the Epicentre kit was used for buccal samples collection. The samples were collected according to manufacturer's instructions. Briefly, buccal cells were collected by inserting the swab from the kit into the mouth of the volunteer and firmly rubbing it against the inside of the cheek for 1 minute. The swab head was placed in the tube, securely closed and stored at 2-4°C in the fridge until DNA extraction.

For the collection of peripheral blood cells, 5ml of whole blood was collected from consenting healthy individuals by a trained clinical nurse. The samples were collected in a sterile purple cap blood collection tubes containing anticoagulants. Thereafter the samples were refrigerated at 2-4°C before DNA extraction (**Section 3.1.3**) or cell isolation (**Section 3.1.4**).

3.1.3. DNA extraction

Genomic DNA was isolated from whole blood of healthy individuals using the QIAamp DNA Mini Kit (Qiagen, UK) and performed according to manufacturer´s instructions. In brief, 200µl of sample was added to a microcentrifuge tube containing 20µl of QIAGEN Protease and mixed with 200µl of buffer AL. The mixture was pulse-vortexed for 15 seconds and incubated at 56°C for 10 minutes. After incubation, 200µl of ethanol was added and mixed by vortexing briefly. The sample was carefully applied on to a QIAamp Mini spin column and centrifuged at 8000rpm for 1 minute. A further 500µl of buffer AW1 was added and the column was centrifuged at 8000rpm for 1 minute followed by addition of 500µl of buffer AW2 and centrifugation at maximum speed for 3 minutes. The spin column was placed in a clean

microcentrifuge tube and 200µl of buffer AE was added, followed by 20 minutes incubation for 5 minutes. After centrifugation at 8000rpm for 1 minute, the flow through was collected and stored at 4ºC for further use.

DNA extraction for Isohelix SK-2S Buccal Swabs was performed using the DNA Isolation kit DDK-50 (Isohelix Ltd) according to manufacturer's instructions. In order to stabilise the DNA, 500µl LS solution and 20µl PK solution was added to the buccal swab tube. The tube was then incubated in a water batch at 60°C for 1 hour. The liquid from the tube was vortexed briefly and transferred into 1.5ml Eppendorf tube, followed by addition of 400µl of CT solution. The tube was centrifuged at 12000 x g for 7 minutes to pellet the DNA. The supernatant was removed and 150µl of TE solution was added to the pellet and incubated for 5 minutes at room temperature. Extracted DNA sample was vortexed briefly and stored at 2-4°C.

3.1.4. Cell isolation

To validate the application of developed methodologies (**Chapters 5 and 6**) to a small numbers of cells representative of embryo biopsies, cells ranging from one to five cells were isolated from cell lines, buccal samples/swabs and blood samples. The cell isolation procedure was carried out in a sterile, clean room by Dr Dagan Wells or Dr Souraya Jaroudi. Prior to isolation of individual cells, samples were prepared as follows:

3.1.4.1. Sample preparation: Cell culture

The cells from confluent cell culture were transferred to a 15ml conical tube and centrifuged at 100 x g for 10 minutes. The supernatant was removed and 0.5-1.0ml of DPBS was added to the pellet and the cell suspension was transferred to a sterile 1.5ml tube and stored at 2-4°C until isolation of individual cells.

3.1.4.2. Sample preparation: Lymphocytes

Isolation of the lymphocytes from whole blood was carried out using the QIAamp DNA Mini Kit (Qiagen, UK) and performed according to the manufacturer´s protocol. In brief, 2ml of freshly collected blood samples from a healthy individual was mixed with 2ml of DPBS. The mixture was then gently layered over 3ml of Ficoll-Plaque Plus (GE Healthcare, UK) and centrifuged at 400 x g for 35 minutes, resulting in the separation of four distinct layers. If the layers were not clear, then a further centrifugation at 500 x g for 10 minutes was performed. The plasma layer was removed and discarded followed by separate collection of the underlying lymphocyte layer, which was then diluted in 6ml of 0.1% of PBS (Fisher Bioreagents).

3.1.4.3. Sample preparation: Buccal cells

After the collection of buccal cells, the swab was moved into a fresh conical tube containing 2ml DPBS. The swab was rotated and squeezed on the side of the tube to release the buccal cells in DPBS. The swab was discarded, and the buccal cell suspension was stored in the fridge.

3.1.4.4. Individual cell isolation

The isolation of cells was carried out in a clean room to prevent contamination. A wash buffer consisting of PBS (Sigma-Aldrich, UK) and 0.1 % PVA (Sigma-Aldrich, UK) was prepared and placed in a sterile petri dish as ~5µl drops (cell wash drops) and ~10µl drop (pipette tip wash drop). In order to avoid sample contamination, the tips were washed frequently in between cell isolation in the pipette wash solution.

For cell isolation, ~10µl of respective cell suspensions (buccal cells, lymphocytes or cultured cells) were transferred initially to the 1st PVA/ DPBS drop and mixed by pipetting. Cells were subsequently transferred to new drops in small quantities until the desired number of cells were isolated (single or clumps of 3 to 5 cells). These isolated cells were then washed in new drops of cell wash buffer and ~2.5µl droplets of the last droplet (containing the isolated cells) were collected on 0.2ml Eppendorf tubes (**Figure 8**). The tubes were centrifuged briefly and stored at -80°C.

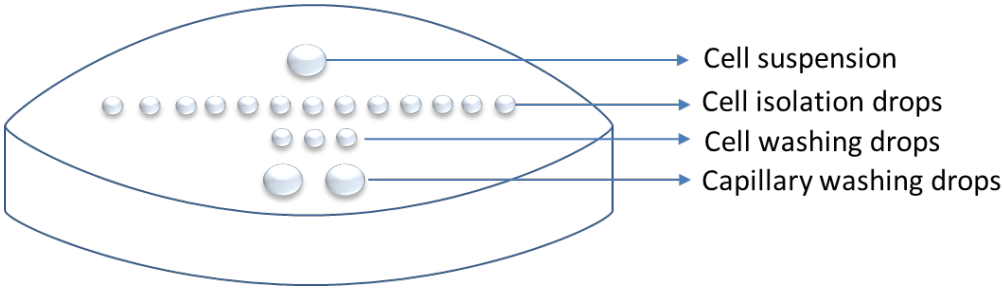


Figure 9. Single cell isolation. The cell suspension is placed on top in the petri dish. The cells are isolated in the middle droplets and the capillary pipette is washed in the bottom washing droplet in between single cell isolations.

3.2. DNA amplification

Genomic DNA (extracted bulk DNA or from isolated cells) was amplified for various downstream applications during the course of the project. Various amplification strategies including whole genome amplification (WGA), targeted amplification using conventional polymerase chain reaction (PCR) and multiplex PCR were used for the purpose. All the amplification reactions were performed in a UV irradiated cold rack in a laminar hood. Reactions involving minute quantities of DNA (isolated cells or embryo biopsies), the reactions were carried out in a clean room.

3.2.1. Conventional PCR

Amplification of specific regions in the genome was carried out using designed primers and Taq polymerase. Depending upon the requirement of respective experiments, several modifications of the conventional PCR amplification were performed including gradient PCR, nested/ hemi-nested PCR and touch down PCR (described in detail in relevant sections). All the PCRs were performed in a 15µl reaction in sterile, irradiated 0.2ml Eppendorf tubes.

In order to test primer specificity to determine the optimal annealing temperature, a gradient PCR was performed as shown in **Table 2**. The annealing temperature depends upon the melting temperature of the primer (Tm) and hence the optimal annealing temperature was determined first for each primer pair using gradient PCR (**Table 3**).

The amplification was carried out either on extracted genomic DNA or cell samples. For genomic DNA, 0.5ul of the sample was added to 14.5µl of the amplification reaction mix (**Table 2**). In case of amplification of cell samples, alkaline lysis was performed prior to PCR. For cell lysis, 0.3µl 1M NaOH (Sigma Aldrich), 0.75µl of 0.1 M DTT (Sigma Aldrich) and 0.45µl H_2O were added to the cell sample, following incubation at 65°C for 10 minutes. The strong alkaline nature of the reaction mixture disrupts the cell membrane and leads to the release of the intracellular content in the solution. After alkaline lysis, 1.5µl of tricine (Sigma Aldrich) was added to each sample, to neutralise the alkalinity of the lysis solution.

Each experiment consisted of a negative control (0.5µl water) to check for any potential contamination of the reagents. The reactions consisted of 0.5µM primers, 0.5mM dNTPs and 1 unit of Taq DNA polymerase in 10X buffer (**Table 2**). The amplifications were carried out in a thermocycler with a heated lid at 105°C and the cycling conditions are described in **Table 3**. To assess the success of amplification, 5µl amplified products were run

on an agarose gel (concentrations ranging from 1% to 4% depending upon the experiment) as described in **Section 3.3.2.1**. The amplified samples were stored at 2-4°C

Table 2. Reaction conditions of conventional PCR

Component	Supplier	Volume (µl)
Nuclease free water	Roche Diagnostics	12.51-x
HotMaster Taq DNA Buffer	5 Prime	1.5
Forward Primer (10µM)	Eurogentec	0.3
Reverse primer (10µM)	Eurogentec	0.3
dNTPs (10mM)	ThermoFisher Scientific	0.3
HotMaster Taq DNA polymerase	5 Prime	0.09
DNA	N/A	x (0.25-0.5)
Final volume		**15**

Table 3. Thermocycler conditions for conventional PCR

PCR step	Cycle Conditions	Number of cycles
Initial denaturation	96°C for 1 minute	1
Denaturation Annealing Elongation	94°C for 15 seconds 55-65°C for 15 seconds 65°C for 45 seconds	15 to 45
Final Extension	65°C for 2 minutes	1
Cooling	Hold at 4°C	1

3.2.3. Multiplex PCR

Multiplex PCR enables simultaneous amplification of numerous genomic loci in a single amplification reaction. Specific details about the primer characteristics and genomic loci pertaining individual experiments are described in Materials and Methods sections of **Chapters 5 and 6**. Multiplex PCR was performed either on extracted genomic DNA or cell samples (following alkaline lysis) in a UV irradiated clean hood.

Relative to the experiment, all the corresponding primer pairs (100µM concentration, Eurogentec) were mixed at an equimolar concentration to make a primer pool. The primer pool was subsequently diluted to make to 10µM concentration which was then used in the multiplex PCR reaction. All the reactions were performed in a 15µl reaction using Qiagen Multiplex PCR kit (Qiagen, Germany). For gradient PCR, different annealing temperatures were tested (**Table 5**). The reaction mixture composition is depicted in **Table 4**.

Table 4. Reaction conditions for multiplex PCR

Component	Supplier	Volume (µl)
Nuclease free water	Roche Diagnostics	7.2-x
Qiagen Multiplex Master Mix	Qiagen	7.5
Primer pool (10µM)	Eurogentec	0.3
DNA		x (0.25-0.5)
Final volume		**15**

Table 5. Thermocycler conditions for multiplex PCR

Heated lid: 105°C		
PCR STEP	**CYCLE CONDITIONS**	**NUMBER OF CYCLES**
Initial denaturation	95°C for 10 minutes	1
Denaturation Annealing	99°C for 10 minutes 55-65°C for 4 minutes	15-45
Final Extension	99°C for 10 minutes	1
Cooling	Hold at 4°C	1

3.2.4. Whole genome amplification (WGA)

The WGA strategies enable rapid and robust amplification of the entire genome from minute quantities of DNA (picograms), generating high DNA yield which can be further used for multiple downstream applications. Two different WGA methods were used for

amplification of samples; Sureplex DNA amplification (Illumina, USA) and Multiple Displacement Amplification (MDA) (Qiagen, Germany).

3.2.4.1. Sureplex amplification

The Sureplex amplification (Illumina, USA) was carried out according to the manufacturer's protocol which consists of three steps; 1) cell lysis, 2) pre-amplification and 3) final amplification. Briefly, 8µl of the lysis mix was added to ~2µl of cell sample followed by incubation at 75°C and denaturation at 95°C. Immediately, 5 µl of pre-amplification step was added and the samples were incubated in a thermocycler (**Tables 6 and 7**). The final amplification step was carried out in a total volume of 75 µl and resulting amplification products stored at 4°C (**Table 7**).

Table 6. Sureplex amplification reaction mix

Reaction step	Reagent	Volume (µl)
1. Cell Lysis	Extraction enzyme dilution buffer	4.8
	Cell extraction buffer	3
	Cell extraction enzyme	0.2
2. Pre-amplification	SurePlex pre-amp buffer	4.8
	SurePlex pre-amp enzyme	0.2
3. Final amplification	Nuclease-free water	34.2
	SurePlex amplification buffer	25
	SurePlex amplification enzyme	0.8

3.2.4.2. Multiple Displacement Amplification (MDA)

The MDA was performed using Qiagen's REPLI-g kit (Qiagen, Germany) according to the manufacturer's recommendations. Briefly, the cells were subjected to alkaline lysis followed by incubation at 65°C for 10 minutes (**Table 8**). Thereafter, isothermal WGA was carried

out by at 30°C for 2 hours (**Table 9**). The amplified samples were stored at 4°C for further downstream processing.

Table 7. Sureplex amplification thermocycler conditions

Heated lid: 105°C		
Reaction step	**Cycle conditions**	**Number of cycles**
1. Cell Lysis	75°C for 10 minutes	1
	95°C for 4 minutes	
	Hold at 10°C	
2. Pre-amplification	95°C for 2 minutes	1
	95°C for 15 seconds	12
	15°C for 50 seconds	
	25°C for 40 seconds	
	35°C for 30 seconds	
	65°C for 40 seconds	
	75°C for 40 seconds	
	Hold at 4°C	1
3. Final amplification	95°C for 2 minutes	1
	95°C for 15 seconds	14
	65°C for 1 minute	
	75°C for 1 minute	
	Hold at 4°C	1

Table 8. MDA reaction conditions

Reagent	**Volume (µl)**
Water SC	9
REPLI-g SC Reaction Buffer	29
REPLI-g SC DNA polymerase	2
Total volume:	**40**

Table 9. MDA incubation conditions

Step	Cycle conditions	Number of cycles
Isothermal amplification	30°C for 120 minutes	1
Enzyme denaturation	65°C 3 minutes	1
	Hold at 4°C	1

3.3. Downstream DNA processes

3.3.1. Measurement of DNA concentration

Concentrations of DNA samples were measured using the Qubit Fluorometer and the Qubit dsDNA HS Assay Kit (Invitrogen) that allows determination of DNA concentration in the range of 10pg/µl to 100ng/µl. Measurement was performed according to the manufacturer's instructions. In brief, the fluorometer was referenced using 10µl of two standards provided with the kit. A working solution was prepared by diluting the Qubit dsDNA HS reagent in Qubit dsDNA HS buffer (1:200). Thereafter, 2µl of samples were mixed with 98µl of working solution, followed by subsequent measurement of DNA concentrations.

3.3.2. Visualisation of DNA

3.3.2.1. Agarose gel electrophoresis

The products obtained after amplification were analysed by agarose gel electrophoresis. An agarose gel (1-4g agarose (Invitrogen, USA) in 100ml 1X TBE buffer; 10µl GelRed (Biotium)) was prepared and 5µl of the samples along with 1µl of 10X BlueJuice Gel Loading Buffer each (Invitrogen, UK) and 5µl of 100bp Low Scale ladder (Fisher Scientific) were loaded into individual wells. The gel was run at 90 V for 60 minutes. Subsequently the gel was analysed on a UV Transilluminator (UVP) and pictures of the gel were captured using a digital camera (Canon) attached to the gel documentation system.

3.3.2.2. Bioanalyzer

Bioanalyzer (Agilent Technologies, USA) facilitates the simultaneous quantification of DNA and measurement of the fragment sizes by automated electrophoresis. The DNA migrates through a network of intricate channels on a chip. A High Sensitivity DNA kit (Agilent Technologies, USA) was utilised to perform the analysis of minute quantities of DNA (ranging from 5pg-500pg) according to the manufacturer's instruction. In brief, a gel-dye mix was prepared by mixing the dye concentrate into the High Sensitivity DNA gel matrix vial. The mixture was vortexed for 10 seconds, centrifuges briefly and the contents were transferred to a column with filter. The tube containing the column was centrifuged at 2240 x g for 10 minutes and the resulting gel-dye mix was collected. A High Sensitivity DNA chip primed and prepared on a chip priming station by addition of 9µl of the gel-dye mix into four dedicated wells (**Figure 10**). Thereafter, 5µl of the DNA marker was added to 11 designated sample wells and one ladder well. One microliter of ladder as well as samples were loaded in their respective wells. The chip was vortexed at 2400 rpm for 1 minute and was placed on the Bioanalyzer instrument. The samples were labelled on the 2100 Expert software (Agilent Technologies, USA) according to their corresponding positions on the chip and processed. The resulting data was analysed using the above-mentioned software and an example of the output is shown in **Figure 10**.

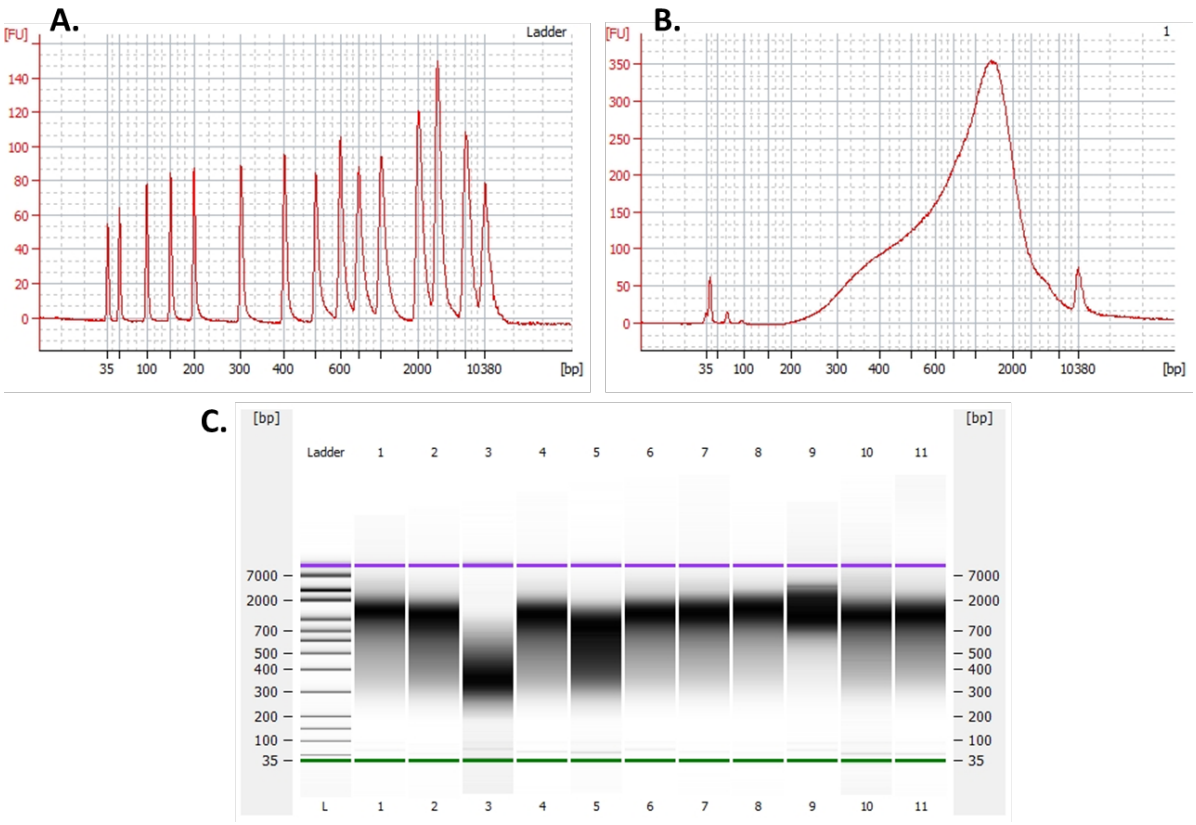


Figure 10. Bioanalyzer images. The figure shows the output from Bioanalyzer instrument. Figure **A.** shows the ladder pattern, **B.** shows the size distribution of a sample and **C.** shows the gel image with size distribution of all samples.

3.3.3. Gel extraction

After PCR, the samples were run on an agarose gel. Thereafter, the fragments were excised from the gel with a clean scalpel and transferred to 1.5µl tubes. DNA was extracted with QIAquick Gel Extraction Kit (Qiagen, UK). The weight of each sample was determined and Buffer QG was added accordingly (1:6 ratio; e.g. 100mg gel in 600µl buffer). After incubation for 10 minutes at 50ºC, one volume of isopropanol was added and the solution applied on a spin column. After centrifugation at 13000 rpm for 1 minute, the column was washed with 0.75ml of buffer PE followed by a second centrifugation step with the same conditions. In order to elute the extracted DNA from the column, 50µl nuclease free water was added and the column centrifuged at 13000rpm for 1 minute.

3.3.4. Next Generation Sequencing (NGS)

Illumina's MiSeq platform was used to sequence samples for either comprehensive chromosomal screening or targeted sequencing of the loci of interest. Samples were prepared using various types of library preparation kits according to the nature of the experiment. Details regarding the specific library preparation protocols are described in the Materials and Methods section of the relevant chapters. The principle behind Illumina's library preparation methods used during the course of this thesis is shown in **Figure 11**.

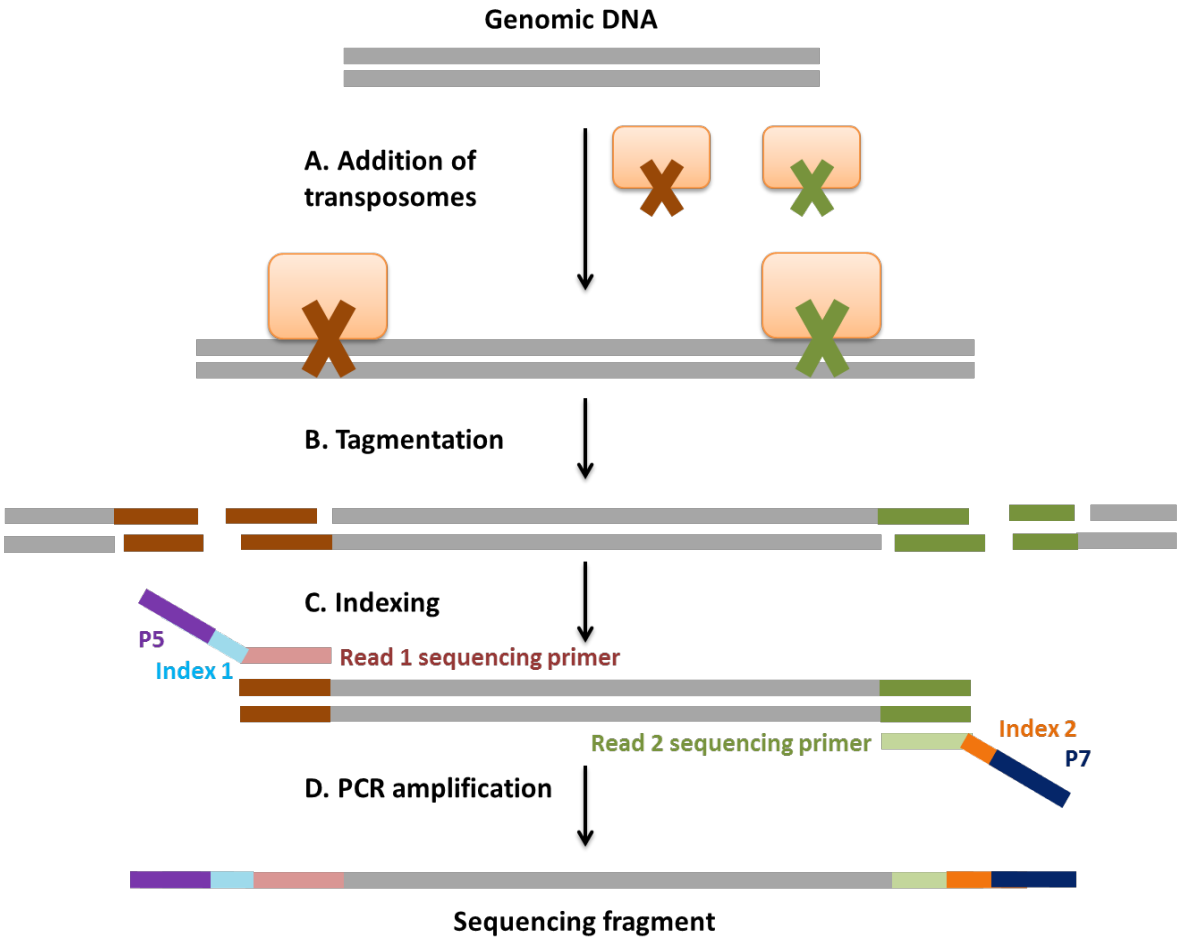


Figure 11. Library preparation principle for Illumina's Nextera protocols. The Nextera library preparation protocol by Illumina uses a transposome mediated adapter ligation followed by indexing of the libraries in subsequent PCR reaction.

3.4. Bioinformatics

3.4.1. Selection of the DNA sequence

All the DNA sequences of interest were retrieved from NCBI database (https://www.ncbi.nlm.nih.gov/). Various genes and regions of DNA for different experimental procedures are described in the relevant sections in **Chapters 5** and **6**. To retrieve specific details about genes and related sequence features, UCSC (https://genome.ucsc.edu/) and Ensemble (http://www.ensembl.org/index.html) genome browsers were also utilised. Detailed description of their specific usage is described in the respective sections.

3.4.2. Primer design

3.4.2.1. Conventional PCR

Primers for various experiments were designed using the online tool Primer 3 (http://primer3.ut.ee/). The standard primer parameters utilised for all primer design are described in **Table 10**.

Table 10. Primer design conditions

Primer conditions	Minimum	Optimal	Maximum
Primer size	18bp	20bp	23bp
Primer Tm	57°C	59°C	62°C
Primer GC%	30%	50%	70%
Product length	Varying		

3.4.2.2. Bisulfite converted DNA PCR

For the detection of methylation, the genomic DNA was treated with sodium bisulfite and amplified using specially designed bisulfite converted DNA primers.

The bisulfite treatment of DNA converts all the unmethylated cytosine into uracil residues and hence the template sequence used for primer design differs from that used for standard primer design. The bisulfite converted primers were designed using Bisulfite Primer Seeker tool by Zymo Research (www.zymoresearch.com/tools/bisulfite-primer-seeker). The standard primer parameters are described in **Table 11**.

Table 11. Primer design conditions for bisulfite converted DNA

Primer conditions	Minimum	Optimal	Maximum
Primer size	24bp	30bp	38bp
Primer Tm	50°C	60°C	66°C
Primer GC%	40%	50%	60%
Product length	Varying		

All the designed primers were purchased from Eurogentec Ltd. (UK) (100µM in TE buffer). Working aliquots of 10µM were prepared from the stock solution and stored at -20°C.

3.4.3. Checking primer parameters

Proper primer design is crucial for the success and efficiency of an experiment. Hence, primer parameters such as specificity, likelihood of cross-dimerization and self-annealing as well as the presence of SNPs in the primer sequences were assessed after primer design.

The self-dimerization and hairpin formation potential of a primer was detected by using the Oligo Calc tool (http://biotools.nubic.northwestern.edu/OligoCalc.html). New primers were designed if a high number of self-annealing or 3'complementarity was observed in the designed primer. Next, the specificity of the primers were checked by using PrimerBlast (https://www.ncbi.nlm.nih.gov/tools/primer-blast/) which aligns the primer sequence to the reference human genome and gives outputs as the regions in the genome complementary to the input sequence. Lastly, in order to detect the presence of any SNPs in the primer

sequence, SNP check (https://secure.ngrl.org.uk/SNPCheck) tool was used and the primers having SNPs near the 3' end were redesigned.

For multiplex PCR, the self- and cross-dimerization potential of the primers was checked using ThermoFisher Scientific's Multiple Primer Analyzer tool. This aids in increasing the efficiency of a multiplex PCR reaction by avoiding primers which potentially cross-dimerise with other primers or self-dimerise.

Chapter 4: A detailed cytogenetic analysis of the incidence of segmental aneuploidies in human oocytes and preimplantation embryos

The aim of this part of the study was to determine the incidence of aneuploidies affecting parts of chromosomes (segmental aneuploidies) during gametogenesis and preimplantation development and investigate their clinical significance. Two widely used comprehensive chromosomal screening (CCS) techniques namely aCGH and low pass NGS were utilised to gain an insight into the origin and factors affecting segmental aneuploidy.

4.1. Introduction

Chromosomal abnormalities in human oocytes and preimplantation embryos are very common. The prevalence of such abnormalities increases with advancing maternal age, affecting about 25% of blastocysts generated by women in their mid-twenties to over 65% of blastocysts from women aged 40 years or over (Munné et al., 2007; Franasiak et al., 2014b; Demko et al., 2016). The high incidence of chromosomal abnormalities in the early human embryo is thought to be the major cause for the relatively low pregnancy rate following single embryo transfer (Papanikolaou *et al.*, 2008). In most cases, aneuploidy results in embryo development arrest or implantation failure (Scott et al., 2012). Of the small proportion of aneuploid embryos that do succeed in establishing a pregnancy, the great majority eventually miscarry at a later stage of pregnancy (Nagaoka et al., 2012).

Hence, the cytogenetic analysis of samples biopsied from the embryo for the purposes of embryo selection was proposed as a way of improving clinical outcomes after IVF (Munne et al., 1993). This screening strategy is termed preimplantation genetic testing for aneuploidy (PGT-A), and has especially gained impetus in the past decade (Vermeesch, Voet and Devriendt, 2016). The reason for the growth in PGT-A utilisation was the development of comprehensive molecular cytogenetic methods capable of examining the entire chromosome complement of cells with high accuracy, such as array comparative genomic hybridisation (aCGH) and Next Generation Sequencing (NGS). Clinical data obtained after the use of such methodologies have generally been encouraging, leading to a wider use of PGT-A, especially in the USA.

Studies describing oocyte and embryo results obtained with the use of CCS methodologies thus far, have mainly focused on the incidence of abnormalities affecting the entirety of the

chromosomes (e.g. Munné, et al., 1995; Fragouli et al., 2013; Yang et al., 2015). However, structural losses or gains affecting chromosomal fragments, resulting in segmental aneuploidy, are also common during gametogenesis and early embryo development (Munné et al., 1995; Voullaire et al., 2000; Wells & Delhanty, 2000a; Vanneste et al., 2009a; Rabinowitz et al., 2012b). Segmental aneuploidies have been associated with miscarriages and the birth of children affected by congenital abnormalities (Brewer et al., 1998, Brewer et al., 1999). However, the clinical relevance and impact of segmental abnormalities in relation to embryo viability and IVF outcome is currently poorly understood.

Segmental imbalances were first observed in murine models methods half a century ago (Vickers, 1969). However, it was only with the advent of advanced molecular cytogenetic techniques that the occurrence of segmental aneuploidy in embryonic cells was first observed (Voullaire et al., 1999). Two studies on human cleavage stage embryos using comparative genomic hybridisation detected numerous segmental imbalances and also demonstrated the occurrence of *de novo* chromosomal breakage during the first few mitoses following fertilisation, giving rise to reciprocal losses/gains of the same chromosome fragment in different cells of the embryo (Voullaire et al., 2000; Wells & Delhanty, 2000b).

Even though the existence of segmental aneuploidy in human gametes and preimplantation embryos has been previously reported, little work has been done to determine the frequency and origin of such abnormalities. Vanneste and colleagues (2009) investigated the incidence of various forms of chromosomal aneuploidies in cleavage stage embryos using SNP arrays and aCGH and found that approximately 70% of embryos contained at least one cell affected by a segmental imbalance. This high prevalence may have implications for natural and assisted reproduction, contributing to low fecundity of humans

and relatively low success rate of IVF treatments. However, the sample size for the study was low (n=23) and all the embryos were derived from a single IVF clinic. In order to verify these results, studies involving considerably more samples from multiple IVF clinics are required.

The mechanism of origin of segmental aneuploidy is different from that of whole chromosomal aneuploidy. A double stranded DNA break, which fails to resolve itself, can lead to a segmental imbalance in subsequent daughter cells (**Figure 12**). Depending on the origin of the error, segmental aneuploidies can be either classified as meiotic or mitotic. Meiotic segmental aneuploidies arise in the oocyte or sperm during one of the 2 meiotic divisions of gametogenesis. Fertilisation of a gamete harboring a segmental abnormality is assumed to lead to an embryo with the same segmental error present in all of its cells (**Figure 13**). Mitotic segmental abnormalities arise during the embryonic cellular divisions taking place post-fertilisation. Mitotic segmental errors are confined to a subset of daughter cells of the embryo leading to a phenomenon known as mosaicism. Specifically, mosaicism can be defined as the presence of two or more distinct cell lines within the same embryo. Various types of segmental aneuploidies are shown in **Figure 14**

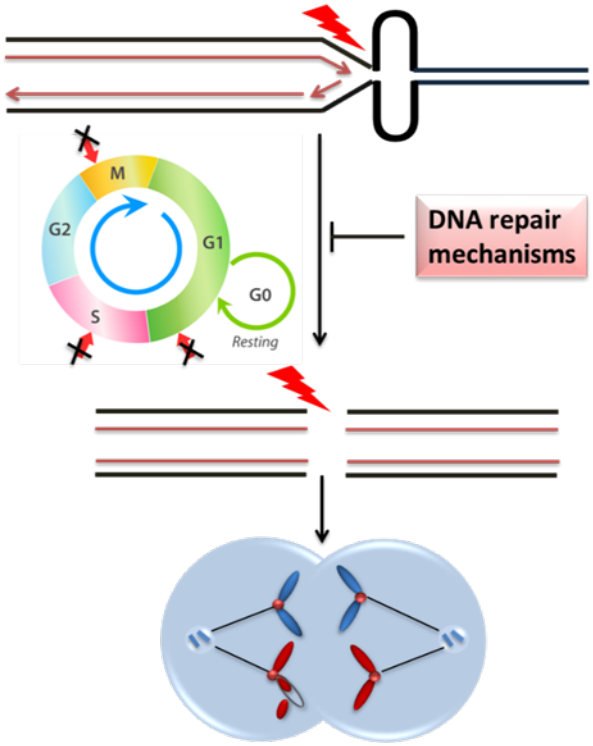


Figure 12. Mechanism of dsDNA breaks. Encounter with DNA secondary structures may lead to stalling of the progressing replication fork. Failure of cell cycle checkpoints to resolve this may lead to dsDNA breaks and subsequent segmental aneuploidy in the daughter cells.

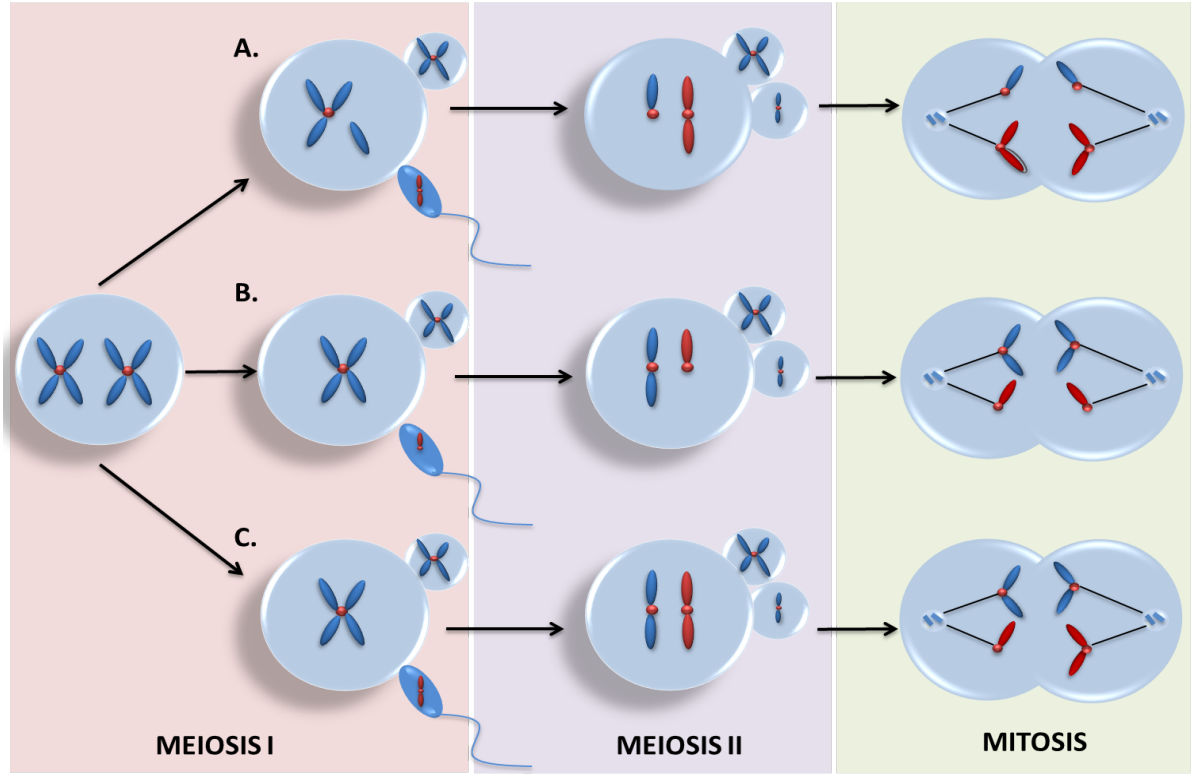


Figure 13. Origin of segmental aneuploidy. Segmental aneuploidy can arise either due to (**A**) chromosomal breakage during replication during meiosis I in oocytes, (**B**) introduction of fragmented DNA by the fertilising sperm or (**C**) during the subsequent mitotic divisions post fertilisation. The first two (**A** and **B**) lead to meiotic segmental aneuploidy present in all the daughter cells while the last (**C**) leads to mitotic segmental aneuploidy, present only in a subset of daughter cells of the resulting embryo.

Mosaicism has been observed in human embryos since the early days of PGD and PGT-A (Delhanty et al., 1997; Munné et al., 1994). It can arise as a result of chromosome malsegregation in a cell of a euploid embryo (some cells would be normal, others abnormal) or in a cell of an aneuploid embryo (no cells would be normal, the embryo would be a mixture of different aneuploid cell types) (reveiwed by McCoy, 2017).

The initial studies involving the analysis of mosaic embryos were performed by fluorescence *in situ* hybridization (FISH). However, the frequency of mosaicism reported by numerous studies using FISH varied widely, ranging from ~30% to 90% (Delhanty et al., 1993; Munne et al., 1994; Baart et al., 2006). FISH cannot assess all of the 24 chromosomes simultaneously and hence its use may not provide a complete picture of mosaicism. However,

with the advent of modern molecular cytogenetic techniques such as aCGH, single nucleotide polymorphism (SNP) array, quantitative real time PCR (qRT-PCR) and next generation sequencing (NGS), detection of all 24 chromosomes simultaneously became feasible. Of all the aforementioned methods, NGS has been shown to provide the highest resolution for the detection of mosaicism in TE biopsies, which are typically composed of several cells (Munné & Wells, 2017).

Recent studies have shown that chromosomal mosaicism involving entire chromosomes can impact the implantation potential and ongoing pregnancy rates highlighting the clinical relevance of such abnormalities (Fragouli et al., 2017; Munné et al., 2017). The clinical outcomes of mosaic pregnancies are likely to be dependent on the chromosome(s) involved and level and distribution of mosaicism in the embryonic and extraembryonic tissues (Robinson et al., 1997; Kalousek, 2000; Wallerstein et al., 2000). Mosaicism confined to the placenta is generally associated with a higher likelihood of fetal viability, but an abnormal outcome may occur if high levels of aneuploidy persist to term in the placenta (Wolstenholme et al., 1994).

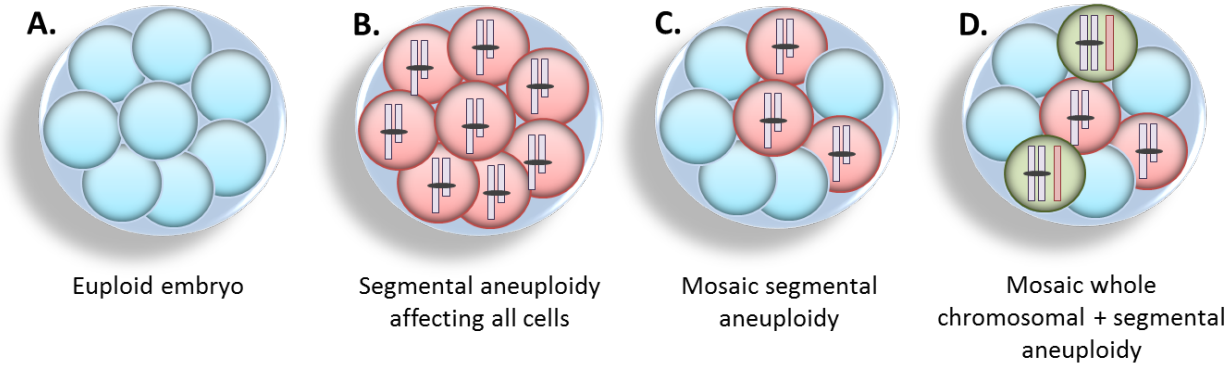


Figure 14. Types of segmental aneuploidy. The diagram shows different types of segmental aneuploidies in comparison to a euploid embryo (**A**). The segmental aneuploidy can affect either all of the cells in an embryo (**B**; meiotic in origin) or a subset of cells giving rise to mosaic segmental aneuploidy (**C** and **D**). Moreover, the segmental aneuploidy can occur either independently (**B** and **C**) or in conjunction with whole chromosomal aneuploidy (**D**).

Apart from a chromosomally viable embryo and ideal uterine conditions, physiologically good quality embryos are also essential for the establishment of a successful pregnancy. The physiological state of an embryo, including its developmental kinetics, metabolism and genetic integrity is dependent on numerous components of the IVF laboratory and culture conditions. The early embryo development is a dynamic process and needs adequate culture media conditions comprising of optimal media composition, correct pH, temperature and gas composition. Several studies confirm that the culture media composition has an impact on the quality of embryos generated during IVF/ ICSI cycles (reviewed by Mantikou et al., 2013).

Currently, there are several IVF culture media available commercially with varying composition. These could be broadly classified as either continuous (single) media systems or sequential media systems. Continuous media systems facilitate the culture and development of embryos from fertilisation to either cleavage or blastocyst stage (Day1 to Day 3/ Day 5 post fertilisation) using the same medium formulation. On the other hand, sequential systems use a series of culture media which differ in composition and concentration of components including glucose, amino acids and pyruvate, between Days 1-3 and Days 3-5 of culture.

Studies on mouse blastocysts have revealed that changes in culture media can cause a significant alteration to the embryonic transcriptome. It was furthermore shown that culture conditions that better mimic the environment present *in vivo*, produced better quality embryos (Rinaudo & Schultz, 2004; Lonergan et al., 2006). Additionally, more deviations in the transcriptome and proteome were observed if culture conditions were devised to cause embryonic stress (Rinaudo & Schultz, 2004; Lonergan et al., 2006). On the other hand, studies on the effect of culture media on human embryos have mainly focused on evaluating the

efficacy of different commercially available culture medias, especially comparing the embryo viability rates, pregnancy rates and overall IVF success rates (Gardsner & Lane, 1997; Aoki et al., 2005; Lonergan et al., 2006; Balaban et al., 2008). However, the major limitation of these studies was that the evaluation of embryos was based on morphological criteria alone. This may introduce observer dependent bias as the morphological observations are time-point specific whereas the development of an embryo is a dynamic process. Moreover, these assessments do not reflect the genomic integrity of the embryos, which is one of the major causes of developmental arrest.

There are numerous culture media formulations available with different compositions of amino acids, nutrients, vitamins, growth factors etc. Other clinical factors in an IVF laboratory such gas composition in incubators, temperature, incubator types, culture oils, are also important in determining the embryo interaction dynamics with the components of culture medium (Swain and Smith, 2011; Kolahi et al., 2012; Sommer et al., 2012). As the mitotic segmental aneuploidies arise during *in vitro* culture of embryos, it is pertinent to assess any potential impact of culture media and other IVF associated conditions on the frequency of such abnormalities, especially considering that such defects may have clinical consequences.

4.2. Study Aims

This part of the project examines the prevalence and origin of segmental aneuploidy at various stages of preimplantation development in a large population of fertilized human oocytes and embryos. These samples were derived from multiple IVF clinics and hence variation in certain aspects of culture conditions could be evaluated in relation to segmental aneuploidy. The results obtained provide an insight into the frequency, origin and nature of segmental imbalances present prior to implantation as well as the likely causes and fate of such abnormalities.

The main objectives of this study were as follows:

1) **Carry out a detailed cytogenetic evaluation of segmental aneuploidies in fertilised oocytes, cleavage stage and blastocyst stage embryos to examine:**
    - The frequency of segmental chromosome errors at various stages of preimplantation development
    - The incidence of partial gains and losses
    - The location of chromosomal breakpoints (leading to segmental aneuploidies) across the human genome
2) **Investigate the origin of segmental aneuploidies. Specifically, to:**
    - Establish the frequency of mitotic and meiotic segmental abnormalities in blastocyst stage embryos
    - Map the mitotic and meiotic chromosomal breakages across the human genome

3) Assess the factors affecting the incidence of segmental aneuploidy. Specifically:

- The effect of female age on the incidence of segmental errors versus whole chromosome errors in oocytes and embryos.
- The effect of different PGT-A indications on the origin of segmental aneuploidy
- The effect of IVF culture conditions on the frequency of segmental aneuploidy in embryos derived from different IVF clinics

4.2. Materials and Methods

4.2.1. Sample details

The PGT-A data obtained from oocytes and embryos was collected during the course of routine clinical work undertaken by the Reprogenetics laboratories (UK and USA). The patients requested oocyte/embryo screening for various reasons, most commonly advanced maternal age or previously unsuccessful IVF treatments. Patients received counselling and a signed consent for embryo screening was obtained. Embryological techniques, including polar body, cleavage stage and blastocyst biopsy were carried out according to standard protocols in each IVF clinic. A total of 31,646 samples, including 452 fertilised oocytes, 10,191 cleavage stage embryos, and 21,003 blastocyst stage embryos were analysed using either aCGH or NGS. There were two main parts to this analysis; 1) detailed cytogenetic evaluation of segmental chromosome errors and 2) investigation of clinical factors affecting the frequency of segmental aneuploidy in human embryos (**Figure 15**).

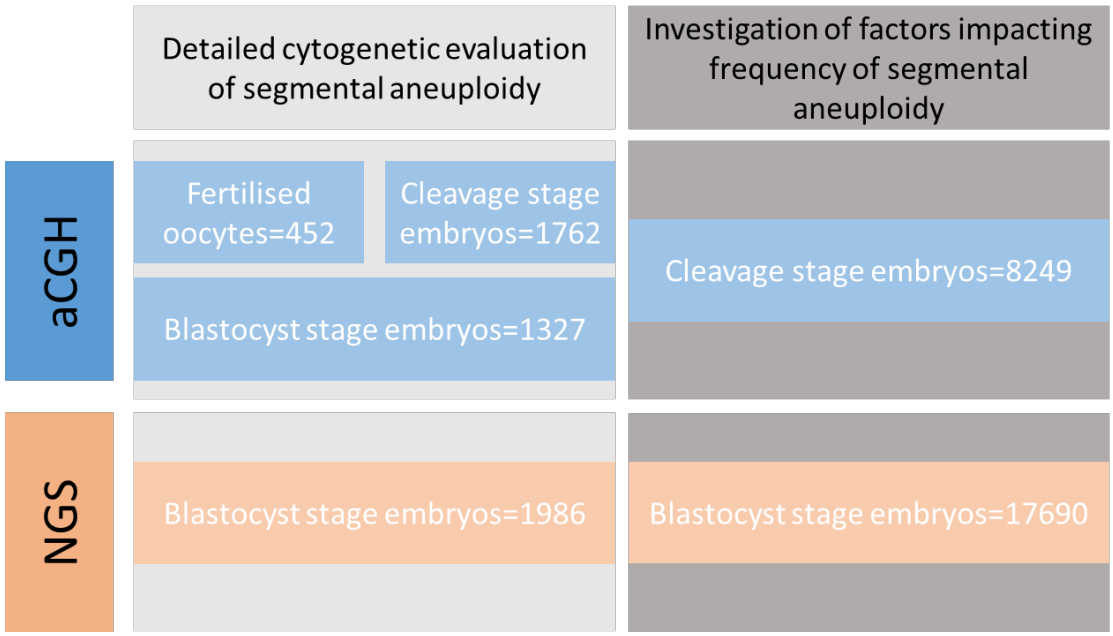


Figure 15. Sample details for segmental aneuploidy assessment. The samples consisted of either fertilised oocytes, cleavage stage or blastocyst stage embryos. The diagram represents the number of samples processed by aCGH and NGS respectively as well as groups them according to the evaluation carried out on them.

4.2.2. Sample preparation and WGA

In all cases of oocyte analysis, both the first and the second polar bodies (PBs) were tested, following sequential biopsy. The blastomere biopsy consisted of removal of a single cell at the cleavage stage (Day 3 post fertilisation). Trophectoderm (TE) biopsy involved the removal of approximately 3-5 cells from the outer trophectoderm layer of the blastocyst stage embryo (day 5 or day 6 post fertilisation). The PB and embryo biopsies were carefully washed and were collected in ~2µl PBS/ 0.1% polyvinyl alcohol (v/v). Subsequently, the biopsied samples were lysed and subjected to WGA using the Sureplex WGA system™ (Illumina, UK) according to the manufacturer's protocol as described in **Section 3.2.4.** (**Chapter 3**).

The WGA products were subsequently processed using either aCGH or NGS.

4.2.2.1. Array CGH

Array CGH was performed using the 24 Sure™ Cytochip V3 microarray (Illumina, UK) which has been previously extensively validated for the CCS of oocytes and embryos (Fragouli et al., 2011; Gutiérrez-Mateo et al., 2011). The procedure was performed according to the manufacturer's instructions (Illumina, UK) (**Figure 3**). Briefly, the amplified DNA, along with male and female reference DNA samples were fluorescently labelled utilizing the 24 Sure Fluorescence Labelling System (Illumina, UK). Thereafter, the fluorescently labelled samples were placed on 24Sure Cytochip microarrays (Illumina, UK) and incubated overnight. Post-incubation, the microarrays were washed and scanned using the InnoScan 710 (Innopsys, France). The resulting images were analyzed using BlueFuse software (Illumina, UK). The criteria for categorizing a segmental aneuploidy were set to be ≥ 15Mb losses or gains of chromosome fragments, with the results of all of the probes within the affected region

exceeding the threshold used by the BlueFuse analysis software. An example of an embryo with a segmental chromosome imbalance identified by array-CGH is shown in **Figure 16**.

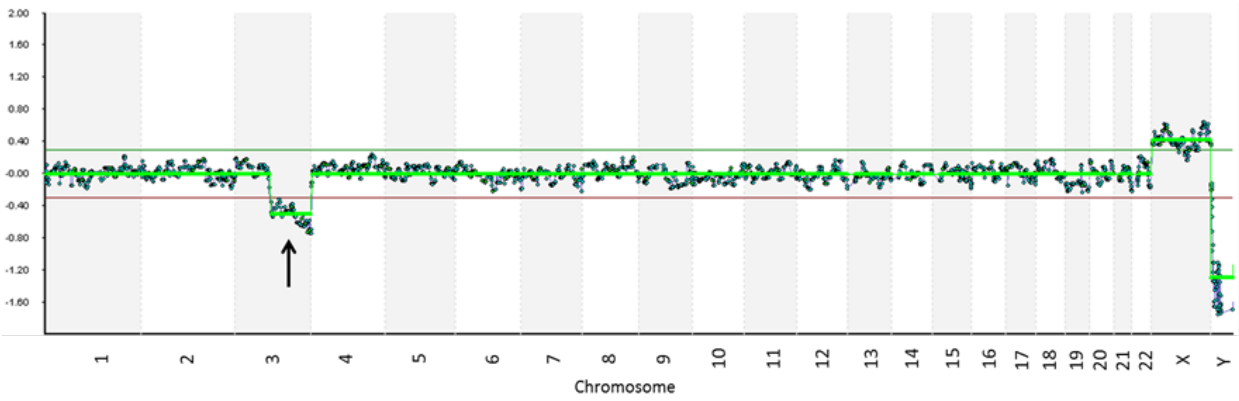


Figure 16. Example of segmental aneuploid aCGH profile. Molecular karyotype of an embryo generated after aCGH showing a segmental loss (indicated by an arrow) of chromosome 3.

4.2.2.2 Next generation sequencing analysis

The Sureplex WGA products were processed to prepare libraries for NGS analysis using the Veriseq PGS pipeline (Illumina, UK) according to the manufacturer's protocol. The protocol was validated for detection of whole chromosomal and segmental aneuploidies (Fragouli et al., 2017). Briefly, the amplified samples were initially quantified using the dsDNA High-Sensitivity (HS) Assay Kit (Qubit®, Life Technologies UK). Thereafter, the diluted DNA (0.2 ng/µl, 1 ng total) was fragmented and simultaneously adapters were added to the fragmented products by a transposome in a tagmentation reaction (**Table 12**). The index sequences were introduced in the DNA samples to enable dual-index sequencing (2x36bp) by a limited PCR amplification using the Nextera PCR master mix. The amplified products were cleaned using the AMPure XP beads (Beckman Coulter, USA) in 1:1 (beads:DNA) ratio. The beads were subsequently washed twice with 80% ethanol solution and were eluted in resuspension buffer after the second wash. The resulting purified libraries were then normalized to equalize the quantity of each sample using the library normalisation reagents (Illumina, UK). The reaction composition and conditions for all of the above-mentioned steps are depicted in **Table 12**.

Table 12. Reaction conditions for library preparation using Veriseq reagents. The table depicts reaction conditions for various steps of library preparation before sequencing.

Reagent	Volume (µl)	Incubation conditions	
(1) Step: Tagmentation			
Amplicon Tagment Mix	5	55°C for 5 minutes Hold at 10°C	
Tagment DNA Bufffer	10		
DNA sample (0.2ng/ µl)	5		
(2) Step: PCR amplification			
Nextera PCR Master Mix	15	72°C for 3 minutes 95°C for 30 seconds	x 1 cycle
index 1 (i7) primers	5	95°C for 10 seconds 55°C for 30 seconds 72°C for 30 seconds	x 12 cycles
index 2 (i5) primers	5		
		72°C for 5 minutes	x 1 cycle
(3) PCR cleanup			
AMPure XP beads	45	2 minutes	
80% ethanol	200	30 seconds x 2 washes air-dry for 15 minutes	
Resuspension buffer	50	2 minutes	
(4) Library normalisation			
LNA1/LNB1 mixture	45	Mix at 1800rpm for 30 minutes and magnetic separation of beads	
cleaned up DNA	20		
LNW1	45	Wash twice on magnetic stand	
0.1N NaOH	30	5 minutes	
LNS1	25		
Final normalised library	**50**		

Equal volumes of the normalised libraries were pooled, denatured and sequenced using the Miseq Sequencing kit V3 (Illumina, UK) on a MiSeq sequencing system (Illumina, UK). The resulting sequencing data was analysed by BlueFuse Multi Software (Illumina, UK). Embryos were categorised as euploid, if the reads for all the autosomal chromosomes aligned to the copy number 2 on Y-axis of the chromosomal profile (**Figure 16**). The sex of the embryo was similarly determined using the copy number on the Y-axis of the chromosomal profile, with a female embryo having copy number 2 for X chromosome and zero for Y-chromosome and a male embryo displaying copy number 1 for both X and Y chromosomes. Embryos were identified as aneuploid if they displayed a deviation from their respective default copy number, with trisomic samples showing a copy number >2 and monosomic samples having a copy number <2. An NGS profile of a segmental aneuploid sample is shown in **Figure 16**.

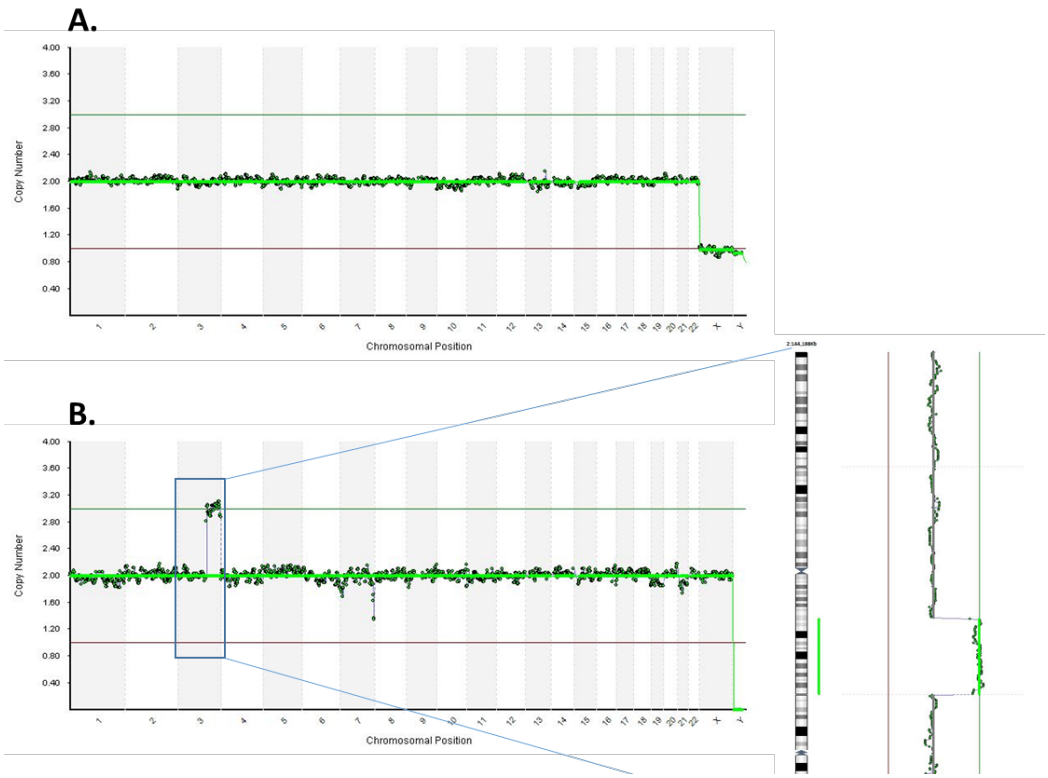


Figure 16. Example of NGS profiles. **A**. Molecular karyotype of a euploid male embryo generated after NGS. **B.** A female NGS profile showing a full segmental gain (non-mosaic) (zoomed in) of chromosome 3.

The Bluefuse Multi V3 software is capable of providing numerical values for exact copy numbers of chromosomes for individual samples. A mosaic diploid-aneuploid sample consists of a combination of cytogenetically normal and abnormal cells. Hence, the chromosomal copy number values generated by the software will be between 2 and 3 for mosaic gains and between 1 and 2 for mosaic losses. An example of a mosaic segmental aneuploidy profile is shown in **Figure 17**.

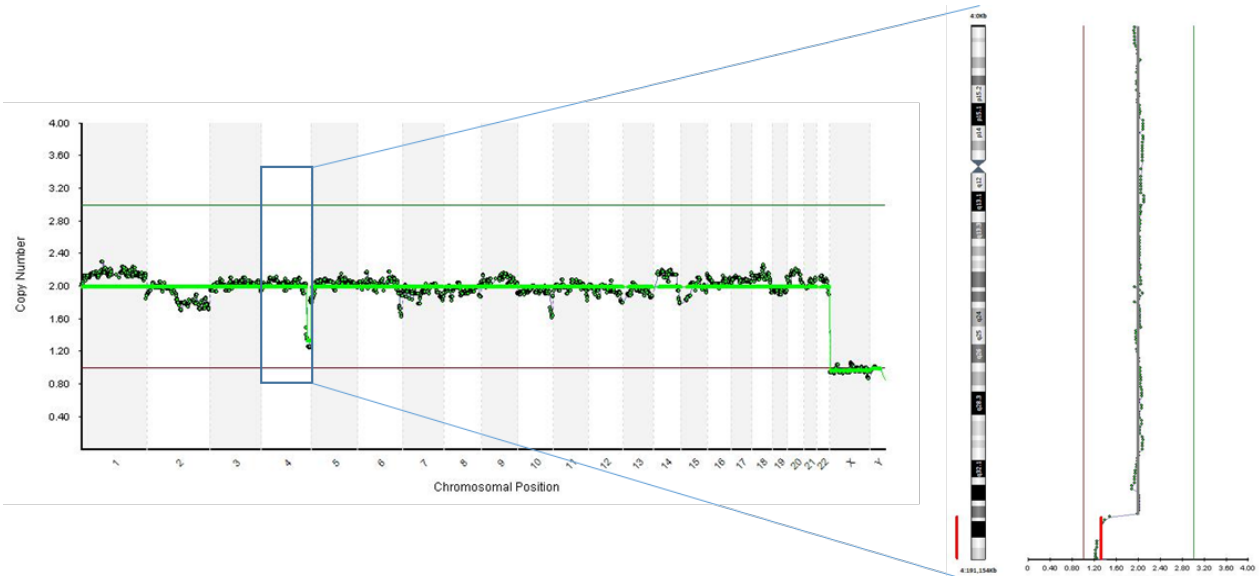


Figure 17. Example of mosaic segmental aneuploidy. Molecular karyotype of a male embryo showing a mosaic segmental loss (zoomed in) of chromosome 4. The profile for the segmental loss shows a copy number of 1.3 which means that if 5 cells were biopsied, approximately 4 cells had a segmental loss of chromosome 4.

4.2.3. Validation of aCGH and NGS for the detection of whole chromosomal and mosaic aneuploidy

We have previously validated the 24Sure™ platform and have confirmed an accuracy of >98% in single blastomeres, polar bodies and trophectoderm samples (Fragouli et al., 2011; Gutiérrez-Mateo et al., 2011; Wells et al.,2014). The sensitivity and resolution of aCGH (24Sure™ platform) for the detection of segmental aneuploidies was established using three distinct cell lines with known segmental aneuploidies (Fragouli et al., 2017). Moreover, an additional 25 embryo samples from 11 patients with different reciprocal translocations were

used to validate the resolution of segmental aneuploidy detection on the 24Sure™aCGH platform (**Table 13**). The embryo samples from these patients were initially analysed utilising the 24Sure+ aCGH platform (Illumina), which has been validated previously for the detection of reciprocal translocations (Fiorentino et al., 2011; Colls et al., 2012). The results from both platforms were compiled and compared for concordance.

The sensitivity and resolution of aCGH and NGS for the detection of whole chromosomal as well as segmental aneuploidies was established using six distinct karyotypically stable aneuploid cell lines. In short, mixing experiments using isolated fibroblast cells from aneuploid and euploid cell lines in different ratios were carried out to establish the sensitivity of aCGH and NGS to detect mosaic aneuploidy.

Table 13. Validation of aCGH platform for detection of segmental aneuploidy

Translocation	Number of embryos
46,XY,t(20;22)(q11.2;q11.2)	1
46,XY,t(7;8)(p22;p22)	3
46,XY,t(1;17)(p36.3;q24.2)	2
46,XX,t(11;22)(q23;q11)	2
46,XY,t(11;16)(q25;p11.2)	2
46,XX,t(5;8)(q13.1;q11.2)	3
46,XX,t(11;16)(q22.2;q22)	3
46,XX,t(3;16)(q21.3;p13.1)	3
46,XX,t(13;15)(q12.3;q15)	5
46,XX,t(3;9)(q27;p24)	1
Total embryos	**25**

4.2.3.1. Mixing experiments for validation of mosaicism detection

In order to analyse the efficacy of NGS to detect mosaicism, mixing experiments using isolated fibroblast cells from aneuploid and euploid cell lines mixed in different ratios were

carried out (Fragouli et al., 2017). The aneuploid cell lines were obtained from the NIGMS Human Genetic Cell Repository at the Coriell Institute for Medical Research (USA) (**Table 14**). The isolated fibroblasts from these cell lines were mixed with lymphocytes from a euploid male (46,XY) in different ratios in order to simulate different levels of mosaicism (**Table 15**)

Table 14. .Cell lines used for validation of aCGH and NGS platforms for aneuploidy screening

Cell line number	Karyotype	Size of chromosomal breakage
GM00526	47,XY,+13	N/A
GM01359	47,XY,+18	N/A
GM04965	48,XXY,+21	N/A
GM00857	45,XO	N/A
GM03047	46,XY,del(10)(p14p12)	19.22Mb
GM00509	46,XX,del13(pter>q14)	
GM01730	46,XX,der(21)(21qter>21p11::Xq11>Xqter)mat	

Mosaic gains affecting the entirety of chromosomes was examined using trisomy 13 (47,XY,+13 (GM00526)), trisomy 18 (47,XY,+18 (GM01359)) and trisomy 21 (48,XXY,+21 (GM04965)) cell lines. Mosaic whole chromosomal losses were investigated by using a monosomy X cell line (45,XO (GM00857)). Segmental chromosomal losses and gains were examined by using three different cell lines carrying (1) a partial loss of 10p (46,XY,del(10)(p14p12) (GM03047)), (2) a partial loss of 13q (46,XX,del13(pter>q14): (GM00509)), and (3) an unbalanced translocation between chromosomes 21 and X (46,XX,der(21)(21qter>21p11::Xq11>Xqter)mat (GM01730)). Different ratios (**Table 15**) of euploid-aneuploid mixes from individual cell lines were further subjected to WGA and analysed using aCGH and NGS respectively.

Table 15. Mixing experiments for the validation of mosaicism detection via aCGH and NGS. Euploid and aneuploid cells were mixed in different ratios to mimic a range of mosaicism scenarios in trophectoderm biopsies.

Number of euploid cells	Number of aneuploid cells	Level of mosaicism
5	0	0%
4	1	20%
3	2	40%
2	3	60%
1	4	80%
0	5	100%

A survey comprising of 19 questions related to different laboratory practices was prepared and sent to 25 North American and UK IVF clinics. The segmental aneuploidy data of the embryos generated by these clinics was compiled and further analysed in relation to different embryo culture media formulations and conditions. The list of questions sent to the clinics regarding their respective IVF practices are listed in **Table 16**.

4.2.5. Statistical analysis

The statistical tests and modelling were carried out in GraphPad Prism. The tests were either non-parametric, correlation or logistic regression analyses as described in the relevant parts of the chapter. The differences in observations were tested using Fisher's exact test (Chi square test wherever applicable) with a 95% confidence interval. A p-value of less than 0.05 was considered to be statistically significant. The distribution of data was checked by using the D'Agostino and Pearson normality test to determine Gaussian distribution. For correlation analysis, Pearson test was used for data with Gaussian distribution whereas for nonparametric data, Spearman test was used.

Table 16. IVF clinics survey questionnaire. The table lists the questions concerning various culture media conditions and practices in an IVF clinic. This data was further analysed to see if any of these factors contribute towards differences in the aneuploidy rates between IVF clinics.

	IVF survey questions
1	Information about IVF clinic:
2	What media (type and brand) is used for egg collection? (e.g. gamete buffer or fertilisation media)
3	What media (type and brand) is used for egg stripping?
4	What type of incubators are used?
5	What is the gas composition of the incubators?
6	What is the temperature of the incubators for embryo culture?
7	What type of culture media system do you use? (Continuous or Sequential)
8	If continuous media is used, what is the type and brand?
9	If continuous media is used, do you perform a changeover/ replenish the media?
10	What type (brand) of sequential media is used?
11	Has your culture media supplier changed in the last two years?
13	When do you perform the embryo checks?
14	What type and brand of media is used for sperm preparation?
15	What methodology is used for sperm preparation?
16	If swim-up method is used, what brand of media is used?
17	How is sperm stored prior to insemination?
18	If PGS is performed on donor cycles, what is the average dosage of FSH administered to the donors?
19	Additional comments:

4.3. Results

The incidence of segmental aneuploidy was assessed in human embryos at various stages of preimplantation development including fertilised oocytes, cleavage stage and blastocyst stage embryos. A total of 31,466 oocyte and embryo samples were analysed using either of the two widely used comprehensive chromosomal screening methodologies namely, aCGH or NGS. The data obtained was subsequently utilised to carry out a detailed cytogenetic assessment of segmental aneuploidy at different stages of preimplantation development, as well as to evaluate various factors affecting the frequency of such abnormalities.

4.3.1. Validation of CCS methods for detection of whole chromosomal and segmental aneuploidy

In order to imitate the different types of mosaic chromosomal abnormalities occurring in TE biopsies, a total of 85 samples, each consisting of five cell mixes (comprising of aneuploid and euploid cells mixed in different ratios) were analysed (**Table 15**). Both NGS and aCGH platforms were successful in detecting the seven different abnormalities including four whole chromosomal and three segmental aneuploidies in samples containing 100% aneuploid cells (**Figures 18 and 19**). NGS was capable of accurately detecting all the different ratios (20%, 40%, 60% and 80%) of mosaic whole chromosomal and segmental abnormalities in diploid-aneuploid cell mixes. However, aCGH was capable of detecting only high levels of mosaicism ranging from 40% to 80%, depending upon the size of segmental aneuploidies (**Figure 20**).

This series of validation experiments clearly demonstrated that the NGS method (VeriSeq, Illumina) selected for PGT-A was capable of detecting mosaicism levels as low as 20% and had the potential to accurately quantify the proportion of aneuploid cells in a sample equivalent to a TE biopsy (**Figure 20**).

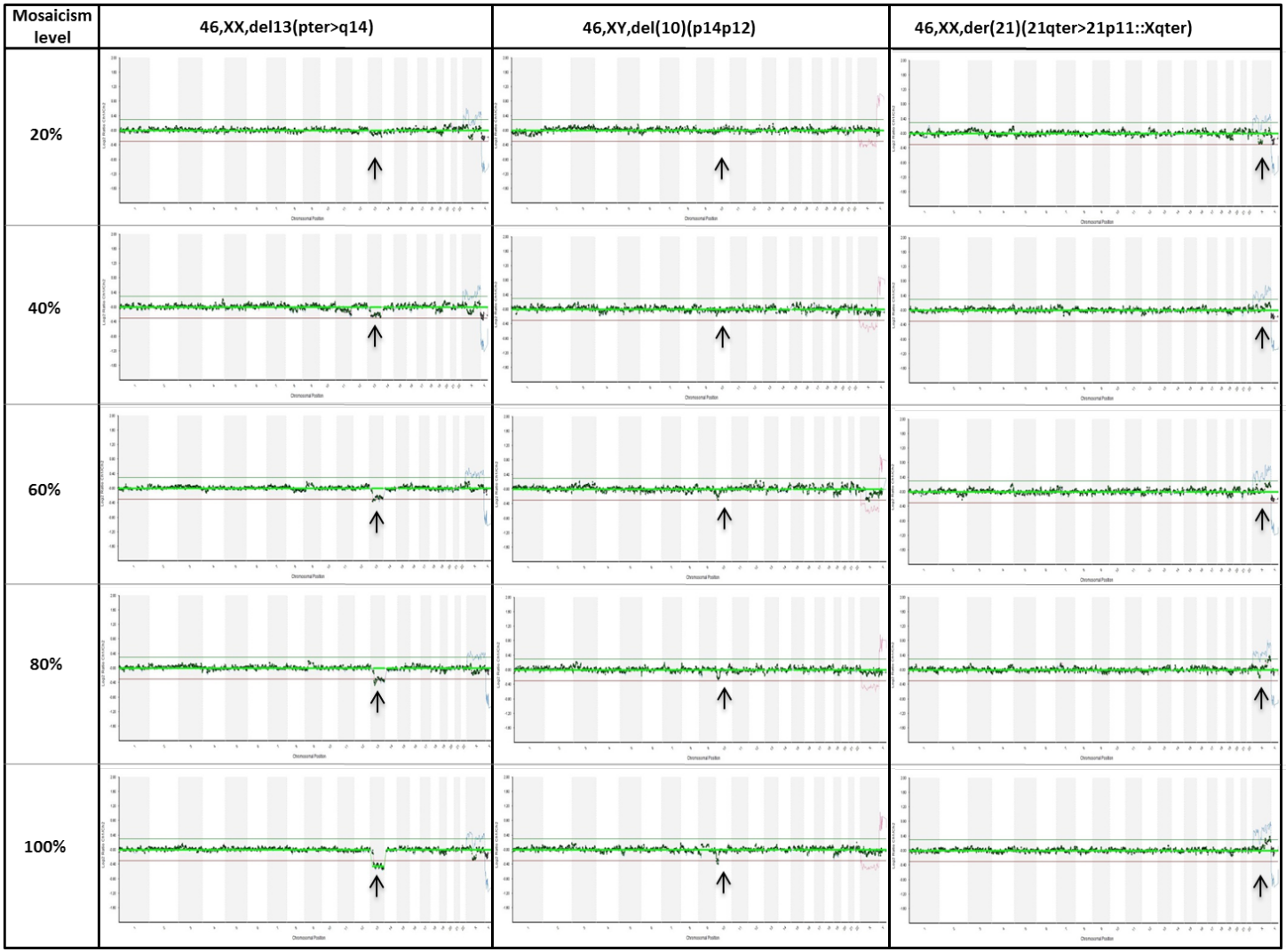


Figure 18. Profiles generated by aCGH for validation of mosaicism detection. The figure shows the profiles generated by aCGH for various levels of mosaicism for three different types of segmental aneuploidies. The position of the segmental aneuploidy for each sample is shown by a black arrow.

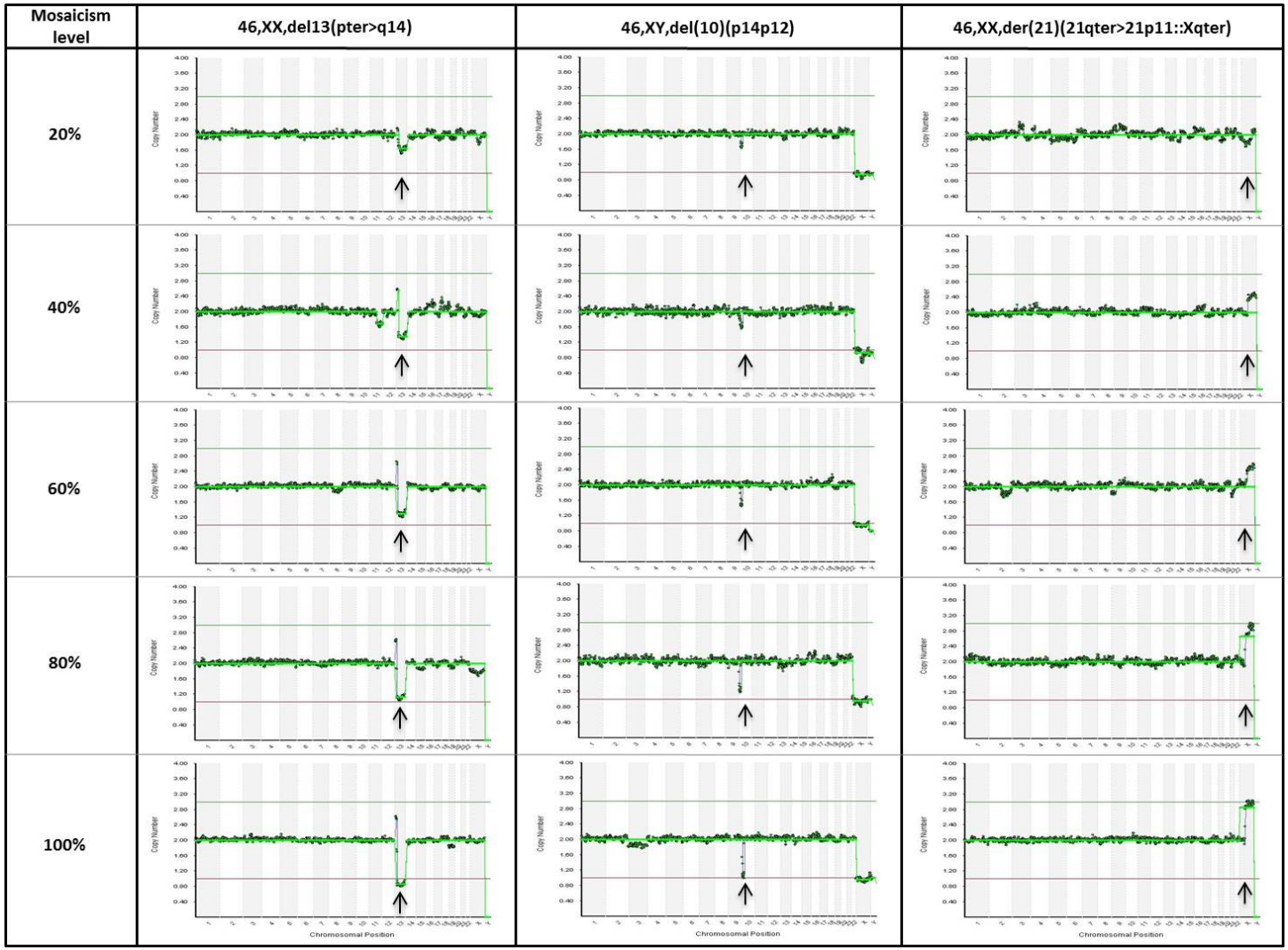


Figure 19. Profiles generated by NGS for validation of mosaicism detection. The figure shows the profiles generated by NGS for various levels of mosaicism for three different types of segmental aneuploidies. The position of the segmental aneuploidy for each sample is shown by a black arrow.

4.3.2. Detailed cytogenetic investigation of segmental aneuploidy using aCGH

Cytogenetic data generated by aCGH was analysed for a total of 3,541 samples comprising of 452 human oocytes, 1,762 cleavage stage and 1,327 blastocyst stage embryos (**Table 16**).

4.3.2.1. Frequency of segmental aneuploidy

A total of 37.5 % (45/120) of patients having their polar bodies analysed had one or more fertilised oocytes affected by segmental aneuploidy, while for the cleavage and blastocyst stages, the percentage of patients having at least one affected sample was 66.5% (167/251) and 29.9% (79/264) respectively (**Table 17**).

Table 16. Patient characteristics

Stage analysis performed	Number of patients	Number of embryos/oocytes	Mean patient age (maternal)	Age range
Oocyte	120	452	40.4	36-46
Cleavage stage	251	1762	38.36	26-47
Blastocyst	264	1327	38.21	28-45

Table 17. Frequency of segmental aneuploidy

Stage analysis performed	Patients with ≥1 affected* embryos/oocytes	Mean age of patients with an affected embryo/oocyte	Age range of patients with an affected embryo/oocyte	Patients without any affected* embryos/oocytes[+]
Oocyte	45 (37.5%)[a,b]	39.41	36-44	75
Cleavage stage	167 (66.5%)[a,c]	39.69	26-46	84
Blastocyst	79 (29.9%)[b,c]	38.40	31-43	185

*Affected by segmental aneuploidy. Statistical comparisons, using Fisher's exact test: (a) p<0.0001; (b) p=not significant; (c) p<0.0001

Table 18. Incidence of segmental aneuploidy in MI and MII stage in oocytes

Stage analysis performed	Number of segmental aneuploidy events
MI (PB 1)	21 (23.33%)[p]
MII (PB 2)	69 (76.66%)[p]

The incidence of segmental aneuploidy differed significantly according to the stage of preimplantation development. A total of 682 samples were found to be affected by segmental aneuploidies. Of all the oocytes analysed, 10.39% (47/452) were observed to carry structural chromosomal errors (**Table 17; Figure 20**). A threefold increase in the incidence of segmental aneuploidies was observed in the second PBs, extruded from oocytes post fertilisation and after completion of meiosis II (MII), as compared to those observed in first PBs after completion of meiosis I (MI) ($P<0.0001$) (**Table 18**). After fertilisation, a significant increase in segmental aneuploidy was observed, affecting 24.29% (428/1762, $p<0.0001$) of cleavage stage embryos. Interestingly, when compared to the cleavage stage, a significant decline in blastocyst stage embryos (15.59%, 207/1327) affected by segmental aneuploidies was observed ($p=0.001$) (**Table 17; Figure 20**). However, the incidence of segmental errors at this stage of development still remained significantly higher when compared to that observed in oocytes ($p=0.0034$).

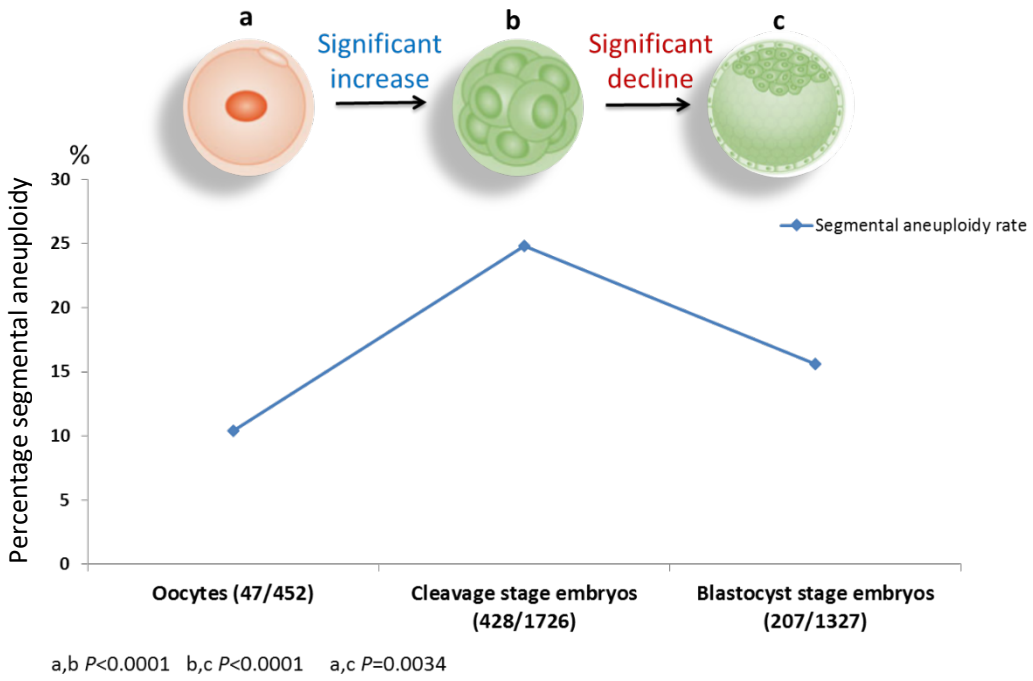


Figure 20. Frequency of segmental aneuploidy at various stages of preimplantation development. There was a significant increase in the incidence of segmental aneuploidy from oocytes to cleavage stage of embryos (P<0.0001) and a significant decline from cleavage to blastocyst stage (P<0.0001). However, no significant difference was observed in the incidence of segmental aneuploidy between oocytes and blastocysts.

Most of the segmental errors scored occurred along with abnormalities affecting whole chromosomes in oocytes (8.4%; 38/452) and embryos (18.4% (352/1762) for cleavage stage embryos; 8.1% (108/1327) for blastocysts). Specifically, 1.99% (9/452) oocytes were affected with only partial chromosome errors, but this rate significantly increased to 5.84% (103/1762; p=0.0013) for cleavage stage embryos. The occurrence of segmental errors being the sole abnormalities at the blastocyst stage was similar to that at cleavage stage (7.46%; 99/1327; p=0.0848) (**Figure 21**). The distribution of segmental aneuploidy affecting all 23 chromosomes was also analysed. This distribution frequency of segmental aneuploidy events across all the chromosomes at various stages of preimplantation development is shown in **Figure 22**.

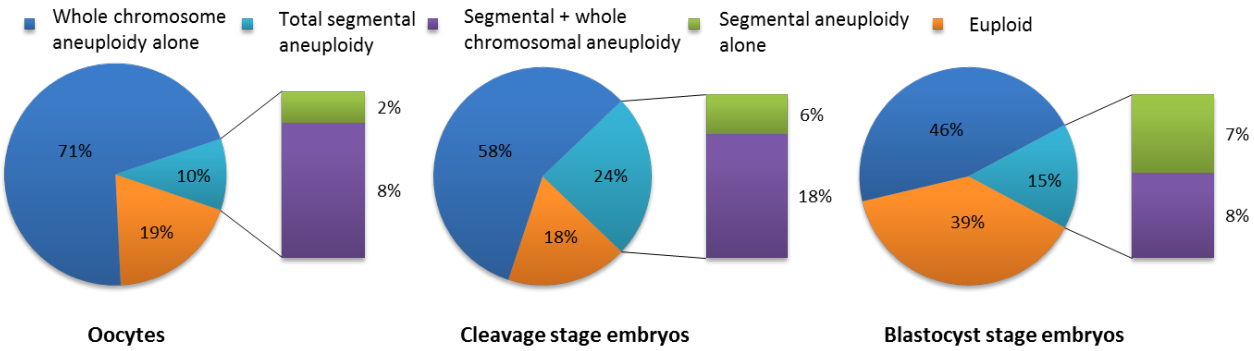


Figure 21. Incidence of segmental aneuploidy at various stages of development. The frequency of segmental aneuploidy increased significantly from oocytes to cleavage stage embryos but decreased from cleavage to blastocyst stage embryos. Most of the segmental imbalances occurred along with other whole chromosomal aneuploidy with 8.4% (38/452) in oocytes, 18.4% (352/1762) in cleavage stage embryos and 8.1% (108/1327) at blastocyst stage. It was rare to see segmental aneuploidies occurring alone in oocytes (9/452; 1.99%) however; its incidence increased significantly in the cleavage (103/1762; 5.85%; p=0013) and blastocyst stage (99/1327; 7.46%; p<0.0001) embryos. No significant difference was observed in the occurrence of segmental aneuploidy alone between cleavage and blastocyst stage embryos

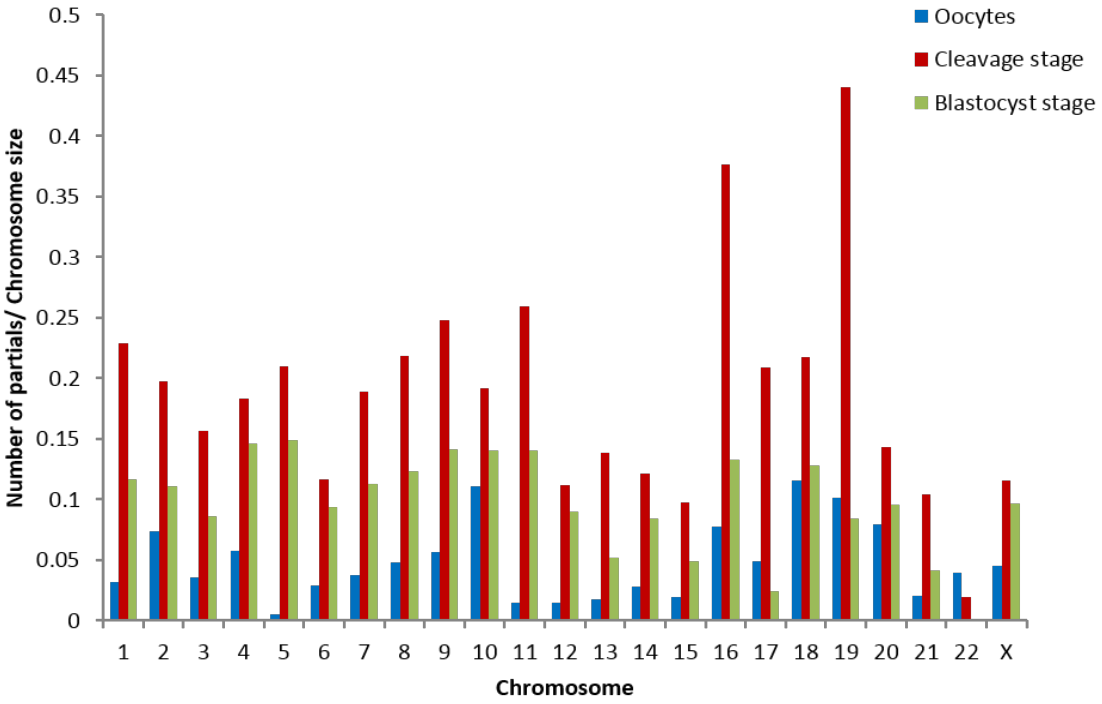


Figure 22. Distribution of number of partial chromosome errors across the genome. Graph depicting the total number of segmental errors per megabase of chromosome length in oocytes (blue), cleavage stage embryos (brown) and blastocyst stage embryos (green) across

4.3.2.2. Maternal age and segmental aneuploidy

The average age of female patients producing one or more oocytes/embryos with a segmental aneuploidy was not significantly different from those who had no affected oocytes/embryos (**Table 17**). To assess the impact of female age on the incidence of aneuploidy, Pearson correlation was applied on whole chromosomal as well as segmental abnormalities data. The data distribution was initially checked by the D'Agostino and Pearson omnibus normality test and was determined to be of Gaussian distribution. A strong correlation was found between advancing maternal age and whole chromosomal aneuploidy across all three stages of preimplantation development ($P<0.05$; **Figure 23**). However, advancing maternal age did not have any significant correlation with the incidence of segmental aneuploidy in oocytes ($P=0.99$), cleavage stage ($P=0.11$) or blastocyst stage embryos ($P=0.92$) (**Figure 23**).

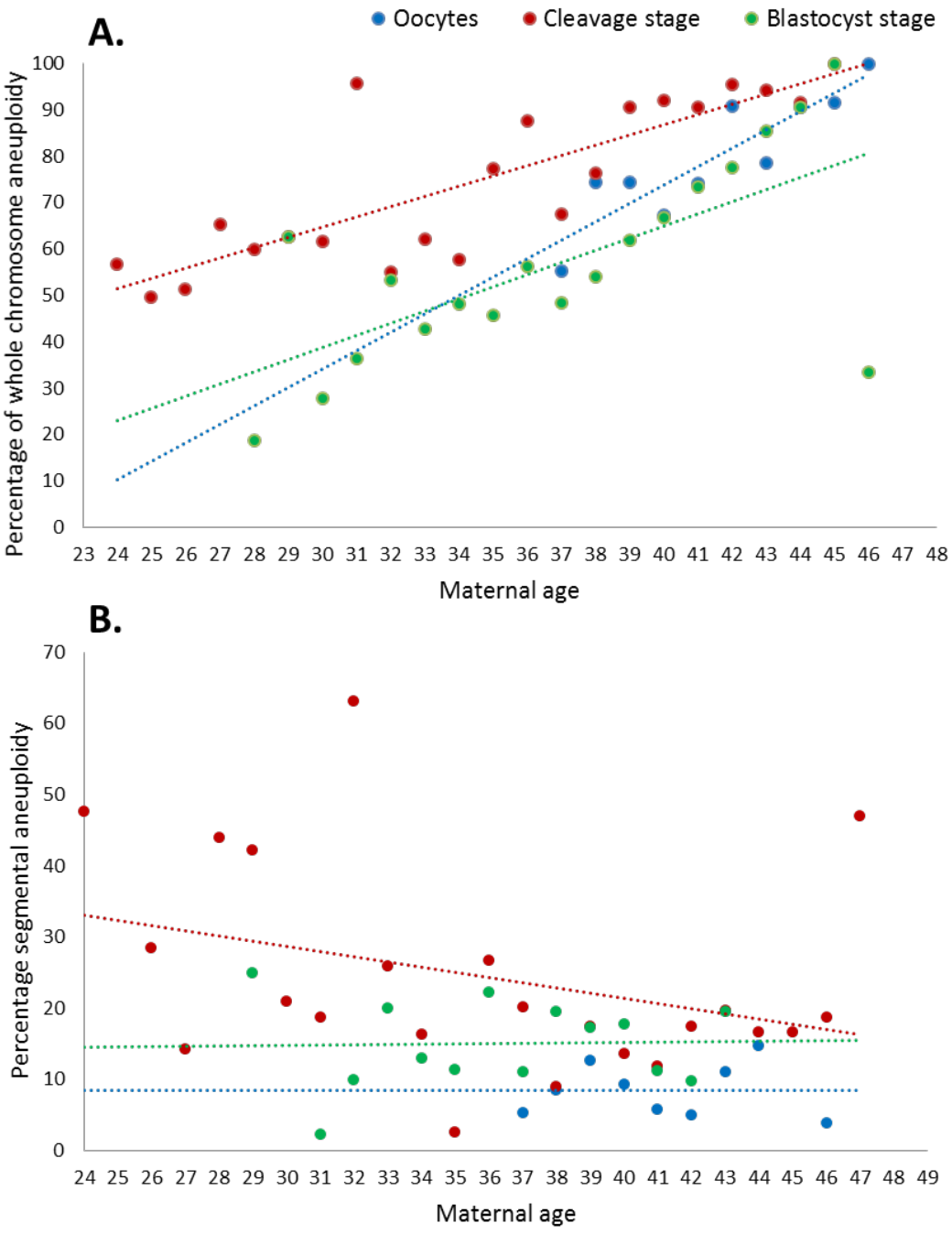


Figure 23. Correlation between aneuploidy and advancing female age. (**A**) A significant correlation (Pearson test) was found between the incidence of whole chromosomal aneuploidy and advancing maternal age at all the three stages of preimplantation development; oocytes (P=0.0005), cleavage stage embryos (P<0.0001) and blastocyst stage embryos (P=0.0013). (**B**) No significant correlation was found between the incidence of segmental aneuploidy and advancing female age at any stages of preimplantation development including oocytes (P=0.9934), cleavage stage embryos (P=0.1105) and blastocysts (P=0.9160).

4.3.2.3. Chromosomal breakage sites

The analysis of the location of chromosomal breaks revealed that ~75% of them occurred at non-centromeric regions while ~25% occurred at or near the centromeres. The distribution pattern of all the chromosomal breakages is in shown in **Figure 24**. Additionally, the location of chromosomal breakages was not entirely random but had a tendency to occur at distinct regions, forming 'hotspots'. Some of the identified hotspots corresponded to known fragile sites in humans (**Figure 24**). Some chromosomes were more susceptible to chromosome breakages compared to others such as chromosomes 16 and 19.

The segmental imbalances were also considered in terms of the site at which chromosome breakage had occurred, and divided into two broad categories: 'distal' (where the break occurred along the chromosome arm, meaning that one of the resulting fragments would not have a centromere), or 'centromeric' (where an entire chromosome arm was involved, giving the possibility that both of the resulting fragments might have a functional centromere). The frequency of centromeric segmental imbalances was essentially the same between the three developmental stages assessed, but this was not the case distal imbalances as described below (**Figure 25**).

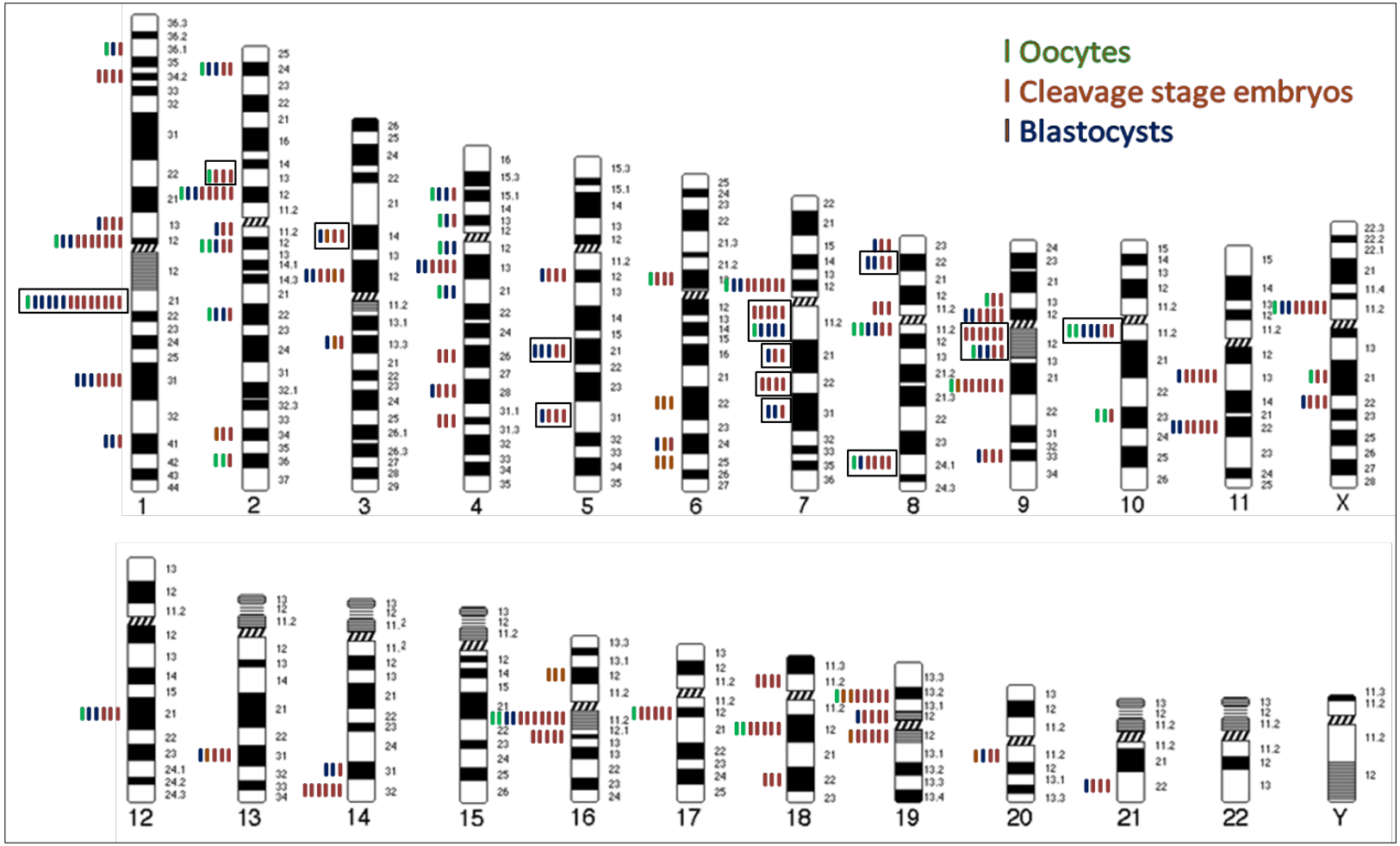
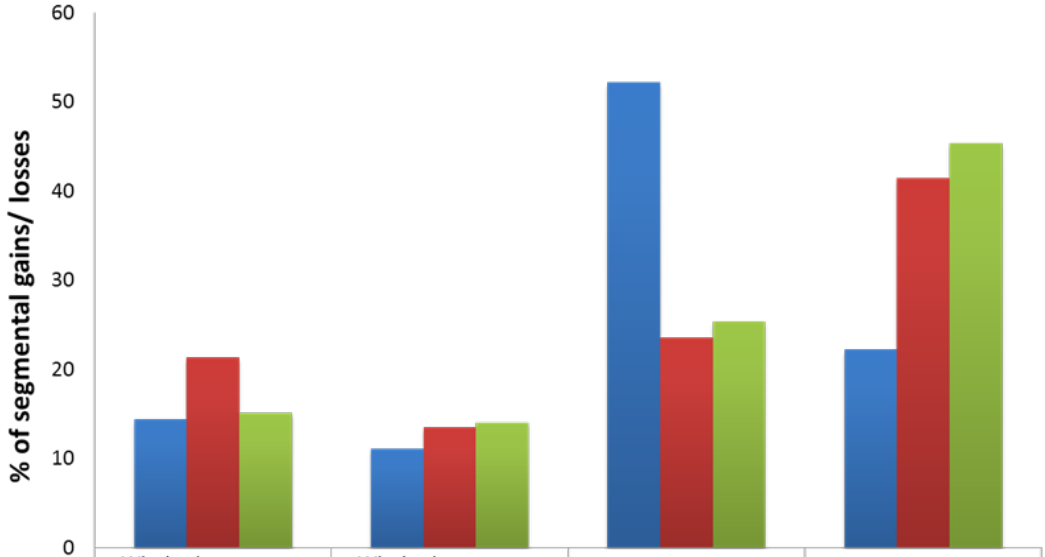


Figure 24. Distribution of chromosomal breakpoints across the human genome. This ideogram shows the locations of chromosomal breakage sites observed in oocytes (green lines), cleavage stage embryos (brown lines) and blastocyst stage embryos (blue lines). Numerous break points formed hotspots at distinct locations on chromosomes. The loci affected by more than 2 segmental aneuploidies are shown on this ideogram. The black rectangular boxes indicate the break points corresponding to known fragile sites in the human genome (Durkin and Glover, 2007).

The segmental aneuploidy was further assessed according to the deletion or duplication of chromosomal material as a result of such abnormalities. The oocytes had approximately 34% more gains of chromosomal material as compared to losses (82/124 vs 42/124). The losses of chromosomal fragments were significantly more frequent in cleavage stage (324/558; p<0.0001) and blastocyst stage embryos (168/275; p<0.0001) as compared to oocytes (42/124) (**Figure 25**). However, there was no significant difference in the relative frequency of segmental losses or gains of chromosomes between cleavage stage and blastocyst stage embryos (p=0.4110), with segmental deletions occurring at a higher rate in both the stages of preimplantation development (**Figure 25**).



	Whole chromosome arm gain	Whole chromosome arm loss	Acentric gain	Acentric loss
Oocytes	14.44	11.11	52.22 (a,b)	22.22 (a,b)
Cleavage stage embryos	21.39	13.53	23.58 (b,c)	41.48 (b,c)
Blastocyst stage ambryos	15.13	14.05	25.4 (a,c)	45.4 (a,c)

(a) $p<0.0001$, (b)$p<0.0001$, (c)$p=1.000$; not significant

Figure 25. Breakage sites leading to segmental gains and losses. The frequency of centromeric segmental gains and losses was similar between oocytes, cleavage and blastocyst stage embryos (p=not significant). However, the oocytes had a higher incidence of acentric gains while the cleavage and blastocyst stage embryos had a significantly higher incidence of acentric losses. Statistical comparison, using Fisher's exact test: (a) p<0.0001, (b) p<0.0001, (c) p=1.000; not significant

The chromosome breakages were further analysed according to the chromosomal sizes. No significant correlation was observed between the chromosomal sizes and breakages per megabase of the chromosomes. However, when the chromosomes with big heterochromatin blocks (chromosomes 1, 9, 16 and 19) were removed, a significant increase in the number of breakages per megabase of chromosomes was observed with increasing chromosomal sizes (P=0.0045; Spearman correlation) (**Figure 26**).

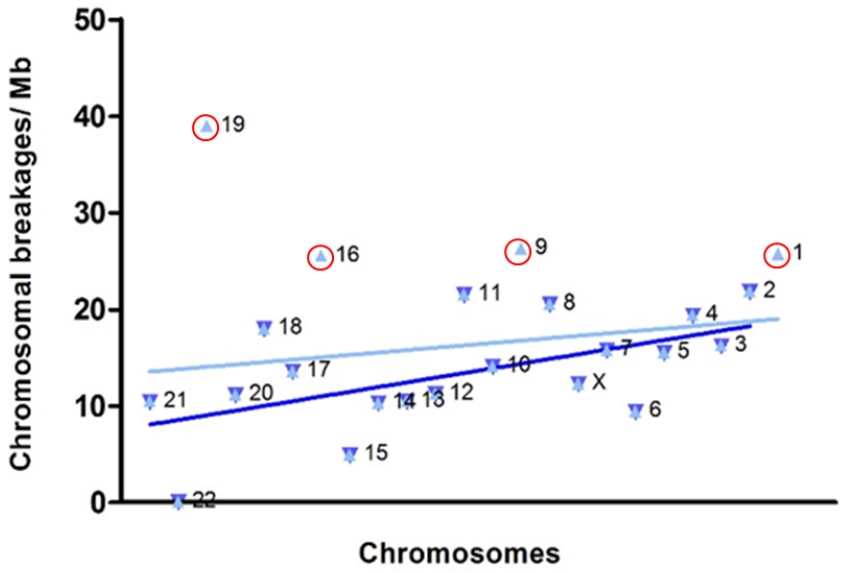


Figure 26. Chromosomal sizes and DNA breakages. No significant correlation was found between the numbers of DNA breakages per megabase of the chromosome with the chromosomal size. However, when the chromosomes with big heterochromatic blocks (1, 9, 16 and 19; circled in red) were removed, a significant increase in number of breakages with chromosomal sizes was observed (P=0.0045; Spearman correlation).

4.3.3. Investigation of the origin of segmental aneuploidy

In order to further investigate the origin of segmental aneuploidy, an additional 1,986 TE biopsies were cytogenetically analysed using NGS. NGS is a much more sensitive method, compared to aCGH. This means that NGS is capable of detecting whole and partial chromosome abnormalities present in all of the biopsied cells in a TE sample, as well as those

that are present in some of the cells of the TE biopsy, indicating that the corresponding embryo might be mosaic.

A total of 70.89 % (246/347) of the patients generating these embryos had one or more blastocysts affected by segmental aneuploidy (**Table 19**). Furthermore, patients referred for PGS for RIF had a significantly higher rate of segmental aneuploidy affecting their blastocysts as compared to those referred for AMA (P<0.0001) and RPL (P=0.0012) (**Table 19** and **Figure 27**). Of 1,986 blastocysts analysed, 22.9% (455/1986) of TE biopsies were chromosomally normal. The overall frequency of segmental aneuploidy was 29.05% (577/1986; **Table 20**) in this cohort of blastocysts. Furthermore, mosaic segmental aneuploidy occurred at a higher frequency as compared to segmental aneuploidy affecting all the cells of a TE biopsy (22.7% v/s 6.35% respectively, P<0.0001) (**Table 20**).

Table 19. Patient characteristics – NGS cohort

Reason for referral	Total number of embryos	Embryos with segmental aneuploidy (rate)	Mosaic segmental aneuploidy (rate)	Segmental aneuploidy affecting all cells (rate)
AMA	830	207 (24.93%)	167 (20.12%)	40 (4.82%)
RPL	403	125 (31.01%)	101 (25.06%)	24 (5.96%)
RIF	753	245 (32.53%)	183 (24.30%)	62 (8.24%)
Total	**1986**	**577 (29.05%)**	**451 (22.71%)**	**126 (6.35%)**

Table 20. Rate of segmental aneuploidy in blastocysts analysed by NGS

Reason for referral	Total patients	Patients with >1 affected embryos/oocytes	Age range	Average age
AMA	160	102	35-47	40.7
RPL	72	46	25-46	38.3
RIF	115	98	24-45	36.4
Total	**347**	**246**	**24-47**	**38.5**

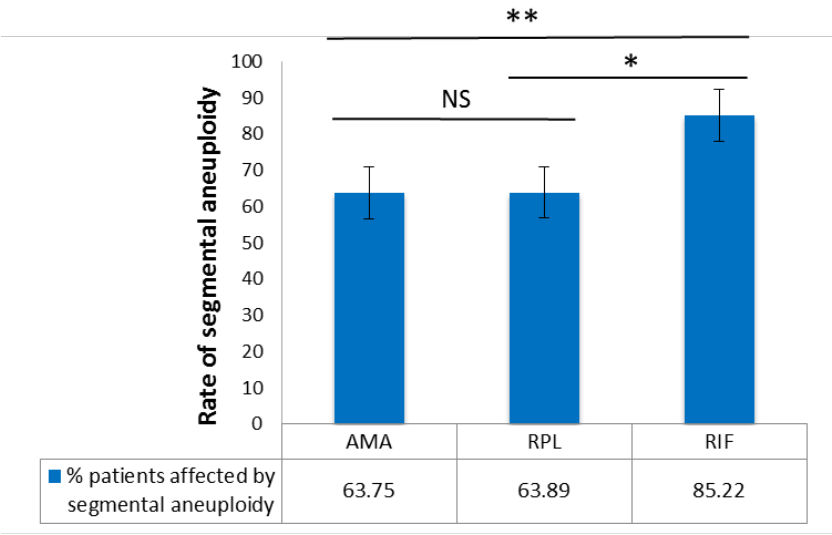


Figure 27. Patients affected by segmental aneuploidy according to reason for referral. A significantly higher proportion of patients referred for RIF generated blastocysts carrying segmental aneuploidy as compared to AMA and RPL patients (**P<0.0001 and RPL *P=0.0012 respectively). However, there was no significant difference between segmental aneuploidy in AMA and RPL patients.

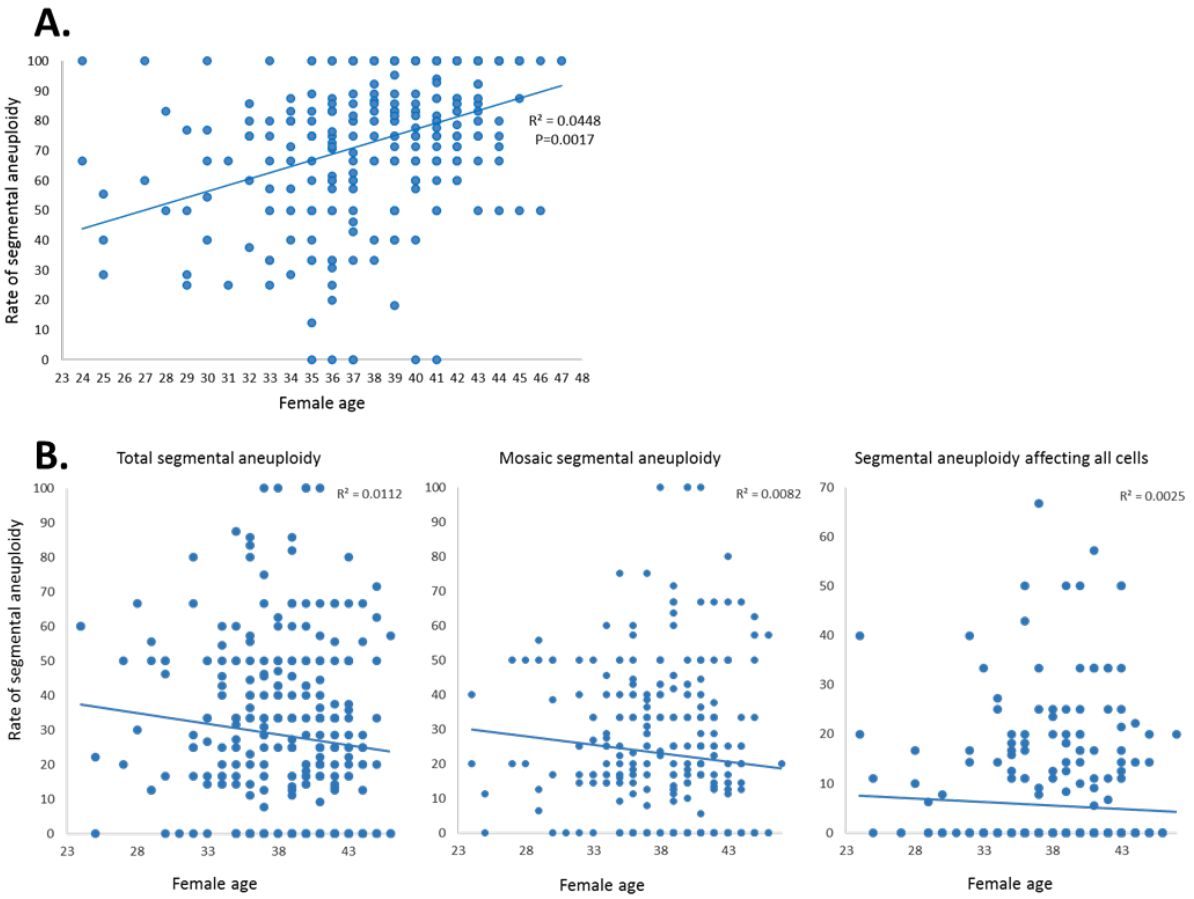


Figure 28. Impact of female age on incidence of segmental aneuploidy. **A.** A significant increase in incidence of whole chromosomal aneuploidy was observed with advancing maternal age (P=0.0017, Spearman correlation). In contrast, **B.** there was no significant correlation observed between advancing maternal age and the incidence of segmental aneuploidy (including mosaic and that affecting all cells).

Upon analysis of female age, no significant difference was observed with the incidence of segmental aneuploidy; including mosaic segmental aneuploidy and that affecting all cells (**Figure 28**). Conversely, the rate of whole chromosomal aneuploidy significantly increased with female age (P=0.0017, Spearman correlation) (**Figure 28**).

Of note, the patients referred for RIF, generated a significantly higher proportion of embryos with segmental aneuploidy affecting all the cells as compared to those referred for AMA (8.2% v/s 4.8%; P=0.0074). The rate of mosaic segmental aneuploidy in embryos of RIF patients was also slightly higher than those generated by patients referred for AMA (24.3% v/s 20.1%; P=0.045). However, there was no significant difference in the frequency of segmental aneuploidy between embryos generated by RIF and RPL patients (**Figure 29**).

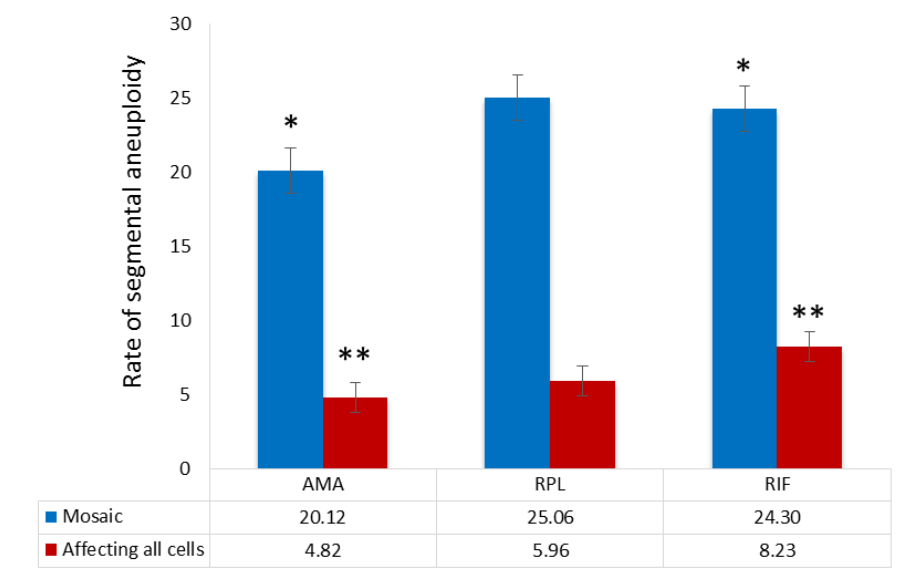


Figure 29. Segmental aneuploidy rates in blastocysts of AMA, RPL and RIF patients. Embryos generated by RIF patients had a significantly higher incidence of segmental aneuploidy affecting all call as compared to those generated by AMA patients (P=0.0074). However, there was no significant difference in rates of segmental aneuploidy between RIF and RPL patients.

* and ** denote statistical significance; P<0.05

4.3.4. Investigation of clinical factors affecting rate of segmental aneuploidy

In order to investigate various IVF related factors affecting the incidence of segmental aneuploidy, an additional 25,939 embryos derived from a total of 25 different IVF clinics were analysed. For this this part of the study, 8,249 cleavage stage embryos and 17,690 blastocyst stage embryos were examined. The cleavage stage embryos were processed using aCGH whereas the blastocyst stage embryos were analysed using NGS (enabling the identification of mosaicism) for their respective chromosomal copy number. Several clinical factors related to IVF such as culture medium type, gas composition of the incubators and incubation temperatures were investigated to identify any possible correlations with the rate of segmental aneuploidy.

4.3.4.1. Rates of segmental aneuploidies across different IVF clinics

The effect of culture media conditions on the rate of segmental aneuploidy in embryos was assessed for 8,249 cleavage stage embryos derived from 18 different IVF clinics (**Table 21**) and 17,690 blastocysts derived from 22 IVF clinics (**Table 22**).

The rate of segmental aneuploidy amongst these clinics significantly varied from 3.3% to 9.3% for cleavage stage embryos **(Figure 30**) and from 8% to 11.5% for the blastocysts (**Figure 31**). Interesting, in blastocysts the rate of mosaic (mitotic) segmental aneuploidy varied significantly amongst the clinics ranging from 3.6% to 13.8% whereas the rate of segmental aneuploidy affecting all the biopsied cells (pure segmental aneuploidy, likely of meiotic origin) did not vary significantly between the different IVF clinics (1%-4.7%) (**Figure 31**).

Table 21. Rate of segmental aneuploidy in blastomeres from 20 different IVF clinics

IVF Clinic	Total number of embryos	Embryos with segmental aneuploidy	Rate of segmental aneuploidy
1	181	6	3.31%
2	157	7	4.46%
3	84	4	4.76%
4	84	4	4.76%
6	263	14	5.32%
7	123	7	5.69%
8	1219	73	5.99%
9	250	15	6.00%
10	919	56	6.09%
11	2866	177	6.18%
12	461	32	6.94%
13	280	20	7.14%
14	406	33	8.13%
15	107	9	8.41%
17	104	9	8.65%
18	126	11	8.73%
19	428	40	9.35%
20	191	18	9.42%
	Total: 8249	**Total: 535**	**Average: 6.49%**

Table 22. Rate of segmental aneuploidy in blastocysts from 23 different IVF clinics

IVF clinic	Total embryos	Segmental chromosome errors present in all of the TE cells (pure)	Rate of pure segmental aneuploidy	Segmental chromosome errors present in part of the TE cells (mosaic)	Rate of mosaic segmental aneuploidy
1	110	3	2.73	4	3.64
2	124	5	4.03	5	4.03
3	299	8	2.68	17	5.69
4	288	8	2.78	17	5.90
5	188	4	2.13	13	6.91
6	544	16	2.94	37	6.80
7	83	1	1.20	7	8.43
8	460	14	3.04	31	6.74
9	1178	56	4.75	65	5.52
10	5453	164	3.01	426	7.81
11	164	4	2.44	13	7.93
12	151	4	2.65	12	7.95
13	2759	76	2.75	226	8.19
14	2186	104	4.76	143	6.54
15	681	21	3.08	57	8.37
16	210	7	3.33	21	10.00
17	502	19	3.78	48	9.56
18	502	19	3.78	48	9.56
19	389	8	2.06	52	13.37
20	101	1	0.99	14	13.86
21	390	13	3.33	46	11.79
22	390	13	3.33	46	11.79
23	538	21	3.90	60	11.15
	Total: 17690	**Total: 589**	**Average: 3.33**	**Total: 1408**	**Average: 7.96**

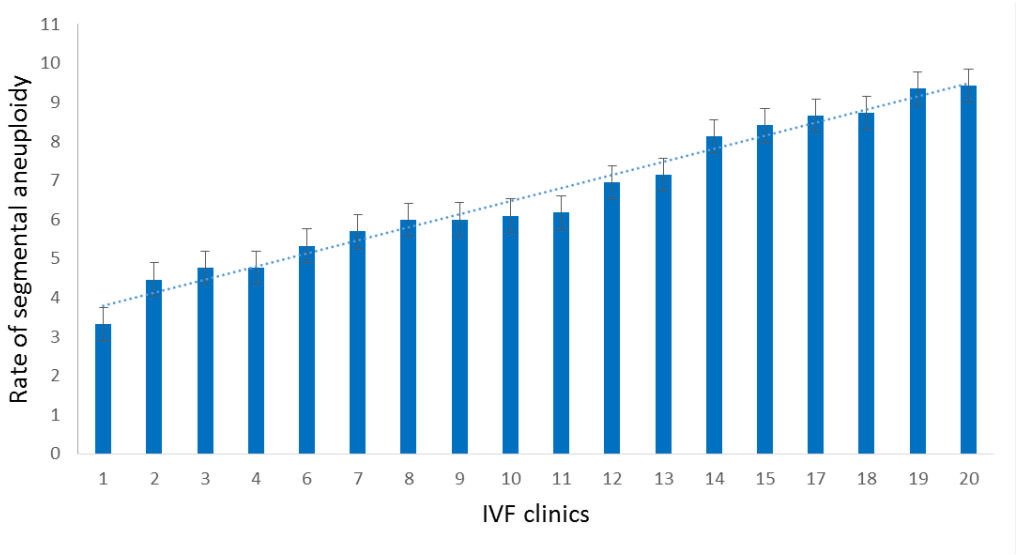


Figure 30. Rates of segmental aneuploidy in cleavage stage embryos from 18 different IVF clinics. The graph depicts the range of percentage of segmental aneuploidies in blastomeres from across 20 different IVF clinics. The trend line depicts the significant variation in frequency of segmental aneuploidy between the first and last IVF clinics.

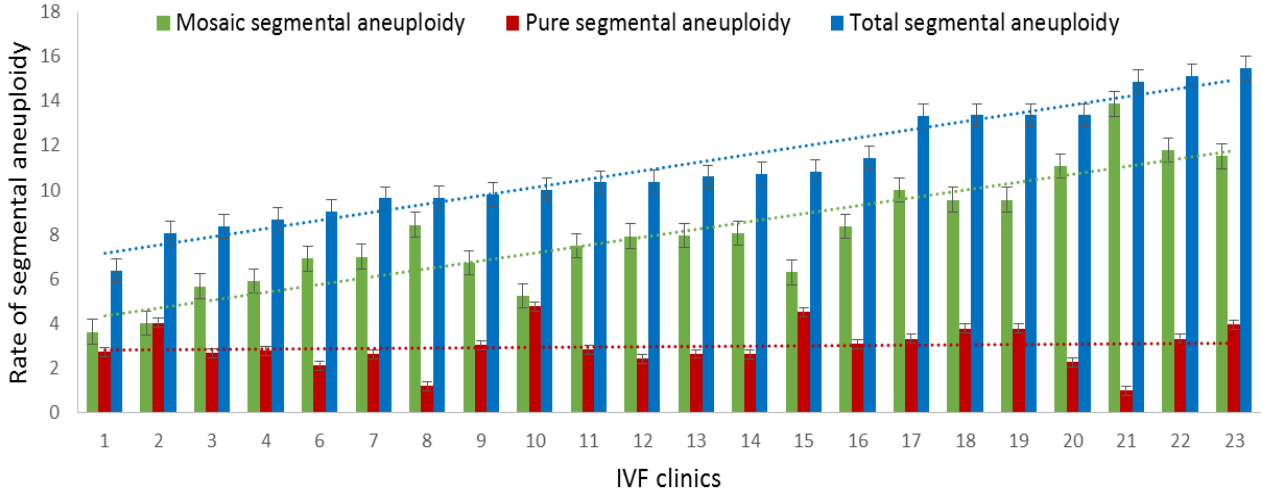


Figure 31. Rates of segmental aneuploidy in blastocysts from 22 different IVF clinics. The graph depicts the range of segmental aneuploidies in trophectoderm biopsies from across 22 different IVF clinics. The green trend line depicts the significant variation in frequency of mosaic segmental aneuploidy between the IVF clinics. However, no significant difference was found between the segmental aneuploidies present in all TE cells across different IVF clinics (brown trend line).

4.3.4.2. Culture media conditions and rate of segmental aneuploidy

Culture media conditions among different clinics were investigated, in an attempt to determine if they had any influence on the incidence of partial chromosome abnormalities seen in embryos generated in these clinics. Of the 25 clinics included in the study, 19 clinics were using continuous media and 6 clinics used sequential media system for embryo culture.

For cleavage stage embryo biopsies subjected to aCGH for comprehensive chromosomal screening, no significant difference in the rate of segmental aneuploidy was observed between clinics using continuous and sequential culture media systems (P=0.1509) (**Figure 32**) (**Appendix A**). For the blastocysts screened with NGS, analysis of mosaic partial errors and those affecting all cells in the TE biopsy was possible. There was a significantly higher rate of mosaic segmental aneuploidy amongst various clinics as compared to pure segmental aneuploidy (P<0.0001, Mann Whitney test; **Figure 33**) Moreover for blastocysts, the rate of pure segmental aneuploidy did not differ significantly between clinics using continuous (range: 0.99% to 4%) and sequential (range: 2.72% to 4.75%) culture media systems (P=0.1596) (**Appendix A**). However, the rate of mosaic segmental aneuploidy was found to be significantly higher in the clinics using continuous culture media as compared to those using sequential media (P=0.036, Mann Whitney test; **Figure 34**). Furthermore, the gas composition and temperature of the incubators across different clinics and their possible correlation with the rate of segmental aneuploidy was assessed using Student's t-test. The percentage of carbon dioxide utilised in incubators ranged from 6% to 7% and that of oxygen was either 5% or 6% amongst various clinics (**Appendix A**). The incubation temperature used by the clinics ranged between 36.4°C to 37 °C (**Appendix A**).

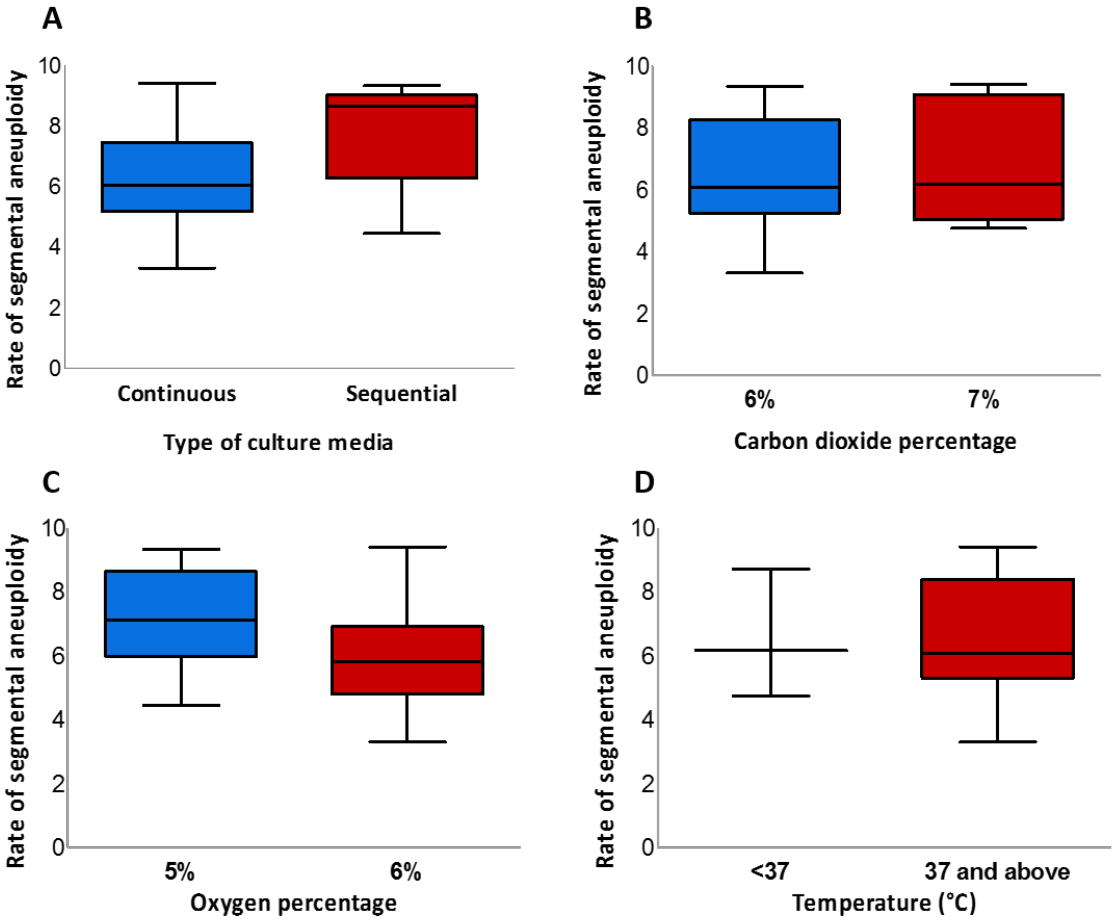


Figure 32. Effect of culture media conditions on rate of segmental aneuploidy (cleavage stage embryos). No significant difference in segmental aneuploidy rates amongst IVF clinics was observed with different culture media systems (**A**), CO_2 and oxygen percentage in the incubator (**B** and **C**) or temperature (**D**). (Mann Whitney test used for statistical comparisons)

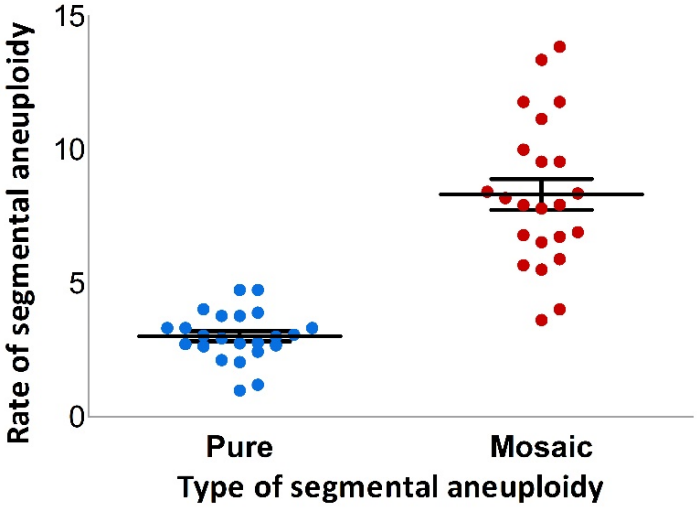


Figure 33. Rates of pure and mosaic segmental aneuploidy in blastocysts. The mosaic segmental aneuploidy occurred at a significantly higher frequency as compared to the pure segmental aneuploidies in blastocysts from all the 23 clinics (P<0.0001, Mann Whitney test). Moreover, there was a large variation in the mosaic segmental aneuploidy rates (SD=2.63) amongst different clinics as compared to the pure segmental aneuploidy (SD=0.92)

For cleavage stage embryos, no significant difference was observed in the rate of segmental aneuploidy amongst clinics using different percentages of oxygen (P=0.25) and carbon dioxide (P=0.73) as well as different temperatures (P=0.95) in the incubators (**Figure 32**). However, for blastocysts a significant increase in the rate of mosaic segmental aneuploidy was observed in clinics using 7% CO_2 as compared to those using incubators with 6% CO_2 (P=0.036) (Figure 24). However, no such difference was observed between mosaic segmental aneuploidy rates and different temperatures (P=0.67) and oxygen percentage (P=0.67) between clinics (**Figure 34**) (**Appendix**).

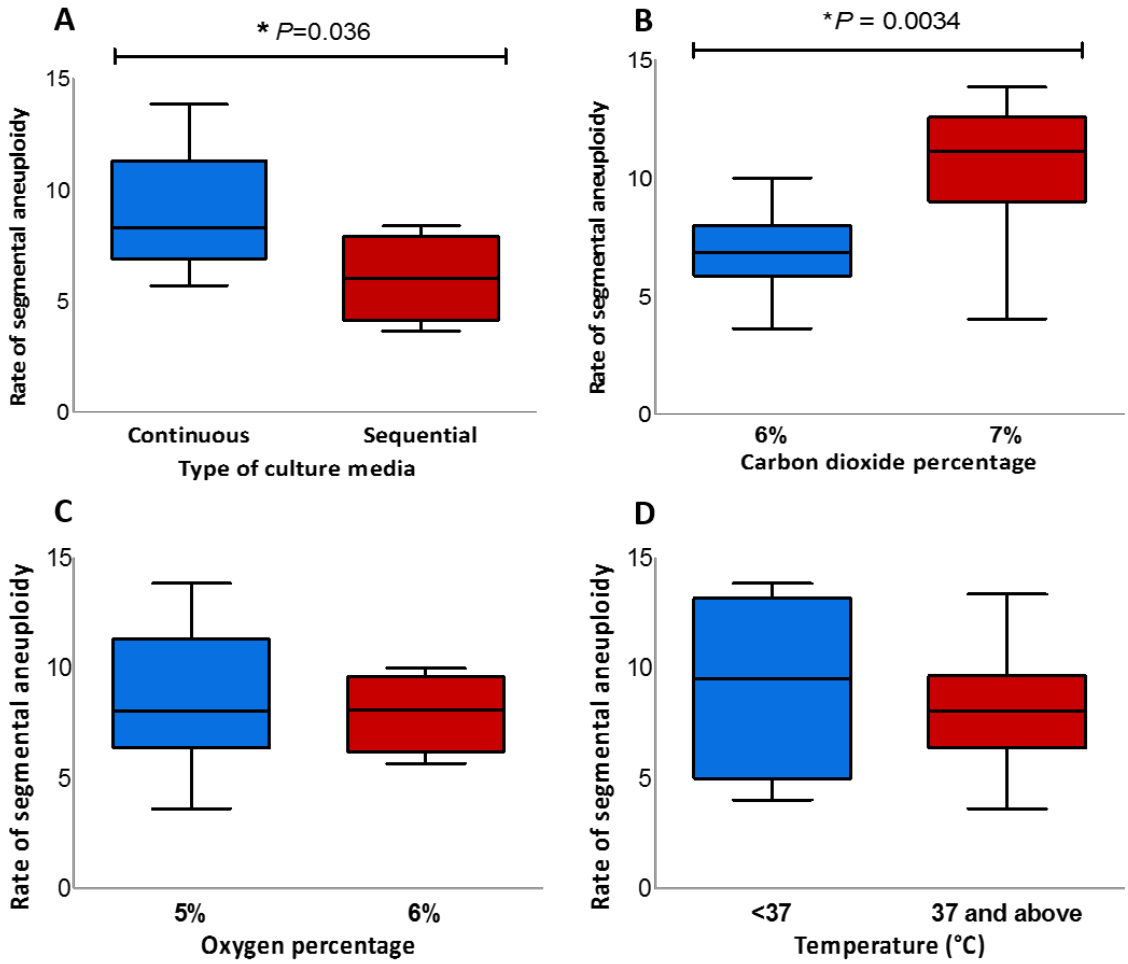


Figure 34. Effect of culture media conditions on rate of segmental aneuploidy (blastocyst stage embryos). Clinics utilising continuously media generated embryos with slightly elevated rates of mosaic segmental aneuploidy as compared to those using sequential media systems (P=0.036; t test). Also, clinics using higher percentage of CO_2 (7%) tend to generate embryos with more segmental aneuploidy (P=0.0034). However, no such difference was observed for oxygen percentage or temperature differences amongst clinics.

4.4 DISCUSSION

DNA double stranded breaks can be induced by various endogenous and exogenous factors such as certain mutagens, oxidative stress and stalling of replication forks during S-phase of the cell cycle. If unrepaired, double stranded DNA breaks will typically culminate in segmental aneuploidy (Khanna and Jackson, 2001; Mehta and Haber, 2014). The stalling of a replication fork may occur either due to DNA damage, lack of sufficient materials for DNA replication, or due to challenges posed to a progressing replication fork by the encounter of DNA secondary structures. In the case of replication stalled replication forks, failure to reinitiate DNA synthesis may lead to a double stranded DNA break at the site of the collapsed replication fork. Moreover, programmed DNA strand breaks that are an essential element of meiotic recombination, occurring during gametogenesis, may also lead to chromosomal breakage if not resolved properly (Richardson & Pandita, 2004). In virtually all cell types (certain tumour cells are a notable exception), the problems that predispose the cell to DNA double stranded breaks induce cell cycle check points, which may in turn pause the cell cycle while an attempt is made to initiate DNA repair pathways (reviewed by Elledge & Zhou, 2000). If the problem cannot be corrected, cell cycle arrest is maintained and apoptotic pathways are activated, eliminating the affected cell (Aguilera and García-Muse, 2013).

4.4.1. Frequency of segmental aneuploidy in human oocytes and preimplantation embryos

The present study investigated the incidence of segmental aneuploidy in a large cohort of human oocytes and embryos at different stages of preimplantation development. The results demonstrate that segmental aneuploidies are common in these early stages of human development and pose important questions regarding the mechanisms of their origin, subsequent fate and clinical impact. Unlike whole chromosomal aneuploidy, which has a

strong correlation with advancing female age, segmental aneuploidy was found to have no correlation with maternal age. Hence, the molecular processes leading to segmental aneuploidy are likely to be distinct from those causing whole chromosomal gains or losses.

Approximately 10% of fertilised oocytes were affected by segmental aneuploidy following both the meiotic divisions. The follicles from which the oocytes are retrieved may differ in size, levels of damaging oxygen radicals and blood supply, affecting the competency of their respective oocytes (Agarwal et al.s, 2005; Tatone et al., 2008). Additionally, disruption of the blood supply to follicles has been shown to impact replication fork progression in certain cell types, which may subsequently lead to chromosomal breakages (Hammond, et al., 2002).

Interestingly, a threefold increase in segmental aneuploidies was observed in the second meiotic division (MII) as compared to the first one (MI) in oocytes. This may be in part due to the pieces of fragmented chromosomes, arising in MI, being tethered to sister chromatids and only becoming apparent as segmental aneuploidy at anaphase of MII after separation of the chromatids and extrusion of second polar body. However, it is also possible that this observation reflects a genuine increase in the frequency of unrepaired double stranded DNA breaks during MII. In the context of IVF, the second meiotic division is completed *in vitro* thus opening up the possibility of an influence of suboptimal culture systems on chromosome integrity. Additionally, a majority of segmental aneuploidies observed in oocytes involved gains of chromosome fragments (losses in the corresponding polar bodies). This is most likely due to the asymmetric cell divisions occurring during meiosis wherein oocyte retains a majority of the cytoplasm compared to polar bodies leading to

fragments of chromosomes without centromeres to have a tendency to remain within the oocytes during cell division.

The incidence of segmental aneuploidies was found to be at its peak during cleavage stage of preimplantation development which is reminiscent of studies looking at losses or gains of whole chromosomes. These have shown that chromosomal malsegregations occur frequently during the first few mitotic divisions, leading to mosaicism in early embryo (Harper et al., 1995; Fragouli et al., 2006). The genomic stability of a cell depends upon active gene expression. However, the embryonic genome in humans becomes active only at the 4-8 cells stage (Braude et al.,1988). The dependency of the early embryo on an ever-diminishing maternal pool of mRNAs, proteins and other resources may also contribute towards the replicative stress leading to chromosomal breaks during the first few mitotic divisions post-fertilisation. Moreover, the lack of dynamic gene expression most likely reduces the capacity of cells to adjust to stressful environment and induce the control of cell cycle checkpoints. The relatively higher rate of chromosomal errors occurring during the first few mitotic divisions suggest that checkpoints, that usually serve to monitor factors such as DNA damage and chromosome alignment on the spindle, may be relaxed or absent. While the additional chromosomal breakages observed in cleavage stage embryos may have arisen spontaneously at that stage of development, another possibility is that they were introduced by the sperm at the time of fertilisation. Certain studies have demonstrated that sperm samples with high level of DNA damage are associated with poorer IVF outcome suggesting the persistence of DNA damage after fertilization resulting in embryo arrest (Spano et al., 2000).

The rate of segmental aneuploidy was observed to decline significantly from cleavage to blastocyst stage of development. Moreover, studying the ratio of percentage of embryos

with only whole chromosomal aneuploidies to percentage of euploid embryos, we observed 2.7 times decline from cleavage stage to blastocyst stage (58:18 versus 46:39). However, embryos with segmental abnormality in addition to whole chromosomal aneuploidy seem to be even more compromised. Relative to euploid embryos, they decline five-fold from the cleavage to blastocyst stage (18:18 versus 8:39). Embryos carrying only segmental chromosomal abnormalities declined by a factor of 1.9 from cleavage to blastocyst stage (6:18 versus 7:39). This suggests that a combination of whole chromosomal and segmental aneuploidy is most lethal for embryo development followed by occurrence of whole chromosomal aneuploidy alone and lastly the presence of isolated segmental abnormality. All of these forms of abnormality display reduced survival from the cleavage to the blastocyst stage in comparison to euploid embryos. The decline in whole chromosomal and segmental aneuploidy during the transition to the blastocyst stage is suggestive of selection against affected cells and/or embryos. This observation was concordant with previous findings showing that fewer chromosomal abnormalities arise after the first couple of mitotic divisions (Fragouli et al., 2014). It is possible that embryos/cells with chromosomal abnormality undergo arrest. Alternatively, affected cells may be eliminated through the initiation of apoptotic pathways.

Upon analysis of the chromosomal breakpoints that resulted in the segmental imbalances, it was observed that these did not appear to be random but rather concentrated at various loci on different chromosomes. Similar to this finding, *de novo* chromosome rearrangements in prenatal samples have been seen to be associated with chromosomal fragile sites (Giardino *et al.*, 2009). Fragile sites are chromosomal regions susceptible to DNA breakage and are mainly associated with the regions of DNA which pose a difficulty during DNA replication most likely due to the presence of DNA secondary structures (Hewett *et al.*,

1998). The partial inhibition of replication at fragile sites may lead to double stranded breaks in the DNA resulting in loss of chromosomal fragments and/or subsequent chromosomal rearrangements. To date, over a 100 different fragile sites have been identified, distributed across the human genome (Durkin and Glover, 2007). Some of the identified hotspots of chromosomal breakpoints in this study lie in the vicinity of such fragile sites, indicating a potential relationship between the two (**Figure 24**). The additional recurrent breakage sites identified in the oocytes and embryos may correspond to novel fragile sites specific to gametogenesis and embryogenesis.

Of note, the heterochromatic blocks on chromosomes 1, 9 and 16 were associated with high number of chromosomal breakages. These chromosomes have the largest regions of constitutive heterochromatin, comprising highly repetitive DNA sequences, which may hinder the replication fork progression, thereby causing it to stall, collapse, and produce DNA breaks (Saksouk et al., 2015). Chromosome 19 was also affected by a disproportionately high number of segmental abnormalities given its relatively small size. This chromosome has the highest GC content amongst all the chromosomes, which may also lead to challenges for DNA replication.

It is not certain whether the segmental aneuploidies investigated in the present study are representative of what might be observed following natural conception, or whether they are in some way associated with the underlying infertility of the patient or the treatments they received (e.g. ovarian stimulation and embryo culture). It is known that *de novo* chromosomal rearrangements, similar to those described here, occur in natural pregnancies at a low frequency as shown by a study based on amniocentesis (Warburton, 1991). However, unbalanced chromosome rearrangements are frequently lethal and many embryos carrying

such errors are likely to be lost early during development, before prenatal testing is undertaken. The data from the current study may be the closest we can come to an estimate of the true rate of segmental aneuploidy around the time of conception, before any selection against abnormalities has occurred.

Based upon the size of the chromosomal fragments involved, we estimate that at least 80% of those seen in oocytes would be incompatible with a viable pregnancy and would either fail to implant of miscarry. This means only ~2% of all oocytes are likely to be affected by a breakage that would be detected during gestation or at birth, although it is possible that this figure may be higher if smaller chromosomal fragments, below the threshold of detection of the array-CGH technology used in this research, also experience loss/duplication in oocytes.

It is important to define the true rate of segmental chromosome imbalances in oocytes and embryos, since a high frequency would be expected to have a negative impact on IVF success rates and lead to miscarriages and congenital abnormalities. A study by Vanneste and colleagues reported that 70% of cleavage stage embryos (day-3/-4 post fertilisation) contained at least one cell with a segmental abnormality, but provided no data concerning the incidence in oocytes or at later preimplantation stages (e.g. blastocyst). Additionally the number of embryos tested was small and all of the data was derived from a single clinic (Vanneste et al., 2009). The results of the current study suggest that the incidence of chromosome breakage at the cleavage stage is actually considerably lower than 70%, which is more in keeping with other investigations using a range of cytogenetic techniques (Voullaire *et al.*, 2000). A limitation of the present investigation is that it did not involve analysis of every cell from the embryos tested. However, extrapolating from the data, it can be estimated that the maximum proportion of human cleavage stage embryos containing segmental imbalance

in at least one of their cells is unlikely to exceed 40%. This assumes that embryos contain 6-8 cells, which is typical for this stage of development, and that each cell is independent in terms of chromosome imbalance occurring. In reality, this likely overestimates the frequency, as some embryos have the same segmental error in every cell due to a meiotic error, while in others the same abnormality, or reciprocal losses/gains, are shared by several cells, resulting from an error in the early mitotic divisions.

It could be concluded from the data analyzed that while segmental imbalances are common in oocytes, they occur at a much higher frequency in preimplantation embryos. There is a high risk of chromosomal breakage during the first few mitotic divisions with terminal regions being affected more frequently. It is probable that this reflects the natural situation although an underlying susceptibility might be exacerbated by the application of assisted reproductive techniques. During the subsequent cell divisions, acentric fragments of chromosomes tend to be lost. As embryonic development progresses from the cleavage to the blastocyst stage, the rate of segmental aneuploidy decreases. Hence, it is highly likely that there is a selection against abnormal embryos or, in the case of mosaicism, against the unbalanced cells they contain. Selection mechanisms could involve apoptosis, which might eventually lead to the demise of the embryo or normalization of the karyotype by elimination of abnormal subpopulations of cells. Importantly, despite the high frequency of segmental aneuploidies in embryos generated using IVF technology, there is no evidence for an increased rate of such abnormalities in children born following fertility treatments (Bonduelle et al., 1995; Wang, & Jin, 2013).

4.4.2. Origin of segmental aneuploidy in preimplantation embryos

To gain further insight into the origin and nature of segmental aneuploidies, detailed cytogenetic evaluation of TE biopsies from approximately 2000 embryos was performed using NGS. The ability of NGS to distinguish between aneuploidies affecting all cells of a TE biopsy and those affecting only a fraction of the biopsied sample (mosaic) can aid in differentiating between aneuploidies of mitotic and possibly meiotic in origin. The mosaic aneuploidies are most likely to have arisen during mitotic divisions, leading to cytogenetically distinct cell lines in the same embryo, whereas those present in all cells are likely to be meiotic in origin, thereby propagating with each cell division and affecting all resultant daughter cells.

A significantly higher proportion of patients were found to be affected by segmental aneuploidy in the cohort of blastocysts analysed by NGS as compared to those analysed by aCGH (29.9% vs 70.89%; $P<0.0001$). Moreover, the overall frequency of segmental aneuploidy was also significantly higher in blastocysts analysed by NGS as compared to those analysed by aCGH (15.59% vs 29.05%). This was in part due to the higher resolution of NGS, which aids in detection of mosaic segmental aneuploidies as compared to aCGH. NGS is currently the most sensitive method for detection of mosaicism in embryo biopsy specimens (Treff & Zimmerman, 2017). The superior capability of NGS for the detection of mosaic segmental aneuploidy was also reflected by the results of validation experiments wherein aCGH was only capable of detecting segmental abnormality when at least 60% of cells were affected, whereas NGS was able to pick up mosaicism at the lowest levels attempted (20% of cells affected) (**Figures 18** and **99**). Therefore, aCGH underestimates the overall frequency of segmental aneuploidy, a majority of which is mosaic in origin (McCoy, 2017).

The NGS results showed that a majority of segmental aneuploidies were mosaic (mitotic in origin), arising post fertilisation, while the others appeared to be present in all the biopsied cells (likely meiotic in origin, derived from one of the gametes) (**Figure 33**). This was reminiscent of the findings of a study, which interrogated the origin of segmental aneuploidies using single nucleotide polymorphisms microarrays (SNP), which included over 300,000 SNPs across the human genome (Konstantinidis et al., 2016). By examining the same SNPs in DNA samples of the parents, it was revealed that a majority of the meiotic segmental aneuploidies were paternal in origin. The analysis showed that unlike meiotic aneuploidies affecting whole chromosomes, more than 95% of which were maternal in origin, a majority of meiotic segmental aneuploidies (~65%), were of paternal in origin. The DNA delivered by the sperm may be fragmented and this finding may be relevant to that possibility. The same study demonstrated that segmental errors of mitotic origin were approximately 2.5 times more common than meiotic segmental aneuploidy. This agrees with the findings of the current research and other published work, in which testing of multiple cells from the same embryos has demonstrated that most segmental abnormalities are mosaic, making it highly likely that they arise during post-zygotic cell divisions.

One of the potential causes of meiotic segmental aneuploidies is functional impairment of DNA repair pathways during early embryonic development. Collaborative work undertaken by our research group has provided direct experimental evidence that human zygotes and cleavage stage embryos have compromised DNA repair processes (Fogarty *et al.*, 2017). In that study, double stranded DNA breaks were induced in human zygotes by using a CRISPR/Cas9-genome editing method. In most cell types, including human embryonic stem cell lines, this process induces a double-strand break in the DNA which then undergoes repair, reconnecting the DNA strands. However, upon inducing such breaks in human zygotes it was

observed that approximately half of the resulting embryos (9/19) displayed a segmental aneuploidy extending from the site of the induced DNA break (p arm of chromosome 6) to the end of the chromosome (Fogarty *et al.*, 2017). This provides the first conclusive proof that human cleavage stage embryos have a deficiency in the repair of double-strand DNA damage and fail to eliminate affected cells during the cleavage stage, as a consequence, may develop segmental aneuploidy. Careful morphokinetic evaluation of embryos using time-lapse microscopy indicated a slowing of the cell cycle in CRISPR/Cas9 treated embryos relative to controls. This is consistent with checkpoint activation and suggests that checkpoint mechanisms are operational at the cleavage stage but are unable to adequately maintain cell cycle arrest and that apoptotic pathways are not triggered as would usually be the case.

It has been well established that the first few mitotic divisions post-fertilisation are subject to high rates of chromosome malsegregation, leading to chromosomal mosaicism (Munné et al., 1994; Bielanska et al., 2002; van Echten-Arends et al., 2011; Fragouli et al., 2013b). As a result, approximately 30% of human blastocysts are mosaic, comprising of two or more cytogenetically distinct cell lines (Fragouli et al., 2017). It is clear from the current work that the period of genetic instability prior to genome activation has much broader and far reaching consequences than has been previously appreciated, impacting not only appropriate division of chromosomes but also the capacity to repair other forms of DNA damage.

Interestingly, the rate of meiotic segmental aneuploidy was significantly higher in the patients referred for RIF as compared to those referred for AMA and RPL (**Figure 27**). Repeated implantation failure (RIF) is defined as the failure of implantation of transferred embryos after 2 IVF cycles. Successful implantation is a complex process with two critical

players; the mother's uterus and the embryo. Problems with the maternal environment, such as abnormal uterine anatomy, non-receptive endometrium and certain immunological conditions of the mother can negatively affect the embryo-uterine cross talk leading to implantation failure (Achache and Revel, 2006). Alternatively, the endometrial-embryo communication can be hampered if the embryo is of compromised quality as a result of abnormalities derived from maternal or paternal gametes or arising during preimplantation development.

Meiotic segmental aneuploidy, present in all the cells of an embryo, may hamper its implantation potential and may lead to early miscarriages. As the segmental aneuploidy involves a gain or loss of only a fragment of the chromosome, the embryo might retain sufficient competence to be able to avoid developmental arrest at early stages of preimplantation development, a common observation for embryos consisting of whole chromosomal aneuploidy. However, segmental abnormalities might not be able to propagate at advanced stages of embryonic or fetal development and potentially lead to implantation failure or clinical pregnancy losses. Studies on early miscarriages have shown that segmental aneuploidies occur frequently in products of conception ranging in frequency from 3% to 6% (Goddijn and Leschot, 2000; van den Berg et al., 2012; Shen et al., 2016). This is comparable to the frequency of meiotic segmental aneuploidy observed in the embryos from the RPL patient cohort in the current study (5.9%; **Figure 29**). In the embryos generated by RIF patients, meiotic segmental aneuploidies were observed to occur at a still higher frequency of 8.3%, significantly elevated with respect to patients having PGT-A for reasons of advanced reproductive age (**Figure 29**). This high incidence of meiotic segmental aneuploidy might potentially compromise the implantation potential of embryos, leading to repeated implantation failure.

4.4.3. Factors affecting frequency of segmental aneuploidy

The observed disproportionate numbers of chromosomal breaks at fragile sites, inducible in other cell types by growing them in suboptimal environment, suggests that currently embryo culture methods may provide inadequate support for key cellular pathways such as those involved in DNA synthesis and replication. As the culture techniques vary between different IVF clinics, it raises the question whether segmental aneuploidies are affected by culture media. In order to assess this possibility, data from a total of 8,249 cleavage stage embryos and 17,690 blastocysts derived from 25 different IVF clinics were analysed. A detailed survey concerning embryological practices was created and provided to over 25 IVF clinics. This survey aimed to gather information on key elements of IVF methodology including type of incubator, concentration of gases, types of culture media and frequency of embryo observation (which involves removal from the carefully controlled and optimised environment of the incubator). For the aforementioned analysis, embryos were analysed at cleavage stage and blastocyst stage of development. The cleavage stage embryos were analysed using aCGH while the blastocyst stage embryos were analysed using NGS. Hence, it was possible to determine the mosaicism levels of the TE biopsies from blastocyst stage embryos. As at the cleavage stage only a single blastomere is biopsied, it was not possible to determine mosaicism level at this stage.

One of the major factors implicated in the incidence of whole chromosomal aneuploidy is advancing maternal age. However, the female age was found to be independent of the occurrence of total segmental aneuploidy including both, meiotic and mitotic in origin (**Figure 28**). This difference can be attributed to separate mechanisms being responsible for producing these two classes of abnormality. Segmental aneuploidy arises due to a double stranded break in the DNA and a failure to correct this by DNA repair mechanisms, leading to

their propagation in subsequent cell divisions. In contrast, whole chromosomal aneuploidy mainly arises due to malsegregation of chromosomes (e.g. non-disjunction, anaphase lag, premature separation of sister chromatids), strongly correlated with advancing maternal age (Kuliev & Verlinsky, 2004; Nagaoka et al., 2012).

Of all the IVF culture related factors analysed, none were clearly demonstrated to affect the incidence of segmental aneuploidies in cleavage stage embryos across different IVF clinics. However, for blastocyst stage embryos, the culture media system and CO_2 concentration appear to be associated with an altered rate of mosaic segmental aneuploidy. As only single cell is analysed from cleavage stage embryos during PGT-A, it is not possible to detect the level of mosaicism in these embryos.

Maintenance of a proper pH in culture media is essential for optimal embryo development. The optimal pH for different media may vary but it usually ranges from 7.2-7.4 (Swain, 2010). The pH of the medium is maintained by the CO_2 concentration in the incubation chamber as well as by the concentration of bicarbonate in the media. The significant increase in the incidence of mosaic segmental aneuploidy observed in this study was seen in relation to higher concentrations (7%) of CO_2 (P=0.0034; **Figure 34**). As raising CO_2 lowers media pH, while lowering CO_2 raises the pH, it is possible that lower pH induces some form of cellular stress in the embryo.

The IVF clinics use either of the two types of culture media systems; continuous or sequential, for culturing the developing embryo *in vitro*. The differences in composition of the oviductal and uterine secretions, as well as changes to the embryo metabolism during the first few days of development, led to the development of sequential media for optimal growth of the embryo till blastocyst stage. Our study showed that for blastocysts, sequential media

strategies where one formulation is used through fertilisation to the cleavage stage and a second is introduced from Day-3 until the blastocyst stage, were associated with small but significantly lower frequencies of segmental aneuploidy than continuous culture strategies ($P<0.036$) (**Figure 34**). However, a majority of clinics used continuous media for the culture of blastocysts as compared to sequential media. Six clinics used sequential media, supplied by four different manufacturers, with an average of 6.01% of blastocysts showing evidence of a mitosis-derived segmental abnormality (range 3.6%-8.3%). Nineteen clinics used continuous media, obtained from four suppliers, and the average mitotic segmental aneuploidy rate was 9.08% (range 5.69%-13.86%). It may be possible that it is not continuous media *per se* that increases the risk of segmental aneuploidy, rather a single commercially available formulation may be responsible for much of the observed increase relative to sequential media. Given the small number of clinics in the sequential media cohort, it is important to interpret these results with caution.

It is noteworthy that examination of rates of non-mosaic segmental aneuploidy can serve as a valuable internal control in these analyses. As non-mosaic abnormalities are presumed to arise prior to embryo culture (in gametes), they should remain constant regardless of the culture conditions employed. Indeed, the frequency of non-mosaic segmental abnormalities were found to be similar across all 23 clinics surveyed (**Figure 33**). However, the incidence of mosaic segmental abnormalities, caused by errors occurring after fertilisation, differed significantly ($P<0.001$), affecting 3.6% to 13.8% of embryos depending on the clinic. Having established that patient factors (including female age and reason for referral) do not influence the incidence of mitotic segmental aneuploidies (mosaic), this further indicates that external culture environment might be responsible for the variations in the incidence of segmental aneuploidy of mitotic origin. As described above, culture system

and CO_2 concentration were associated with altered rates of mosaic segmental aneuploidy, but they had no impact on non-mosaic abnormalities.

The analyses undertaken during the course of this study provides evidence that certain aspects of embryo culture conditions are important for the maintenance of genetic stability, with inevitable consequences for embryo viability. Exposure of an embryo to one suboptimal component of a culture system may predispose it to becoming more vulnerable to a second stressor, as has been well documented for atmospheric oxygen and individual culture, as well as for oxygen and ammonium (reveiwed by Wale & Gardner, 2016). Although far from straight forward, analysing the interactions that exist between the human embryo and its environment, in carefully controlled experiments, will facilitate the creation of more effective and safer treatments for an infertile couple.

4.4.4. Summary

In summary, the results obtained in this study showcase the incidence of segmental aneuploidy in greater detail than had been previously possible, shedding light on their origin and ultimate fate. Unlike whole chromosomal aneuploidy, segmental aneuploidy does not have any link to maternal age. Patients with recurrent implantation failure were associated with occurrence of higher rates of meiotic segmental aneuploidy in their embryos, suggesting that impaired DNA repair mechanism(s) or stressors responsible for induction of DNA strand breaks (e.g. oxidative stress) might be a part of their pathology. This may aid in enhanced patient management, providing opportunities for early identification or diagnosis of patients likely to experience RIF and perhaps the possibility of treating them through the use of dietary supplements that could support DNA repair pathways.

The study furthermore confirms that segmental aneuploidy mainly arises during the first few mitotic divisions following fertilisation. Moreover, a deficiency of DNA double-stranded break repair, uniquely affecting early embryos prior to their genome activation, renders the human cleavage stage embryo particularly susceptible to DNA damage. This is the most likely explanation for the high frequency of *de novo* segmental aneuploidy observed at cleavage stage of embryonic development. Segmental aneuploidies are less common in blastocyst stage embryos, presumably due to elimination of cells/embryos carrying such abnormalities. Importantly, the data obtained during the present study indicated that certain IVF related factors, especially culture media and CO_2 may influence the rate of segmental aneuploidy, suggesting that there might be a potential of minimising the DNA double stranded breaks resulting in segmental aneuploidies *in vitro* by using optimised culture conditions.

Hence, the study successfully determined the frequency of segmental aneuploidy at various stages of preimplantation development, characterised the origin and cytogenetic locations of such breakages and explored the factors affecting the frequency of their occurrence.

Chapter 5: Exploring blastocoel fluid and spent culture media as non-invasive sources of embryonic DNA

This chapter focused on developing non-invasive methods to explore embryonic DNA present in blastocoel fluid and spent culture media samples derived from blastocyst stage embryos. Briefly, amplification methodologies capable of amplifying minute quantities of fragmented DNA were developed and validated on blastocoel fluid and spent media samples. The subsequent WGA products were subjected to low pass next generation sequencing for chromosomal copy number analysis and the results were compared and corroborated with their corresponding TE biopsy.

5.1. Introduction

The live birth rate following IVF and ICSI remains fairly low despite continuous advancements in the field of ART. The latest report from Society for Assisted Reproductive Technologies (SART) shows that live birth rate in women after ART procedures was 29.2% (SART report, 2014). To maximise the chances of pregnancies, often multiple embryos are transferred but this increases the risk of multiple gestation and associated complications (Ledger et al., 2005). Hence, it is crucial to develop methods which facilitate the identification of embryos with the greatest likelihood of producing a healthy pregnancy.

Several methods for embryo selection have been proposed which include both invasive and non-invasive techniques. Invasive methods entail performing an embryo biopsy for the purpose of chromosomal (or other genetic) testing. Currently, only invasive methods are used for routine 'screening' of embryos for their chromosomal constituents (Brezina and Kutteh, 2015). These procedures are expensive and require skilled personnel and specialist equipment in order to carry them out. Also, there are concerns about the potential for iatrogenic damage to the embryo during biopsy procedure (Joris et al., 1999). Consequently, more infertility practitioners are considering non-invasive ways of embryo selection.

Proposed non-invasive methods for embryo selection include 1) embryo morphology 2) morpho-kinetics of embryo growth observed by time-lapse photography, 3) oxygen consumption of developing embryo, 4) various biochemical markers (metabolites, proteins, etc.) in the embryo culture medium and 5) oxidative stress subjected to the embryo (reviewed by Rodgaard et al., 2015; Sallam et al., 2016). The final aim of non-invasive analysis is to find biomarkers for embryo viability without subjecting it to an intrusive biopsy procedure. However, each of the above mentioned non-invasive strategies has its limitations, hampering their introduction into routine clinical practice.

More recently, for the purpose of non-invasive screening of the embryos, spent culture medium (in which the embryo develops) as well as blastocoel fluid (found in the cavity of blastocyst stage embryos) have been explored as potential sources of embryonic biomarkers, especially genetic material.

5.1.1. Spent culture media

Spent culture media has been extensively explored for the presence of biomarkers of embryo viability. The constituents of interest in the culture medium can be categorised as a) genetic material (genomics), b) proteins translated from mRNA (proteomics), c) end products of cellular processes (metabolomics) and d) small non-coding RNA which play a role in gene regulation (reviwed by Rodgaard et al., 2015) (**Figure 35**). The analysis of these molecules has proved to be difficult in part due to their limited quantities present in the culture media which pose subsequent technical challenges to downstream processing and analysis.

Stigliani et al. first reported the presence of mitochondrial and nuclear DNA in culture media and found a correlation between quantity of DNA and embryo quality (Stigliani et al., 2013, 2014). Thereafter, several studies have reported results on chromosomal copy number analysis or genetic diagnosis from embryonic DNA derived from spent media using WGA followed by either aCGH or NGS (Xu et al., 2016; Feichtinger et al., 2017; Hammond et al., 2017; Rodgaard et al., 2015). This is analogous to non-invasive prenatal testing (NIPT) from maternal blood and if successful, non-invasive preimplantation testing (NI-PGT) of embryos would potentially eliminate the need for micromanipulation.

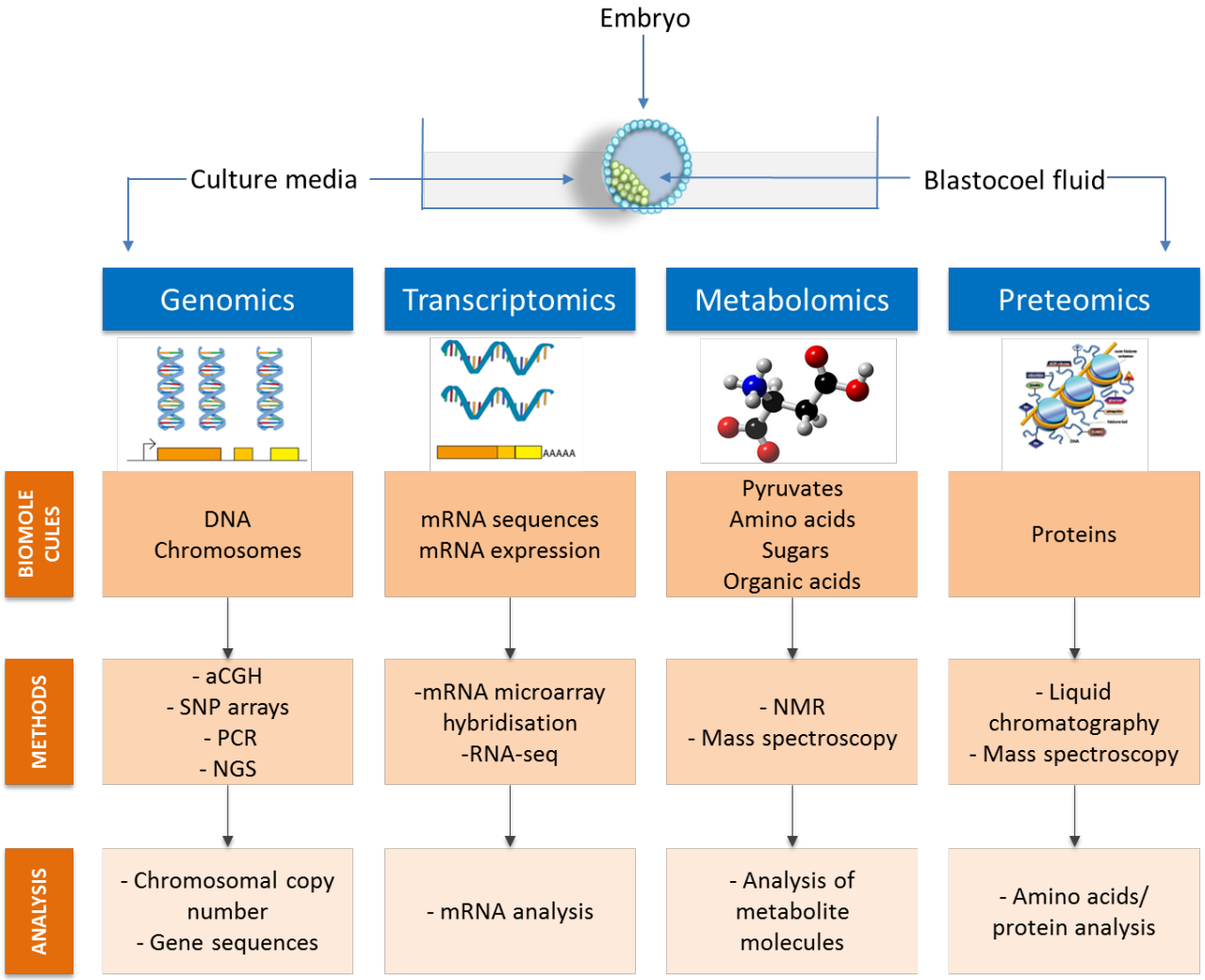


Figure 35. Non-invasive methods for determination of embryo viability. The diagram broadly shows four major areas of non-invasive methodologies; Genomics, Transcriptomics, Metabolomics and Proteomics, along with the biomolecules assessed in each discipline as well as their corresponding assessment methods and analysis outputs.

5.1.2. Blastocoel fluid

The process of compaction in a normally developing human embryo begins at the 8-cell stage and results in formation of tight junctions between the cells of the embryo (Iwata et al., 2014). After compaction, the cells start differentiating into ICM and TE lineages and migrate to their distinct locations, forming a cavity within the embryo. The TE cells start expressing a variety of transport molecules, including sodium pumps which leads to accumulation of fluid known as blastocoel fluid (BF) inside this cavity (Barcroft et al., 2003). The transit of molecules to and fro from BF is highly regulated and it is a source of embryonic proteins and extruded DNA (Watson et al., 2004). Moreover, the blastocoel cavity is separated from the outer environment by a monolayer of TE cells which are linked together by tight junctions thus preventing any contaminants from culture media entering into the BF. Hence, blastocoel fluid can potentially serve as a sterile source of embryonic proteins and DNA.

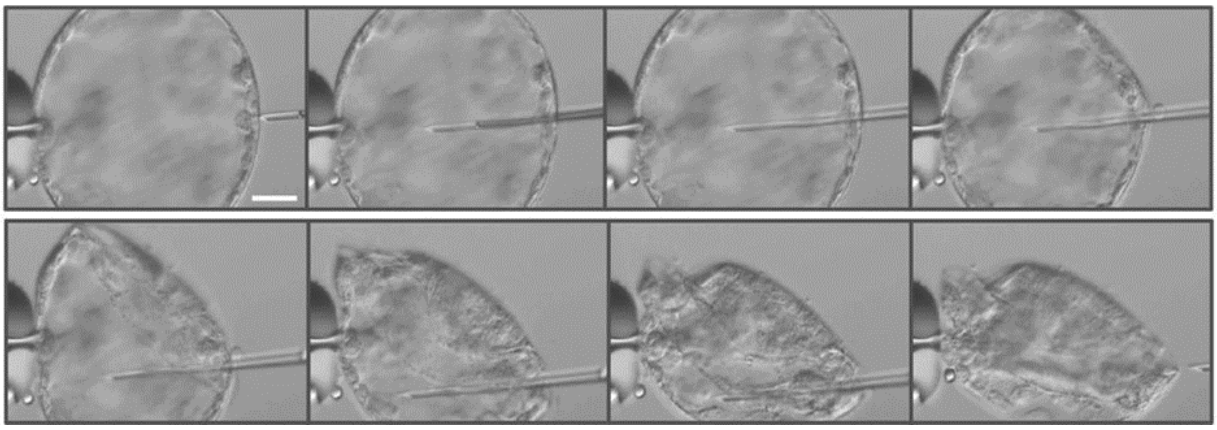


Figure 36. Blastocentesis. The diagram shows various steps of blastocentesis wherein ~5nl of blastocoel fluid from the embryonic cavity of a blastocyst is being aspirated using a micropipette while the blastocyst is being held in place by a vacuum pressure through another micropipette. Image source: Poli et al., 2015.

Jensen and colleagues first showed the presence of proteins in human BF, thus paving way for exploring it for biomarkers of embryo viability (Jensen et al., 2012). The extraction of

BF from embryonic cavity is performed by a procedure known as blastocentesis (Luna et al., 2013; Poli et al., 2013). During blastocentesis, approximately 5nl of BF is aspirated from a fully expanded blastocyst at Day 5 or Day 6 post fertilisation using a micropipette as shown in **Figure 36**.

A recent study characterised and quantified proteins present in individual BF samples by a targeted proteomics approach (Poli et al., 2015). The study established a preliminary correlation between *GAPDH* gene expression and H2A proteins present in BF with chromosomal ploidy of corresponding embryos. However, the detection of proteins from BF is technically challenging using mass spectroscopy due to the limited quantities of proteins present in such samples (Jensen *et al.*, 2014). Hesnce, it is challenging to implement such an assay clinically for routine embryo viability assessment and further studies need to be performed to determine the efficacy of proteome analysis in blastocoel fluid.

Blastocoel fluid has also been explored as a source of embryonic DNA for non-invasive PGT-A (NI PGT-A). The presence of DNA was first shown in blastocoel fluid by Palini and colleagues in 2013 (Palini et al., 2013). Since then, numerous groups have explored blastocoel fluid as a source of embryonic DNA for the purpose of non-invasive PGT-A and PGD (Assou et al., 2014; Gianaroli et al., 2014; Jensen et al., 2012; Luna et al., 2013; Poli et al., 2013). However, most of these studies have reported low chromosomal copy number concordance rates between the embryonic DNA present in the blastocoel fluid and the corresponding TE biopsy

5.1.3. Study aims

The main aim of this part of the project was to develop sensitive molecular methodologies for exploring blastocoel fluid and spent culture media for any extruded embryonic genomic DNA. Development of amplification strategies during the course of this project was based on the hypothesis that DNA in blastocoel fluid and spent culture media is likely to be fragmented in nature and present in minute quantities (similar to cell free DNA in blood plasma).

More specifically, the project aimed to:

1) Develop a Y-chromosome assay for non-invasive genetics approaches

2) Develop molecular methodologies for capture and amplification of minute amounts of fragmented genomic DNA. The following three amplification strategies were developed and optimised for this purpose:

- Direct dsDNA adapter ligation-based amplification
- Homopolymer tailing based dsDNA adapter ligation-based amplification
- Ligation mediated multiple displacement amplification (MDA)

3) Explore human blastocoel fluid spent culture media for embryonic DNA

4) Validation of the developed non-invasive preimplantation genetic testing for aneuploidy (NI PGT-A) assay on blastocoel fluid and spent media samples from human embryos.

5.2. Materials and methods

5.2.1. Sample characteristics

The development and optimisation of protocols during the course of this study were performed on isolated buccal cell samples collected from healthy male and female volunteers.

For the validation of the developed WGA protocol, 26 blastocoel fluid and 78 spent media samples derived from a total of 17 patients undergoing IVF treatment were used. The samples were collected at Oregon Reproductive Medicine clinic (USA) from fully expanded human blastocysts, undergoing PGT-A for various reasons, most common being advanced maternal age. Appropriate IRB (Institutional Review Board) approval was obtained to conduct this study.

5.2.2. Sample collection

Isolation of buccal cells and genomic DNA extraction during the protocol optimisation phase was performed as described in **Sections 3.1.4**.

Laser assisted TE biopsies of blastocysts for PGT-A were performed according to the IVF clinics' standard procedures. The blastocoel fluid samples were collected from fully expanded blastocysts at either Day-5 or Day-6 post fertilisation, depending upon the embryo's development rate. Briefly, using a micropipette blastocoel fluid samples were aspirated from blastocoel cavity into ~2ul droplet of 0.1% PBS/PVA wash buffer inside a 0.2ml Eppendorf tube. The samples were immediately stored at -80°C until the amplification step.

The spent media samples were collected either after a) culturing the embryos from Day-3 to Day-5 post fertilization (fresh embryo culture) or b) thawing cryopreserved blastocysts overnight in ~3-5 µl of culture media droplets (frozen embryo culture). For fresh

culture, embryos were placed in 3-5µl of Quinn's Advantage Cleavage Media (Sage, Denmark) until the cleavage stage and then transferred to a 3-5µl drop of Quinn's Advantage Blastocyst Media (Sage, Denmark) medium untill the blastocyst stage of development. The spent media droplet (exposed to embryo from cleavage to blastocyst stage of development) was collected in its entirety in a 0.2ml Eppendorf tube after transferring the embryo to a new drop of media for a TE biopsy for PGT-A (**Figure 37**).

The cryopreserved blastocysts were thawed in 3µl of Quinn's Advantage Blastocyst Media (Sage, Denmark) and cultured overnight. Thereafter, the embryo was transferred to a new media droplet and the spent culture media (from overnight culture) was collected and stored at -80°C. In addition, control media droplets were also collected which did not have any embryo exposure but were incubated in a similar fashion to spent media droplets.

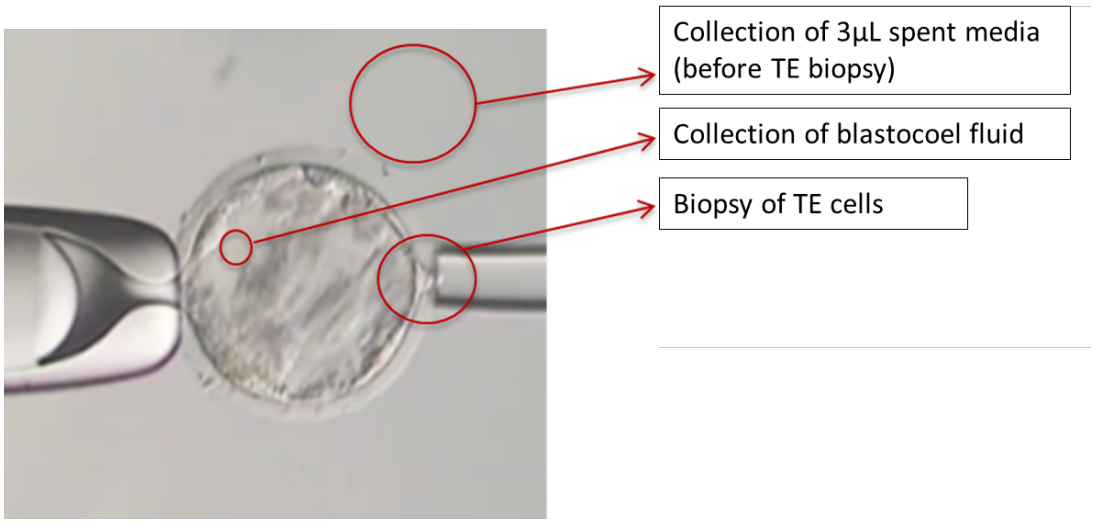


Figure 37. Sample collection. The diagram shows a fully expanded human blastocyst. The blastocoel fluid was aspirated using an ICSI needle and the TE biopsy was performed using a laser. Approximately 3-5µl of spent media droplet was collected after embryo culture.

5.2.3. Development of Y chromosome assay

In order to detect the presence of Y chromosome in blastocoel fluid and spent media samples, a multiplex PCR assay targeting 6 multicopy genes specific to Y-chromosome was

designed. The amplicon sizes of these genomic loci ranged from 77 to 138bp (**Table 23**). The primer design was carried out as described in **Section 3.4.2**.

The preliminary validation of the Y-chromosome assay was performed on human male and female genomic DNA controls. Thereafter, the assay was optimised on isolated single cells from human male and female buccal samples. The specificity of each of the primer pairs was tested in single PCR reactions using gradient PCR at temperatures ranging from 55°C-63°C as described in **Section 3.2.1**. Thereafter, gradient multiplex PCR consisting of all the six primer pairs was also carried out at annealing temperatures ranging from 55°C-63°C. The PCR protocols are described in detail in **Section 3.2.3**.

Table 23. Y-chromosome assay amplicon sizes and primer sequences.

Gene name	Number of copies	Amplicon size (bp)	Primer sequences
DAZ	4	77	F: 5' CATCAACAGCAGTGCAGACT 3' R: 5' AATGTGAGGGACCTTAGCCG 3'
RBMY	6	138	F: 5' GCACCTGCCACGCATATAGT 3' R: 5' TACCCAGAGAAGGCGGATTC 3'
TSPY	~35	101	F: 5' AGTGGAAGGAAGATGGTGGG 3' R: 5' GGAGTGGAATGAGAAGCCCT 3'
CDY	4	118	F: 5' ACACCCACTAATGTCGCAGA 3' R: 5' GTCTGTTGTCCCATTGGCTG 3'
BPY2	3	112	F: 5' TGCAGTTGTACCCAGGTGAT 3' R: 5' CAGGCAGAAAGGGAGACTCA 3'
CYorf16/ FAM197Y9	~35	121	F: 5' TCTCCCAGGCCATTCATGTT 3' R: 5' TCCGTGTGAGGTGGACTAAC 3'

5.2.4. Development of amplification protocols for non-invasive genetic approaches

In order to amplify minute quantities of fragmented DNA, potentially present in spent culture media and blastocoel fluid, three amplification strategies were designed and developed. Each one of these is described in detail below:

5.2.4.1. Double stranded adapter ligation mediated amplification method

For capturing and amplifying short fragments of DNA, double stranded adapters (L1+L2 sequences) were ligated to blunt ended DNA, followed by amplification using primers complementary to the ligated adapter sequences (**Figure 37**). The adapter and primer sequences are described in **Table 24**. Briefly, the DNA was blunt ended using Quick BluntingTM kit (NEB, UK) and the dsDNA adapters were ligated using the enzyme T4 ligase (Thermo Fisher Scientific). Thereafter, adapter ligated DNA fragments were further amplified using Taq polymerase (5'Prime) and primers specific to known sequences in the adapters. The reaction conditions and incubation times are shown in **Table 25** and the optimisation steps are described in detail in **Section 3.1.4**.

Table 24. Adapter and primer sequences.

Name	Sequence
P1	5' AATGATACGGCGACCACCGAGATCTACACTCTTTCCCTACACGA 3'
P2	5' CAAGCAGAAGACGGCATACGAGAT 3'
P3	5'CAAGCAGAAGACGGCATACGAGATGTGACTGGAGTTCAGACGTGTGCTCTTCCGATCTG GGGGGGGGGGGGGGG-3'
L1	5'-AATGATACGGCGACCACCGAGATCTACACTCTTTCCCTACACGACGCTCGGGGGGG-3'
L2	5'-AATGATACGGCGACCACCGAGATCTACACTCTTTCCCTACACGACGCTCGGGTTTTTTT-3'

Table 25. Reaction conditions for double stranded adapter ligation mediated amplification method.

Reaction conditions		Incubation conditions	
Reagents	**Volume (µl)**	**Temperature (°C)**	**Time**
b) Blunting			
10X blunting buffer	0.5	70	10 minutes
1mM dNTP mix	0.5		
Blunting enzyme	0.2		
c) Ligation			
dsDNA adapter (30µM) (L1+L2)	2	22	14-16 hours
T4 DNA ligase (5U/L)	2.5 or 1.25	65	10 minutes
T4 DNA ligase buffer	1	95	2 minutes
dNTPs	1	95	2 minutes
d) Amplification			
Hot start Master Taq polymerase	1	30°C	120 minutes
Hot start Master Taq buffer	3	65°C	3 minutes
Water	0.7	4°C	Hold
Primer P1+P2 or P1+P3 (10µM)	0.3		

5.2.4.2. Homopolymer tailing mediated adapter ligation method.

To increase the efficiency of adapter ligation mediated amplification, a homopolymer tailing based amplification approach was optimised. Briefly, a homopolymer tail of cytosine residues (approximately 20bp) was added to the 3’ end of blunt ended and phosphorylated DNA followed by ligation of a double stranded adapter (Eurogentec, UK) carrying seven protruding guanine residues at the 5’end, complementary to the homopolymer cytosine tail (Eurogentec, UK) (**Figure 37**). The homopolymer tail enables annealing-assisted ligation of the double stranded adapter and thereby aids in increasing the overall efficiency of ligation as the nature of hydrogen bond between 7 dC:dG base pairs is extremely stable. The adapter ligated molecules were amplified using the user-defined sequence at 5’ end of the adapter along with another primer containing region of complementarity with the homopolymer tail merged to a second user defined sequence in the adapter molecule using Taq polymerase (5’ Prime) (**Figure 37**). The amplification was carried out using either primer pair P1+P2 or P1+P3 (**Table**

26). The reaction conditions for the aforementioned steps are described in **Table 26** and the optimisation steps along with corresponding results are detailed in **Section 3.2.3**.

5.2.4.3. Modified WGA method

In order to capture any fragmented DNA as well as any intact DNA present in spent media and blatocoel fluid samples, a modified WGA method was developed. The modified WGA method consisted of four key steps as shown in **Figure 37**. All the reaction conditions and incubation times are described in **Table 27**. Briefly, the samples were initially subjected to an alkaline treatment in order to lyse any intact cells and digest any cellular fragments present. Thereafter, the fragments of DNA were blunt ended using Quick Blunting^{TM} kit (NEB, UK). A 60bp long artificial oligonucleotide derived from pUC19 vector was used as a 'linker' DNA sequence in order to aid the formation of long concatenated DNA fragments (**Figure 129**). The concatenation was carried out using T4 DNA ligase (Thermo Fisher Scientific) and the subsequent long, linear and/ or circular concatamers were used as a template for whole genome amplification by MDA (REPLI-g kit; Qiagen, UK).

Table 26. Reaction conditions for homopolymer tail mediated amplification method.

Reaction conditions		Incubation conditions	
Reagents	**Volume (µl)**	**Temperature (°C)**	**Time**
a) Blunting			
10X blunting buffer	0.5	70	10 minutes
1mM dNTP mix	0.5		
Blunting enzyme	0.2		
b) Homopolymer tailing			
5x buffer terminal transferase	4	37	1 hour
dCTP (10mM)	0.9		
ddCTP (1mM)	0.1		
Terminal transferase enzyme	0.5		
c) Adapter Ligation			
L1 (30µM)	2	23	1 hour
T4 DNA ligase (5U/L)	1		
T4 DNA ligase buffer	3		
f) Amplification			
10x Buffer	5	95	2 minutes
Hot Master taq	1	95 65 72	30 sec 30 sec x 20cycles 120 sec
10mM dNTPs	2		
water	14		
Primers (P1+P2 or P1+P3)	1	4	hold

Table 27. Reaction conditions and incubation times for various steps of modified MDA

Reaction conditions		Incubation conditions	
Reagents	**Volume (µl)**	**Temperature (°C)**	**Time**
a) Alkaline lysis			
DTT (0.1M)	0.70	65	10 minutes
NaOH (1M)	0.3	4	hold
b) Blunting			
Tricine (0.4M)	2	22	30 minutes
10X blunting buffer	0.5	70	10 minutes
1mM dNTP mix	0.5		
Blunting enzyme	0.2		
c) Ligation			
Artificial oligo (1ng, 100pg, 10pg or none)	1	22	14-16 hours
T4 DNA ligase (5U/L)	1	65	10 minutes
T4 DNA ligase buffer	1	95	2 minutes
d) MDA			
Repli-g buffer	29	30°C	120 minutes
Repli-g polymerase	2	65°C	3 minutes
Water	9	4°C	Hold

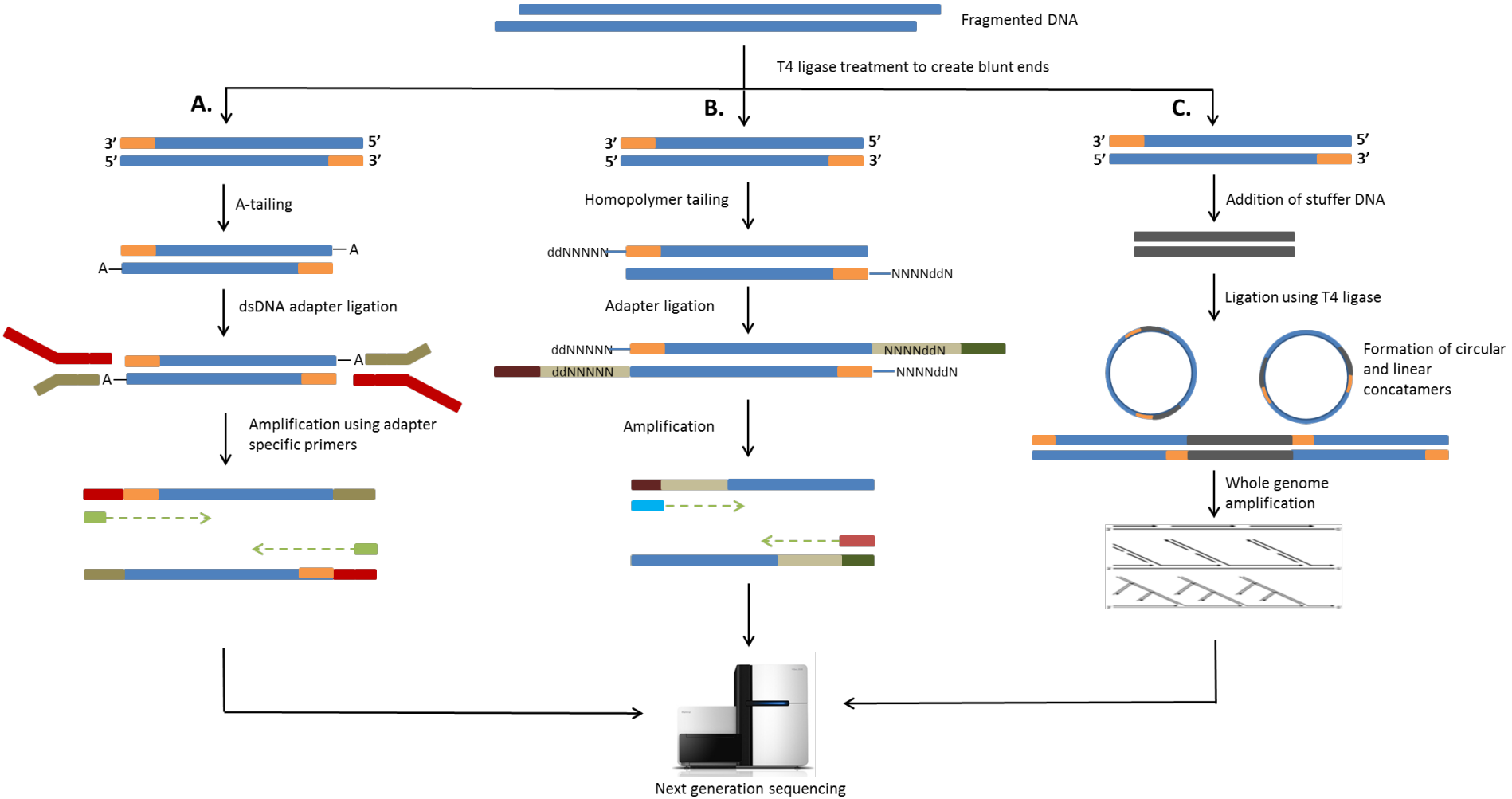


Figure 37. Amplification strategies for fragmented DNA. The fragmented DNA was initially blunt ended for all the three methods. **Method A** consisted of adenylating the blunt ended fragments, followed by adapter ligation and subsequent PCR based amplification. **Method B** entailed homopolymer tailing (cytosine residues) of blunt ended DNA followed by ligation of adapters consisting of poly-G tails. Amplification was carried out using primers complimentary to adapter sequences. Method C involved concatenation of blunt ended DNA fragments along with short artificial oligonucleotides with the aid of T4 ligase resulting in formation of linear and circular concatamers. These were further amplified using MDA.

5.2.5. Next generation sequencing

The amplified samples were subjected to next generation sequencing in order to determine their corresponding chromosomal copy number. The samples for sequencing were prepared using Nextera DNA library preparation kit (Illumina, UK) according to the manufacturer's protocol (**Figure 11**) (**Table 28**). In brief, 50ng of amplified DNA sequences were fragmented and Illumina adapters were simultaneously attached to these DNA fragments in a reaction known as 'tagmentation'. Thereafter, the tagmented DNA sequences were cleaned using Zymo spin columns (Zymo, USA) in order to get rid of any excess transposase enzyme to prevent over fragmentation of samples. Sample specific 'indices' were introduced in a PCR reaction and the resultant amplified products were cleaned using Agencourt AMPure XP magnetic beads (Beckman Coulter, Germany). The resulting libraries were quantified using Quibit (as described in **Section 3.3.2**) and library size distribution was visualised using Bioanalyser (as described in **Section 3.3.2**). The nanomolar (nM) concentration of each sample was calculated using the formula $(\frac{library\ concentration}{660 * avg\ library\ size}) \times 10^6$. Based on these calculation, the samples were normalised to 4nM concentration.

The final 4nM normalised libraries were denatured using 0.2N NaOH and 12pM of the denatured libraries were subjected to paired-end sequencing using MiSeq Reagent kit v2 (300 cycles) on a MiSeq sequencing instrument (Illumina, UK).

Table 28. Library preparation steps for NGS. Nextera DNA library preparation kit was used for library

Reaction conditions		Incubation conditions	
Reagents	**Volume (µl)**	**Temperature (°C)**	**Time**
a) Tagmentation			
DNA (2.5ng/µl; 50ng total)	20	55	10 minutes
TD Buffer	25	10	Hold
TDE1 enzyme	5		
b) Amplification of libraries			
Index 1 (i7)	5	72	30 minutes
Index 1 (i5)	5	98	10 minutes
NPM	15	5 cycles of:	
PPC	5	98	10 seconds
Cleaned up tagmented products	20	63	30 seconds
		72	3 minutes
		10	Hold
c) Library normalisation to 4nM			
d) Denaturation			
4nM library	5	Room temperature	10 minutes
0.2N NaOH	5		

5.2.6. Chromosomal copy number analysis

An analysis pipeline for chromosomal copy number detection was developed using the Nexus Copy Number™ software by Biodiscovery, USA. The software enables copy number analysis by using a 'reference' dataset generated from numerous 'euploid' samples. For reference creation, BAM files from several euploid spent media samples (based on the embryo karyotype determined following embryo biopsy and conventional PGT-A) were uploaded to MultiScale BAM reference Builder (Biodiscovery, USA). The reference builder contains several modifiable parameters which aid in developing a custom analysis pipeline tailored for particular sample type (**Figure 38**). During the development phase of the analysis

pipeline, several alterations were made to these parameters and numerous combinations of spent media samples were tested to generate most adequate reference for analysis. The BAM files of samples along with the appropriate reference were then loaded on the Nexus software and the subsequent analysis was performed. **Figure 39** shows Nexus profiles for chromosomal copy number analysis.

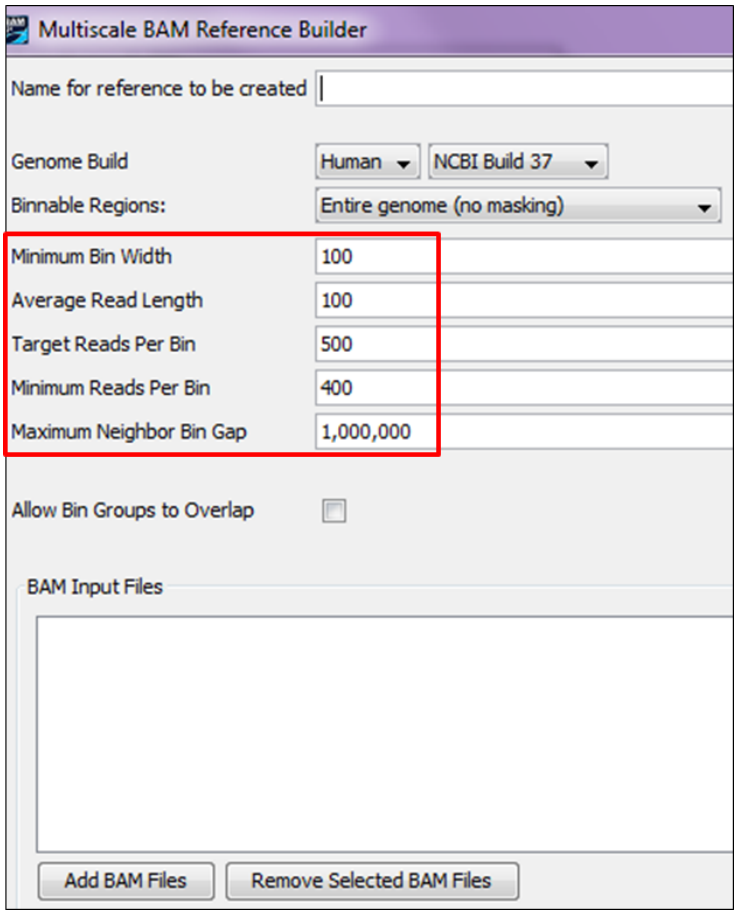


Figure 38. Reference builder for chromosomal copy number analysis. Multiscale reference builder from Nexus Biodiscovery software was utilised for creation of references for chromosomal copy number analysis. The BAM files from euploid samples were used to create a reference against which other spent media samples were normalised. The red box shows the specific parameters used for chromosomal copy number analysis of NGS data from blastocoel fluid and spent media samples.

5.2.7. Sensitivity and Specificity calculation

The sensitivity and specificity of modified MDA method for chromosomal copy number analysis of spent media samples with respect to TE biopsy were calculated. The

formula used for sensitivity calculation was: $sensitivity = \frac{True\ positive}{True\ positive + False\ negative}$ and specificity calculation was: $specificity = \frac{True\ negative}{True\ negative + False\ positive}$. The positive predictive value (PPV) was calculated by using the formula $PPV = \frac{True\ positive}{True\ positive + False\ positive}$ and the negative predictive value (NPV) was calculated with the formula: $NPV = \frac{True\ negative}{False\ negative + True\ negative}$.

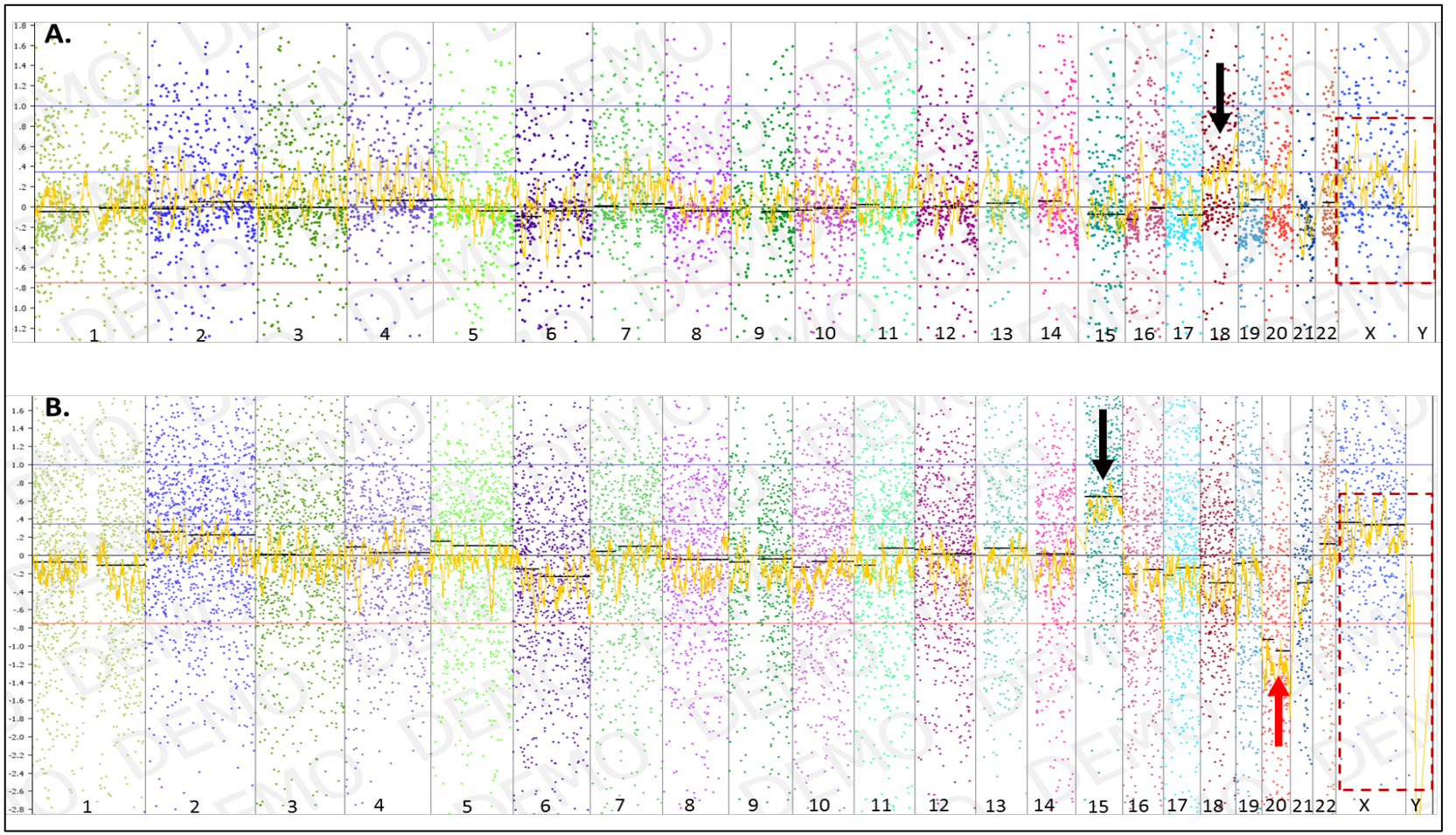


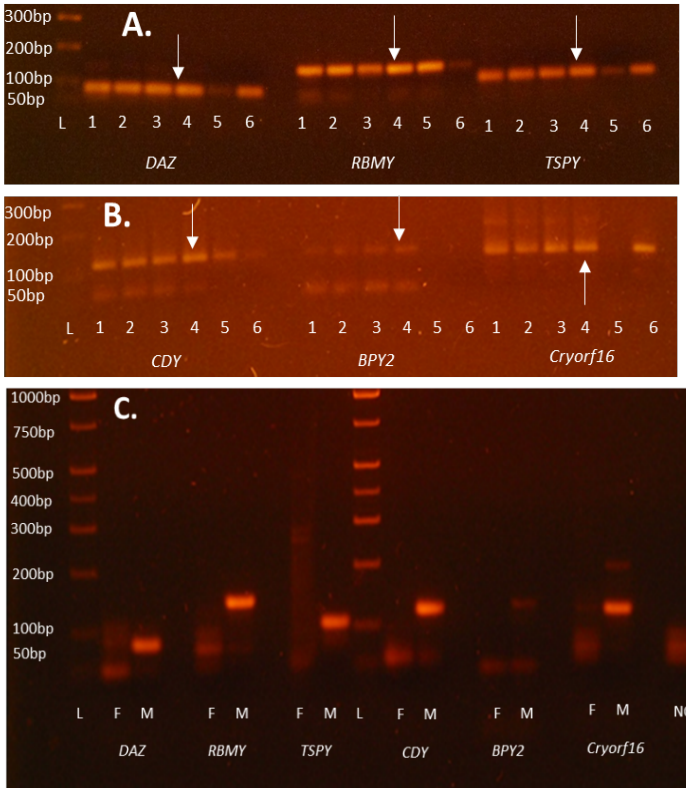
Figure 39. Nexus chromosomal copy number profiles showing profiles of aneuploid spent media samples. The karyotype of sample **(A)** is 47, XY,+18. And that of sample **(B)** is 46,XX,+15,-20. The gains of chromosomes are depicted with a black arrow and the loss is depicted with a red arrow. The red boxes show the sex chromosomes for each sample. Each spot in the chromosomal profile corresponds to a 'bins' of equal size (1Mb) into which the entire genome has been divided. Reads are placed into bins corresponding to the chromosomal regions to which they map and the number of reads in each bin, relative to the number seen in the reference dataset, provides an indication of copy number.

5.3. Results

5.3.1. Development and validation of Y-chromosome assay

The Y chromosome assay was developed using six Y-chromosome specific multicopy genes; *DAZ*, *RBMY*, *TSPY, CDY, BPY2* and *CRYORF16.* The specificity all the 6 primer pairs was tested, and the optimum annealing temperature was determined by performing a gradient PCR at 6 different temperatures (58°C, 58.8°C, 60°C, 61.3°C,62.9°C,64°C) on human genomic DNA control (**Figure 40**). Although distinct bands corresponding to the amplicon sizes of individual genes were observed for most of the gradient annealing temperatures; 62.9°C was determined to be the optimal annealing temperature based on the intensity of amplification bands.

In order to determine the specificity of primers for Y-chromosome, singleplex PCR reactions were performed on male and female genomic DNA controls for all the 6 genes. Although some primer dimers and non-specific products were obtained for female controls, specific bands corresponding to the 6 Y-specific amplicon sizes were obtained only for all the male genomic DNA samples. Additionally, a multiplex PCR for all the 6 amplicons was performed on isolated buccal cells from a healthy male and healthy female. Distinct and bright bands of expected amplicon sizes were obtained in all of the male single cell samples and the positive control. However, only primer dimers were observed in the female single cell sample (**Figure 40**).



Gene name	Amplicon size (bp)	Observed on gel?
DAZ	77	✔
RBMY	138	✔
TSPY	101	✔
CDY	118	✔
BPY2	112	✔
Cryorf16	121	✔

Figure 40. Y-chromosome assay. Agarose gel image **A** and **B** show the PCR products for each of the 6 Y-chromosome specific amplicons .at different temperatures where 1=58°C, 2=58.8°C, 3=60°C, 4=61.3°C, 5=62.9°C, 6=64°C .Gel image C shows the amplification products from all the 6 Y-specific genes on female (F) as well as male (M) genomic DNA. Gene specific amplicons were only observed for male samples but not for female samples.

Multiplex PCR products for Y-chromosome for isolated single buccal cells from male (M1, M2, M3, M4, M5) and female (F) are shown in gel image **D**. Distinct bands were observed for all the male cells but only primer dimers were observed for female sample.

NC= negative control; PC=positive control

5.3.2. Testing the hypothesis

The amplification strategies for this study were developed and optimised based on the hypothesis that the cell-free DNA present in blastocoel fluid and spent culture media might be fragmented in nature and present in minute quantities (in picograms). In order to demonstrate that conventional WGA methods are not capable of amplification of highly fragmented DNA, different concentrations (ranging from 1ng to 1pg) of a complex mixture of over 200 short amplicons from different loci across the human genome (ranging from 77bp-150bp) were amplified using MDA and Sureplex amplification methods. For MDA amplified samples, faint smears were observed on the agarose gel only for 1ng and 0.1ng of amplicon samples but the lanes with 10pg and 1pg samples were clear. However, a clear band at ~150bp for the positive control for all samples was observed on the gel. Primers targeting *PLCz* amplicon (~150bp) in the mixture of amplicons was used as a positive control (**Figure**

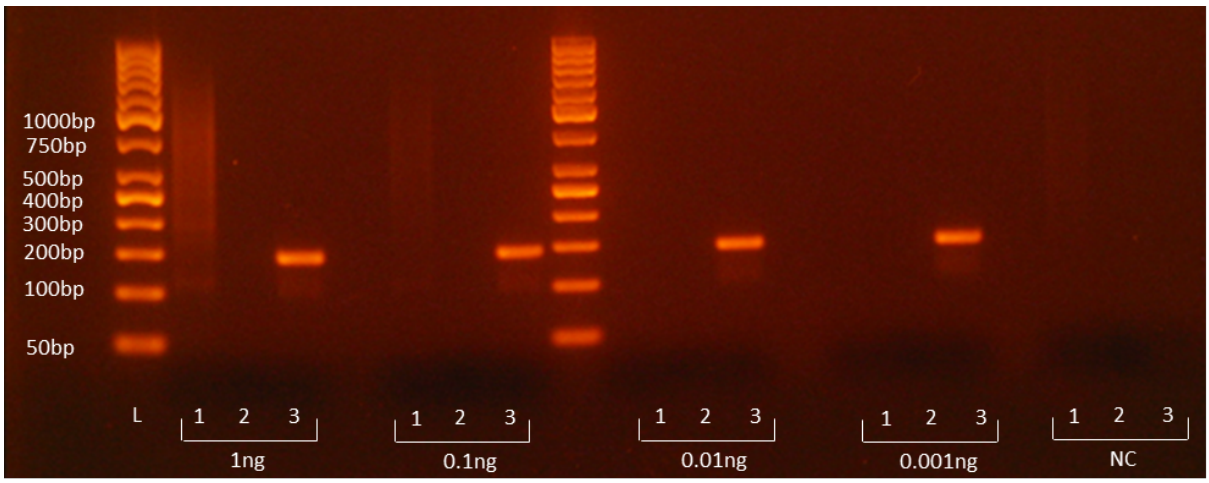


Figure 41. WGA using Sureplex and MDA on complex mixture of amplicons. The gel image depicts different concentrations of complex mixture of amplicons ranging from 77-150bp amplified using MDA (**1**) and Sureplex (**2**). No amplification bands were observed for these samples. The positive control (sample **3**) for all the concentrations showed a distinct band of ~150bp which was the expected band size from PLCz control amplicon present in the mixture of input amplicons.

NC= negative control; L=ladder

5.3.3. Development and optimisation of amplification methodology

5.3.3.1. Method A: Blunting + adapter ligation (Direct adapter ligation method)

The validation of Method A comprised of blunting the ends of various concentrations (1ng, 100pg, 10pg and 1pg) of a known 150bp amplicon from the PLCz gene, followed by double stranded adapter ligation and subsequent amplification of adapter ligated PLCz fragments. For each sample concentration, two different reaction concentrations were used for each of the three aforementioned steps (**Figure 42**). Post adapter ligation, the ensuing amplification should yield ~250bp sized amplicons. However, only a high level of primer dimers and distinct non-specific PCR products (~60bp-120bp) were observed for samples amplified with this strategy. It seemed likely that these non-specific products originated from inter-adapter ligation and subsequent amplification of adapter dimers.

5.3.3.2. Method B: Blunting + homopolymer tailing + adapter ligation (Homopolymer tailing mediated adapter ligation)

In order to increase the efficiency of ligation step, homopolymer tail mediated adapter ligation was employed as an amplification strategy. Various concentrations (1ng, 100pg and 10pg) of 150bp PLCz amplicons were subjected to blunting, cytosine homopolymer tailing and adapter ligation followed by PCR using known sequences from the adapter. **Figure 43** depicts the optimisation steps for the homopolymer tailing amplification strategy. In brief, for each sample, blunting was either performed by (A) T4 DNA polymerase or (B) Klenow enzyme. A controlled homopolymer tail of cytosine of approximately 20bp was added to blunt ended DNA samples followed by dsDNA adapter ligation. The adapter ligated molecules were thereafter amplified using adapter specific primers (P1+P2) and half of the amplified products were subjected to a PCR cleanup using magnetic beads (1.5x) (**Figure 43**).

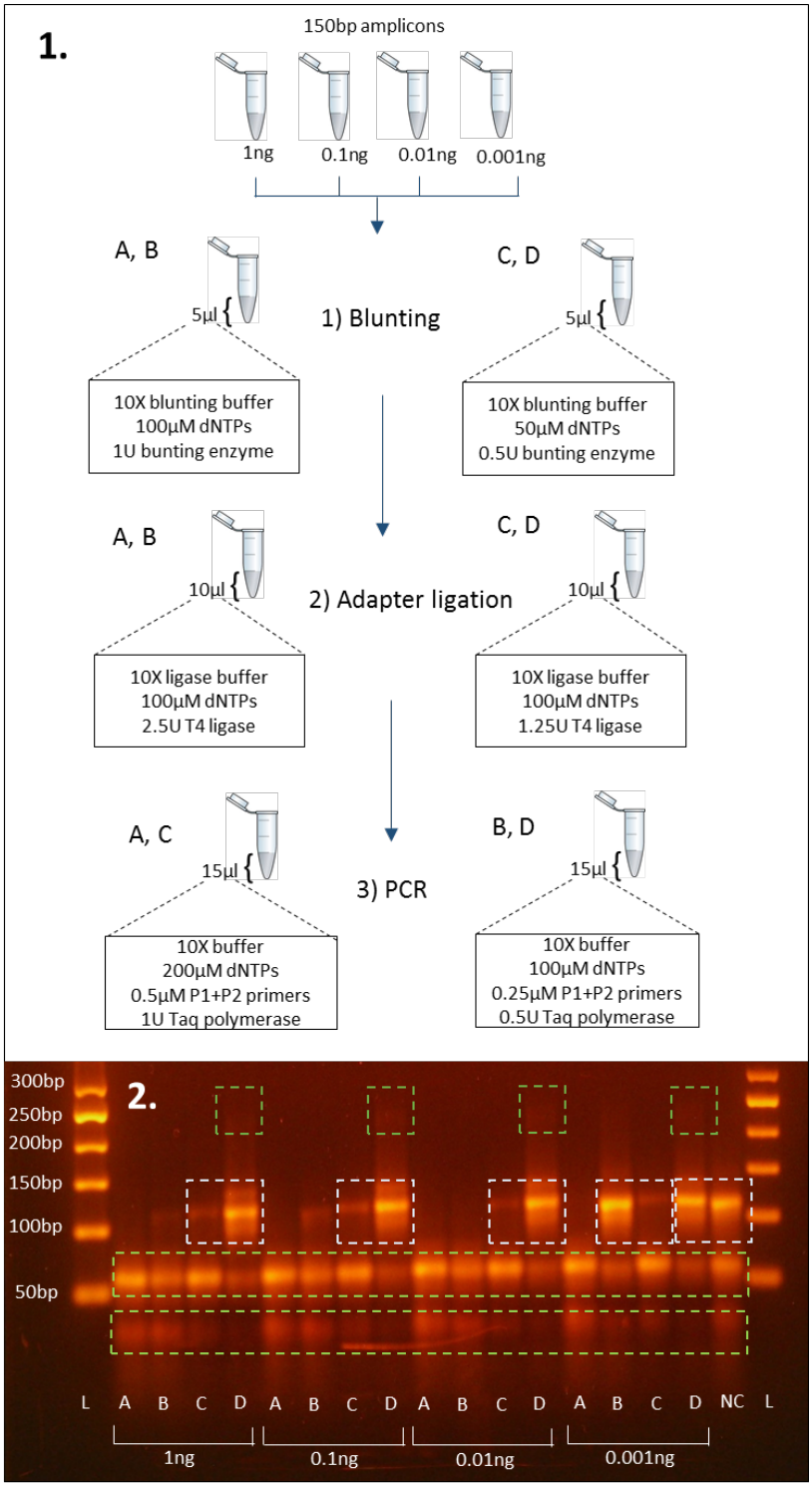


Figure 42. Amplification method A: Direct adapter ligation based amplification. The diagram **1** shows the different optimisation reaction conditions for various steps of direct adapter ligation based amplification method on different concentrations of a 150bp PLCz amplicon (1ng, 0.1ng, 0.01ng and 0.001ng). The agarose gel image (**2**) shows the amplification products after PCR using the adapter ligation method. Very faint bands of expected product size of ~250bp was observed for 1ng and 0.1ng input samples (marked in green box) with reaction conditions D. For rest of the samples, only primer dimers and non-specific amplification products were observed (highlighted in yellow and white boxes).

NC=negative control; L=ladder

A faint band of expected amplicon size of ~280bp was observed on the agarose gel for the PCR cleaned up products of 1ng and 0.1ng samples (subjected to reaction conditions A). However, for all the other samples, primers dimers and non-specific products of <100bp were observed (**Figure 43**).

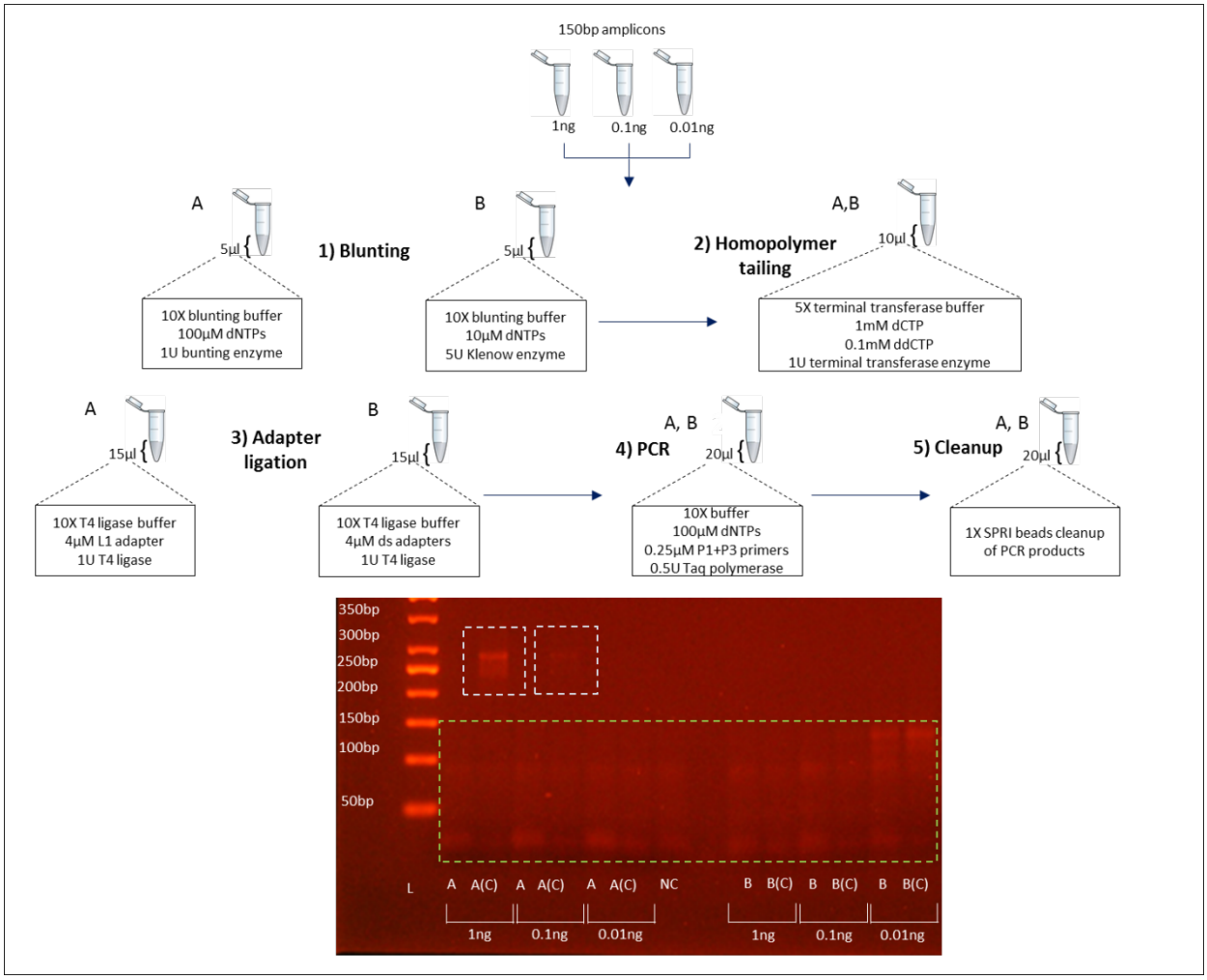


Figure 43. Amplification method B: Homopolymer tail mediated adapter ligation amplification method. The diagram shows two optimisation steps; A and B, consisting of different reaction conditions for various steps (1=Blunting; 2=Homopolymer tailing; 3=adapter ligation; 4=PCR; 5=PCR cleanup) of the homopolymer tail mediated amplification protocol. Amplification products of expected size of ~280bp were observed for PCR cleaned up products of 1ng and 0.1ng of input samples subjected to reaction conditions A and amplified using P1+P2 primers.

NC=negative control; L=ladder

Further amplification using P1+P2 and P1+P3 primer sets on the cleaned-up PCR products of reaction conditions A generated smears of expected product size of ~280bp. The

intensity of the bands increased with sample concentration (1ng>0.1ng>0.01ng). Moreover, primer set P1+P3 gave a better amplification intensity for the expected product size even with lower concentration of input DNA (0.01ng) (**Figure 44**). Smears of primer dimers ranging from 25bp to 90bp were observed for all the samples, with P1+P2 primers generating more primer dimers as compared to P1+P3 primer set (**Figure 44**).

Additionally, in order to verify the presence of PLCz amplicon in the adapter ligated fragments observed at ~280bp, gel extraction was performed on P1+P3 products of 1ng and 0.01ng samples followed by amplification using PLCz specific primers. A distinct product of 150bp was observed for both the samples confirming the presence of PLCz amplicon in the gel extracted products.

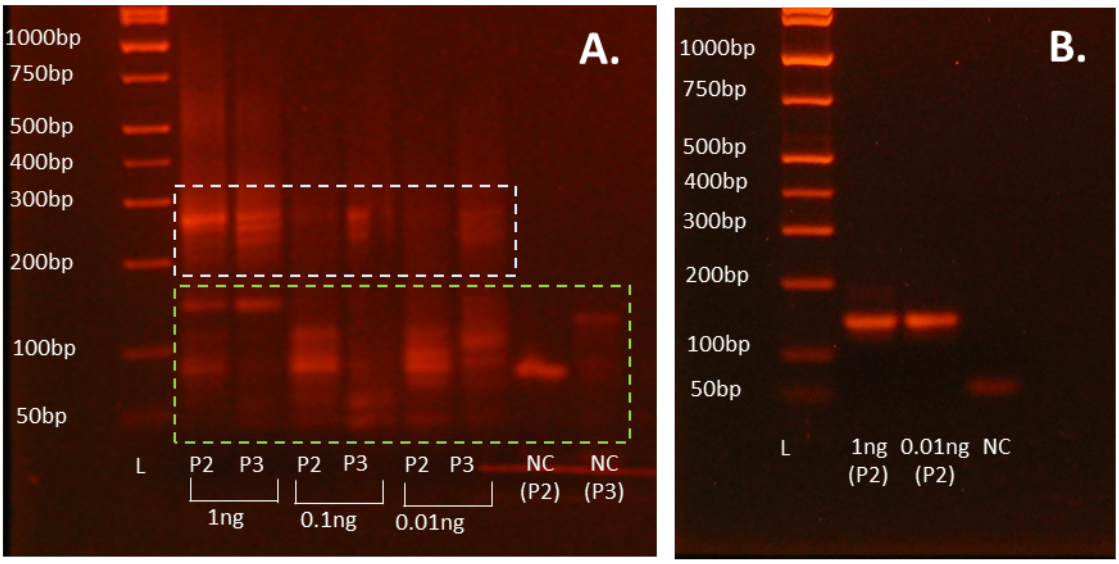


Figure 44. Amplification method B: PCR using P1+P2 and P1+P3 primer sets: A. Amplification of cleaned up PCR products of reaction conditions A using P1+P2 and P1+P3 primer sets yielded products of expected size of ~280bp for all DNA concentration (white box). However, P+P3 primer set was observed to generate products of brighter intensity. All the samples also generated primer dimers ranging in size from 50bp-150bp (yellow box). **B**. Amplification of gel extracted products (~280bp) from gel A with PLCz specific primers gave the expected product size of 150bp.

NC=negative control; L=ladder

In order to verify the results obtained above on a more complex mixture of DNA fragments, PCR products (ranging from 77bp-138bp) from Y-chromosome specific multiplex PCR (**Section 3.2.3**) were utilised in different concentrations (1ng, 0.1ng and 0.01ng). Additionally, two isolated single buccal cell samples (C1, C2) from a male were enzymatically fragmented using NEBNext dsDNA Fragmentase (New England Biolabs, UK) into amplicons ranging from 100-200bp and further processed using the homopolymer tailing mediated amplification protocol (**Figure 45**).

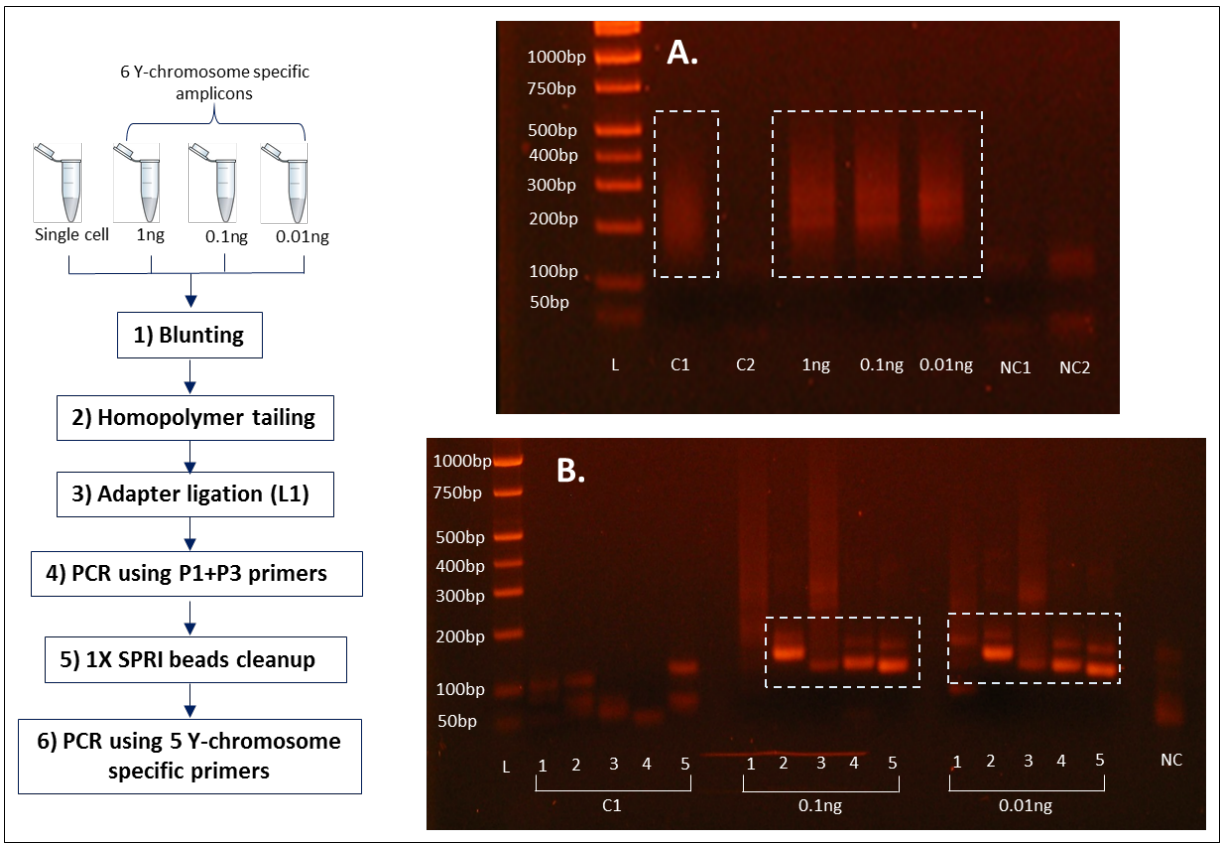


Figure 45. Validation of amplification method B on mixture of short amplicons: A. Agarose gel image A shows amplification products from fragmented male single cells (C1, C2) and different concentrations of Y-chromosome assay (1ng, 0.1ng, 0.01ng) after homopolymer tailing mediated amplification. Only one of the single cell samples, C2, failed to amplify but the rest of the samples showed a smear of amplification between 150-350bp (shown in white boxes). **B.** Amplification of 5 Y-chromosome specific genes (1=*DAZ* (77bp), 2=*RBMY* (138bp), 3=*CDY* (118bp), 4=*Cryorf16* (121bp), 5=*BPY2* (112bp)), was performed on Gel extracted products (150-250bp) from Gel A for samples C1, 0.1ng and 0.01ng. Sample C1 yielded only one expected amplicon size of 112bp for gene *BPY2* (5). The 0.1ng and 0.01ng samples showed 4 expected amplicon sizes from 4 genes, RBMY (138bp), CDY (118bp), Cryorf16 (121bp), BPY2 (112bp) (shown in white boxes).

NC=negative control; L=ladder

On the agarose gel, smears of products ranging from ~150bp to ~350bp were observed for cell sample 1 (C1) as well as for 1ng, 0.1ng and 0.01ng of Y-chromosome assay samples. DNA was extracted from the smears observed on the gel (250pb-350bp band) for C1, 0.1ng and 0.01ng samples and amplified using 5 Y-chromosome specific primers (*DAZ* (77bp), *RBMY* (138bp), *CDY* (118bp), *Cryorf16* (121bp), *BPY2* (112bp)). For cell sample C1, faint band of expected amplicon size of 112bp was observed only for the gene *BPY2*. For 0.1ng and0.01ng samples, distinct bands corresponding to 4 Y-specific genes (*RBMY* (138bp), *CDY* (118bp), *Cryorf16* (121bp), *BPY2* (112bp)) were observed along with faint bands of non-specific products for some of the amplified amplicons (**Figure 45**).

5.3.3.3. Method C: Blunting + ligation + WGA (Ligation mediated WGA)

The last method to be developed for the purpose of exploring the genetic constituents of blastocoel fluid and spent media was based on the principle of concatenation of a mixture of small DNA fragments which in turn would serve as a template for MDA. Different concentrations (1ng, 0.1ng, 0.01ng and 0.001ng) of PCR amplified Y-chromosome assay products were subjected to amplification either by (A) MDA or (b) T4 ligase mediated ligation followed by MDA (**Figure 46**). For MDA amplified samples, very faint amplification bands were observed on the agarose gel for 1ng and 0.1ng samples, however no products were obtained for 0.01 and 0.001ng samples. A bright and long amplified DNA smear was observed for the positive control. For samples amplified by MDA after DNA ligation, a distinct amplification pattern was observed for 1ng sample, which decreased in the intensity with declining concentrations of the samples (1ng<0.1ng<0.01ng<0.001ng) (**Figure 46**).

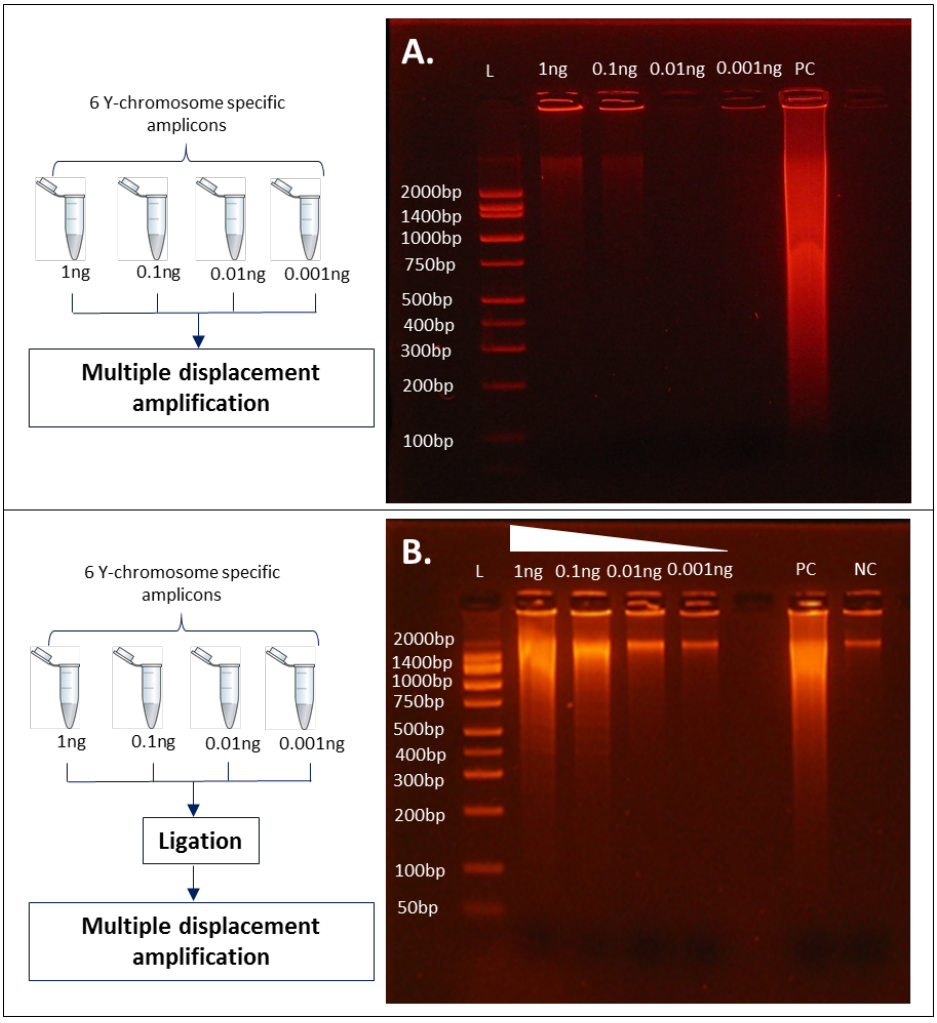


Figure 46. Method C: MDA of DNA fragments with and without DNA ligation A. Gel image shows the amplification of different concentrations of Y-chromosome specific assay products (1ng, 0.1ng, 0.01ng, 0.001ng) using MDA. No optimal amplification was observed for any of these samples. **B.** The samples were subjected to T4 ligase mediated DNA ligation followed by MDA and a decreasing efficiency of amplification was observed with decreasing concentration of DNA fragments in samples (1ng<0.1ng<0.01ng<0.001ng).

NC=negative control; PC=positive control; L=ladder

In the next set of experiments, either 100ng, 10ng or 1ng 'linker' DNA was added to 1ng, 0.1ng, 0.01ng and 0.001ng samples of multiplex PCR products of Y-chromosome assay. Thereafter the samples were blunt-ended by T4 polymerase, ligated to form concatamers using T4 ligase and subsequently amplified by MDA (**Figure47**). All the samples showed clear amplification bands on agarose gel (**Figure 47**). These MDA products were cleaned up using magnetic SPRI beads (1x) followed by amplification of 2 genes, *DAZ* and *RBMY* from the Y-chromosome assay.

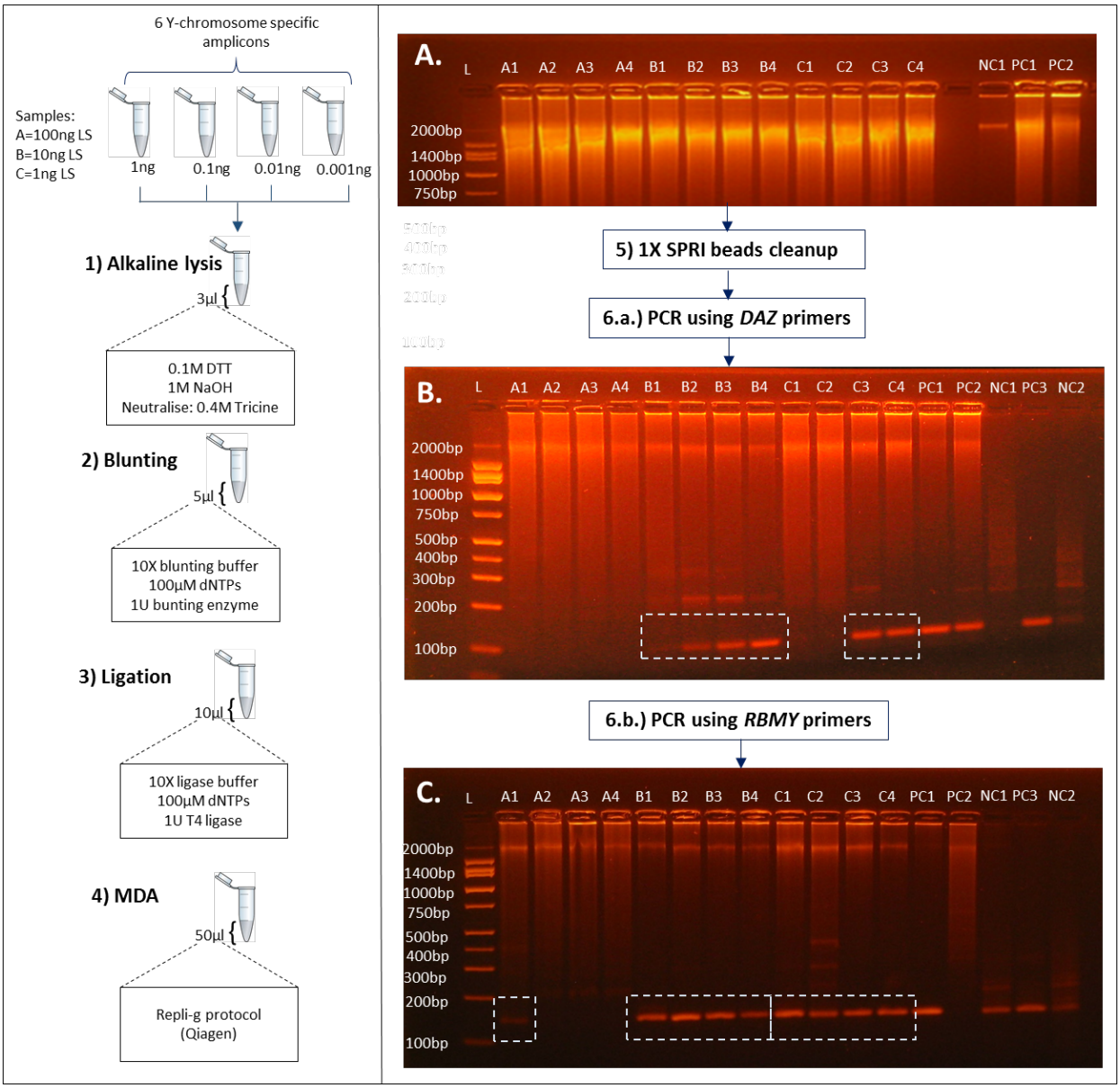


Figure 47. Method C: Addition of linker DNA for ligation mediated MDA A. Successful MDA amplification was obtained for all the samples from Y-chromosome multiplex assay (1=1ng, 2=0.1ng, 3= 0.01ng, 4=0.01ng) after addition of either A=100ng linker DNA, B=10ng linker DNA or C=1ng linker DNA. **B.** Beads cleaned up products of the above MDA samples were amplified using primers for *DAZ* gene. No products were obtained for samples containing 100ng linker DNA (A1, A2, A3, A4). Amplicons of expected size of 77bp were obtained for B1, B2, B3, B4, C3 and C4 samples (shown in white boxes). **C.** Amplification using *RBMY* primers resulted in amplicons of expected size of 138bp for all the samples consisting 10ng (B) and 1ng linker DNA (C) as well as 1ng Y-chromosome assay sample containing 100ng linker DNA (A1) (shown in white boxes). However, no amplification was obtained for rest of the samples containing 100ng linker DNA (A2, A3, A4).

NC=negative control; PC=positive control; L=ladder; LS=linker DNA sequence

For *DAZ* gene, distinct 77bp bands corresponding to the expected amplicon size were observed for 0.1ng, 0.01ng and 0.001ng of samples containing 10ng linker DNA and for samples with 1ng linker DNA added, distinct amplification bands were seen only for 0.01ng and 0.001ng samples. However, no products were seen for *DAZ* and *RBMY* genes in any of the samples (1ng, 0.1ng, 0.01ng, 0.001ng) wherein 100ng linker DNA was added (**Figure 47**). All the samples containing 10ng and 1ng linker DNA showed a clear band at expected 138bp for *RBMY* gene, however no amplification products were obtained for the samples containing 100ng of the linker DNA (**Figure 47**).

In order to determine the successful concatenation of DNA fragments, the MDA samples were further amplified by Y-chromosome assay primers using Klentherm enzyme (without 5' -> 3' exonuclease activity) (Genecraft, Germany) and also subjected to restriction digestion using AluI enzyme (New England Biolabs, UK) (**Figure 48**). For Klentherm amplification reaction, a ladder-like pattern of amplified bands was observed for 0.1ng, 0.01ng and 0.001ng samples containing 10ng and 1ng linker DNA (**Figure 48**). However, only a smear of amplified products was observed for the samples containing 100ng linker DNA as well as for 1ng of samples containing varying amount of linker DNA (**Figure 48**).

For the restriction digested samples, a district ladder pattern of digested amplicons was observed for samples containing 10ng linker DNA (B1, B2, B3, B4), followed by comparatively less restricted digested fragments for samples containing 1ng linker DNA (C1, C2, C3, C4). However, no such ladder like pattern of restriction digested products was observed for samples without any linker DNA (A1, A2, A3, A4) (**Figure 48**).

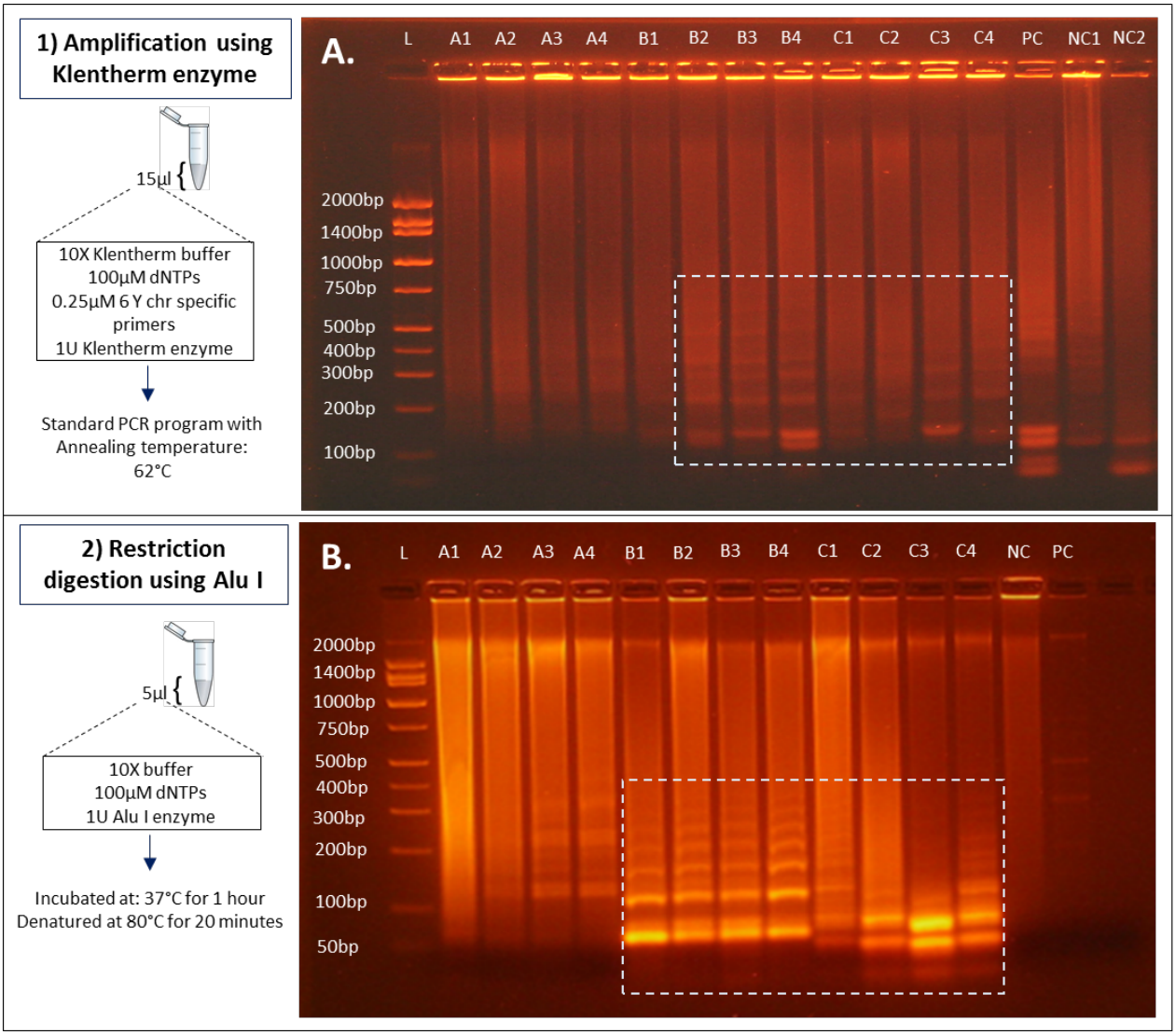


Figure 48. Verification of concatenation by ligation mediated MDA A. Klentherm amplification of ligation mediated MDA products resulted in ladder like pattern of amplicons for all input concentrations of Y-chromosome assay samples (1=1ng, 2=0.1ng, 3= 0.01ng, 4=0.01ng) containing 10ng (B) or 1ng (C) of linker DNA. **B**. Restriction digestion of samples using AluI enzyme gave a distinct ladder pattern for samples containing 10ng linker DNA (B1, B2, B3, B4) and comparatively less restriction digested fragments for samples containing 1ng of linker DNA (C1, C2, C3, C4).

NC=negative control; PC=positive control; L=ladder

5.3.7. Experimental Validation of Method C

Following the optimisation of the modified MDA protocol, an experimental validation was conducted on samples comprising of isolated single cells as well as different concentrations of a complex mixture of over 200 short amplicons ranging from 77bp-120bp (**Figure 49**). These amplicons were generated from a Real Time PCR (RT PCR) assay developed for comprehensive chromosomal copy number analysis by Ms Katharina Spath in the Wells' group.

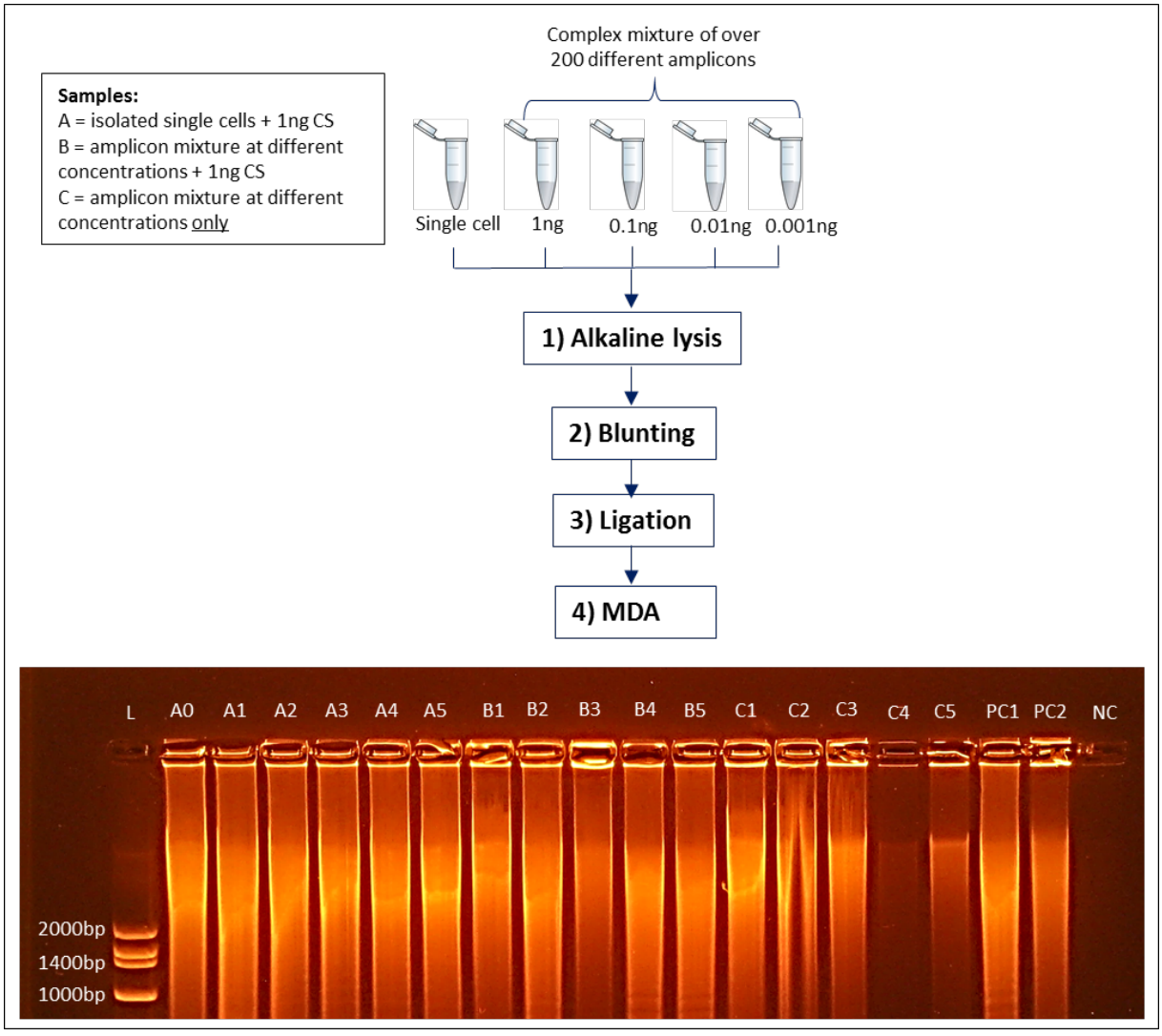


Figure 49. Experimental validation of method C: ligation mediated MDA. Various concentrations (1=10ng, 2=1ng, 3=0.1ng, 4=0.01ng, 5=0.001ng) of a complex mixture of over 200 amplicons from different genomic loci were subjected to ligation mediated MDA with either 1ng of linker DNA (B) or no linker DNA at all (C). Additionally, isolated single cells (A) were also subjected to ligation mediated MDA after the addition of 1ng of linker DNA. Amplification was observed for all samples except 0.01ng and 0.001ng samples without any linker DNA (C4, C5).

NC=negative control; PC=positive control; L=ladder

Successful WGA was obtained for all samples except 0.01ng and 0.001ng samples wherein the linker DNA was not added (C4, C5) (**Figure 49**).

Eight of the samples (A1, B1, B2, B3, B4, C1, C2, C3) amplified by MDA were sequenced using Illumina's 150bp paired-end sequencing chemistry (**Section 3.4**). The sequencing data was subsequently analysed to determine the frequency of different ligation junctions encountered within the 150bp read sequences. Depending upon the presence of ligation junctions in the sequencing reads, the sequences were categorised into 5 types: 1) single genomic site only (no ligation junction encountered in the 150bp sequenced reads), 2) genomic chimeras within the same chromosome (two distinct sequences from same chromosome ligated together), 3) genomic chimeras between chromosomes (two sequences from different chromosomes ligated together), 4) genomic chimeras with linker DNA (genomic sequence ligated with linker DNA) and 5) linker DNA chimeras (linker DNA sequences ligated to each other).

For the single cell sample (A1), a majority of mapped sequences were single genomic loci (94.42%) followed by genomic chimeras within the chromosomes (3.66%), linker DNA chimeras (1.03%), genomic chimeras between chromosomes (0.52%) and genomic + linker DNA chimeras (0.36%). The proportion of linker DNA chimeras for MDA samples (processed with 1ng of linker DNA), increased with decreasing input amplicon concentration in the samples (B1 (0.19%) < B2 (4.2%) < B3 (46.78%) < B4 (71.55%) < B5 (98.58%) (**Appendix B**; **Figure 50**). Overall, the frequency of chimeric sequences containing genomic DNA (inclusive of all types of chimeras containing genomic loci) declined with decreasing initial amplicon concentration in the samples (B1 (99.81%) > B2 (95.80%) > B3 (53.22%) > B4 (28.45%) > B5 (1.42%)) (**Figure 50**).

More specifically, the proportion of 1) single genomic sites was found to be in the descending order for the following samples: B3 (10.35%) > B2 (5.48%) > B1 (3.94%) > B4 (3.92%) > B5 (0.21%); 2) for genomic chimeras between chromosomes the order of sequences was: B2 (54.78%) > B3 (22.56%) > B1 (17.81%) > B4 (2.70%) > B5 (0.10%); 3) for genomic chimeras between chromosomes: B5 (0.22%) > B4 (0.91%) > B3 (3.64%) > B2 (29.65%) > B1 (75.49%) and 4) the percentages of chimeras between genomic and linker DNA was observed to be in the order: B4 (20.935) > B3 (16.66%) > B2 (5.88%) > B1 (2.57%) > B5 (0.89%) (**Appendix B**; **Figure 50**).

The analysis of sequences from MDA samples which did not contain any linker DNA (C1, C2, and C3) nevertheless revealed a small proportion of sequences with linker DNA (0.01% for each of the samples) which might have arisen due to contamination during sample handling (**Figure 50**). However, the analysis of genomic sequences showed that a majority of mapped reads were genomic chimeras between chromosomes (C1 (86.32%) > C2 (70.74%) > C3 (70.31%)), followed by genomic chimeras within the same chromosomes (C3 (27.92%) > C2 (25.52%) > C1 (9.96%)) and the lowest representation of sequences in these samples was of sequences consisting a single genomic loci only (C2 (3.69) < C1=(3.67%) < (C3=(1.74)).

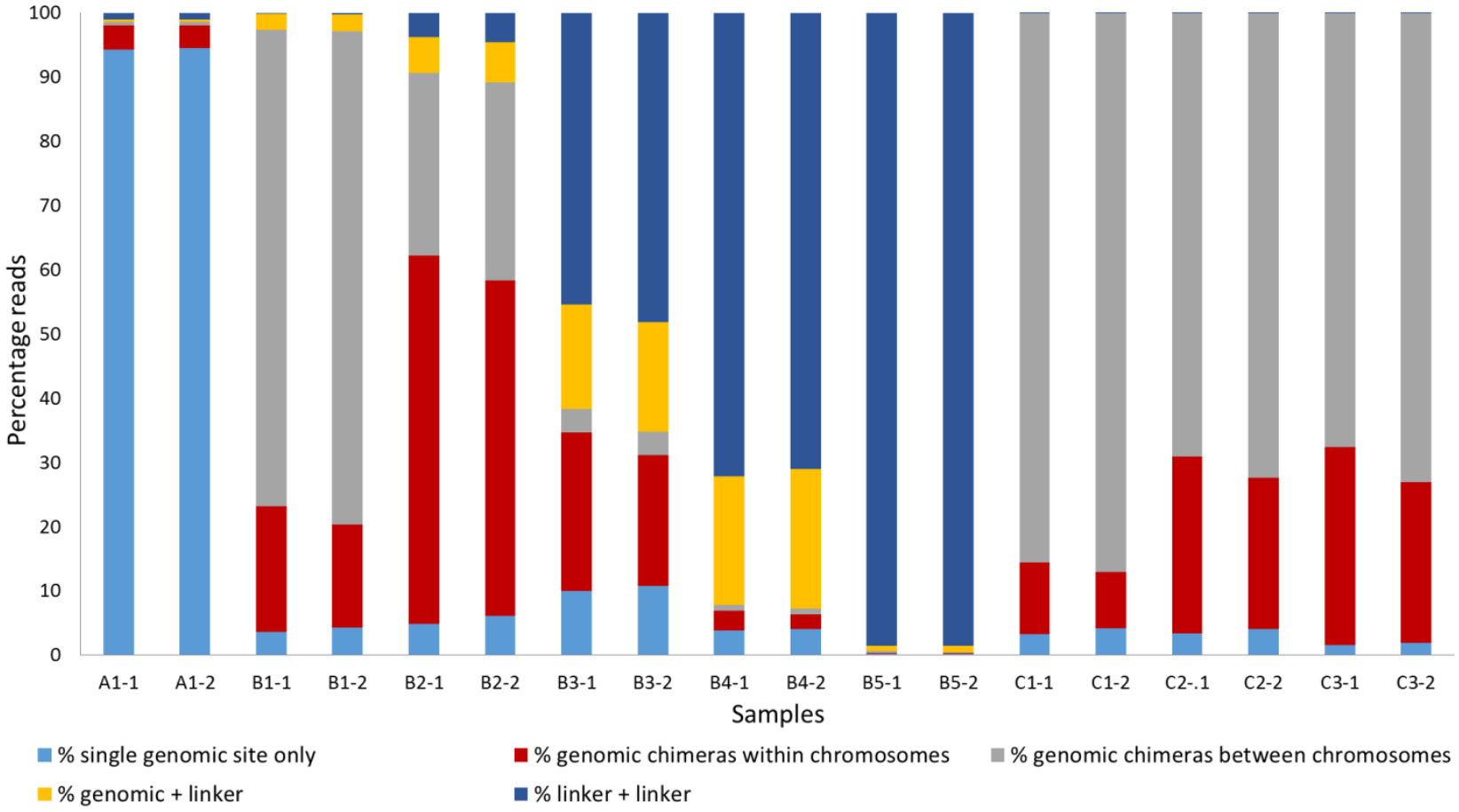


Figure 50. Experimental validation of method C: Sequencing data analysis. The analysis of the 150bp sequencing reads from ligation mediated MDA samples revealed 4 different types of chimeras; 1) genomic chimeras within the same chromosome (brown), 2) genomic chimeras between different chromosomes (grey), 3) genomic+linker DNA chimeras (yellow) and 4) chimeras between linker DNA sequences (dark blue) This graph depicts different proportions of single genomic loci and chimeras amongst the 8 MDA samples subjected to paired end sequencing wherein 1=1st read and 2=2nd read sequence for each sample.

5.3.8. Clinical validation of Method C

The developed modified MDA method (ligation mediated MDA) was further applied to blastocoel fluid and spent culture media from either freshly cultured or frozen-thawed blastocysts.

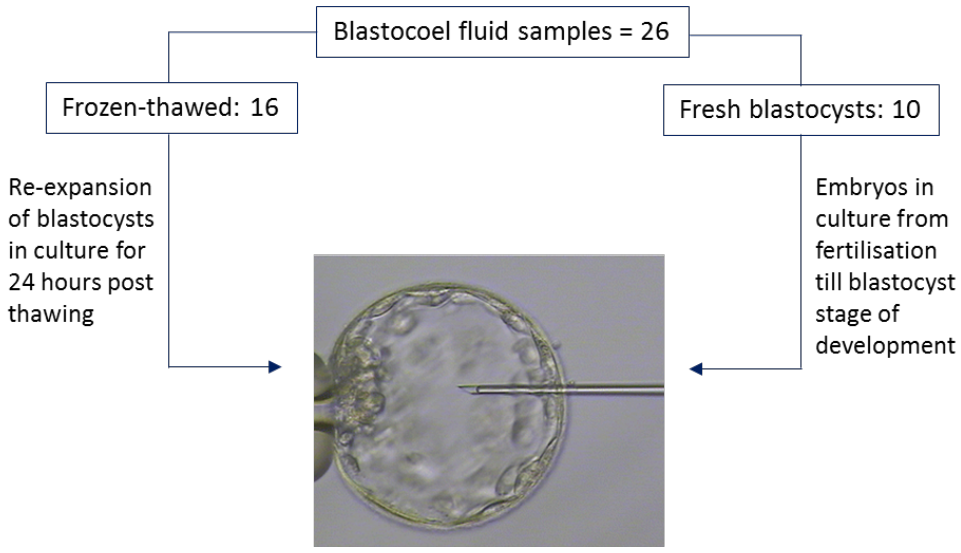
5.3.8.1. Amplification of Blastocoel fluid and spent media samples

A total of 26 blastocoel fluid (BF) samples, including 16 samples from frozen-thawed embryos and 10 samples from freshly cultured blastocysts were subjected to WGA using modified MDA method and the amplified products were subsequently sequenced. Only 30% (3/10) of blastocoel fluid samples from freshly cultured embryos were successfully amplified (optimal for chromosomal copy number analysis using NGS) whereas none of the BF samples derived from frozen thawed embryos optimally amplified (**Figure 51**).

The spent media samples were derived from either fresh Day-3 to Day-5 embryo culture (n=45) or overnight culture of frozen thawed embryos (n=33). These were subsequently amplified by one of the three WGA methods; Sureplex (Illumina, UK), MDA (Qiagen, UK) or modified MDA (**Figure 51**).

For spent media samples from fresh culture, the amplification success rate was significantly higher with the modified MDA method as compared to MDA (66.7% vs 20%; p=0.023; **Figure 52**). However, there was no significant difference between the amplification rates of Sureplex with respect to MDA and modified MDA methods (46.7% vs 20% and 66.7% respectively; **Figure 52**). In the case of spent media samples derived from frozen-thawed embryos, the amplification rate was significantly higher with modified MDA protocol as compared to both, Sureplex (100% vs 50%; p=0.015) and MDA method (100% vs 25%;

p=0.0011; **Figure 52**). No significant difference was observed between optimal amplification rates of Sureplex and MDA amplified samples.



Type of BF sample	Frozen thawed blastocyst	Fresh blastocyst
Number of samples	16	10
Optimally amplified*	0 (0%)	3 (30%)

Figure 51. Amplification of DNA from blastocoel fluid samples by modified MDA method. A total of. 26 blastocoel fluid (BF) samples, including 16 samples from frozen thawed embryos and 10 from fresh embryo cultures, were aspirated and amplified by modified MDA method. A 30% success rate of optimal amplification was obtained for BF samples derived from fresh embryo cultures. However, none of the BF samples from frozen thawed embryos amplified optimally.

*=optimally amplified samples wherein the sequencing quality was optimal for downstream chromosomal copy number analysis

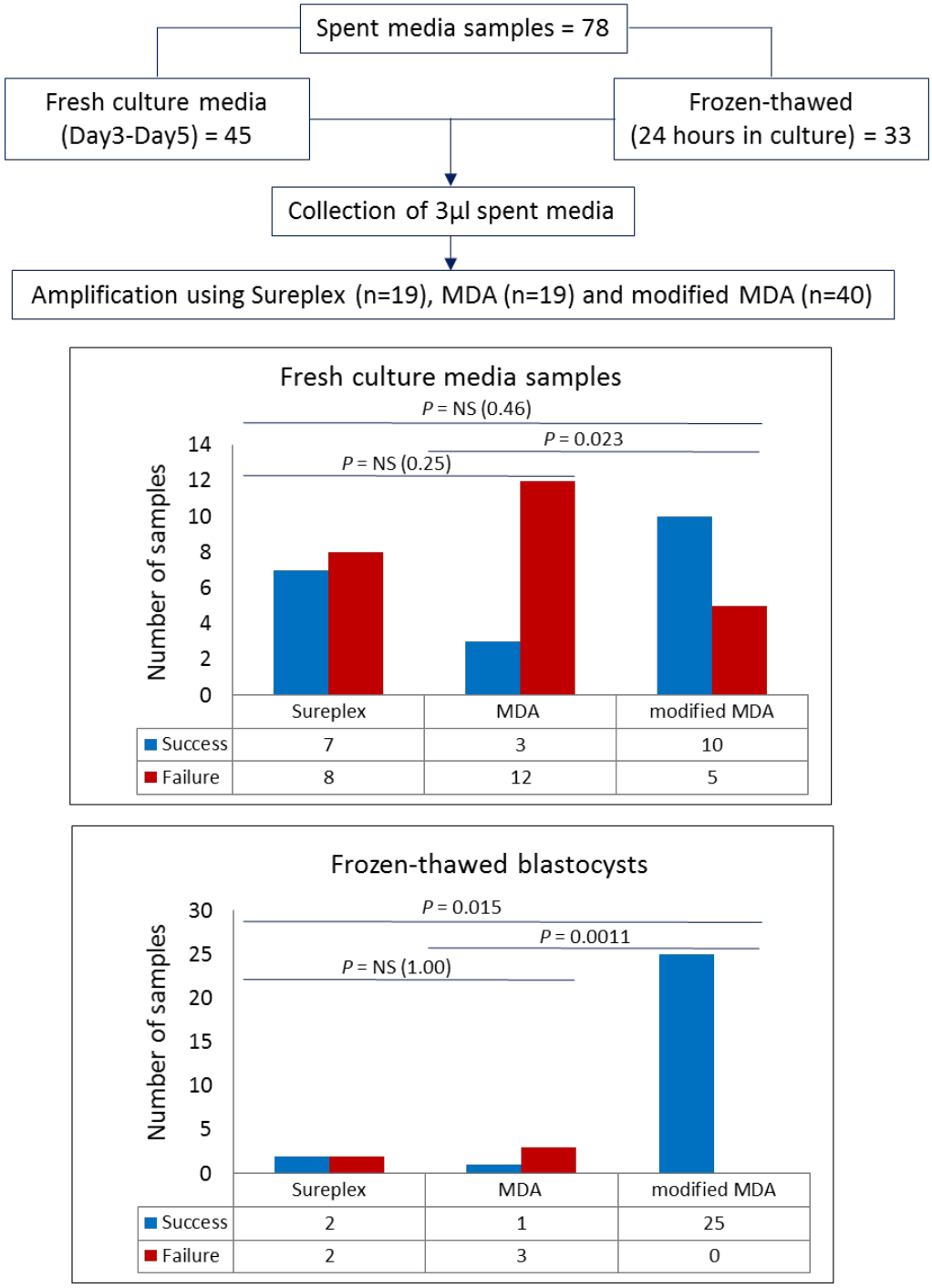


Figure 52. Amplification of DNA from spent culture media samples. Spent media samples derived from frozen thawed embryos (n=33) and fresh embryo cultures (n=45) were subjected to WGA with either a) Sureplex, b) MDA or c) modified MDA. For samples from fresh embryo cultures, success of amplification was significantly higher for modified MDA as compared to MDA (66.7% vs 20%; p=0.023). Additionally, the amplification success rate for samples from frozen thawed blastocysts was significantly higher for modified MDA samples in comparison to Sureplex and MDA amplified samples (100% vs 50% and 25% respectively; p<0.05).

5.3.8.2. Analysis of genomic DNA from blastocoel fluid and spent media

The analysis of sequencing data obtained from blastocoel fluid samples showed that the total proportion of reads mapping/aligning to the human genome ranged between 0.2%-4.46% for frozen-thawed embryos and between 35.74%-71.9% for freshly cultured embryos (**Figure 53**). Similarly, for spent culture media samples, the percentage of total mapped reads ranged from 21.23%-83.3% for frozen thawed embryos and 25.6%-81.1% for fresh embryo cultures (**Figure 55**) (**Appendix B**).

The 150bp mapped sequencing reads either aligned to a single chromosomal locus in the genome or comprised of chimeric sequences (different sequences ligated together). The chimeric sequences were categorised into four classes: 1) genomic chimeras between different chromosomes, 2) genomic chimeras within the same chromosome, 3) genomic and linker DNA chimeras, and 4) linker DNA chimeras only. The proportions of different chimeric sequences are depicted in **Figures 53, 54 and 55** for each of the blastocoel fluid and spent media samples (**Appendix B**).

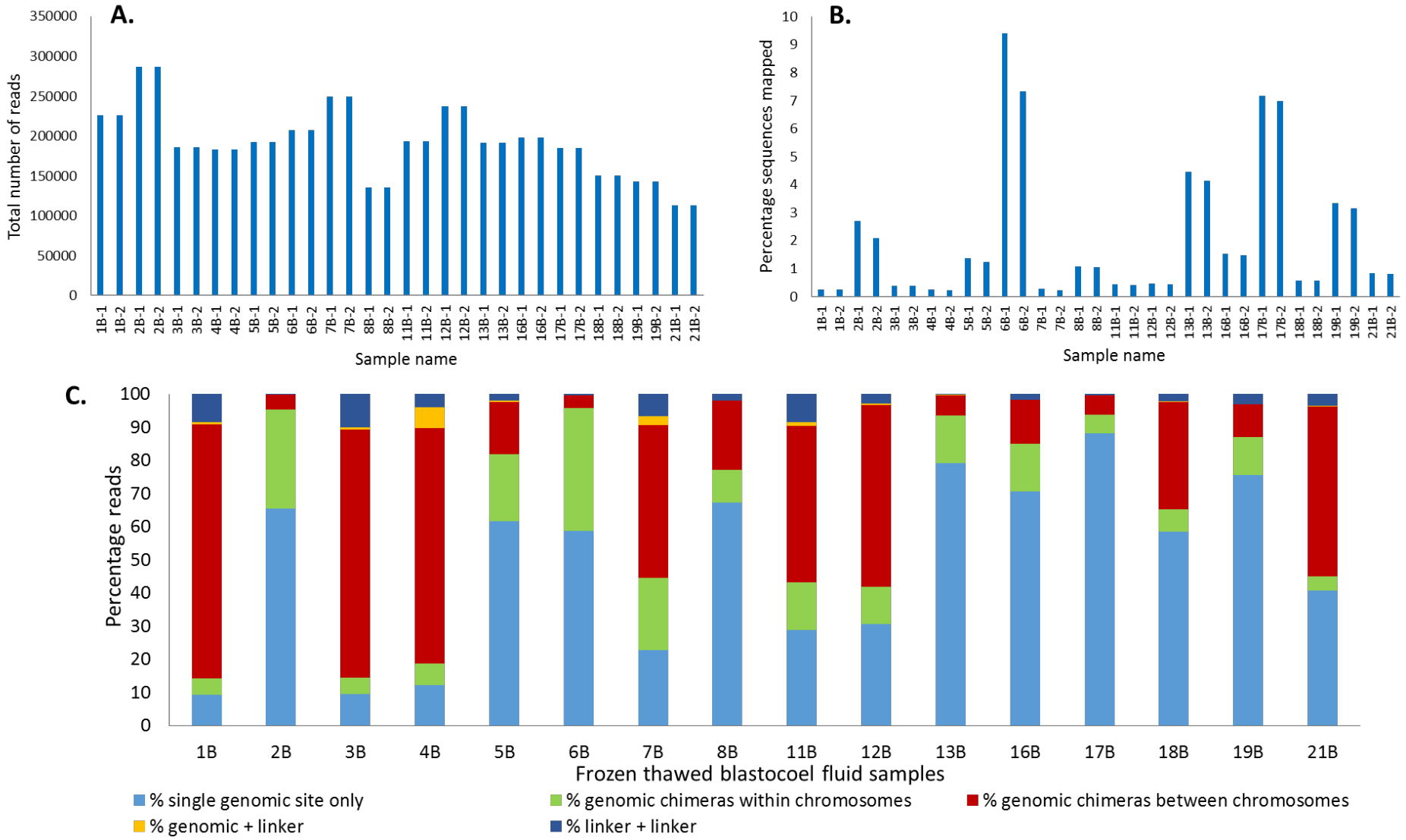


Figure 53. Analysis of sequencing reads of blastocoel fluid samples from frozen-thawed embryos The Bar graph **A** shows the total number of sequencing reads (paired end reads, 1=1st read; 2=2nd read) obtained and the graph **B** shows the percentage of these reads which mapped to human genome. **C.** The proportions of different chimeras for each sample are depicted in this bar graph.

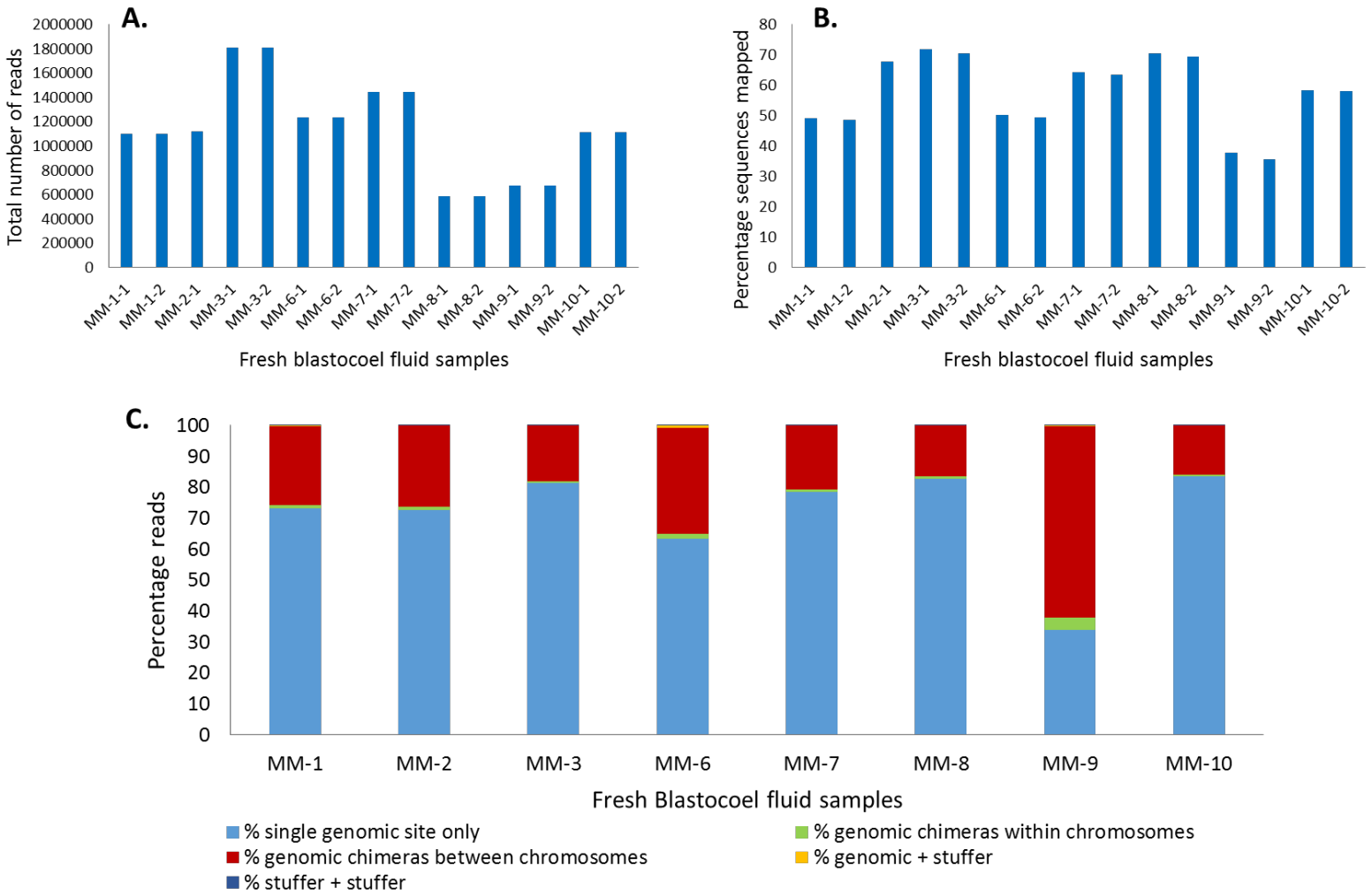


Figure 54. Analysis of sequencing reads of blastocoel fluid samples from fresh embryo cultures The Bar graph **A** shows the total number of sequencing reads (paired end reads, 1=1st read; 2=2nd read) obtained and the graph **B** shows the percentage of these reads which mapped to human genome. **C.** The proportions of different chimeras for each sample are depicted in this bar graph.

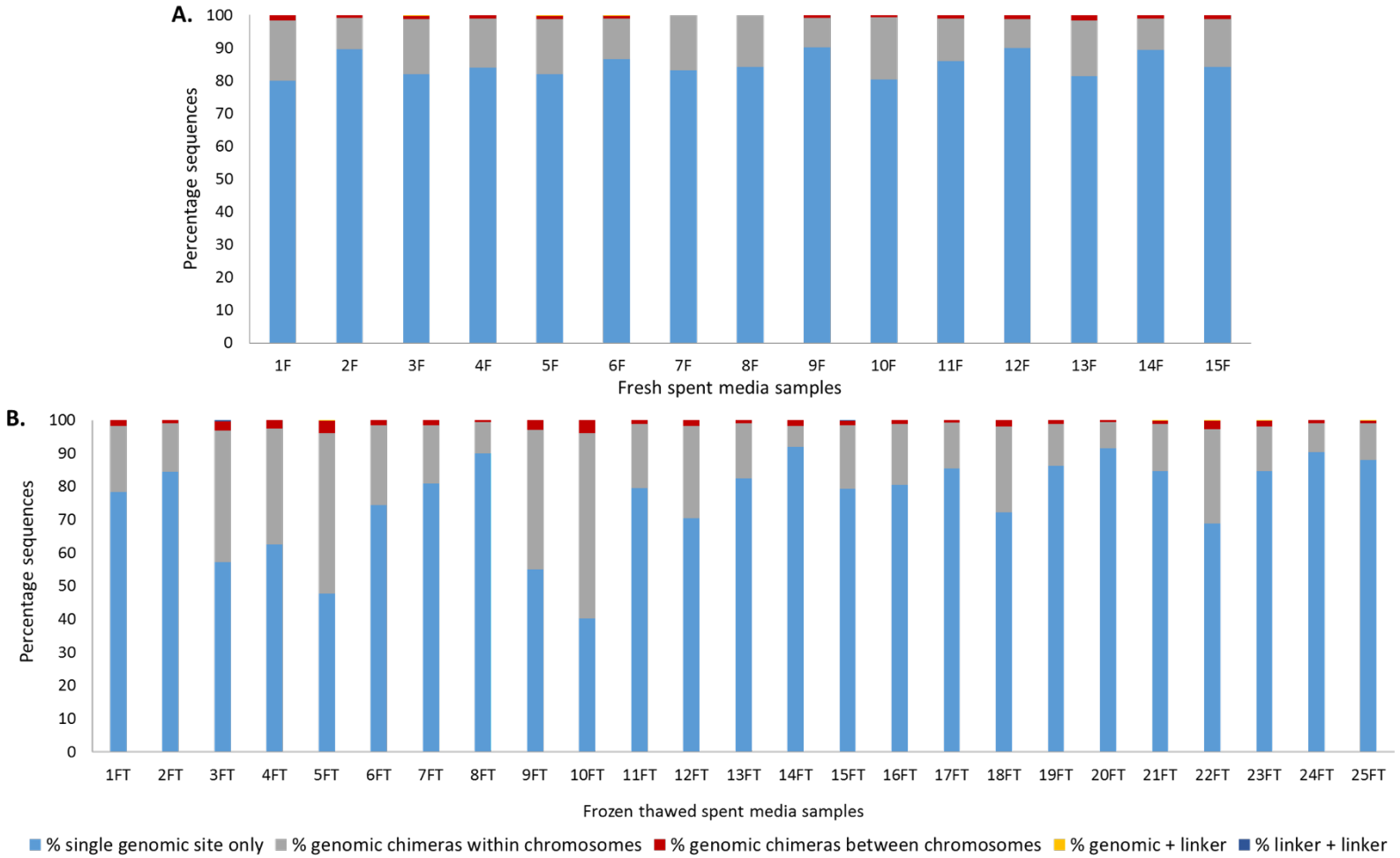


Figure 55. Analysis of sequencing reads of spent media samples The Bar graphs **A** and **B** depict the proportions of sequences consisting of single genomic locus as well as different types of chimeras for each spent media sample from either fresh (F) or frozen thawed (FT) embryo culture.

Upon further analysis of chimeric sequences, blastocoel fluid samples from fresh embryo culture had a significantly higher proportion of chimeric sequences within the same chromosome as compared to blastocoel fluid samples from frozen-thawed embryos ($P<0.05$; 1way Anova with Dunn's test) (**Figure 56**). The proportion of genomic chimeras within the same chromosome was comparable between blastocoel fluid samples and spent media samples from fresh as well as frozen-thawed embryo cultures (**Figure 56**). Ligation between two DNA sequences from different chromosomes gave rise to reads with genomic chimeras between different chromosomes. Such chimeras were observed in a significantly higher proportion in blastocoel fluid samples from frozen-thawed embryos as compared to blastocoel fluid samples from freshly cultured embryos as well as spent media samples ($P<0.05$; 1way Anova with Dunn's test). However, no significant difference was observed between spent media samples and blastocoel fluid samples from freshly cultured embryos for genomic chimeras between chromosomes (**Figure 56**).

Furthermore, linker DNA was present in some of the sequencing reads. The percentage of chimeras with linker and genomic DNA was significantly higher in blastocoel fluid samples than in spent media samples obtained from frozen-thawed embryos ($P<0.05$; 1way Anova with Dunn's test). However, the spent media samples from fresh embryo cultures had a significantly higher rate of genomic and linker DNA chimeras as compared to those from frozen thawed embryos. The chimeras consisting of only linker DNA were found in significantly higher proportion in blastocoel fluid from frozen thawed embryos as compared to blastocoel fluid and spent media samples from fresh embryo cultures ($P<0.05$; 1way Anova with Dunn's test) (**Figure 56**).

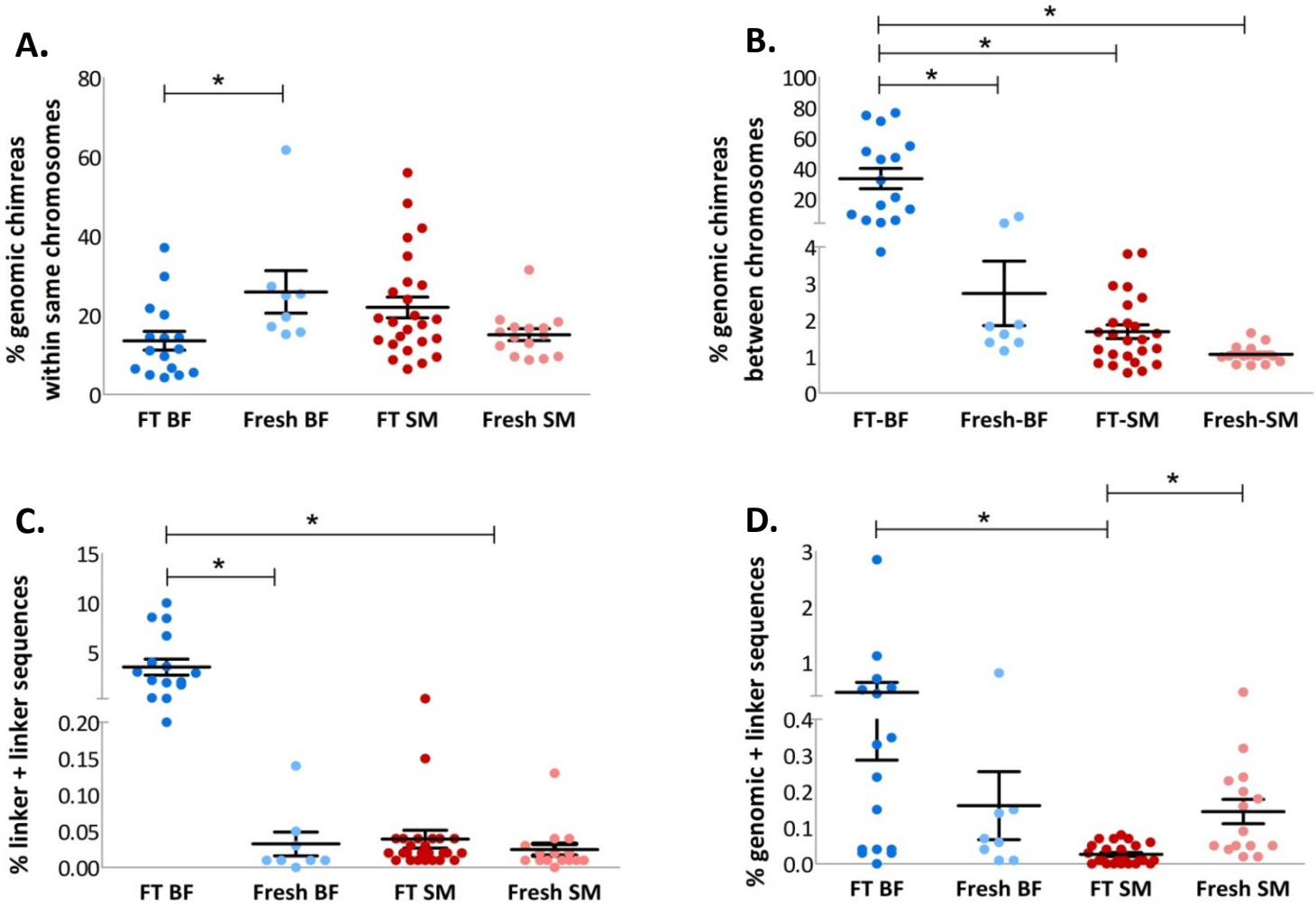


Figure 56. Analysis of chimeric sequences in spent media and blastocoel fluid samples. A. A significantly higher proportion of genomic chimeras within the same chromosome were observed for Fresh BF as compared to those from FT BF samples (P<0.05; 1way Anova, Dunn's test). **B.** For genomic chimeras between different chromosomes, a significantly higher proportion of such sequences were observed for FT BF samples as compared to other samples (P<0.05; 1way Anova, Dunn's test). **C** and **D.** Similarly, a significantly higher percentage of liker DNA chimeras was observed for blastocoel fluid samples from frozen thawed embryos as compared to spent media samples.

FT BF: Blastocoel fluid samples from frozen thawed embryos; **Fresh BF**: Blastocoel fluid samples from fresh embryo cultures
FT SM: Spent media samples from frozen thawed embryos; **Fresh SM**: Spent media samples from fresh embryo cultures

5.3.8.3. Chromosomal copy number analysis

The sequencing data from blastocoel fluid and spent media samples was further utilised for chromosomal copy number analysis and compared to the chromosome complement of their respective trophectoderm biopsies. The concordance rates between these samples and their corresponding TE biopsies were analysed separately as 1) karyotype, 2) euploidy, 3) aneuploidy and 4) individual chromosome concordance rates.

Only samples with optimal amplification were analysed for chromosomal copy number to compare and corroborate the karyotypes with that of their corresponding TE biopsies. The blastocoel fluid samples from frozen-thawed embryos failed to generate optimal sequencing results. For blastocoel fluid samples from fresh embryo cultures, the karyotype concordance rate with respect to TE biopsy was 66.66% (2/3), euploidy and aneuploidy concordance rate was 100% (2/2 and 1/1 respectively) and concordance at individual chromosome level was 99.28% (137/138) (**Table 28**) (**Appendix B**).

Spent media samples were amplified using either Sureplex, MDA or modified MDA method. The karyotype concordance rate was highest for Sureplex amplified samples from frozen thawed embryos, although the sample size was extremely small (100%; 2/2) followed in descending order by modified MDA samples from frozen thawed embryos (80%; 20/25), modified MDA samples from fresh embryo culture (70%; 7/10), Sureplex amplified samples from fresh embryo culture (57.14%; 4/7) and MDA amplified samples from frozen thawed embryos (33.34%; 1/3) (**Table 28**) (**Appendix B**). The individual chromosomal concordance rates for spent media samples are depicted in Table.

Table 28. Concordance rates for blastocoel fluid and spent media samples with respect to their corresponding TE biopsies

			Karyotype concordance rate	Euploidy concordance rate	Aneuploidy concordance rate	Individual chromosome concordance rate
1. Blastocoel fluid	modified MDA	Fresh culture	66.67% (2/3)	100% (2/2)	100% (1/1)	99.28% (137/138)
2. Spent media	modified MDA	Frozen-thawed	80% (20/25)	85.7% (6/7)	100% (18/18)	99.39% (1143/1150)
		Fresh (Day3-Day5 culture)	70% (7/10)	87.5% (7/8)	100% (2/2)	99.57% (458/460)
	MDA	Frozen-thawed	33.34% (1/3)	33.34% (1/3)	N/A	95.56% (132/138)
	Sureplex	Frozen-thawed	100% (2/2)	100% (2/2)	N/A	100% (92/92)
		Fresh (Day3-Day5 culture)	57.14% (4/7)	75% (3/4)	100% (3/3)	99.06 % (319/322)

The rates of false positives and false negatives for all the samples are shown in **Table 29**. The number of blastocoel fluid samples was very low (n=3) and the rate of false positive (0/2) and false negatives (0/1) was 0% in this group (**Table 29**).

Amongst spent media samples, the rate of false positives was lowest for Sureplex amplified samples from frozen thawed embryos (0%; 0/2) followed in increasing order as following: modified MDA samples from fresh embryo culture (12.5%; 1/8) < modified MDA samples from frozen thawed embryos (14.29%; 1/7) < Sureplex amplified samples from fresh embryo culture (25%; 1/4) < MDA samples from frozen thawed embryos (**Table 29**). No false negatives were observed for spent media samples amplified by modified MDA from frozen thawed embryos (0/18) and Sureplex amplified samples from fresh embryo culture (0/3) (**Table 29**). Modified MDA samples from fresh embryo culture had a false negative rate of 50% (1/2) but the sample size was very small (n=2) (**Table 29**).

Sensitivity and specificity rates were calculated for spent media samples amplified only by modified MDA method as the number of samples for Sureplex and MDA cohorts was considered too small to provide a reliable representation. The sensitivity for spent media samples from frozen thawed embryos amplified by modified MDA was 100% and specificity was 85.71%. Additionally, the samples from fresh embryo cultures had a sensitivity of 100% and specificity of 87.5%. The positive predictive value (PPV) for spent media samples from frozen thawed embryos was 94.74% and 66.67% for samples from fresh embryo cultures. Lastly, the negative predictive value (NPV) was calculated to be 100% for frozen thawed embryos and 100% for fresh embryo cultures.

Table 29. Rate of false positives and false negatives for blastocoel fluid and spent media samples with respect to their corresponding TE biopsies

			False positive rate	False negative rate
1. Blastocoel fluid	modified MDA	Fresh culture	0% (0/2)	0% (0/1)
2. Spent media	modified MDA	Frozen-thawed	14.29% (1/7)	0% (0/18)
		Fresh (Day3-Day5 culture)	12.5% (1/8)	0% (0/2)
	MDA	Frozen-thawed	66.67% (2/3)	N/A
	Sureplex	Frozen-thawed	0% (0/2)	N/A
		Fresh (Day3-Day5 culture)	25% (1/4)	0% (0/3)

5.4. Discussion

Currently, analysis of DNA from an embryo biopsy of a cleavage stage or blastocyst stage embryo is the gold standard for comprehensive chromosomal screening as well as preimplantation genetic diagnosis for monogenic disorders (Fragouli et al., 2011; Handyside et al., 2010; Munné et al., 1993; Sermon et al., 2016). However, this approach is invasive and necessitates highly skilled personnel along with expensive micromanipulators to perform the biopsies. In recent years, non-invasive sources of embryonic DNA such as blastocoel fluid and spent culture media have been explored with the ultimate aim of developing non-invasive chromosomal screening and genetic diagnosis methods (Hammond et al., 2016; Liu et al., 2017; Poli et al., 2013; Xu et al., 2016).

The main aim of this study was to develop an accurate non-invasive method for comprehensive chromosomal analysis of the embryo by utilising either blastocoel fluid or spent culture media. The study was successful in developing an approach for whole genome amplification of minute quantities (>1pg) of fragmented DNA which was further utilised for subsequent chromosomal copy number analysis of human embryonic DNA present in blastocoel fluid and spent media samples. Moreover, it was possible to accurately determine the sex of embryos from DNA derived from blastocoel fluid and spent media samples using the Y-chromosome assay. This non-invasive sexing assay has a potential application in distinguishing between male and female embryos for sex-linked disorders. The Y-chromosome assay consisted of a multiplex reaction which generated amplicons ranging from 77bp-138bp from 6 multicopy genes on Y-chromosome (**Figure 40**). The presence of multiple targets for primer annealing gives an increased likelihood that at least one locus will be successfully amplified when Y-chromosome material is present, even if highly degraded or if

the amount of DNA present is the equivalent of less than one cell. Using the Y-chromsome assay, all of the male samples from WGA products of blastocoel fluid and spent media were correctly identified with respect to genders of their corresponding TE biopsies.

5.4.1. Development of WGA method for minute quantities of fragmented DNA

Amplification of the entire genome is often technically challenging, especially for small quantities of DNA. Whole genome amplification facilitates global amplification of even minute amounts of DNA and provides sufficient quantities for further downstream analyses. In the past two decades, advances in WGA methods have enabled chromosomal screening and genetic diagnosis of human embryos from single or a small number of cells (Wells et al., 1999; Hellani et al., 2008; Johnson et al., 2010; Treff et al., 2010). DNA present in single cells is generally intact and appropriate storage and transportation measures are undertaken to prevent any potential DNA degradation prior to amplification. However, sometimes DNA degradation in cells occurs due to certain endogenous or external factors resulting in DNA fragmentation. The fragmentation of DNA reduces efficiency of PCR and impedes adequate amplification (Chung et al., 2004; Mccord et al., 2011; Putkonen et al., 2010). It was hypothesized that DNA present in blastocoel fluid and spent culture media would potentially be fragmented in nature. The main aim of this project was to develop an amplification method suitable for whole genome amplification of minute quantities of fragmented DNA.

Through sequencing of blastocoel fluid samples, Zhang and colleagues (2016) found two DNA fragmentation patterns; a majority of fragments ranged between 160-220bp and a small proportion was between 300-400bp. The majority population of DNA fragments was similar in size range of nucleosome spacing on DNA strand and was reminiscent of cell free DNA seen in circulating plasma of human blood (Mouliere and Rosenfeld, 2015). However,

the method used by Zhang and colleagues for determining the fragment size of DNA in blastocoel fluid entails adapter ligation followed by amplification using known sequences in the adapters. This method is sensitive to the size of DNA fragments and it is very likely that long DNA sequences (>1kb) cannot be captured by such an amplification strategy, thereby distorting the size distribution in blastocoel fluid samples. This concern is further reinforced by the fact that the amplification success rate obtained in this study was 72.7% (8/11) using the PicoPlex WGA method. The input size specifications for PicoPlex amplification as recommended by the manufacturer, Rubicon, is over 500bp and the average product size post WGA is bertween 300-500bp. Hence, if only <500bp DNA fragments are present in blastocoel fluid sample, the success rate of amplification using PicoPlex perhaps would be reduced.

In order to assess whether the existing whole genome amplification methods are capable of amplifying fragmented DNA successfully, an experiment was performed using different concentrations (1ng, 0.1ng, 0.01ng, 0.001ng) of a complex mixture of short amplicons ranging from 77-150bp encompassing at least 4 loci from each of the 24 chromosomes. Faint amplification smears were observed for 1ng concentration of amplicons amplified using MDA whereas no amplification was observed for any concentration of samples subjected to Sureplex amplification. This demonstrated that the two widely used WGA methods; Sureplex and MDA, used for CCS and PGD of human embryos, are not suitable for amplifying limited quantities of fragmented DNA.

To develop a method capable of capturing and amplifying a small amount of fragmented DNA, initially a direct adapter ligation based method was developed and tested. Briefly, different concentrations (ranging from 1ng to 1pg) of a known 150bp amplicon from *PLCz* gene were subjected to double stranded adapter ligation following blunting of the DNA

fragments. Subsequently, primers complementary to adapter sequences were used to amplify the ligated products. However, very faint bands of expected product size of ~250bp were observed but these were accompanied by large quantities of primer dimers in each sample. Blunt end ligation involves covalent joining of two blunt ended DNA molecules present in close proximity and is carried out by a DNA ligase enzyme (Ferretti and Sgaramella, 1981). As compared to cohesive end ligation, blunt end ligation is a relatively less efficient process especially when the input DNA concentration is low.

To circumvent this issue, a homopolymer tail mediated adapter ligation method was carried out. The principle of this method was described by Lazinski & Camilli (2013) for DNA cloning and library preparation from low input DNA samples. For our application, a homopolymer cytosine tail of controlled length (~20bp) was added to 3' termini of double stranded DNA fragments. This homopolymer tail enables annealing-assisted ligation of a defined hybrid adapter carrying a poly-G tail complementary to the poly –C homopolymer tail of the DNA fragment. Subsequently, the adapter ligated DNA fragments are further amplified by using primers complimentary to known sequence in the adapters. During the course of the method development, several optimisation steps were carried out on a known 150bp PLCz amplicon ranging in concentration from 1ng to 10pg. Of all the optimisation steps, faint product bands of expected size of ~280bp were observed increasing in intensity with sample concentration in the order 1ng<0.1ng<0.01ng. The expected products were observed with primer set P1+P3. However, primer set P1+P2 did not yield any products in the expected size range. The primer P3 has an increased specificity due to the presence of a poly-G tail which partially anneals to the homopolymer tail in addition to the complimentary sequence on the hybrid adapter. Due to the stable nature of the dC:dG base pairs, this ligation event is extremely efficient. Gel extraction of the 280bp product obtained after amplification with

P1+P3 primer set was subjected to further amplification using *PLCz* primers for the original insert. A distinct 150bp product was obtained of the expected size after this amplification which provided the proof of principle of this method, demonstrating successful amplification of a relatively small fragment of DNA.

In order to assess whether the homoploymer tailing mediated adapter ligation method is applicable to a more complex mixture of fragmented DNA, various concentrations (1ng, 0.1ng and 0.01ng) of 6 amplicons (ranging from 77bp-138bp) from the Y-chromosome assay were amplified. In addition, DNA from 2 isolated male buccal cells was initially enzymatically fragmented into approximately 120bp fragments and thereafter amplified by homopolymer tailing mediated adapter ligation amplification. Product smears ranging in size from 250-350bp were obtained for all the input samples from Y-chromosome assay and one buccal cell sample, C1. It is possible that the cell might have been lost during the attempt to transfer it to the sample tube. The gel extracted products (250-350bp) from the successfully amplified samples were further amplified using primers for 5 genes from Y-chromosome assay. Successful amplification of 4 genes was obtained in 0.1ng and 0.01ng samples whereas only 2 genes successfully amplified in the buccal cell sample C1. It can be inferred that either the quality of DNA present in the single buccal cell was partially degraded or the random enzymatic fragmentation resulted in fragments which lacked either one (or both) of the primer binding sites thereby leading to amplification failure.

The direct adapter ligation (Method A) and homopolymer tail mediated adapter ligation (Method B) methods would yield libraries compatible for sequencing on lllumina platforms as the adapters ligated to the DNA fragments during these methods contain Illumina chemistry compatible sequences. However, Method A generated extensive primer

dimers, especially for low molecular weight samples. Both of these methods seem to work for relatively shorter fragments of DNA of uniform size but if the DNA fragments vary in amplicon sizes then it might pose a problem during subsequent sequencing. Moreover, the methods were developed on the hypothesis that the DNA present in blastocoel fluid and spent culture media might be fragmented in nature and the size of these fragments would be approximately 180bp, similar to nucleosome sized DNA fragments. In order to address the possibility of the presence of fragmented as well as longer, intact DNA sequences within these samples, a modified amplification method based on DNA ligation and MDA was developed.

It has been suggested by Shamonki et al. (2016) that spent culture media contains cell free DNA, in part due to the lack of observation of any intact cells in these samples. However, it is possible that lysing cells are present in culture media which may contain an intact nucleus. Hence, it is possible that these non-invasive sources of embryonic DNA contain a complex mixture of fragmented as well as intact DNA. In order to address this possibility, a modified MDA method was developed based on the principle of ligation of fragmented DNA in order to form long DNA concatamers which further serve as an ideal template for MDA. In theory, the method would be able to capture fragmented DNA by ligation mediated amplification and the long, intact DNA sequences would be amplified by standard MDA in the same reaction. The principle behind ligation mediated MDA to amplify complex mixture of short DNA fragments was first described by Shoaib et al. in 2008. Based on the same principle, a modified MDA method was developed for our application.

To test the proof of principle of modified MDA, different concentrations of PCR amplified Y-chromosome assay products were subjected to amplification by conventional MDA and modified MDA. The absence of products for conventional MDA amplified samples

suggests that the sample does indeed contain short fragments of DNA (which cannot be efficiently amplified by MDA). This is because phi29-DNA polymerase based Multiple Displacement Amplification requires a template at least 2 kilobase long for successful amplification (Dean *et al.*, 2002). For samples amplified by modified MDA, amplification efficiency was observed to decrease with decreasing concentration (1ng< 0.1ng< 0.01ng< 0.001ng). It is likely that small concentrations of DNA fragments do not generate long enough concatamers post ligation to serve as optimal templates for phi29 polymerase. To circumvent this issue, a fixed quantity of a 60bp artificial oligonucleotide derived from pUC19 vector (linker DNA) was added to the ligation reaction which aided in generating longer concatenated templates and resulted in successful amplification of picogram quantities of input DNA fragments. By performing PCRs for two genes (*DAZ* or *RBMY*) from Y-chromosome assay on cleaned up modified MDA products (>750bp), only samples wherein the linker DNA was added during WGA successfully amplified for all concentrations of input samples (1ng, 0.1ng, 0.01ng, 0.001ng).

Furthermore, amplification of modified MDA products by Klentherm DNA polymerase (lacking 5'-3' exonuclease activity) with Y-chromosome assay primers generated a ladder like pattern of amplicons. This proves that the concatenation worked with the aid of linker DNA in these samples and the amplicons from Y-chromosome assay were ligated into long concatamers be before WGA. In order to assess the incorporation of linker DNA into the ligated concatamers, restriction digestion was performed using AluI enzyme as the linker DNA has a restriction site for AluI. A ladder-pattern of DNA bands was observed only for samples containing linker DNA which indicated that the linker DNA was present in the successfully amplified products of these samples.

5.4.2. Experimental validation of modified MDA method

Next, experimental validation of modified MDA method was carried out on different concentrations of a complex mixture of over 200 amplicons as well as isolated single cells from buccal samples. Samples containing different concentrations of the mixture of amplicons (10ng, 1ng, 0.1ng, 0.01ng and 0.001ng), to which linker DNA was added during modified MDA process, were all successful in amplification. However, lower concentrations of complex amplicon samples (0.01ng and 0.001ng) without the addition of the linker DNA failed to yield optimal WGA products. Hence, it could be inferred that addition of the linker DNA aids in formation of long concatamers of DNA fragments of optimal length to serve as a template for phi29 polymerase mediated MDA, especially for low concentration of input samples. This is in line with the experimental findings of Shoaib and colleagues (2008) who demonstrated that addition of an artificial oligonucleotide was necessary for optimal amplification of low concentrations of fragmented DNA.

The analysis of sequencing data of these modified MDA samples revealed the presence of four types of chimeric sequencing reads based on different types of ligation junctions; which comprised of a combination of either genomic sequences from the same chromosome, genomic sequences from different chromosomes or linker DNA sequences. A majority of sequencing reads from single cell samples consisted of a single genomic loci (without any ligation junctions) as the DNA would be intact in the nucleus of these isolated cells. A small percentage of genomic chimeras within the same chromosome (3.66%) in sequencing reads of single cell samples were also observed. Several studies have reported the presence of chimeric sequences in the products amplified by phi29 enzyme due to the formation of hyperbranched structures during the strand displacement activity of MDA process (Lasken and Stockwell, 2007; Tu *et al.*, 2015). Thus, this hyperbranching provides

numerous binding positions to DNA polymers which tend to choose a close position from the branching polymers within the same chromosome in order to generate a thermodynamically stable structure.

For samples consisting of a complex mixture of amplicons and linker DNA, only a small percentage of sequencing reads were found to contain single genomic loci (3.92% - 10.35%). However, for 0.001ng sample, very small proportion of single genomic loci was detected Hence, it can be concluded that > 0.01ng concentration of DNA fragments can be amplified using the developed modified MDA approach. Excluding the 0.001ng sample, with respect to decreasing concentration of input DNA fragments (1ng<0.1ng<0.01ng), the proportion of genomic + linker DNA sequences was found to increase whereas the percentage of genomic chimeras between different chromosomes was observed to decrease. This can be explained by the fact that with decreasing concentration of input DNA, more fragments will ligate to linker DNA as compared to each other hence giving rise to more genomic + linker DNA chimeras as opposed to genomic chimeras between different chromosomes. Moreover, the representation of linker + linker DNA chimeras was observed to increase with decreasing input DNA concentration, a finding in line with expected results as in absence of genomic DNA fragments, the linker DNA ligate to each other and amplify during subsequent MDA.

Collectively, the results from experimental validation of modified MDA approach proved the method's proof of principle and demonstrated its applicability to minute quantities (>0.01ng) of complex mixture of fragmented DNA.

5.4.2. Clinical validation of modified MDA method on blastocoel fluid and spent media samples

Of all the three developed methods for amplification of fragmented DNA, modified MDA method was used to assess the DNA present in blastocoel fluid and spent media samples from human embryos. Modified MDA method performed better than the other two adapter ligation based amplification approaches during the optimisation and validation phase of this study.

Out of the 26 blastocoel fluid amplified by modified MDA, only 30% of samples from fresh embryo cultures successfully amplified. However, optimal amplification was not observed from any of the blastocoel fluid samples from frozen thawed blastocysts. The practice of collapsing blastocyst cavity prior to vitrification is already used by some laboratories as studies have shown that this increases the embryo's survival rate post thawing (Hiraoka & Kinutani, 2004; Mukaida et al., 2006). The vitrified blastocysts used for this study were thawed and placed in culture medium overnight which led to re-expansion of the collapsed blastocoel cavity. However, the amount of DNA accumulating during this re-expansion period (<24 hours) would be comparatively less than that accumulating during fresh embryo culture wherein DNA is potentially accumulated in blastocoel cavity for one (Day-5 embryo) or two days (Day-6 embryo). A potential explanation for the low success rate of amplification of blastocoel fluid from fresh embryo culture can be the degraded nature of DNA present in these samples. A previous study on cell death in human embryos using differential labelling showed that cell death occurred in both, inner cell mass and trophectoderm of normally fertilised embryos (Hardy et al., 1989). Hence, DNA found in blastocoel fluid may come from dead or dying cells from inner cell mass and trophectoderm and can therefore be degraded in nature.

A recent study by Zhang et al. (2016) reported a 72.7% (8/11) amplification success rate of blastooel fluid. This was in line with a few more studies on WGA of blastocoel fluid samples using PCR-based methods which reported the amplification efficiency of 63% (60/96) (Tobler *et al.*, 2015), 76.5% (39/51) (Gianaroli et al., 2014), 80% (4/5) (Palini et al., 2013) and 82% (95/116) (Magli *et al.*, 2016) respectively. A possible explanation for discrepancy in the amplificaton success rates between our study and that reported previosuly could be how the amplification 'success' was defined. In the present study, amplification was defined as successful only if the WGA products were of optimal quality for downstream sequencing and chromsomal copy number analysis. Degraded DNA can also yield WGA products on an agarose gel but such an amplification can prove to be suboptimal for downstream processes such as aCGH, qPCR or NGS.

The use of spent IVF culture media from blastocyst stage embryos for the purpose of non-invasive chromosomal screening of embryos was first reported by Shamonki et al. (2016). Since then several groups have published studies on the feasibility of using spent culture media for the purpose of non-invasive genetic testing for aneuploidy. The amplification success rates of DNA from spent media reported by these groups have approximately ranged between 70 to 85% (Shamonki et al., 2016; Xu et al., 2016; Feichtinger et al., 2017). Even though differences in culture media conditions and ensuing volumes used for amplification might explain the differences in the amplification success rates amongst various groups, the method used for WGA might also have contributed to the observed differences. In order to compare the efficiencies of different WGA methods; spent media derived from frozen thawed as well as fresh embryo cultures were subjected to amplification by Sureplex, MDA or modified MDA method.

Overall, DNA amplification rates were superior in the samples amplified with modified MDA compared to those amplified by Sureplex and MDA methods: 87.5% (35/40) versus 47.37% (9/19) and 21.05% (4/19) respectively (P<0.005). Of note, the media samples which failed to amplify mainly belonged to the cohort frozen (at -20°C) for over a month before amplification. The preliminary data analysis demonstrates modified MDA to be superior for spent media samples as compared to the most commonly used WGA methods (Sureplex or MDA).

Sureplex and MDA methods are widely used clinically for single cell WGA especially for the purpose of PGT-A and PGD (Handyside et al., 2010; Thornhill et al., 2005). Sureplex amplification utilises the combination of multiple strand displacement pre-amplification and PCR based amplification for WGA. The use of quasi-random primers generates products ranging from 300-500bp from DNA template of >500bp (Czyz et al., 2015). On the other hand, MDA relies on phi29 mediated isothermal amplification which utilises strand displacement activity to generate amplification fragments >10kb from long DNA templates (Paez *et al.*, 2004). The fact that modified MDA method was superior to Sureplex and MDA for amplifying DNA from spent culture media suggests that the DNA fragments found in such samples are at least a couple of kilobases, but not long enough to serve as template for phi29 based conventional MDA. If the DNA fragments in spent media were of the size of nucleosome bound DNA (~180bp), we wouldn't obtain about 50% amplification success rate with Sureplex (which requires >500bp long template) as observed during our study. Moreover, the fact that after ligating the DNA fragments during modified MDA method, the amplification success rate was significantly higher as compared to other WGA methods, proves that DNA is indeed fragmented in nature in spent media but not to the extent we initially hypothesised. Hence, the modified MDA method is best suited amongst the three amplification methods to salvage

the large fragments of DNA present in spent media samples thereby resulting in optimal amplification for chromosomal copy number analysis.

5.4.3. Analysis of nature of DNA fragments in blastocoel fluid and spent media samples

The analysis of chimeras generated during the modified MDA process helped shed some light on the nature of DNA in spent media and blastocoel fluid samples. The blastocoel fluid samples from frozen-thawed embryos had a significantly higher proportion of genomic chimeras between chromosomes as compared to blastocoel fluid samples from fresh embryo cultures and spent media samples. It can be inferred that the fragment size of DNA present in blastocoel fluid from frozen thawed embryos is smaller than in blastocoel fluid samples from fresh embryos and spent media samples from both, fresh and frozen thawed embryos. This was further supported by the observation that the percentage of linker+linker DNA chimeras were significantly higher in blastocoel fluid samples from frozen thawed embryos than blastocoel fluid samples from freshly cultured embryos as well as spent media samples. As there was no significant difference in proportion of genomic chimeras between chromosomes in spent media samples, it could be inferred that the DNA fragments are of similar size in spent media samples from either fresh or frozen-thawed cultures.

As seen from the validation experiments, the proportion of genomic + linker DNA chimeras increase with decreasing input DNA concentration. It was observed that the blastocoel fluid samples from frozen thawed embryos had a significantly higher amount of genomic + linker DNA sequences as compared to spent media samples from frozen thawed embryos. Hence the DNA concentration in blastocoel fluid samples from frozen thawed embryos was comparatively lower. Moreover, it seemed that DNA in spent media samples from fresh embryo cultures was relatively lower as compared to that present in spent media

samples from frozen-thawed embryos as the genomic+linker DNA percentage was significantly higher in spent media samples from fresh embryo cultures. Taking all the data from different types of chimeras into consideration, it can be inferred that embryonic DNA present in blastocoel fluid from frozen thawed embryos seems to be more fragmented and less in concentration as compared to blastocoel fluid from fresh embryo cultures and spent media samples (from both, fresh and frozen thawed embryos).

After the activation of human genome at Day-3 post fertilisation, the cellular differentiation begins at the morula stage leading to lineage segregation of cells into ICM and TE (reviewed by Niakan et al., 2012). Cell death has been reported to occur in even normally developing embryos, in both ICM and TE (Amit *et al.*, 2000). This suggests a possible role of apoptosis in the regulation of cell number and embryo development and these dying cells could be a source of DNA in the blastocoel fluid. Hence, the blastocoel fluid derived from freshly cultured embryos will have DNA accumulating in it from these sources during the course of embryo development (from morula till blastocyst stage). However, in the case of frozen thawed embryos, the previously collapsed blastocoel cavity re-expands and is in culture for a relatively shorter time, thereby potentially limiting the amount of DNA shed in the blastocoel cavity.

Even though the chimeric sequences between blastocoel fluid from fresh embryo culture and that from spent media from either fresh or frozen thawed embryos did not vary significantly, suggesting a similarity in DNA fragment sizes amongst these samples, the quality of amplification and sequencing reads was sub-optimal for blastocoel fluid samples.

5.4.4. Analysis of chromosomal content of blastocoel fluid and spent culture media

Some of the whole genome amplified samples subjected to NGS failed to yield optimal sequencing results. For chromosomal copy number analysis, only samples with quality score <8.5 on Nexus software were included for analysis. Hence for concordance calculations, the number of blastocoel fluid samples amplified by modified MDA and spent media samples amplified by MDA and Sureplex were fairly low as the sequencing quality of these samples was not optimal. The number of samples with their chromosomal complement analysed were fairly low for blastocoel fluid samples as well as MDA and Sureplex amplified spent media samples for any sort of comparison between the chromosomal concordance rates.

Most of the spent media samples generated adequate chromosomal copy number profiles which were then analysed for concordance rates with their corresponding TE biopsies. The karyotype concordance between spent media samples (amplified by modified MDA) and TE biopsy was 80% for frozen thawed embryos and 70% for embryos from fresh cultures. The ploidy concordance rate was similar for spent media samples from both, fresh and frozen thawed embryos.

The false positive rate for spent media samples from frozen thawed embryo was 14.29%. The false positives observed in spent culture media most likely arose due to mosaicism. Mitotic aneuploidy is observed commonly during embryonic development resulting in mosaicism (Fragouli et al., 2013; Munné et al., 1994). It is possible that these mitotically aneuploid cells were shed in spent media during embryo culture and were later detected as false positives. There were no false negatives observed for spent media samples obtained from frozen thawed embryos.

One of the main concerns about NI-PGTA using spent media is the potential contamination from maternal cumulus cells which might result in false negative results. Hence, only patients undergoing ICSI fertilization (which warrants removal of cumulus cells) can be safely offered this test in future. Also, usage of sequential media wherein the embryo is transferred to a different media droplet from Day-3 to Day-5/6 growth might help in reducing the chances of maternal DNA contamination.

5.4.5. Summary

The clinical efficacy of non-invasive PGT-A still remains to be fully established. Even though numerous studies have published reports on the applicability of the method using either blastocoel fluid or spent culture media, the specificity and sensitivity reported by most of the groups have remained fairly modest for a clinical application (Feichtinger et al., 2017; Gianaroli et al., 2014; Hammond et al., 2016; Shamonki et al., 2016; Tobler et al., 2015). However, Xu et al. (2016) have reported clinical application of NI-PGTA using spent media from frozen-thawed embryos and shown a high rate of specificity and sensitivity. This discrepancy in results is due to the biological, clinical and technical variability associated with the non-invasive assays which include differences in culture media systems and conditions utilised in different IVF clinics, timing of the sample collection and differences in amplification systems and downstream processing carried out by different groups. Hence, it is pertinent to develop a universal non-invasive PGTA assay.

In summary, a modified MDA method was developed and validated for amplifying and assessing the genetic contents of blastocoel fluid and spent culture media. The data analysis demonstrates modified MDA to be superior for spent media samples as compared to the most commonly used WGA methods (Sureplex or MDA). The results confirm that the analysis of

media represents a promising strategy for non-invasive PGT, frequently yielding genetic material, which is representative of the embryo when appropriately amplified. While further experiments need to be performed to verify this data on larger sample sizes, results are encouraging.

Chapter 6: Investigating imprinting landscape of preimplantation embryos

The main aim of this chapter was to develop a method capable of detecting imprinting perturbations at multiple DMRs simultaneously in cells derived from preimplantation human embryos. It further endeavoured to characterise the methylation patterns of 20 imprinted genes in TE and ICM samples from euploid human blastocysts.

6.1. Introduction

Genomic imprinting is one of the best studied examples of epigenetic regulation in placental mammals. In autosomal cells, genes are generally biallelically expressed, i.e. both maternal and paternal alleles are expressed at a particular locus. However, genomic imprinting, results in the expression of a single parental copy in certain genes (Reik and Walter, 2001). One allele of the imprinted gene is epigenetically silenced while the other remains transcriptionally active.

Genomic imprinting in mammals was discovered in the 1980s as a result of nuclear transplantation experiments in mouse involving uniparental embryos (embryos having two copies of either the maternal or paternal chromosomes) and uniparental disomy (embryos with both copies of certain chromosomes from one of the parents) (Surani et al. 1984; McGrath and Solter 1984). The mice parthenogenetic experiments showed that embryos containing two maternal genomes (gynogenotes) or two paternal genomes (androgenotes) were unable to survive past mid-gestation (McGrath and Solter); thus demonstrating that both parental genomes were necessary for the development of viable embryos. This introduced the concept of genomic imprinting and imprinted genes (Barton and Surani, 1984).

6.1.1. Elements of imprinted genes

Seventy percent of the CpG dinucleotides in the genome are methylated with the exception of CpG islands (CPIs). CPIs are regions of the genome which are rich in CpG dinucleotides, generally found in or close to promoter regions and protected from methylation. However, CPIs are subject to methylation in the inactive X-chromosome in females, in differentially methylated regions (DMRs) of imprinted genes and in cancer cells. DMRs display different methylation patterns for the male and female alleles and play a crucial

role in silencing one of the two parental alleles in imprinted genes. The majority (80%) of imprinted genes occur in clusters and share common DMRs and other regulatory elements (Reik and Walter, 2001). The pattern of differential methylation in DMRs is established during germ cell maturation and often maintained during embryonic development. However, occasionally modifications in the methylation patterns of the DMRs occur during development, which lead to tissue specific expression of imprinted genes (Reik and Walter, 2001).

Imprinted gene clusters can be regulated by imprinting control regions (ICRs) or control elements (CE) which coordinate and control the expression of two or more imprinted genes (Reik and Walter, 2001). ICRs are rich in CPIs and can be up to several kilobases in length. The allelic methylation at most of the ICRs originates during oogenesis and is only occasionally established during spermatogenesis.

6.1.2. Genomic imprinting life cycle

The maintenance of methylation at imprinted loci during the first wave of genome-wide demethylation after fertilisation remains a challenging question. The paternal genome undergoes active demethylation in the pronuclear stage unlike the maternal genome. Hence it might be that the methylated paternal DMRs acquire a specialized chromatin structure which protects them from remodelling and demethylation. The maternally methylated DMRs seem to be enzymatically protected against demethylation, but the enzymes involved remain unknown (Sasaki and Matsui, 2008).

The resetting of the imprints in the germ cells takes place in two stages; the erasure and the reestablishment of the imprints. In mice, a genome wide demethylation in the germ cells leads to the erasure of imprints and is completed in both sexes by embryonic day 12-13

(E12-13) (Hajkova et al., 2002; Lee et al., 2002). Erasure is followed by establishment of the imprinting marks by *de novo* methylation which begins at late foetal stage and continues after birth until the development of mature germ cells. The oocytes are in a meiotic arrest and methylation occurs during their growth, which is not complete until just prior to ovulation. Contrarily, the establishment of paternal methylation marks on the imprinted genes is completed before meiosis by the round spermatid stage during spermatogenesis (Hajkova *et al.*, 2002).

After the imprints are established, maintained and transmitted from parent cells to daughter cells during replication, only the maternal or paternal allele is expressed in these cells. Imprinted genes are largely regulated by epigenetic modifications of promoter sequences, silencer sequences (DNA sequence where repressor molecule binding leads to transcriptional silencing), boundary elements (DNA sequences positioned between enhancer and promoter, preventing their interaction) and overlapping of antisense transcripts (Li & Sasaki, 2011). Therefore, the differential methylation of parental alleles in specific elements of imprinted gene regulates expression majorly at transcriptional level by using the transcriptional control mechanisms.

6.1.3. Assisted reproductive techniques and epigenetics

Assisted reproductive techniques (ARTs), involving the manipulation of gametes in a laboratory, have been utilized to treat infertility for four decades. As the epigenetic reprogramming occurs during the critical phases of gametogenesis and embryogenesis, environmental disruption during these processes could be detrimental.

ART involves ovarian stimulation in order to produce multiple eggs in a single menstrual cycle. As the methylation and establishment of the imprints is completed just prior

to ovulation, the retrieval of partially methylated oocytes may disrupt the imprinting patterns (Gicquel *et al.* 2008). Furthermore, numerous mouse studies explored the effect of culture media on imprinting patterns in oocytes and developing embryos, demonstrating the sensitivity of the imprints to the culture environment (Mann *et al.* 2004; Khosla *et al.* 2001). Moreover, the incidence of imprinting disorders such as Beckwith-Wiedeman and Angelmann syndrome has been found to be increased in children born after ART compared to those conceived naturally (Amor and Halliday, 2008; Lennerz et al., 2010; Maher et al., 2003; Rossignol et al., 2006; Sutcliffe et al., 2006).

6.1.4. Aims

To date, it has been difficult to investigate imprinting defects in human embryos. The main limitation is the availability of reliable techniques that allow the detection of methylation patterns at multiple loci simultaneously, especially in few cells. Therefore, the main aim of this project was to develop a technique that is capable of assessing methylation patterns at a large number of important imprinted loci in preimplantation embryo biopsy specimens.

More specifically, the sub-aims were:

Sub-aim 1: To optimize a bisulfite sequencing method suitable for assessing multiple imprinted loci in embryo biopsy specimens

Sub-aim 2: To assess differences in the patterns of DNA methylation at imprinted loci in cells of the trophectoderm and inner cell mass derived from euploid blastocysts

6.2. Materials and Methods

6.2.1. Bioinformatics

6.2.1.1. Selection of DMRs for imprinted genes panel

A list of 20 characterised differentially methylated regions (DMRs) implicated in genomic imprinting was compiled from various sources including literature, websites (www.geneimprint.com) and online tools (http://epigenomegateway.wustl.edu/). **Table 30** shows the full list of the DMRs included in this study with the germline-specific origin of methylation and the associated imprinted disorders. The methylation status of the chosen DMRs associated with different imprinted genes was further visualised in different types embryonic stem (ES) cells using the epigenome web-browser (http://epigenomegateway.wustl.edu/) (**Figure 57**).

Moreover, the methylation levels in trophoblast (from *in vitro* differentiated cells from a male embryo originated from H1-hESC) was averaged over all the DMRs included in the panel in order to verify the methylated status of the chosen DMRs for the study (**Figure 58**).

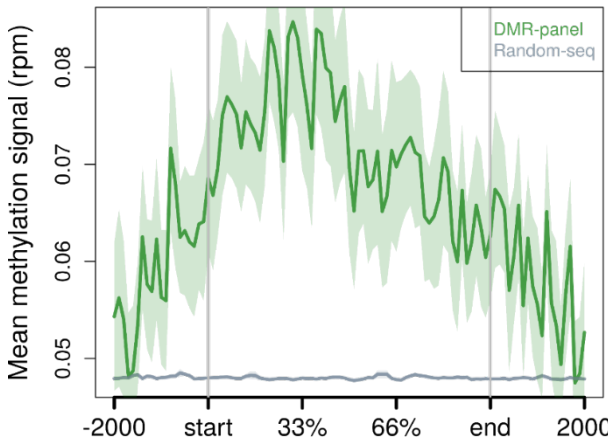


Figure 57. Methylation status of chosen DMRs in trophoblast cells from a human embryo. The figure shows the methylation level in trophoblast averaged over all DMRs in the imprinted genes panel. The methylation profile is cantered over each DMR and the surrounding 2kb region around DMRs is also shown. The DMR-panel is compared with 100,000 randomly generated sequences (each 3000bp long). Overall, the DMR-panel regions have relatively higher methylation level compared to randomly generated sequences and surrounding regions. This analysis was performed by a bioinformatician, Siddharth Sethi.

Table 30. List of DMRs included in the development of imprinted genes panel.

DMR	Chr	Extent of DMR			Number CpGs	Methylation origin	Germline derived	Associated disease
		Start	Finish	Size				
DIRAS3	1	68515433	68517545	2112	88	M	Oocyte gDMR	MLID
ZDBF2	2	207114583	207136544	21961	439	P	Sperm gDMR-secondary DMR	
NAP1L5	4	89618184	89619237	1053	57	M	Oocyte gDMR	MLID
PLAGL1	6	144328078	144329888	1810	143	M	Oocyte gDMR	TNDM; MLID
IGF2R	6	160426558	160427561	1003	74	M	Oocyte gDMR	MLID
GRB10	7	50848726	50851312	2586	171	M	Oocyte gDMR	MLID
PEG10	7	94285537	94287960	2423	119	M	Oocyte gDMR	MLID
MEST	7	130130122	130134388	4266	226	M	Oocyte gDMR	MLID
H19	11	2018812	2024740	5928	250	P	Sperm gDMR	SRS/BWS
KCNQ1OT1	11	2719948	2722259	2311	192	M	Oocyte gDMR	BWS (rare Sotos syndrome)
IG-DMR	14	101275427	101278058	2631	64	P	Sperm gDMR	TS14/KOS14
MEG3	14	101290524	101293978	3454	188	P	No-secondary DMR	TS14/KOS14
SNRPN/SNURF	15	25200004	25201976	1972	113	M	Oocyte gDMR	PWS/AS
ZNF597-1	16	3481801	3482388	587	29	M	Oocyte gDMR	
ZNF597-2	16	3492828	3494463	1635	76	P	No-secondary DMR	
PEG3	19	57348493	57353271	4778	221	M	Oocyte gDMR	MLID
NNAT	20	36148604	36150528	1924	135	M	Oocyte gDMR	
GNAS-NESP	20	57414039	57418612	4573	257	P	No-secondary DMR	PHP
GNAS-AS1	20	57425649	57428033	2384	128	M	Oocyte gDMR	PHP
GNAS-XL	20	57428905	57431463	2558	200	M	Oocyte gDMR	PHP

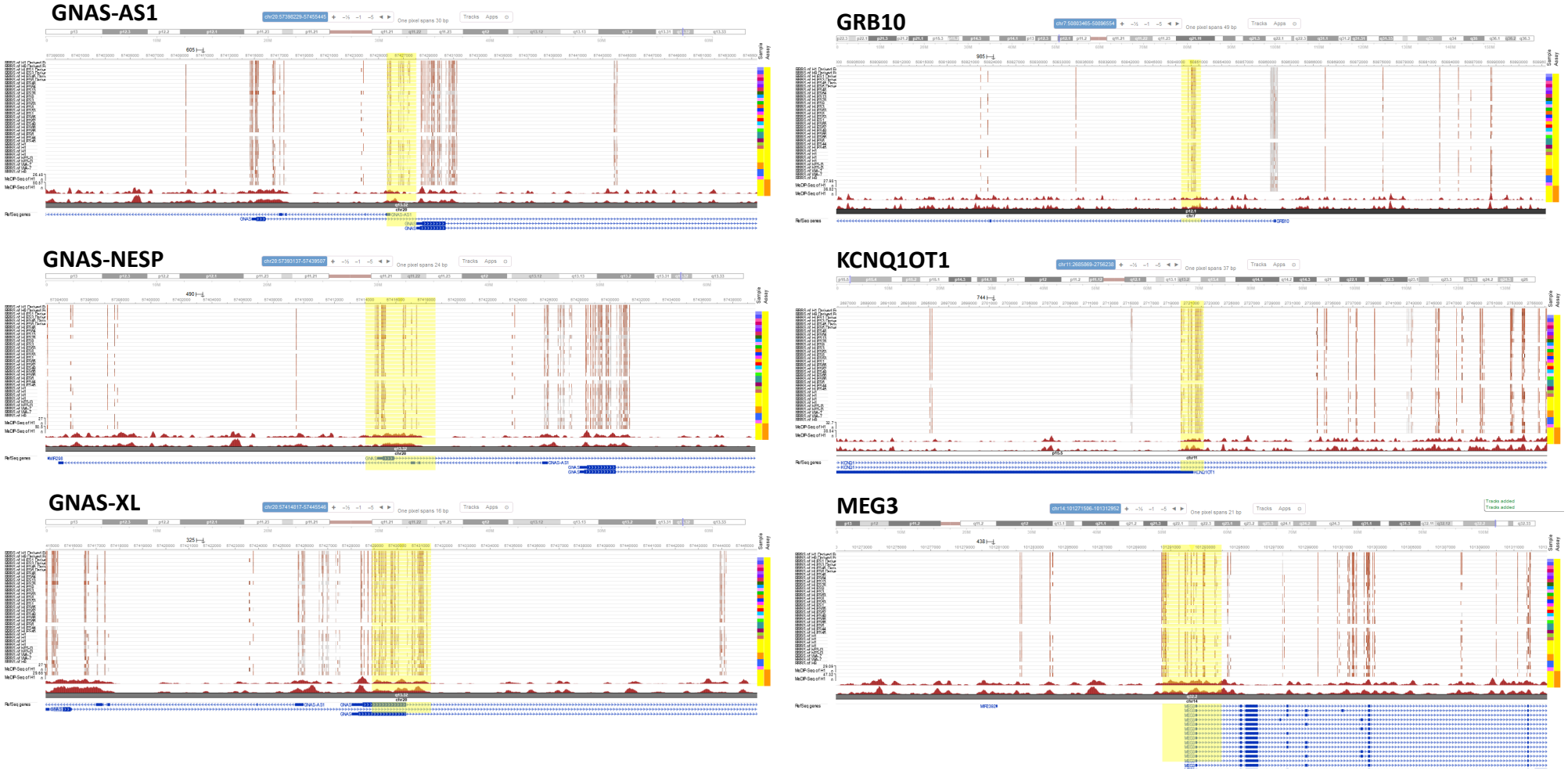


Figure 58. Methylation status of DMRs of imprinted genes panel in ES cells. The figure shows the methylation status of 6 imprinted genes for various embryonic stem (ES) cells (each horizontal line represents methylation data from different types of stem cells) obtained from the epigenome web browser. The red lines represent the CpG enrichment and depict CpG islands for each DMR. The yellow highlighted regions are the DMRs included in the imprinted genes panel for our study. Hence, this shows that the regions included in our study are known to be methylated in various types of embryonic stem cells.

6.2.1.2. Bisulfite converted DNA primer design

In order to investigate the methylation patterns associated with the above-mentioned 20 DMRs in human embryos, an imprinted genes panel consisting of 23 primer pairs from the DMRs of interest was developed. The primers for this panel were designed as described in **Section 3.4.2**. The list of the primers is shown in **Table 31**.

Table 31. List of primers designed for imprinted genes panel.

Primer pair number	Primer name	Primer sequencing	Amplicon size
1	DIRAS3-F	GAAAGATTTGGTTTTAGTTTTAGGGA	217
	DIRAS3-R	ATAAACTCTTAAAATATCCAATTAATTACC	
2	ZDBF2-F	TATAGGAAGTTTGTTTATATGGGTAGGTG	229
	ZDBF2-R	TCCTCTTCTCTCTAAAATCTATCAATAACA	
3	NAP1L-F	GGGGTTTTTTAGTTATTTGATTAGT	202
	NAP1L-R	AAAACCCTCCTAAACCTCTAC	
4	NAP1L5-F	GATATTTTGGGAAAAATAAAATTAGGT	300
	NAP1L5-R	AAATATAATAACATCTATAAACCCCT	
5	PLAGL1-F	TTATGTGTTAAGTAAGTAATTTTTGAGTTTAG	198
	PLAGL1-R	TAAAAACACCCAACTTAAATCCTCC	
6	IGF2R-F	GGGATAGTGGGAGTTGTTTAGG	245
	IGF2R-R	CCCACAACACCAAACTAATAACC	
7	GRB10-F	TGGTTATATAATATTGTTTTATGGTTGG	247
	GRB10-R	CTCTCCAAATACTCAAATAAACTCC	
8	PEG10-F	GTTTGGTTTAGGTGTGGGATTTTAT	228
	PEG10-R	CCCAAACCTTTAAAACTTAATTTCC	
9	MEST-F	TGGTGGGTTTAATAGAGTTTGTTGT	290
	MEST-R	CCTAAATACCCCAACTCTTTCCTTA	
10	H19-F1	TTTAGATTGTGATGTGAGTTATTATTGT	281
	H19-R1	AAATAAATTTACCCACAAATATTCCC	
11	H19-F2	GGGTTGTGATGTGTGAGTTTGT	164
	H19-R2	AAACTTCCCATTCAATCTTAAATACC	
12	KCNQ1OT1-F	GGTAGGATTTTGTTGAGGAGTTTT	300
	KCNQ1OT1-R	CACACCCAACCAATACCTCATA	
13	MEG3-F1	AGTTGGGATTATAGGTATTATGTTTGGA	292
	MEG3-R2	AAATAACCCCATCCCTAATATTCAA	
14	MEG3-F2	GGATTTATTGGAGGATTTTGGATT	243
	MEG3-R2	AACCCCTCACTAACCTTATCACAA	
15	SNRPN/SNURF-F1	GGGGTATTAGAAGGGGTAGTAGTAT	267
	SNRPN/SNURF-R1	CCAAACATCACCTAACCTATCAATC	

Primer pair number	Primer name	Primer sequencing	Amplicon size
16	SNRPN/SNURF-F2	GTGGGTATATTAGGGTGATTGTAGTTT	260
	SNRPN/SNURF-R2	CCTAATCCACTACCATAACCTCCTC	
17	ZNF597-F1	GTGTAGTTGGTGGTTAAGTTGGAGA	254
	ZNF597-R1	CTTACTCCCTAAAACTCAACAAAA	
18	ZNF597-F2	ATGTAGTGGATATGGTTAGGTATATGG	221
	ZNF597-R2	AAATCTCCAACTTAACCACCAACTA	
19	PEG3-F1	TGAGTTTGGTTTTGGATTTTATTTT	249
	PEG3-R1	ATTCATTCATTCTATACCATCTTTACC	
20	PEG3-F2	GGAGGTGAGGGTGTTTTTAGTTT	195
	PEG3-R2	ACTCACCCCTTCCCCTATTATTAC	
21	NNAT-F	TGAAGTAGAGGATTTGGGTTTAAAAT	213
	NNAT-R	CCCCAATCCCTAACCTACAAAT	
22	GNAS-NESP-F	AGAAAGATTAGTTTTAAATAAGTTGGTTT	243
	GNAS-NESP-R	TTAATTATCAACTCTAAAACCTAAACTCC	
23	GNAS-AS1-F	ATTAAGGTTATTAGGTGGTGTGGGT	249
	GNAS-AS1-R	CTAATCAATCAACTCCTTTAACCCC	

6.2.2. Experimental methodologies

6.2.2.1. Sample characteristics

The optimisation of the protocols were performed on isolated buccal cells and control human male and female genomic DNA as described in **Section 3.1**. As controls, Zymo's methylated human genomic DNA was used (CambridgeBioScience, UK) as 100% methylation control whereas WGA products (using MDA) from genomic DNA were used as unmethylated control.

Inner cell mass and TE cells from 9 human embryos were used to assess the imprinting landscape of 23 imprinted loci included in this study. Surplus embryos during IVF cycles were donated for research to RMA, New Jersey/ Foundation for embryonic competence (USA). Appropriate IRB ethics were acquired to use these embryos for this particular study. All the embryology related protocols were performed by an embryologist from Foundation for embryonic competence, Katherine Scott. In brief, each embryo was split into three

trophectoderm biopsies and one inner cell mass biopsy. Moreover, the embryos had previously undergone PGT-A and all the embryos utilised for this study were chromosomally euploid. Of all the biopsies, one TE and ICM biopsy for each embryo was used for this study.

6.2.2.2. Bisulfite conversion of DNA

The EZ DNA Methylation-Direct Kit (Zymo Research) was utilized for bisulfite treatment of genomic DNA. Proteinase K, CT conversion reagent and M-reaction buffer were prepared prior to the experiment as per the manufacturer's protocol. For the bisulfite treatment of genomic DNA derived from whole blood or methylated and unmethylated controls (Zymo Research, UK), 20µl of samples were added to 130µl of CT conversion reagent and incubated for 3.40 hours at 64^{o}C. For the bisulfite treatment of embryo biopsies (ICM and TE), the protocol was slightly changed to ensure complete conversion and to prevent sample loss. Cell lysis of embryo biopsies was carried out using Proteinase K. The overall reaction volume after cell lysis was 5ul, and therefore only 35 µl of CT conversion reagent was added. Post-incubation, samples were loaded along with 600µl of M-binding buffer onto a Zymo-Spin IC column and centrifuged. Samples were subsequently washed and cleaned up with 100µl of M-wash buffer and 200µl of M-desulphonation buffer respectively followed by centrifugation. The bisulfite converted samples were then eluted in a 10µl elution buffer by centrifugation and stored at -80^{o}C for future use. All centrifugation steps were carried out at 16,000 x g for 30 seconds.

6.2.2.3. PCR on bisulfite converted DNA

Initially, the amplification efficiency and specificity of designed primers was tested on bisulfite converted genomic control DNA using gradient PCR as described in **Section 3.2.3**. The annealing temperatures ranged from 55°C to 65°C.

In order to avoid primer dimer formation and ensure optimal amplification of all the loci, an initial pre-amplification including all the 23 primers was performed using Qiagen multiplex PCR kit (Qiagen, Germany). Thereafter, the primers were split into two pools and 1µl of pre-amplification products were further amplified separately in multiplex reaction with both the pools. The sequencing of the two primer pools are shown in **Table 32**. The reaction conditions for these multiplex PCRs are described in **Tables 33 and 34**.

Table 32. Primer pool 1 and 2 for multiplex PCR

Primer pool 1	Primer pool 2
ZDBF2	*DIRAS3*
NAP1L	*IGF2R*
NAP1L5	*GRB10*
PLAGL1	*MEST*
PEG10	*H19-1*
H19-2	*KCNQ1OT1*
MEG3-2	*MEG3-1*
SNURF-2	*SNURF-1*
ZNF597-1	*ZNF597-2*
GNAS-AS1	*PEG3-1*
NNAT	*PEG3-2*
	GNAS-NESP

Table 33. PCR reaction conditions for multiplex PCR

Component	Company	Volume (µl)
Nuclease free water	Roche	3.5
Multiplex master mix	Qiagen	7.5
Primer pool	Eurogentec	1
DNA		Up to 5µl
Final volume		**15**

Table 34. Thermocycler reaction conditions for multiplex

PCR step	Cycle conditions	Number of cycles
Initial denaturation	95°C for 15 minutes	1
Denaturation Annealing Elongation	94°C for 30 seconds 59°C for 90 seconds 72°C for 1 minute	15 (for pre-amplification) and 35 (for final amplification)
Final Extension	60°C for 10 minutes	1
Cooling	Hold at 4°C	N/A

6.2.3.4. Bisulfite sequencing

DNA libraries for sequencing from the amplified products were constructed using Accel-NGS 2S Plus DNA library kit (Swift Bioscience, USA) according to manufacturer's instructions. A dual indexing library preparation kit was used for samples preparation as some of the amplicons to be sequenced were between 150-300bp.

The DNA sequencing was performed on a MiSeq instrument by using MiSeq Reagent Kit v3 (300 cycles) (Illumina, UK). The reaction and incubation conditions for library preparation steps are described in detail in **Table 35**. After library normalisation, 4nM of pooled libraries were denatured with 0.2N NaOH and a final concentration of 12pM of denatured library molecules were loaded on the reagent cartridge for subsequent sequencing.

6.2.3.5. Data Analysis

The data obtained after bisulfite sequencing was converted into BAM files (which can be aligned to the human genome) using Bismark software. This part of the analysis was performed by Mr Siddharth Sethi. Thereafter, the BAM files were aligned to human genome (H19 assembly) and the subsequent DNA sequences were visualised on Integrated Genome

Viewer (IGV) software. For each of the CpG sites from the 23 loci of imprinted genes panel, percentage of cytosines and thymine nucleotides were analysed for every sample. The presence of cytosine at a CpG site was inferred as the particular locus being methylated whereas the presence of thymine was deduced as the unmethylated locus.

The methylation levels between different samples were statistically analysed using 1-way Anova with Dunn's Multiple Comparison Test. The statistical analyses were performed using GraphPad Prism software.

Table 35. Library preparation and sequencing conditions for bisulfite sequencing

Reaction conditions		**Incubation conditions**	
Reagents	**Volume (µl)**	**Temperature (°C)**	**Time**
a) Repair I: Dephosphorylation			
DNA amplicons	40	37	10 minutes
Repair I master mix	20		
1x magnetic beads cleanup			
b) Repair II: End repair			
Repair II master mix	50	20	20 minutes
1.2x magnetic beads cleanup			
c) Ligation I: 1st adapter ligation (3' end)			
Ligation I master mix	30	25	15 minutes
1.2x magnetic beads cleanup using PEG NaCl solution			
d) Ligation II: 2nd adapter ligation (5' end)			
Ligation II master mix	50	40	10 minutes
1.2x magnetic beads cleanup using PEG NaCl solution			
e) PCR library amplification			
Indexing primers	5	98	30 seconds
PCR master mix	25	5 cycles of:	
1.4x magnetic beads cleanup		98	10 seconds
		60	30 seconds
		68	60 seconds
		10	Hold
c) Library normalisation to 4nM			
d) Denaturation			
4nM library	5	Room temperature	10 minutes
0.2N NaOH	5		

6.3. Results

6.3.1. Development of imprinted genes panel

In order to study the imprinting landscape in human embryos, a primer panel consisting of 23 DMRs from 20 imprinted genes was developed. The specificity of the primers was initially tested by performing singleplex gradient PCR of each primer pair separately, with annealing temperature ranging from 55°C to 65°C. Amplicons of expected size and optimal intensity were obtained for all the primer pairs at 65°C annealing temperature.

Multiplex PCR consisting of all the 23 primer pairs was observed to form a lot of primer dimers when bisulfite converted DNA was amplified using all the primers simultaneously. In order to circumvent this issue, the primers were split into 2 pools using the predictions from Multiplex primer analyser tool (ThermoFisher Scientific), such that each pool consisted of primers with minimal possibility form cross-dimers. After an initial pre-amplification of 15cylcles with all the 23 primer pairs, the pre-amplification products were further subjected to multiplex PCR using each primer pool separately. The initial pre-amplification step was performed at three different annealing temperatures (58, 59 and 60°C). Thereafter, a gradient PCR using 6 different annealing temperatures (ranging between 55°C – 65°C) was performed using the two primer pools on pre-amplified bisulfite converted genomic DNA. Also, the second PCR was performed using two different primer concentrations; either 50μM or 10μM. Agarose gel images of the gradient PCR products amplified by the two primer pools are shown in **Figure 59**.

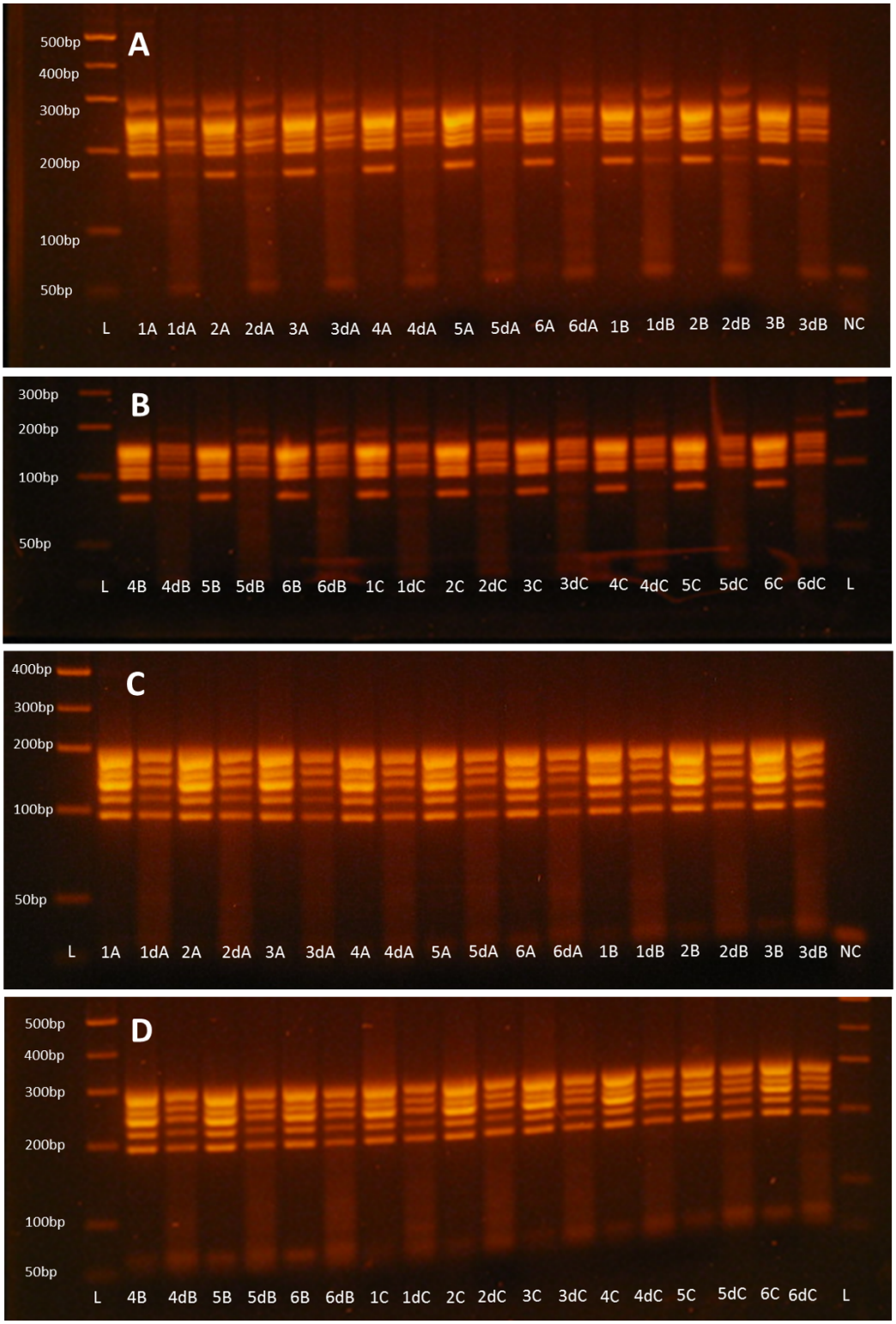


Figure 59.Optimisation of imprinted genes primer panel. The initial pre-amplification was performed at 3 annealing temperatures, A=58°C; B=59°C and D=60°C. The second amplification using either primer pool 1 or 2 was performed at 6 annealing temperatures; 1=53.2°C, 2=54.5°C, 3=55.5°C, 4=57.8°C, 5=60°C and 6=61.8°C with either 50µM or 10µM concentration of primer pool. Gel images **A** and **B** show the gradient PCR products of primer pool 1 whereas gel images **C** and **D** show the products of amplification with primer pool 2.

6.3.2. Overall methylation level analysis: trophectoderm and inner cell mass specific

Trophectoderm (TE) as well as inner cell mass (ICM) cells from a total of 9 euploid human embryos were subjected to bisulfite sequencing by using an imprinted genes panel developed during the course of this project. All the 23 DMRs in the TE and ICM samples were successfully amplified and sequenced. However, for methylation analysis only CpG sites with more than 100 sequences present in the sample were included in the methylation analysis.

Upon interrogating overall methylation levels (inclusive of all the 304 CpG loci in the imprinted genes panel) for each of the TE and ICM samples, no significant difference was obtained between the methylation levels in the samples and control human genomic DNA ($P<0.05$) (**Figure 60**). The methylation levels amongst the 9 ICM and TE samples ranged between 27.99%-42.48% and that of genomic DNA control was observed to be 48.02%. Moreover, the overall methylation level for unmethylated DNA control sample was 4%. There was a significant difference between the methylation levels between unmethylated DNA control and ICM and TE samples as shown in detail in **Figure 60** ($P<0.05$). No significant difference was observed upon comparison of overall methylation levels between each of the 9 individual ICM and TE samples (**Figure 60**). The percentages of methylation at individual CpG sites for control DNA, TE and ICM samples are shown in **Table 36** (**Appendix C**).

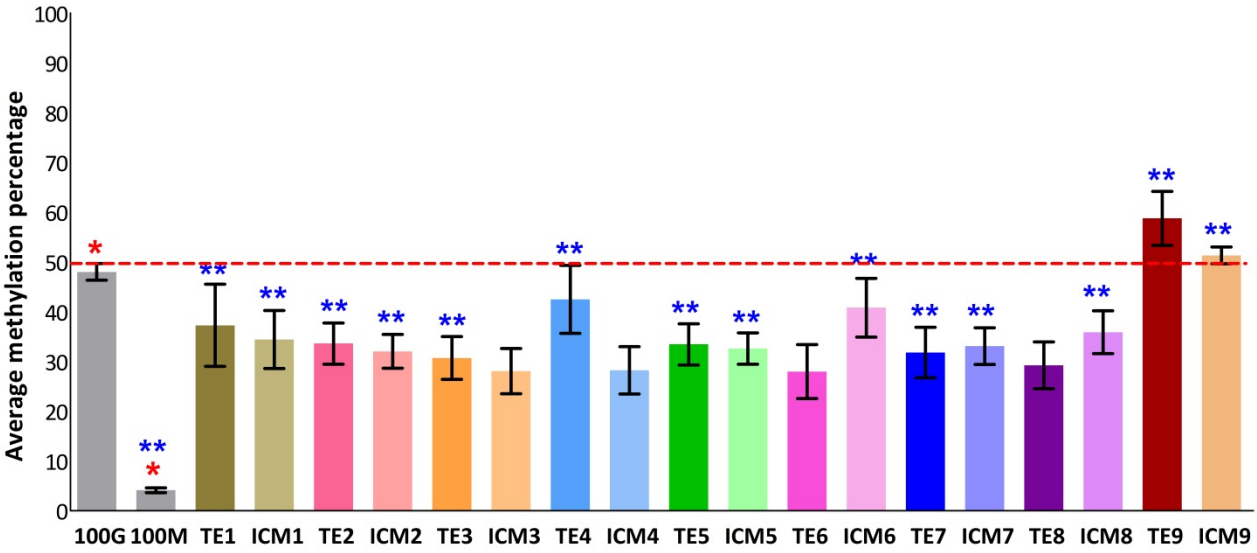


Figure 60. Overall methylation levels in human preimplantation embryos. The overall methylation percentage amongst the 304 CpG sites analysed from the imprinted genes panel did not differ significantly between the genomic control DNA samples (100G) and 9 TE and ICM samples derived from human blastocysts. However, there was a significant difference between genomic DNA control and unmethylated DNA control (100M) sample (P<0.001). Moreover, a significant difference between methylation level of unmethylated control (100M) and several TE and ICM samples was observed (P>0.05). Red asterix = significant difference in methylation between genomic DNA control and other samples; Blue asterix = significant difference between unmethylated control and other samples.

The red dotted line depicts 50% methylation level.

6.3.2. Overall methylation level analysis: Imprinted genes specific

Furthermore, the methylation levels for each of the 23 DMRs was analysed for genomic DNA control, unmethylated DNA control and human blastocysts (TE and ICM biopsy). The average methylation percentage for all the ICM and TE samples was calculated specific to each individual DMR of the imprinted genes panel.

No significant difference in the methylation levels was observed between the genomic DNA control, TE and ICM samples for *DIRAS3*, *NAP1L*, *SNURF2*, *GNAS-AS1* and *NNAT* DMRs. However, for other DMRs a significant difference was observed either between genomic DNA control, TE or ICM samples as shown in detail in **Figure 60** (p<0.05; 1way Anova with Dunn's test).

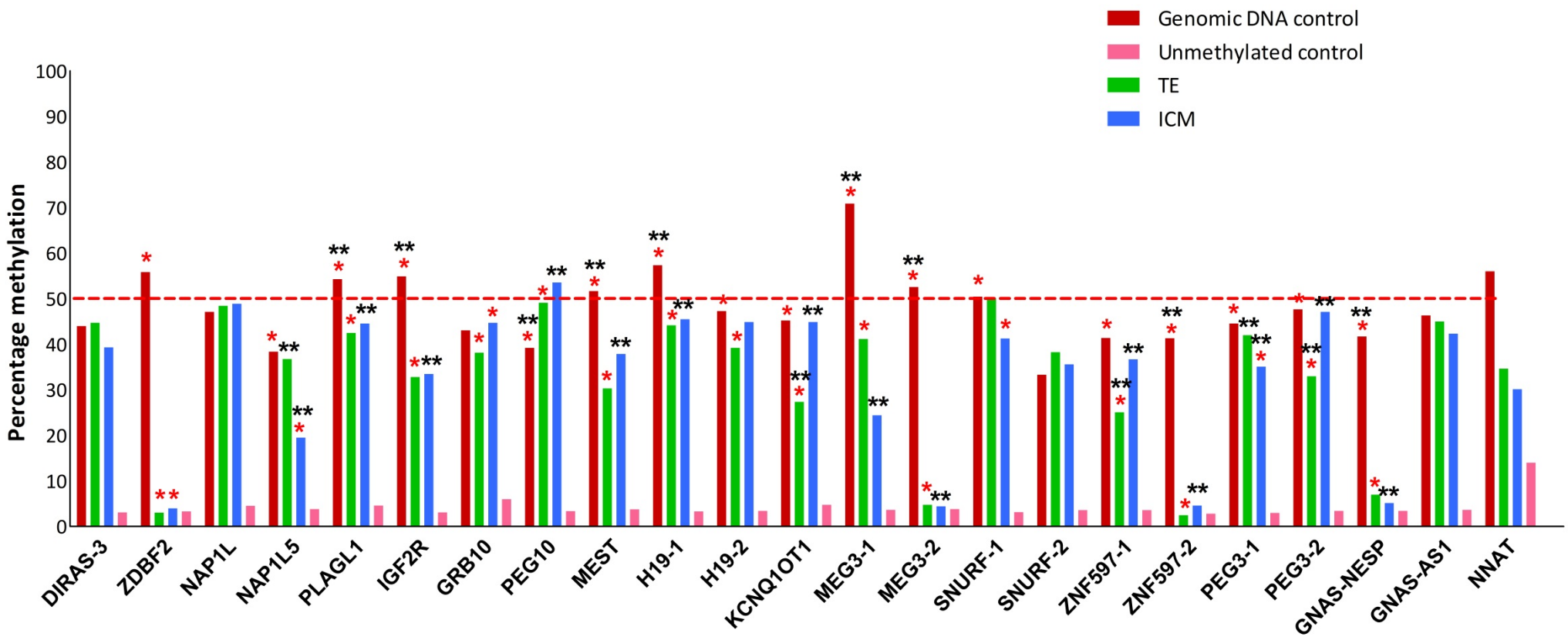


Figure 61 .Methylation level analysis for individual imprinted genes. The figure shows the methylation levels for each of the 23 DMRs for genomic DNA control, unmethylated control, TE and ICM samples. A significant methylation difference was observed between genomic DNA control and TE/ ICM samples for all the DMRs except *DIRAS3*, *NAP1L*, *SNURF-2*, *GNAS-AS1* and *NNAT*. For these 5 DMRs no significant difference in methylation levels was observed between the genomic control and TE/ ICM samples. The red and black asterix represent significant between methylation levels amongst methylated and unmethylated controls, ICM and TE samples.

The red dotted line depicts 50% methylation level.

6.3.3. Imprinting landscape for 20 imprinted genes in TE and ICM from euploid blastocysts

An imprinting landscape of TE cells and ICM from 9 human blastocysts for 20 imprinted genes was constructed by utilising the methylation data obtained from bisulfite sequencing of 23 DMRs.

Out of the 23 DMRs analysed, the methylation level for 19 DMRs between TE cells and ICM was similar as shown in **Figure**.**61** However, methylation level of 4 DMRs namely, *NAP1L5*, *GRB10*, *KCN1OT1* and *PEG3* were significantly different between TE cells and ICM cells. For *NAP1L5*, the methylation level was significantly higher in TE cells as compared to ICM (37% vs 19.48%; P<0.05). Whereas for *GRB10*, *KCNQ1OT1* and *PEG3* DMRs, the methylation level was significantly higher in ICM than in TE cells (44.7% vs 38%; 44.89% vs 27%; 47.1% vs 33% respectively; P <0.05) (**Table 36**).

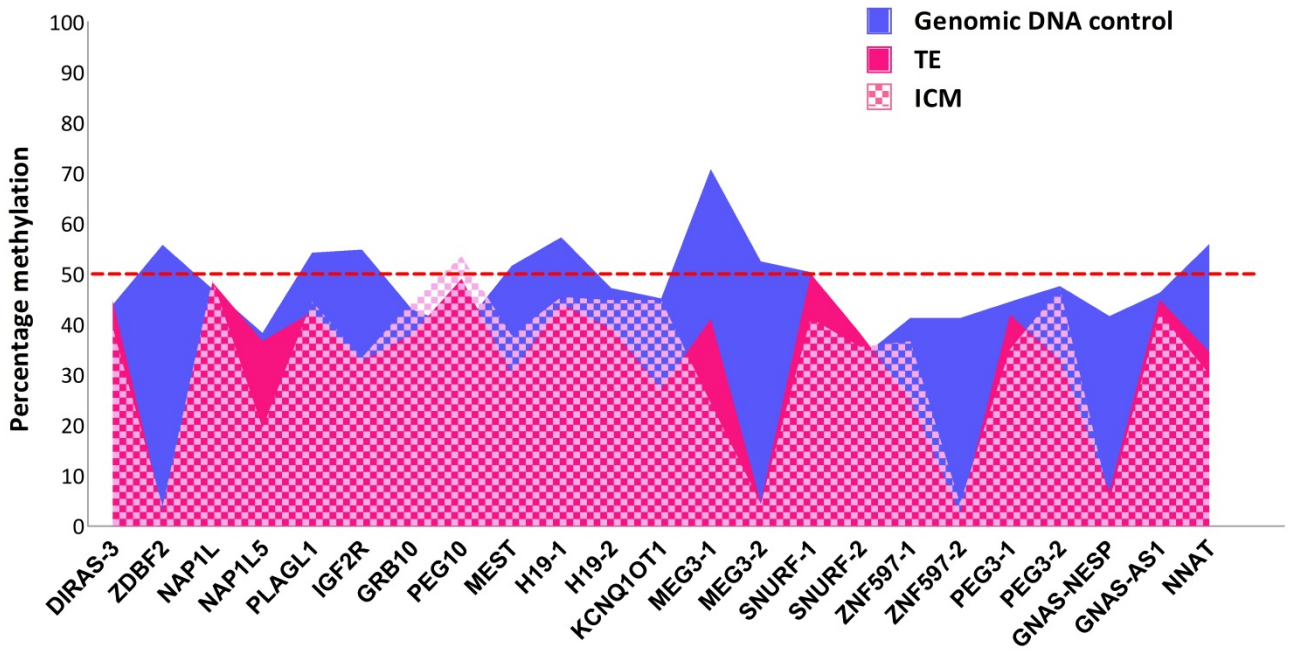


Figure 62. Methylation landscape for 20 imprinted genes from their corresponding DMRs. The graph shows the comparison of methylation levels for 23 DMRs for genomic control DNA, TE and ICM samples. The DMRs *ZDBF2*, *MEG3-2*, *ZNF597-2* and *GNAS-NESP* were observed to be hypomethylated for TE and ICM samples as compared to genomic DNA control.

The red dotted line depicts 50% methylation level.

In comparison to genomic DNA control, four DMRs including *ZDBF2*, *MEG3-2*, *ZNF597-2* and *GNAS-NESP* were found to be hypomethylated (ranging from 2.5-7% methylation) in TE and ICM samples from 9 blastocysts (**Table 36**).

Table 36. Average methylation levels for control DNA, TE and ICM samples. The DMR samples highlighted in brown show regions with hypomethylation.

Gene name	Genomic DNA control (%)	Unmethylated control (%)	TE (%)	ICM (%)
DIRAS-3	44.00	3.11	44.70	39.33
ZDBF2	55.83	3.33	3.04	3.98
NAP1L	47.13	4.56	48.44	48.87
NAP1L5	38.36	3.79	36.77	19.48
PLAGL1	54.29	4.57	42.46	44.57
IGF2R	54.90	3.10	32.79	33.49
GRB10	43.03	6.00	38.15	44.70
PEG10	39.23	3.38	49.09	53.55
MEST	51.69	3.75	30.30	37.86
H19-1	57.33	3.33	44.18	45.51
H19-2	47.30	3.40	39.20	44.88
KCNQ1OT1	45.23	4.77	27.37	44.89
MEG3-1	70.88	3.63	41.13	24.39
MEG3-2	52.58	3.83	4.77	4.42
SNURF-1	50.43	3.14	50.10	41.27
SNURF-2	33.31	3.56	38.27	35.58
ZNF597-1	41.35	3.57	25.09	36.72
ZNF597-2	41.30	2.80	2.49	4.60
PEG3-1	44.55	3.00	42.01	35.10
PEG3-2	47.67	3.44	32.95	47.12
GNAS-NESP	41.72	3.44	6.97	5.15
GNAS-AS1	46.33	3.67	44.98	42.31
NNAT	56.00	14.00	34.65	30.11

6.3.4. CpG site specific methylation levels

The **Figures 62-69** depict CpG site specific methylation at each DMR for genomic DNA control, unmethylated control and individual TE and ICM samples. For each DMR, CpG site specific variation in methylation levels is shown along with inter sample variation amongst each of the 9 TE and ICM samples (**Figures 62-69**).

The average methylation level for each of the 9 TE and ICM samples was compared with methylation level of genomic control DNA for individual DMRs of the imprinted genes panel. The methylation level differences are depicted in **Table 37** wherein the samples having significantly different methylation (imprinting errors) than control genomic DNA are shown with a tick mark. Of note, only three DMRs; *DIRAS3*, *SNURF* and *NANT*, showed no significant differences in methylation for any of the TE and ICM samples with respect to genomic DNA control (**Table 37**).

The site specific DMR methylation analysis revealed imprinting perturbations in TE and ICM samples ranging from 11.11% to 77.78% of samples for various DMRs as detailed in **Table 37**. Interestingly, a significantly higher proportion of imprinting errors was observed for TE samples across the 23 DMRs as compared to ICM samples (P=0.0142; Mann Whitney test).

Table 37. Differences in methylation status. The table shows the differences in methylation status between genomic DNA control and individual TE and ICM samples for each DMR analysed. The ticks represent a significant difference between the sample and control genomic DNA (P<0.05; Dunn's test)

DMR	TE1	ICM1	TE2	ICM2	TE3	ICM3	TE4	ICM4	TE5	ICM5	TE6	ICM6	TE7	ICM7	TE8	ICM8	TE9	ICM9	% TE	% ICM
DIRAS-3																			0.00	0.00
ZDBF2	✓	✓					✓	✓	✓		✓	✓			✓				55.56	33.33
NAP1L	✓												✓						22.22	0.00
NAP1L5	✓	✓					✓												22.22	0.00
PLAGL1	✓																		11.11	0.00
IGF2R	✓										✓	✓					✓	✓	33.33	22.22
GRB10	✓				✓				✓		✓		✓		✓				66.67	0.00
PEG10							✓					✓							11.11	11.11
MEST					✓		✓				✓		✓		✓				55.56	0.00
H19-1			✓			✓							✓						22.22	11.11
H19-2											✓								11.11	0.00
KCNQ1OT1					✓	✓							✓		✓	✓			33.33	22.22
MEG3-1		✓			✓	✓					✓	✓				✓			22.22	44.44
MEG3-2	✓	✓	✓	✓	✓	✓	✓	✓			✓	✓		✓	✓	✓	✓		77.78	77.78
SNURF-1																			0.00	0.00
SNURF-2			✓																11.11	0.00
ZNF597-1							✓	✓	✓				✓						33.33	11.11
ZNF597-2	✓	✓	✓		✓	✓	✓	✓	✓	✓	✓				✓	✓	✓		88.89	55.56
PEG3-1								✓			✓								11.11	0.00
PEG3-2	✓																		11.11	0.00
GNAS-NESP	✓	✓	✓	✓	✓	✓	✓	✓	✓	✓	✓	✓	✓					✓	77.78	77.78
GNAS-AS1							✓												11.11	0.00
NNAT																			0.00	0.00

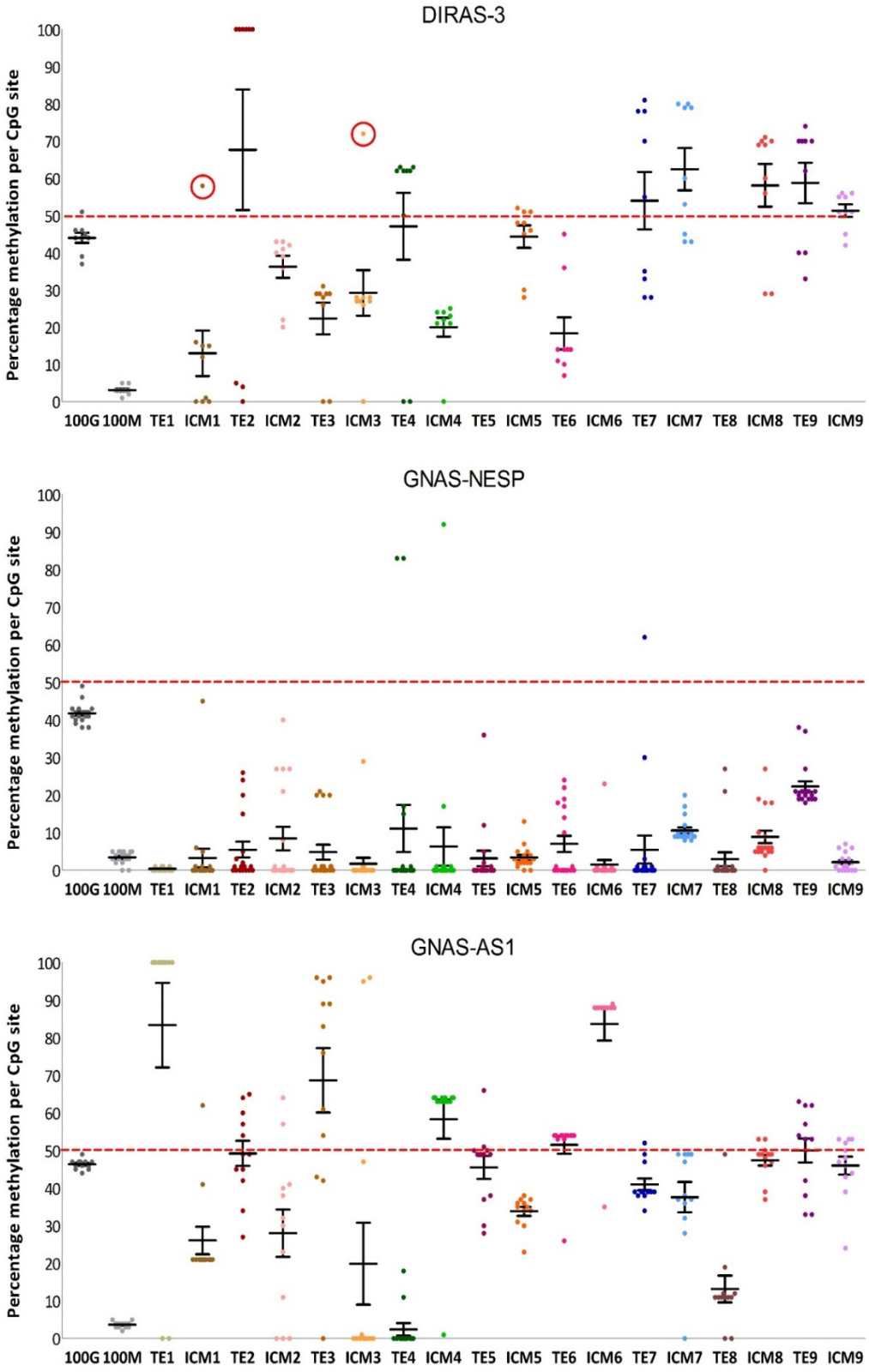


Figure 63. CpG specific methylation for TE and ICM samples. The graphs show CpG site specific methylation level for each of the 9 TE and ICM samples along with genomic DNA control (100G) and unmethylated control (100M) for *DIRAS3*, *GNAS-NESP* and *GNAS-AS1* DMRs.

The dots encircled in red circles show an example of methylation level variation at individual CpG sites. The red dotted line depicts 50% methylation level.

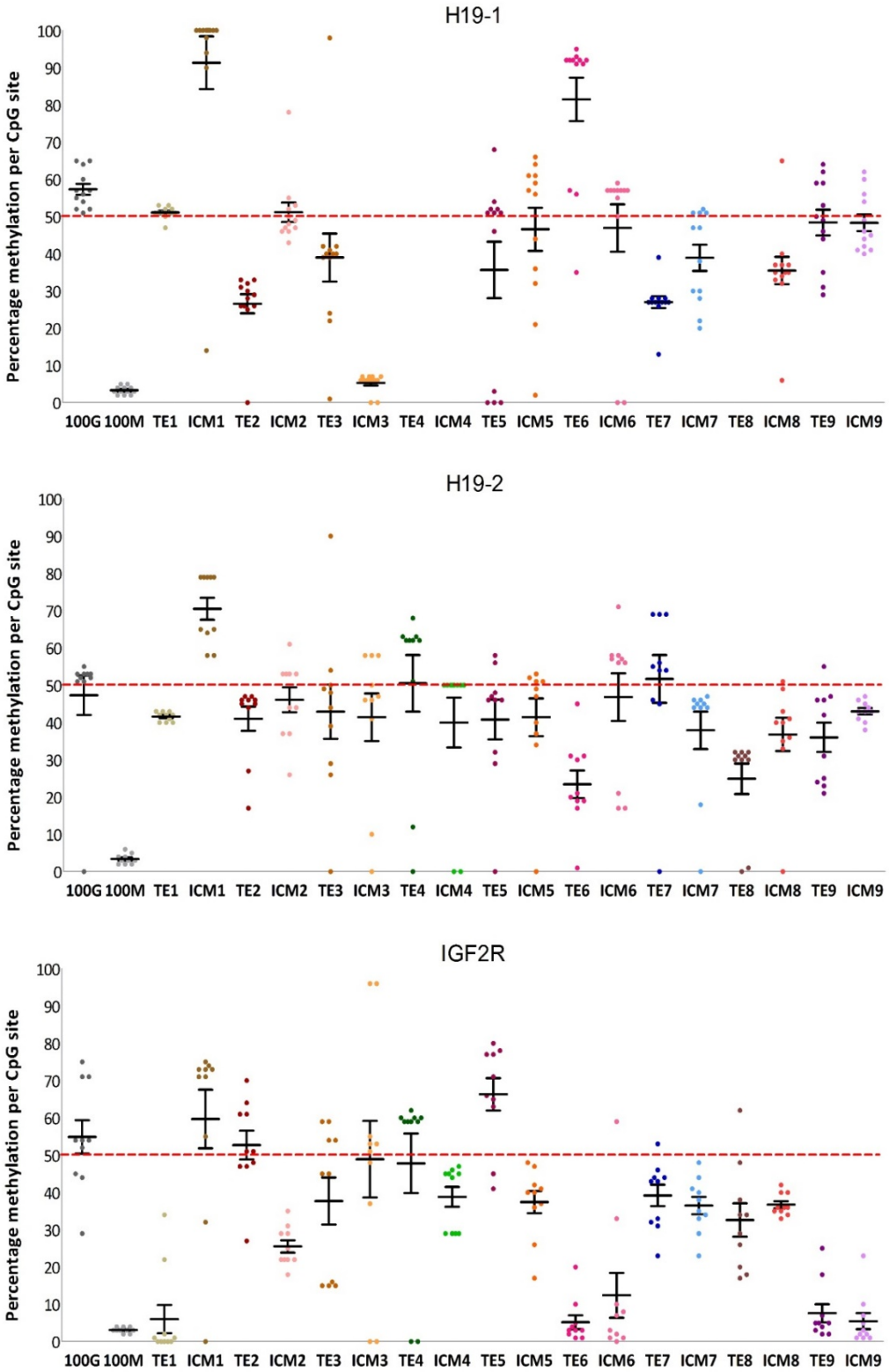


Figure 64. CpG specific methylation for TE and ICM samples. The graphs show CpG site specific methylation level for each of the 9 TE and ICM samples along with genomic DNA control (100G) and unmethylated control (100M) for *H19-1*, *H19-2* and *IGF2R* DMRs.

The red dotted line depicts 50% methylation level.

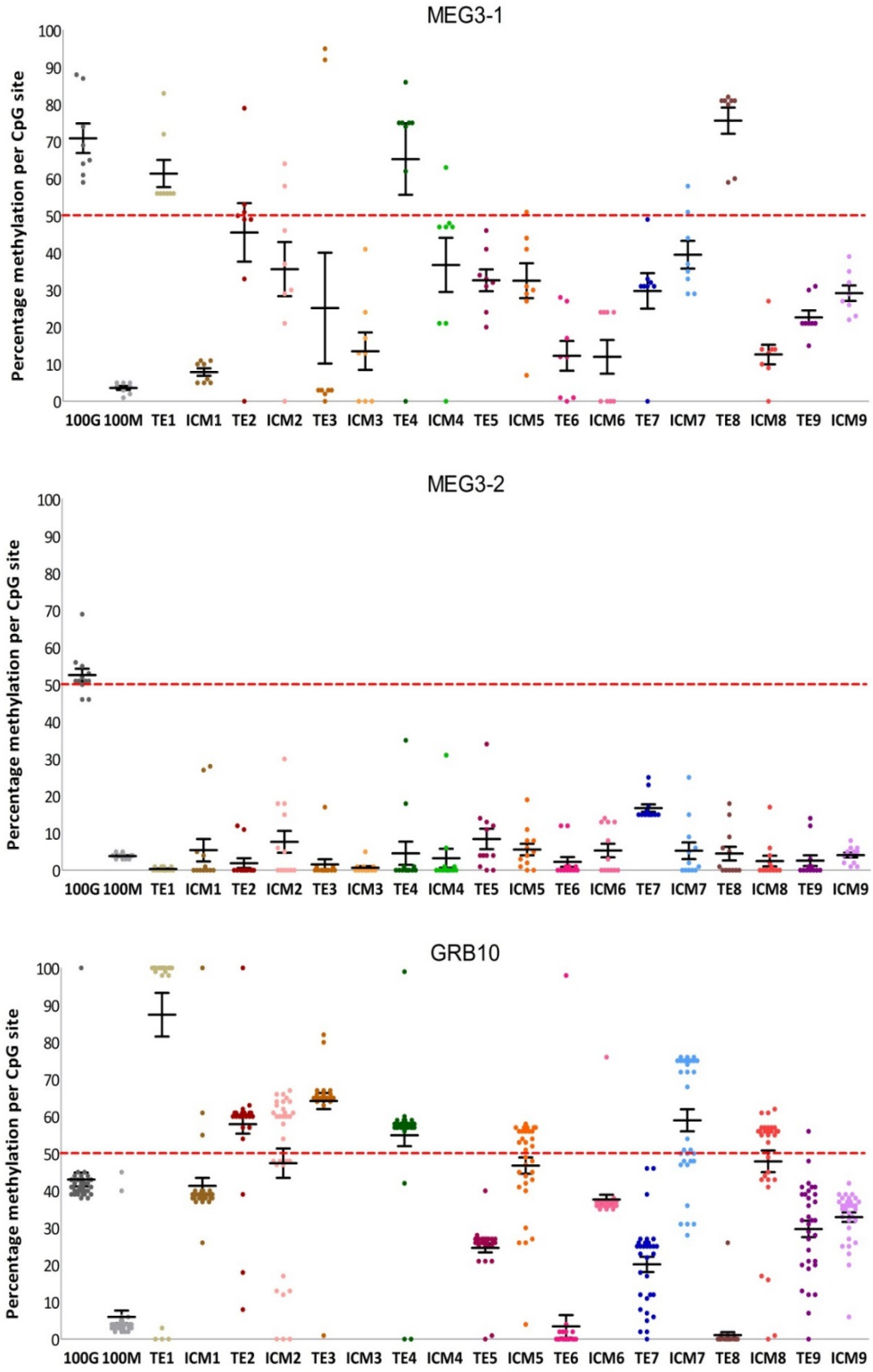


Figure 65. CpG specific methylation for TE and ICM samples. The graphs show CpG site specific methylation level for each of the 9 TE and ICM samples along with genomic DNA control (100G) and unmethylated control (100M) for *MEG-1*, *MEG-2* and *GRB10* DMRs.

The red dotted line depicts 50% methylation level.

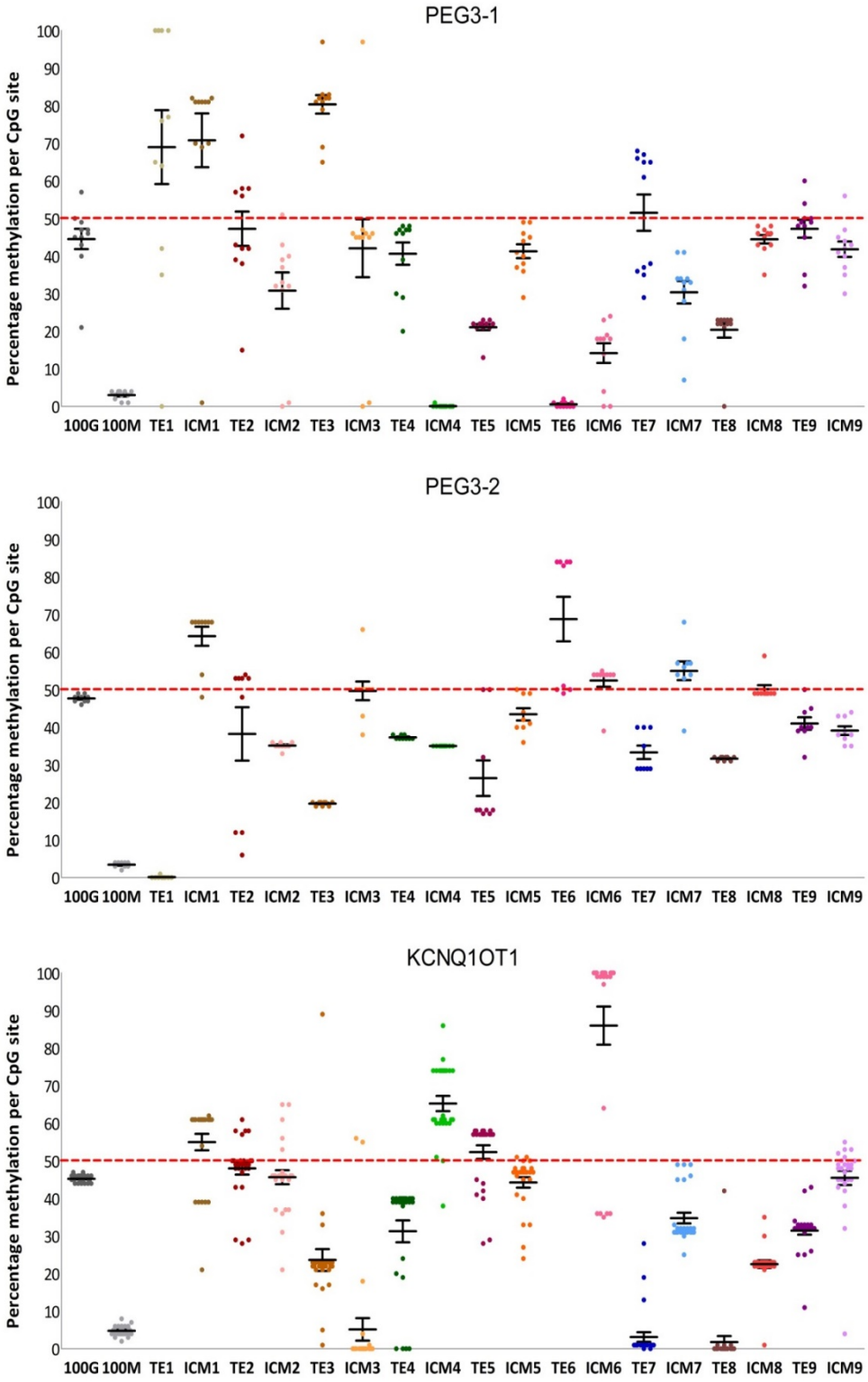


Figure 66. CpG specific methylation for TE and ICM samples. The graphs show CpG site specific methylation level for each of the 9 TE and ICM samples along with genomic DNA control (100G) and unmethylated control (100M) for *PEG3-1*, *PEG3-2* and *KCNQ1OT1* DMRs.

The red dotted line depicts 50% methylation level.

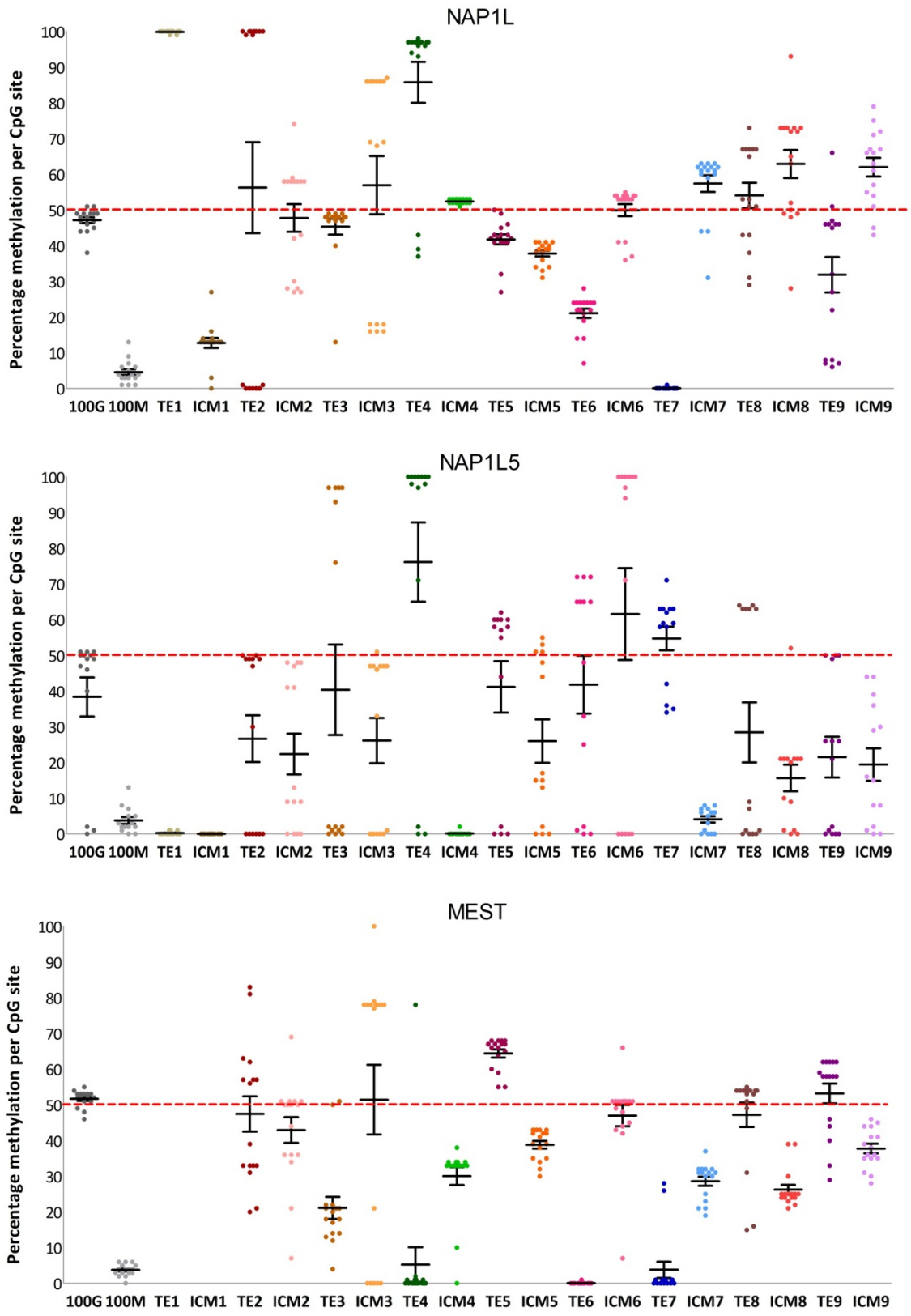


Figure 67. CpG specific methylation for TE and ICM samples. The graphs show CpG site specific methylation level for each of the 9 TE and ICM samples along with genomic DNA control (100G) and unmethylated control (100M) for *NAP1L*, *NAP1L5* and *MEST* DMRs.

The red dotted line depicts 50% methylation level.

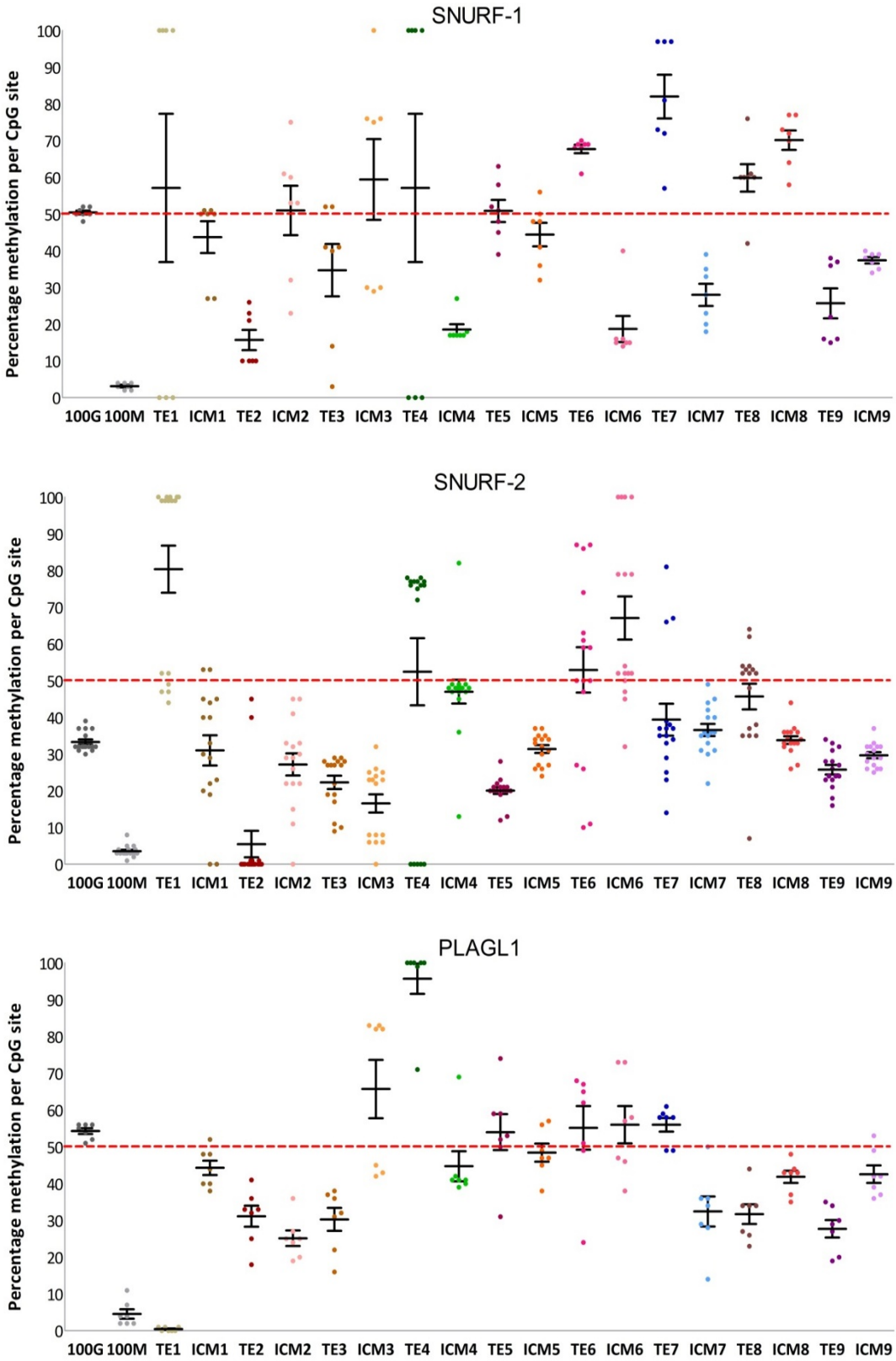


Figure 68. CpG specific methylation for TE and ICM samples. The graphs show CpG site specific methylation level for each of the 9 TE and ICM samples along with genomic DNA control (100G) and unmethylated control (100M) for *SNURF-1*, *SNURF-2* and *PLAGL1* DMRs.

The red dotted line depicts 50% methylation level.

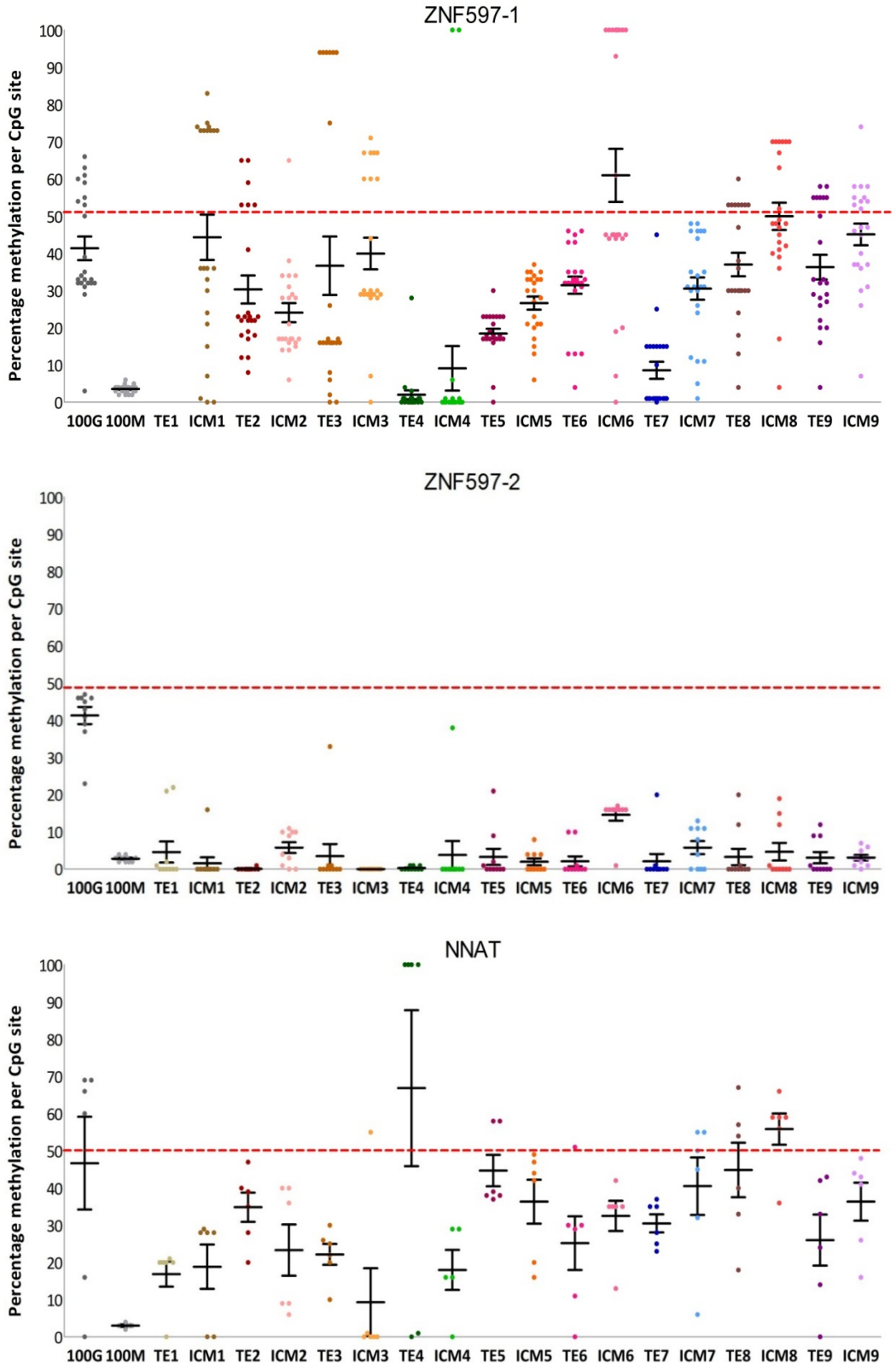


Figure 69. CpG specific methylation for TE and ICM samples. The graphs show CpG site specific methylation level for each of the 9 TE and ICM samples along with genomic DNA control (100G) and unmethylated control (100M) for *ZNF597-1*, *ZNF597--2* and *NNAT* DMRs.

The red dotted line depicts 50% methylation level.

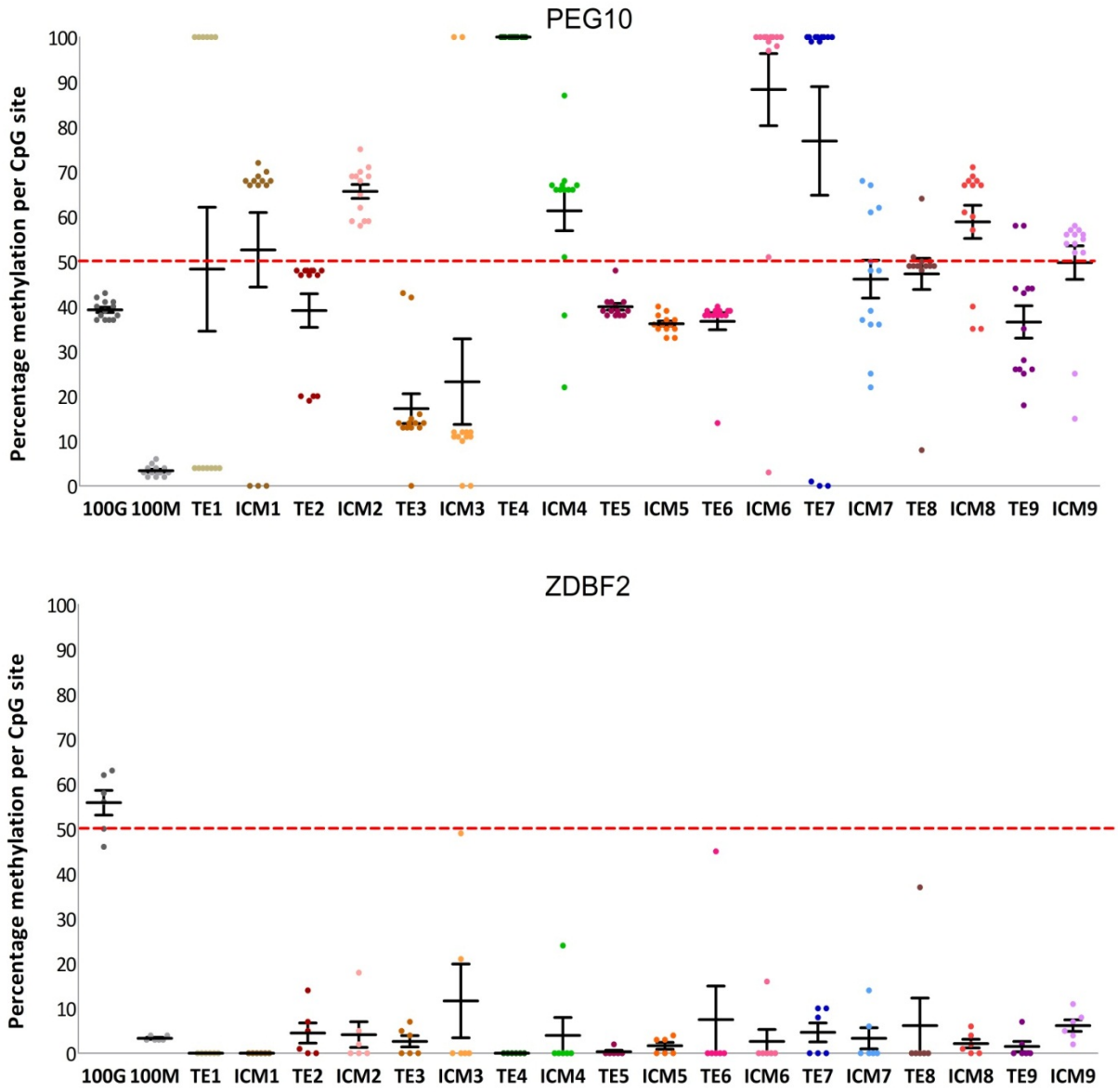


Figure 70. CpG specific methylation for TE and ICM samples. The graphs show CpG site specific methylation level for each of the 9 TE and ICM samples along with genomic DNA control (100G) and unmethylated control (100M) for *PEG10* and *ZDBF2* DMRs.

The red dotted line depicts 50% methylation level.

6.4. Discussion

Genomic imprinting is a classic example of epigenetic regulation during mammalian development which leads to exclusive expression of one of the two parental alleles (Reik and Walter, 2001). The development of preimplantation embryos involves several critical stages including fertilization, cell cleavage, morula and blastocyst formation, which are regulated both genetically as well epigenetically (Li, 2002). Moreover, the imprinting pattern is laid down in the oocyte and spermatozoa in a sex specific manner during gametogenesis. In the oocytes, the establishment of epigenetic marks occurs late and is finished just prior to ovulation. Hence, environmental disruption during these critical stages may lead to abnormal embryo development (Wale and Gardner, 2016).

6.4.1. Need for detection of imprinting perturbations

It has been well established that several imprinted genes are expressed during placental development and play an important role in determining the mother-offspring relationship (Fowden et al., 2006). Moreover, any disruption to the epigenetic marks caused during development may lead to imprinting disorders (reviewed by Butler, 2009).

Advances in single cell sequencing methodologies have facilitated the exploration of methylation landscape at single cell level in human preimplantation embryos. Recently, genome-wide methylation patterns at CpG sites have been characterised in human gametes and preimplantation embryos using Reduced Representation Bisulfite Sequencing (RRBS) and single-cell method (Smallwood et al., 2011; Smith et al., 2014; Clark et al., 2017). However, the large size of human genome poses technical challenge for whole-genome bisulfite sequencing especially with respect to the genome coverage and reproducibility of the method when sequencing the genome of a single or small number of cells (Suzuki and Bird, 2008). PCR

based targeted sequencing of certain imprinted and developmentally important genes have been employed to enrich genomic targets prior to sequencing. However, multiple targets cannot be easily included in the same PCR assay for methylation studies due to technical challenged posed by reduced complexity of bisulfite converted genome. Till date, studies looking at imprinted genes in human preimplantation embryos have looked at a maximum of 3 imprinted loci simultaneously in a single sample (Denomme et al., 2016; Geuns et al., 2013; Shi et al., 2014; White et al., 2015).

The main aim of this study was to develop a targeted approach for methylation detection at 23 DMRs of interest in order to interrogate the imprinting landscape of 20 imprinted genes in human preimplantation embryos. For the purpose, a multiplex PCR based bisulfite sequencing approach was developed to detect the methylation status of 20 imprinted genes simultaneously. After extensive optimisation of the multiplex PCR, a primer panel of 23 DMRs was developed and validated on different concentrations of bisulfite converted genomic DNA control.

Unlike conventional PCR, the PCR design and optimisation for bisulfite converted DNA is technically challenging. As all the unmethylated cytosine residues are converted to uracil resides post bisulfite treatement, the GC content of bisulfite converted DNA greatly reduces. This further decreases the complexity of the genome and reduces the primer specificity. Due to the low GC content, the annealing temperature of primers decrease and the length of primers for bisulfite converted DNA increases because of specificity issues. Cumulatively, these factors make multiplex PCR on bisulfite converted DNA difficult as more number of long and low complexity primers increases the likelihood of primer dimer formation. However, with careful primer and PCR design, these hurdles could be overcome.

For the development of this imprinted genes primer panel, initially a single multiplex reaction was performed which resulted in formation of a lot of primer dimers. To circumvent this issue, the primers were split into two pools based on the predictions on cross-dimers formation tendency using the Multiple primer analyser tool (ThermoFisher Scientific). Thereafter, a pre-amplification was performed with the entire primer panel before using these pre-amplified products for further amplification by the two primer pools separately. The optimal annealing temperature and primer concentration were determined during the optimisation phase and the results were validated on different concentrations (100ng, 10ng, 1ng, 0.1ng) of bisulfite converted genomic DNA control (data not presented). To test the proof of principle, the method was then applied to a small number of bisulfite converted ICM and TE samples from donated blastocysts followed by NGS which revealed the presence of all the successfully amplified 23 DMRs in these samples.

There is a dearth of literature on the imprinting landscape in human preimplantation embryos. To our knowledge, this is the first study to develop and apply a multiplex PCR based bisulfite sequencing approach to analyse 20 imprinted genes simultaneously in two embryonic cell lineages, trophectoderm and inner cell mass, from blastocyst stage euploid human embryos.

6.4.2. Imprinting patterns in TE and ICM samples

Assisted reproductive techniques (ARTs) involve gamete manipulation as well as extended periods of embryo cultures (e.g. when embryos are cultured until the blastocyst stage *in vitro*) at a crucial time when epigenetic marks are being established in the genome (Reik and Walter, 2001). As reviewed by Huntriss & Picton (2008), several studies have found

an association between ART and imprinting disorders and suggested that the ART techniques predispose embryos to imprinting errors.

Blastocyst represents an important stage of preimplantation embryo development, marking the first cell differentiation in mammalian development and resulting into formation of TE and ICM lineages. The TE would later on give rise to placenta and the ICM gives rise to embryo proper and extraembryonic tissues (Dyce et al., 1987). The transcriptional profiles of these cell types differ which in turn is regulated by DNA methylation (Guo *et al.*, 2010).

Upon analysing the overall methylation levels at the 304 CpG sites from the 23 DMRs, methylation was comparable between genomic DNA control and TE and ICM samples derived from the 9 blastocysts. This shows that the overall methylation at the imprinted loci studied here remains conserved even after differentiation of the embryonic cells into TE and ICM lineages. This would be in line with the expectation from a normally developing embryo wherein the methylation marks at imprinted loci are conserved up till differentiation into PGCs at a later stage of foetal development (Li & Sasaki, 2011). However, the global DNA methylation, specific to cell lineage, has been shown to be higher in TE cells in mouse embryos as compared to ICM (Nakanishi *et al.*, 2012).

Also, at individual imprinted DMR level, no significant differences in methylation levels were observed between TE and ICM for a majority of the DMRs (19/23) included in the study. However, the methylation level for 4 DMRs, *NAP1L5*, *GRB10*, *KCN1OT1* and *PEG3* were significantly different between TE cells and ICM cells. Additionally, an imprinting landscape was created for TE and ICM samples utilising the data on methylation levels of 23 DMRs from all the blastocysts. The methylation levels for most of the DMRs for ICM and TE samples was comparable with that of genomic control DNA, however, four DMRs (*ZDBF2, MEG3-2,*

ZNF597-2 and *GNAS-NESP*) were observed to be severely hypomethylated at these DMRs (ranging between 2.5%-7%). A large scale study assessing loss of imprinting in human pluripotent cells also found the highest level of loss of imprinting (LOI) at the *ZDBF2, MEG3-2* and *GNAS* loci using RNA sequencing data (Bar et al., 2017). They furthermore found that genes regulated by paternally methylated gDMRs (*ZDBF2, MEG3-2, ZNF597*) were significantly more prone to LOI than those regulated by maternally methylated DMRs. The loss of methylation observed at the 4 DMRs might indicate loss of imprinting for these genes but this can only be fully confirmed by looking at their respective gene expression levels.

6.4.3. CpG site specific methylation patterns for ICM and TE samples

Upon in depth analysis of the methylation patterns at individual CpG sites per TE and ICM sample, a huge variability in methylation levels was observed across numerous DMRs. Imprinting perturbations were observed in TE and/ or ICM samples in comparison to genomic DNA control for all the DMRs included in the study except *DIRAS3*, *SNURF-1* and *NNAT* DMRs. Moreover, imprinting perturbations were observed to occur at a higher frequency in TE samples as compared to ICM samples (P=0.0142). Studies in mice have observed a selective loss of imprinting in the placenta in comparison to midgestation mouse embryos derived from *in vitro* culture (Mann, 2004; de Waal *et al.*, 2014). Hence, there seems to be preferential relegation of aberrantly methylated cells to extraembryonic lineages.

Research has mainly been focused on studying the imprinting patterns of *H19*, *KCNQ1OT1* and *SNRPN* genes in preimplantation human embryos mainly due to their importance in growth and development (Denomme et al., 2016; Ibala-Romdhane et al., 2011; Khoueiry et al., 2013; Shi et al., 2014). Epigenetic errors in *KCNQIOT1* gene have been observed in over 90% of Beckwith–Wiedemann syndrome (BWS) cases in ART conceived

children as compared to 50% of cases in general population whereas H19 methylation perturbations are seen in 17% of BWS cases of ART population as compared to 5% in general population (DeBaun et al., 2003; Maher et al., 2003; Sutcliffe et al., 2006; Lennerz et al., 2010; Rossignol et al., 2006).

Two studies observed methylation perturbations in *SNRPN* gene in 89% (Geuns *et al.*, 2003) of cleavage stage embryos and 67% (White et al., 2015) of blastocyst stage embryos. However, we observed methylation errors in 11% (1/9) of trophectoderm samples for *SNRPN* DMR. For *KCNQ1OT1* gene, methylation errors were seen in 10% of cleavage stage embryos (Shi et al., 2014), 56% of poor quality blastocysts (Khoueiry *et al.*, 2013) and 31% in good quality blastocysts (White et al., 2015). For the present study, methylation errors at *KCNQ1OT1* locus was found in 33% (3/9) TE samples and 22% ICM samples (2/9) which was comparable to the findings of White et al. study. Lastly, for *H19* gene, imprinting errors have been reported in 17% of cleavage stage embryos (Shi et al., 2014) and 8-14% blastocysts (Shi et al., 2014; White et al., 2015) which are comparable to the findings of our study wherein 22% TE samples and 11% ICM samples were found to carry imprinting errors.

Mouse models have been highly instrumental in studying the effects of ARTs on genetic imprinting but only a few studies have looked at the human counterparts in preimplantation embryos (reviewed by Hudson et al., 2010). Most of these studies were performed on morphologically poor quality embryos that were deemed unsuitable for transfer. We have utilised chromosomally euploid embryos with good morphological quality to establish the imprinting landscape in two earliest cell lineages, TE and ICM, from preimplantation blastocysts. Overall, our findings are in line with other studies which have

shown that imprinting errors occur at a high frequency in both human and mouse preimplantation embryos.

Even though a high rate of imprinting perturbations has been observed in preimplantation human embryos, the frequency of imprinted genes disorders in children conceived after ART remains fairly low (Eroglu and Layman, 2012). A possible explanation for this discrepancy could be that imprinting errors could lead to embryo developmental arrest and implantation failure. A study by Lorthongpanich et al., (2013) showed that failure to maintain DNA methylation at multiple imprinted loci resulted in chimeric mice displaying unpredictable phenotypes and culminated in developmental arrest. They further showed that mouse pronuclear transfer aided in amending the epigenetic defects.

To sum up, the high frequency of imprinted errors observed in human blastocysts in this study was in line with previous studies showing high variability of methylation levels between preimplantation embryos of both, humans and mouse. This study furthermore showed imprinting patterns of 20 imprinted genes for TE and ICM biopsies, which has not been reported previously.

6.4.4. Study limitations

The sequencing depth obtained for the samples analysed in the study was relatively low (ranging from a few hundred to thousand reads per CpG locus). This was in part due to technical difficulties encountered during the sequencing procedure. However, in comparison to previous studies, which assessed the methylation imprints by sequencing <100 clones, the sequencing reads obtained during the study with NGS was much higher and hence should suffice for preliminary methylation analysis of imprinted genes. However, the sequencing

procedure would be repeated for the samples included in this study and the results will be compared to those obtained for the first sequencing run.

The unmethylated control sample was observed to be approximately 4% methylated after bisulfite sequencing. As amplification of DNA cannot retain methylation marks of its original DNA template, the unmethylated control was created by whole genome amplification (WGA) of genomic DNA using MDA method. It is possible that a small portion of the original template was also retained in the WGA products used as unmethylated control, thereby resulting in a small percentage of methylation being observed in this control. There also exists the possibility of the bisulfite conversion procedure less than 100% efficient which results in some of the unmethylated CpGs being unconverted into uracil residues.

While it is most likely that the variation observed in methylation levels amongst individual TE and ICM is due to true biological difference in the methylation of these samples, it could be argued that PCR bias and allele drop-out during amplification of bisulfite converted samples might have resulted in methylation difference amongst these samples. However, methylation analysis of individual CpG sites revealed a significant variation between CpGs corresponding to a single DMR from the same sample. As these CpGs within same DMR correspond to a single amplicon, it is highly unlikely that amplification bias or allele drop out would have contributed to this observed difference. Hence, it can be inferred that most likely the observed methylation variations within the same DMR for a particular ICM or TE sample are true biological differences in IVF generated human blastocysts.

6.5.5. Summary

Current methods used for the assessment of gamete and embryo quality, including the morphological assessment as well as more advanced genetic testing such as preimplantation genetic testing for aneuploidy (PGT-A), cannot assess epigenetic errors. Therefore, there is an urgent need to develop methods that allow testing of epigenetic patterns during gametogenesis and early embryo development in relation to ART and infertility, providing novel insights into the origin of imprinting anomalies in human embryos. Additionally, new methodologies may assist in improving the ART practice in order to reduce imprinting defects.

In summary, the present study was successful in proving the proof of principle for the developed targeted approach to detect methylation status of 20 imprinted genes simultaneously in human embryos. It is the first study to report the methylation status of a huge number of imprinted genes in trophectoderm and inner cell mass samples, derived from the same blastocyst. In future, RNA sequencing experiments would be performed on a separate TE biopsy from the same blastocysts included in this study, in order to compare the gene expression level of the imprinted genes with the methylation levels detected during the course of this study.

Chapter 7: Final conclusion

This chapter summarises the primary findings of the thesis and discusses them in the context of past and prospective research. It also mentions the contribution to the field and scope of future research in the field of infertility, assisted reproduction and reproductive genetics.

7.1. Synopsis of thesis:

It was estimated that approximately 48.5 million couples worldwide were affected by infertility in 2010 alone, with the number on the rise since then (Mascarenhas et al., 2012). The past four decades has seen a great progress in infertility treatments, starting with the successful birth of the first 'test tube' baby in 1978 following IVF (Steptoe & Edwards, 1978). With the unique accessibility to human oocytes and preimplantation embryos granted by IVF treatments, the field of reproductive biology has since developed immensely (reviewed by Harper et al., 2017; Matzuk & Lamb, 2008).

Even though IVF is used routinely as an established treatment for infertility, the success rates remain fairly low. One of the biggest challenges encountered during IVF is the selection of the most viable embryo for transfer. The embryo viability is dependent on several vital molecular processes with chromosomal aneuploidy being one of the most well studied factors responsible for a negative IVF outcome (Delhanty et al., 1993; Munné et al., 1994; Rabinowitz et al., 2012; Wells & Delhanty, 2000).

This project endeavoured to investigate certain underexplored chromosomal and molecular processes, in context of IVF, vital during gametogenesis and embryogenesis. Hence, the project was divided into three crucial parts; (A) analysis of data generated from cytogenetic examination of human oocytes and preimplantation embryos, (B) development and validation of novel techniques to investigate the blastocoel fluid and spent culture media for embryonic DNA and (C) development of a method to explore imprinting landscape of preimplantation embryos.

A. The cytogenetic examination of human oocytes and preimplantation embryos

So far, research has mainly focused on the gains or losses affecting entire chromosomes in context of embryo viability (Fragouli et al., 2013; Munné et al., 1993; Wells & Delhanty, 2000). However, oocytes and embryos are frequently affected by partial losses and gains, which only affect fragments of chromosomes (Vanneste *et al.*, 2009a). Although the phenomena of chromosome breakage and segmental imbalance have been considered interesting oddities of the human preimplantation embryo, little work has been undertaken to define their true frequency, mechanism of origin, or clinical significance. In the light of lack of literature on the subject, the study aimed to address certain outstanding questions about the frequency, origin and clinical implications of segmental aneuploidy in human oocytes and preimplantation embryos.

It could be concluded from the data analysed here that the segmental imbalances occur at a considerable frequency in oocytes and preimplantation embryos. There is a high risk of chromosomal breakage during the first few mitotic divisions with non-centromeric regions being affected more frequently than the centromeric regions. During the subsequent cell divisions, these fragments of chromosomes are lost. As embryonic development progresses from the cleavage to the blastocyst stage, the rate of segmental aneuploidy decreases. Hence, it is highly likely that there is a selection against the abnormal cells/embryos.

Additionally, the study also found that patients experiencing recurrent implantation failure were associated with higher rate of meiotic segmental aneuploidy. It is pertinent to take into account the origin of segmental aneuploidies (meiotic or mitotic) and the site of

chromosomal breakage (acentric or centromeric) before selecting the most appropriate embryo for transfer.

B. Genetic analysis of spent culture media samples and blastocoel fluid extracted from the embryonic cavity of blastocyst stage embryos (5/6 days post fertilisation).

Currently, the standard PGD and PGT-A practice utilises DNA derived from cell(s) biopsied from embryos. Along with the requirement of skilled personnel and expensive equipment to facilitate the biopsies, there is speculation that biopsy procedure might adversely affect the embryo viability (Devroey and Van Steirteghem, 2004). To circumvent these problems, blastocoel fluid and spent culture media have been explored as non-invasive sources of embryonic DNA (Gianaroli et al., 2014; Luna et al., 2013, Shamonki et al., 2016).

The aim of this part of the project was to develop a method potentially capable of isolating and amplifying the minute amount of DNA present in blastocoel fluid and spent culture media. Three strategies were thereby designed and optimised in order to amplify any genetic material in the blastocoel fluid; (A) direct adapter ligation based amplification method (B) homopolymer tailing mediated amplification method and (C) ligation mediated MDA method. Following optimisations of all the three methods, the ligation based MDA approach (method C) seemed most plausible for application to blastocoel fluid and spent media samples. In addition, a Y-chromosome assay was developed which successfully identified all the male embryos.

The experimental and clinical validation of ligation based MDA method showed that DNA from blastocoel fluid was too fragmented and low in concentration for optimal amplification. However, the spent culture media samples were found to harbour amplifiable DNA which was subsequently utilised for chromosomal copy number analysis. The

concordance rates between the spent media samples and TE biopsy from the corresponding embryos were promising and showcased the potential feasibility of non-invasive PGT-A in future.

C. Assessment of methylation patterns of imprinted genes in preimplantation embryos.

Genomic imprinting, wherein a gene is expressed in a parent of origin fashion, is a classic example of epigenetics and plays a crucial role during growth and development. There is a growing body of evidence that ART could lead to imprinting perturbations (Gicquel *et al.*, 2003). However, little is known about the origin and long term implications of these imprinting errors. Methylation of one of the parental alleles of an imprinted gene 'silences' it, leading to gene expression of the other parental allele alone. As the methylation and establishment of the imprints is completed just prior to ovulation, the retrieval of partially methylated oocytes may disrupt the imprinting patterns. Furthermore, numerous mouse studies have explored the effect of culture media on imprinting patterns in oocytes and developing embryos, demonstrating the sensitivity of the imprints to the culture environment (Mann et al., 2004; Khosla et al., 2001).

To date, it has been difficult to investigate perturbations in imprinting patterns in human gametes and embryos in part due to a low amount of genetic material available for analysis. Moreover, studies have mainly focused on a few imprinted genes due to the technical challenges arising during simultaneous detection of methylation patterns of a large number of imprinted genes (Denomme & Mann, 2012; Brenna .et al., 2009; White et al., 2015). Therefore, the aim of this part of the study was to develop a technique capable of assessing methylation patterns of CpG islands of ~20 characterised imprinted genes simultaneously embryonic biopsies.

A panel of primers for 23 DMRs corresponding to 20 imprinted genes was developed using bioinformatics tools and a multiplex PCR based bisulfite sequencing method was developed. The method was applied to TE and ICM biopsies from 9 euploid human blastocysts. An imprinting landscape was successfully established for the 23 DMRs included in the study for TE and ICM samples derived from the same embryo. Moreover, the imprinting perturbations were demonstrated to occur at a considerable frequency in human preimplantations embryos, a finding in line with imprinting studies in human and mouse embryos (Ibala-Romdhane et al., 2011; Shi et al. , 2014; Vrooman & Bartolomei, 2016; White et al., 2015). To our knowledge, this is the first study to develop a targeted approach to interrogate methylation status of a large number of imprinted genes simultaneously in TE and ICM lineages derived from euploid human blastocysts.

7.2 Study Limitations

The studies undertaken during this thesis had several limitations which are acknowledged and discussed in each chapter individually. Some of these limitations will be discussed here in context of current state of research in the field of reproductive genetics.

It was recently shown by Van Der Aa et al. (2013) that a possible artefact in chromosomal copy number assignmnet for individual chromosomal regions can arise from asynchrony of DNA replication across the genome. The study demonstarted that the early replicating areas of the genome have a higher copy number than the late replicating ones during S-phase of cell cycle. However, while this is a theoretical possibility of a segmental imbalance artefact applicable to any study assessing chromosomal copy numer based on DNA quantification, there is still no convincing evidence yet of this artefact to have occurred.

All the non-invasive PGT-A studies undertaken to date have compared the chromosomal complement obtained from spent culture media/blastocoesl fluid to the trophectoderm biopsy of their corresponding embryo. However, this form of comparison likely overestimates discrepancies in concordance rates, since mosaicism is highly prevalent in preimplantation embryos. The true efficacy of the non-invasive PGT-A method could be established if the obtained chromosomal results from such assays were to be compared with that of the entire embryo. However, availability of a large cohort of embryos donated for research is limited.

7.3. Future research

The evaluation of the chromosome content has been performed for more than two decades on DNA derived from embryo biopsies via molecular cytogenetic techniques. However, it is speculated that the invasive nature of embryo biopsy may have an adverse impact on embryo viability. This has led to a drive to explore non-invasive sources of embryonic DNA, such as blastocoel fluid and spent culture media. Although a few studies have reported promising results, the feasibility of clinical application of non-invasive PGT-A remains to be established with further technical optimisations and validations. However, from data available so far, including from this study, it seems highly likely that non-invasive PGT-A may provide an alternative to existing PGT-A methods which require embryo biopsy. In fact, the clinical validation of the non-invasive method developed during the course of this study is currently underway. Most importantly the current study involves multiple IVF centres and aims to optimise and validate the non-invasive assay in different culture systems.

Although aneuploidy is known to be a major factor leading to negative IVF outcome, about one third of embryos known to be euploid fail to implant. Hence in recent years interest

has sparked in the exploration of other factors, underlying embryonic viability. One of these factors is mitochondrial DNA content which has been shown to be correlated with the implantation potential of euploid embryos. Another emerging area of interest is the epigenetic regulation in preimplantation embryos and its impact on embryonic development. In fact, the findings of this study show that imprinting errors are fairly common in euploid blastocysts suggesting a potential impact on embryo viability. However, these findings need to be ascertained with further studies in a larger sample cohort. In addition, the future work for this study involves expansion of the developed imprinted genes panel in order to incorporate all the characterised imprinted loci in the human genome along with gene expression studies to confirm the observed imprinting perturbations.

References

Achache, H. and Revel, A. (2006) 'Endometrial receptivity markers, the journey to successful embryo implantation', *Human Reproduction Update*. Oxford University Press, 12(6), pp. 731–746.

Agarwal, A., Gupta, S. and Sharma, R. K. (2005) 'Role of oxidative stress in female reproduction.', *Reproductive biology and endocrinology : RB&E*. BioMed Central, 3, p. 28.

Aguilera, A. and García-Muse, T. (2013) 'Causes of Genome Instability', *Annual Review of Genetics*, 47(1), pp. 1–32.

Amit, M. *et al.* (2000) 'Clonally derived human embryonic stem cell lines maintain pluripotency and proliferative potential for prolonged periods of culture', *Developmental Biology*, 227(2), pp. 271–278.

Angell, R. (1997) 'First-meiotic-division nondisjunction in human oocytes.', *American journal of human genetics*. Elsevier, 61(1), pp. 23–32.

Aoki, V. W. *et al.* (2005a) 'Comparison of four media types during 3-day human IVF embryo culture', *Reproductive BioMedicine Online*, 10(5), pp. 600–606.

Aoki, V. W. *et al.* (2005b) 'Comparison of four media types during 3-day human IVF embryo culture', *Reproductive BioMedicine Online*, 10(5), pp. 600–606.

Assou, S. *et al.* (2011) 'Dynamic changes in gene expression during human early embryo development: from fundamental aspects to clinical applications', *Human Reproduction Update*. Inserm, 17(2), pp. 272–290.

Assou, S. *et al.* (2014) 'Non-invasive pre-implantation genetic diagnosis of X-linked disorders', *Medical Hypotheses*, 83(4), pp. 506–508.

Baart, E. B. *et al.* (2006) 'Preimplantation genetic screening reveals a high incidence of aneuploidy and mosaicism in embryos from young women undergoing IVF', *Human Reproduction*, 21(1), pp. 223–233.

Baart, E. B. *et al.* (2007) 'Milder ovarian stimulation for in-vitro fertilization reduces aneuploidy in the human preimplantation embryo: A randomized controlled trial', *Human Reproduction*. Cambridge Reviews in Human Reproduction, Cambridge University Press, Cambridge, 22(4), pp. 980–988.

Balaban, B. *et al.* (2008) 'A randomized controlled study of human Day 3 embryo cryopreservation by slow freezing or vitrification: vitrification is associated with higher survival, metabolism and blastocyst formation', *Human Reproduction*. Oxford University Press, 23(9), pp. 1976–1982.

Bar, S. *et al.* (2017) 'Large-Scale Analysis of Loss of Imprinting in Human Pluripotent Stem Cells', *Cell Reports*, 19(5), pp. 957–968.

Barcroft, L. C. *et al.* (2003) 'Aquaporin proteins in murine trophectoderm mediate transepithelial water movements during cavitation', *Developmental Biology*, 256(2), pp. 342–354.

Battaglia, D. E. *et al.* (1996) 'Influence of maternal age on meiotic spindle assembly in oocytes from naturally cycling women', *Human Reproduction*. Oxford University Press, 11(10), pp. 2217–2222.

Bedford, J. M. (1970) 'The Saga of Mammalian Sperm from Ejaculation to Syngamy', in *Mammalian Reproduction*. Berlin, Heidelberg: Springer Berlin Heidelberg, pp. 124–182.

Biase, F. H. *et al.* (2008) 'Global poly(A) mRNA expression profile measured in individual bovine oocytes and cleavage embryos.', *Zygote (Cambridge, England)*, 16(1), pp. 29–38.

Bielanska, M., Tan, S. L. and Ao, A. (2002) 'Chromosomal mosaicism throughout human preimplantation development in vitro: incidence, type, and relevance to embryo outcome.', *Human reproduction (Oxford, England)*. Oxford University Press, 17(2), pp. 413–419.

Biggers, J. D. (2002) 'Thoughts on embryo culture conditions.', *Reproductive biomedicine online*, 4 Suppl 1(June), pp. 30–8.

Blockeel, C. *et al.* (2008) 'Prospectively randomized controlled trial of PGS in IVF/ICSI patients with poor implantation.', *Reproductive biomedicine online*. Elsevier, 17(6), pp. 848–854.

Boivin, J. *et al.* (2007) 'International estimates of infertility prevalence and treatment-seeking: potential need and demand for infertility medical care', *Human Reproduction*, 22(6), pp. 1506–1512.

Bonduelle, M. *et al.* (1995) 'Comparative follow-up study of 130 children born after intracytoplasmic sperm injection and 130 children born after in-vitro fertilization.', *Human reproduction (Oxford, England)*. Oxford University Press, 10(12), pp. 3327–31.

Bonduelle, M. *et al.* (2002) 'Neonatal data on a cohort of 2889 infants born after ICSI (1991-1999) and of 2995 infants born after IVF (1983-1999).', *Human reproduction (Oxford, England)*, 17(3), pp. 671–94.

Braude, P., Bolton, V. and Moore, S. (1988) 'Human gene expression first occurs between the four- and eight-cell stages of preimplantation development.', *Nature*, 332(6163), pp. 459–461.

Brewer, C. *et al.* (1998) 'A chromosomal deletion map of human malformations.', *American journal of human genetics*, 63(4), pp. 1153–9.

Brewer, C. *et al.* (1999) 'A chromosomal duplication map of malformations: regions of suspected haplo- and triplolethality--and tolerance of segmental aneuploidy--in humans.', *American journal of human genetics*, 64(6), pp. 1702–1708.

Brezina, P. R., Anchan, R. and Kearns, W. G. (2016) 'Preimplantation genetic testing for aneuploidy: what technology should you use and what are the differences?', *Journal of Assisted Reproduction and Genetics*, 33(7), pp. 823–832.

Brezina, P. R. and Kutteh, W. H. (2015) 'Clinical applications of preimplantation genetic testing', *BMJ*, 350(feb19 3), pp. g7611–g7611.

Butler, M. G. (2009) 'Genomic imprinting disorders in humans: A mini-review', *Journal of Assisted Reproduction and Genetics*, 26(9–10), pp. 477–486.

Caixeta, E. S. *et al.* (2009) 'Effect of follicle size on mRNA expression in cumulus cells and oocytes of Bos indicus: An approach to identify marker genes for developmental competence', *Reproduction, Fertility and Development*, 21(5), pp. 655–664.

Calogero, A. E. *et al.* (2003) 'Sperm aneuploidy in infertile men', *Reproductive biomedicine online*, 6(3), pp. 310–317.

Chang, M. C. (1959) 'Firtilization of rabbit ova in vitro', *Nature*. Nature Publishing Group, 184(4684), pp. 466–467.

Chatziparasidou, A. *et al.* (2015) 'Sperm aneuploidy in infertile male patients: A systematic review of the literature', *Andrologia*, 47(8), pp. 847–860.

Chavez, S. L. *et al.* (2012) 'Dynamic blastomere behaviour reflects human embryo ploidy by the four-cell stage', *Nature Communications*, 3, p. 1251.

Chung, Denise T Drábek, Jirí Opel, Kerry L Butler, John M McCord, B. R. (2004) 'A study on the effects of degradation and template concentration on the amplification efficiency of the STR Miniplex primer sets.', *Journal of forensic sciences*, 49(4), pp. 733–740.

Clark, S. J. *et al.* (2017) 'Genome-wide base-resolution mapping of DNA methylation in single cells using single-cell bisulfite sequencing (scBS-seq)', *Nature Protocols*, 12(3), pp. 534–547.

Colls, P. *et al.* (2009) 'Increased efficiency of preimplantation genetic diagnosis for aneuploidy by testing 12 chromosomes', *Reproductive BioMedicine Online*. Elsevier, 19(4), pp. 532–538.

Cooper, G. M. (2000) 'Meiosis and Fertilization', in *The Cell, A Molecular Approach*. Sinauer Associates.

Cooper, T. G. *et al.* (2009) 'World Health Organization reference values for human semen characteristics', *Human Reproduction Update*, 16(3), pp. 231–245.

Cox, G. F. *et al.* (2002) 'Report Intracytoplasmic Sperm Injection May Increase the Risk of Imprinting Defects', *Am. J. Hum. Genet*. Elsevier, 71(1), pp. 162–164.

Czyz, Z. T., Kirsch, S. and Polzer, B. (2015) 'Principles of Whole-Genome Amplification', in. Humana Press, New York, NY, pp. 1–14.

Dailey, T. *et al.* (1996) 'Association between nondisjunction and maternal age in meiosis-II human oocytes.', *American journal of human genetics*. Elsevier, 59(1), pp. 176–84.

Dean, F. B. *et al.* (2002) 'Comprehensive human genome amplification using multiple displacement amplification', *Proceedings of the National Academy of Sciences*, 99(8), pp. 5261–5266.

DeBaun, M. R., Niemitz, E. L. and Feinberg, A. P. (2003) 'Association of In Vitro Fertilization with Beckwith-Wiedemann Syndrome and Epigenetic Alterations of LIT1 and H19', *The American Journal of Human Genetics*, 72(1), pp. 156–160.

Debrock, S. *et al.* (2010) 'Preimplantation genetic screening for aneuploidy of embryos after in vitro fertilization in women aged at least 35 years: a prospective randomized trial', *Fertility and Sterility*, 93(2), pp. 364–373.

Delhanty, J. D. A. *et al.* (1993) 'Detection of aneuploidy and chromosomal mosaicism in human embryos during preimplantation sex determination by fluorescent in situ hybridisation, (FISH)', *Human Molecular Genetics*, 2(8), pp. 1183–1185.

Delhanty, J. D. A. *et al.* (1997) 'Multicolour FISH detects frequent chromosomal mosaicism and chaotic division in normal preimplantation embryos from fertile patients', *Human Genetics*. Springer-Verlag, 99(6), pp. 755–760.

Demko, Z. P. *et al.* (2016) 'Effects of maternal age on euploidy rates in a large cohort of embryos analyzed with 24-chromosome single-nucleotide polymorphism-based preimplantation genetic screening', *Fertility and Sterility*, 105(5), pp. 1307–1313.

Denomme, M. M. *et al.* (2016) 'Epigenetic dysregulation observed in monosomy blastocysts further compromises developmental potential', *PLoS ONE*. Edited by O. El-Maarri. Public Library of Science, 11(6), p. e0156980.

Denomme, M. M. and Mann, M. R. W. (2012) 'Genomic imprints as a model for the analysis of epigenetic stability during assisted reproductive technologies.', *Reproduction (Cambridge, England)*, 144(4), pp. 393–409.

Devroey, P. and Van Steirteghem, A. (2004) 'A review of ten years experience of ICSI', *Human Reproduction Update*, 10(1), pp. 19–28.

Diez-Juan, A. *et al.* (2015) 'Mitochondrial DNA content as a viability score in human euploid embryos: Less is better', *Fertility and Sterility*, 104(3), p. 534–541.e1.

Dressler, D. and Potter, H. (1982) 'Molecular mechanisms in genetic recombination.', *Annual review of biochemistry*. Annual Reviews 4139 El Camino Way, P.O. Box 10139, Palo Alto, CA 94303-0139, USA, 51(12), pp. 727–761.

Dumollard, R. *et al.* (2009) 'Mitochondrial function and redox state in mammalian embryos', *Seminars in Cell and Developmental Biology*, 20(3), pp. 346–353.

Durkin, S. G. and Glover, T. W. (2007) 'Chromosome Fragile Sites (2007).pdf', *Annual Review of Genetics*, 41(1), pp. 169–192.

Dyce, J. *et al.* (1987) 'Do trophectoderm and inner cell mass cells in the mouse blastocyst maintain discrete lineages?', *Development (Cambridge, England)*, 100(4), pp. 685–98.

van Echten-Arends, J. *et al.* (2011) 'Chromosomal mosaicism in human preimplantation embryos: A systematic review', *Human Reproduction Update*. Oxford University Press, pp. 620–627.

Eichenlaub-Ritter, U. *et al.* (2004) 'Spindles, mitochondria and redox potential in ageing oocytes.', *Reproductive biomedicine online*, 8(1), pp. 45–58.

Eroglu, A. and Layman, L. C. (2012) 'Role of ART in imprinting disorders', *Seminars in Reproductive Medicine*. NIH Public Access, 30(2), pp. 92–104.

Evers, J. L. (2002) 'Female subfertility', *The Lancet*, 360(9327), pp. 151–159.

Fauser, B. C. *et al.* (1999) 'Minimal ovarian stimulation for IVF: appraisal of potential benefits and drawbacks.', *Human reproduction (Oxford, England)*, 14(11), pp. 2681–6.

Feichtinger, M. *et al.* (2017) 'Non-invasive preimplantation genetic screening using array comparative genomic hybridization on spent culture media: a proof-of-concept pilot study', *Reproductive BioMedicine Online*. Elsevier, 34(6), pp. 583–589.

Ferretti, L. and Sgaramella, V. (1981) 'Specific and reversible inhibition of the blunt end joining activity of the T4 DNA ligase', *Nucleic Acids Research*. Oxford University Press, 9(15), pp. 3695–3705.

Fiorentino, F. *et al.* (2014) 'Development and validation of a next-generation sequencing-based protocol for 24-chromosome aneuploidy screening of embryos', *Fertility and Sterility*, 101(5), p. 1375–1382.e2.

Fogarty, N. M. E. *et al.* (2017) 'Genome editing reveals a role for OCT4 in human embryogenesis', *Nature*. Nature Publishing Group, 550(7674), pp. 67–73.

Fowden, A. L. *et al.* (2006) 'Imprinted genes, placental development and fetal growth', *Hormone Research*, 65(SUPPL. 3), pp. 50–58.

FOWLER, R. E. and EDWARDS, R. G. (1957) 'Induction of superovulation and pregnancy in mature mice by gonadotrophins', *The Journal of endocrinology*, 15(4), pp. 374–384.

Fragouli, E. *et al.* (2006) 'Comparative genomic hybridization analysis of human oocytes and polar bodies', *Human Reproduction*. Oxford University Press, 21(9), pp. 2319–2328.

Fragouli, E. *et al.* (2011) 'Cytogenetic analysis of human blastocysts with the use of FISH, CGH and aCGH: Scientific data and technical evaluation', *Human Reproduction*, 26(2), pp. 480–490.

Fragouli, E. *et al.* (2013a) 'The origin and impact of embryonic aneuploidy', *Human Genetics*. Springer Berlin Heidelberg, 132(9), pp. 1001–1013.

Fragouli, E. *et al.* (2013b) 'The origin and impact of embryonic aneuploidy', *Human Genetics*, 132(9), pp. 1001–1013.

Fragouli, E. *et al.* (2015) 'Altered Levels of Mitochondrial DNA Are Associated with Female Age, Aneuploidy, and Provide an Independent Measure of Embryonic Implantation Potential', *PLoS Genetics*. Edited by S. K. Kim. Public Library of Science, 11(6), p. e1005241.

Fragouli, E. *et al.* (2017) 'Analysis of implantation and ongoing pregnancy rates following the transfer of mosaic diploid–aneuploid blastocysts', *Human Genetics*, 136(7), pp. 805–819.

Fragouli, E. *et al.* (2017) 'Analysis of implantation and ongoing pregnancy rates following the transfer of mosaic diploid–aneuploid blastocysts', *Human Genetics*.

Fragouli, E. and Wells, D. (2011) 'Aneuploidy in the human blastocyst', *Cytogenetic and Genome Research*, 133(2–4), pp. 149–159.

Franasiak, J. M. *et al.* (2014a) 'The nature of aneuploidy with increasing age of the female partner: a review of 15,169 consecutive trophectoderm biopsies evaluated with comprehensive chromosomal screening', *Fertility and Sterility*, 101(3), p. 656–663.e1.

Franasiak, J. M. *et al.* (2014b) 'The nature of aneuploidy with increasing age of the female partner: A review of 15,169 consecutive trophectoderm biopsies evaluated with comprehensive chromosomal screening', *Fertility and Sterility*, 101(3), p. 656–663.e1.

Fulka, H. *et al.* (2004) 'DNA methylation pattern in human zygotes and developing embryos', *Reproduction*. Society for Reproduction and Fertility, 128(6), pp. 703–708.

Gabriel, A. S. *et al.* (2011) 'Array comparative genomic hybridisation on first polar bodies suggests that non-disjunction is not the predominant mechanism leading to aneuploidy in humans', *Journal of Medical Genetics*, 48(7), pp. 433–437.

Gardner, D. K. *et al.* (2015) 'Diagnosis of human preimplantation embryo viability', *Human Reproduction Update*, 21(6), pp. 727–747.

Gardner, D. K. and Lane, M. (1998) 'Culture of viable human blastocysts in defined sequential serum-free media.', *Human reproduction (Oxford, England)*. Oxford University Press, 13 Suppl 3(suppl 3), p. 148–159; discussion 160.

Gardner, D. K. and Wale, P. L. (2013) 'Analysis of metabolism to select viable human embryos for transfer', in *Fertility and Sterility*, pp. 1062–1072.

Gardner, D. and Lane, M. (1997) 'Culture and selection of viable blastocysts: a feasible proposition for human IVF?', *Human Reproduction Update*. Oxford University Press, 3(4), pp. 367–382.

Geuns, E. *et al.* (2003) 'Methylation imprints of the imprint control region of the SNRPN-gene in human gametes and preimplantation embryos', *Human Molecular Genetics*, 12(22), pp. 2873–2879.

Gianaroli, L. *et al.* (2005) 'Frequency of aneuploidy in sperm from patients with extremely severe male factor infertility', *Human Reproduction*. Oxford University Press, 20(8), pp. 2140–2152.

Gianaroli, L., Magli, M. C., *et al.* (2014) 'Blastocentesis: A source of DNA for preimplantation genetic testing. Results from a pilot study', *Fertility and Sterility*, 102(6), pp. 1692–1699.

Gianaroli, L., Magli, M. C., *et al.* (2014) 'Blastocentesis: a source of DNA for preimplantation genetic testing. Results from a pilot study.', *Fertility and sterility*. Elsevier, 102(6), p. 1692–9.e6.

Giardino, D. *et al.* (2009) 'De novo balanced chromosome rearrangements in prenatal diagnosis', *Prenatal Diagnosis*, 29(3), pp. 257–265.

Gicquel, C. *et al.* (2003) 'In vitro fertilization may increase the risk of Beckwith-Wiedemann syndrome related to the abnormal imprinting of the KCN1OT gene.', *American journal of human genetics*. Elsevier, 72(5), pp. 1338–41.

Gleicher, N., Kushnir, V. A. and Barad, D. H. (2014) 'Preimplantation genetic screening (PGS) still in search of a clinical application: A systematic review', *Reproductive Biology and Endocrinology*. BioMed Central, 12(1), p. 22.

Goddijn, M. and Leschot, N. J. (2000) 'Genetic aspects of miscarriage', *Best Practice & Research Clinical Obstetrics & Gynaecology*, 14(5), pp. 855–865.

Griesinger, G. *et al.* (2006) 'GnRH agonist for triggering final oocyte maturation in the GnRH antagonist ovarian hyperstimulation protocol: A systematic review and meta-analysis', *Human Reproduction Update*. Oxford University Press, 12(2), pp. 159–168.

Griffin, D. K. *et al.* (1992) 'Dual fluorescent in situ hybridisation for simultaneous detection of X and Y chromosome-specific probes for the sexing of human preimplantation embryonic nuclei', *Human Genetics*, 89(1), pp. 18–22.

Grobstein, C. (1985) 'The early development of human embryos', *J Med Philos*, 10(3), pp. 213–236.

Guo, G. *et al.* (2010) 'Resolution of Cell Fate Decisions Revealed by Single-Cell Gene Expression Analysis from Zygote to Blastocyst', *Developmental Cell*, 18(4), pp. 675–685.

Gutiérrez-Mateo, C. *et al.* (2011) 'Validation of microarray comparative genomic hybridization for comprehensive chromosome analysis of embryos', *Fertility and Sterility*, 95(3), pp. 953–958.

Hajkova, P. *et al.* (2002) 'Epigenetic reprogramming in mouse primordial germ cells', *Mechanisms of Development*, 117(1–2), pp. 15–23.

Hamatani, T. *et al.* (2004) 'Age-associated alteration of gene expression patterns in mouse oocytes', *Human Molecular Genetics*, 13(19), pp. 2263–2278.

Hamatani, T. *et al.* (2006) 'Global gene expression profiling of preimplantation embryos.', *Human cell*, 19(3), pp. 98–117.

Hammond, E. M. *et al.* (2002) 'Hypoxia Links ATR and p53 through Replication Arrest', *Molecular and Cellular Biology*, 22(6), pp. 1834–1843.

Hammond, E. R. *et al.* (2017) 'Characterizing nuclear and mitochondrial DNA in spent embryo culture media: genetic contamination identified', *Fertility and Sterility*, 107(1), p. 220–228.e5.

Hammond, E. R., Shelling, A. N. and Cree, L. M. (2016) 'Nuclear and mitochondrial DNA in blastocoele fluid and embryo culture medium: Evidence and potential clinical use', *Human Reproduction*. Oxford University Press, 31(8), pp. 1653–1661.

Handyside, A. H. *et al.* (1990a) 'Pregnancies from biopsied human preimplantation embryos sexed by Y-specific DNA amplification', *Nature*, 344(6268), pp. 768–770.

Handyside, A. H. *et al.* (1990b) 'Pregnancies from biopsied human preimplantation embryos sexed by Y-specific DNA amplification.', *Nature*. Nature Publishing Group, 344(6268), pp. 768–770.

Handyside, A. H. *et al.* (2010) 'Karyomapping: A universal method for genome wide analysis of genetic disease based on mapping crossovers between parental haplotypes', *Journal of Medical Genetics*. Elsevier, 47(10), pp. 651–658.

Handyside, A. H. *et al.* (2012) 'Multiple meiotic errors caused by predivision of chromatids in women of advanced maternal age undergoing in vitro fertilisation.', *European journal of human genetics : EJHG*. Nature Publishing Group, 20(7), pp. 742–7.

Handyside, A. H. (2013) '24-chromosome copy number analysis: A comparison of available technologies', *Fertility and Sterility*, 100(3), pp. 595–602.

Hansis, C. *et al.* (2001) 'Analysis of Oct-4 expression and ploidy in individual human blastomeres.', *Molecular human reproduction*, 7(2), pp. 155–61.

Hardarson, T. *et al.* (2008) 'Preimplantation genetic screening in women of advanced maternal age caused a decrease in clinical pregnancy rate: A randomized controlled trial', *Human Reproduction*, 23(12), pp. 2806–2812.

Harper, J. *et al.* (2010) 'What next for preimplantation genetic screening (PGS)? A position statement from the ESHRE PGD Consortium steering committee', *Human Reproduction*, 25(4), pp. 821–823.

Harper, J. C. *et al.* (1995) 'Mosaicism of autosomes and sex chromosomes in morphologically normal, monospermic preimplantation human embryos', *Prenatal Diagnosis*. John Wiley & Sons, Ltd., 15(1), pp. 41–49.

Harper, J. C. *et al.* (2017) 'Recent developments in genetics and medically assisted reproduction: from research to clinical applications', *European Journal of Human Genetics*. Oxford University Press, 2017(3).

Harrison, R. H. *et al.* (2000) 'Lack of cell cycle checkpoints in human cleavage stage embryos revealed by a clonal pattern of chromosomal mosaicism analysed by sequential multicolour FISH [In Process Citation]', *Zygote.*, 8(3), pp. 217–224.

Hassold, T. *et al.* (1996) 'Human aneuploidy: Incidence, origin and etiology', in *Environmental and Molecular Mutagenesis*, pp. 167–175.

Hassold, T. and Hunt, P. (2001) 'To err (meiotically) is human: the genesis of human aneuploidy', *Nat Rev Genet*, 2(4), pp. 280–291.

Hassold, T. and Sherman, S. (2000) 'Down syndrome: genetic recombination and the origin of the extra chromosome 21', *Clinical Genetics*, 57(2), pp. 95–100.

Hellani, A. *et al.* (2008) 'Successful pregnancies after application of array-comparative genomic hybridization in PGS-aneuploidy screening', *Reproductive BioMedicine Online*, 17(6), pp. 841–847.

Hewett, D. R. *et al.* (1998) 'FRA10B structure reveals common elements in repeat expansion and chromosomal fragile site genesis.', *Molcel*, 1(6), pp. 773–781.

Hiraoka, K. *et al.* (2004) 'Blastocoele collapse by micropipetting prior to vitrification gives excellent survival and pregnancy outcomes for human day 5 and 6 expanded blastocysts', *Human Reproduction*. Oxford University Press, 19(12), pp. 2884–2888.

Holubcová, Z. *et al.* (2015) 'Human oocytes. Error-prone chromosome-mediated spindle assembly favors chromosome segregation defects in human oocytes.', *Science (New York, N.Y.)*, 348(6239), pp. 1143–7.

Hook, E. B., Cross, P. K. and Schreinemachers, D. M. (1983) 'Chromosomal Abnormality Rates at Amniocentesis and in Live-Born Infants', *JAMA*. American Medical Association, 249(15), p. 2034.

Hudson, Q. J. *et al.* (2010) 'Genomic imprinting mechanisms in embryonic and extraembryonic mouse tissues', *Heredity*. Europe PMC Funders, 105(1), pp. 45–56.

Huntriss, J. D. *et al.* (2013) 'Variable imprinting of the MEST gene in human preimplantation embryos', *European Journal of Human Genetics*, 21(1), pp. 40–47.

Huntriss, J. and Picton, H. M. (2008) 'Epigenetic consequences of assisted reproduction and infertility on the human preimplantation embryo', *Human Fertility*, 11(2), pp. 85–94.

Ibala-Romdhane, S. *et al.* (2011) 'Analysis of H19 methylation in control and abnormal human embryos, sperm and oocytes', *European Journal of Human Genetics*, 19(11), pp. 1138–1143.

Iourov, I., Vorsanova, S. and Yurov, Y. (2010) 'Somatic Genome Variations in Health and Disease', *Current Genomics*, 11(6), pp. 387–396.

Jacobs, K. *et al.* (2017) 'Mitotic spindle disruption in human preimplantation embryos activates the spindle assembly checkpoint but not apoptosis until Day 5 of development', *MHR: Basic science of reproductive medicine*. Oxford University Press, 23(5), pp. 321–329.

Jensen, P. L. *et al.* (2012) 'Proteomic Analysis of Human Blastocoel Fluid and Blastocyst Cells', *Stem Cells and Development*. Mary Ann Liebert, Inc. 140 Huguenot Street, 3rd Floor New Rochelle, NY 10801 USA, 22(7), pp. 1126–1135.

Jensen, P. L. *et al.* (2014) 'Proteomic analysis of bovine blastocoel fluid and blastocyst cells', *Systems Biology in Reproductive Medicine*. Taylor & Francis, 60(3), pp. 127–135.

St. John, J. C. *et al.* (2010) 'Mitochondrial DNA transmission, replication and inheritance: A journey from the gamete through the embryo and into offspring and embryonic stem cells', *Human Reproduction Update*, 16(5), pp. 488–509.

Johnson, D. S. *et al.* (2010) 'Preclinical validation of a microarray Method for full molecular karyotyping of blastomeres in a 24-h protocol', *Human Reproduction*, 25(4), pp. 1066–1075.

Jones, K. T. and Lane, S. I. R. (2013) 'Molecular causes of aneuploidy in mammalian eggs.', *Development (Cambridge, England)*, 140(18), pp. 3719–30.

Joris, H. *et al.* (1999) 'Reduced survival after human embryo biopsy and subsequent cryopreservation', *Human Reproduction*. Oxford University Press, 14(11), pp. 2833–2837.

Kalousek, D. K. (2000) 'Pathogenesis of chromosomal mosaicism and its effect on early human development', *American Journal of Medical Genetics*, 91(1), pp. 39–45.

Katz-Jaffe, M. G., McReynolds, S., *et al.* (2009) 'The role of proteomics in defining the human embryonic secretome', *Molecular Human Reproduction*. Humana Press, Ottowa, New Jersey, 15(5), pp. 271–277.

Katz-Jaffe, M. G., McCallie, B. R., *et al.* (2009) 'Transcriptome analysis of in vivo and in vitro matured bovine MII oocytes', *Theriogenology*, 71(6), pp. 939–946.

Katz-Jaffe, M. G., Gardner, D. K. and Schoolcraft, W. B. (2006) 'Proteomic analysis of individual human embryos to identify novel biomarkers of development and viability', *Fertility and Sterility*, 85(1), pp. 101–107.

Katz-Jaffe, M. G., Trounson, A. O. and Cram, D. S. (2004) 'Mitotic errors in chromosome 21 of human preimplantation embryos are associated with non-viability', *Molecular Human Reproduction*, 10(2), pp. 143–147.

Khanna, K. K. and Jackson, S. P. (2001) 'DNA double-strand breaks: signaling, repair and the cancer connection.', *Nature genetics*, 27(3), pp. 247–54.

Khoueiry, R. *et al.* (2013) 'Abnormal methylation of KCNQ1OT1 and differential methylation of H19 imprinting control regions in human ICSI embryos', *Zygote*, 21(2), pp. 129–138.

Kiessling, A. A. *et al.* (2009) 'Evidence that human blastomere cleavage is under unique cell cycle control', *Journal of Assisted Reproduction and Genetics*. Springer, 26(4), pp. 187–195.

Kuliev, A. and Verlinsky, Y. (2004) 'Meiotic and mitotic nondisjunction: Lessons from preimplantation genetic diagnosis', *Human Reproduction Update*. Oxford University Press, 10(5), pp. 401–407.

Kushnir, V. A. *et al.* (2017) 'Systematic review of worldwide trends in assisted reproductive technology 2004–2013', *Reproductive Biology and Endocrinology*, 15(1), p. 6.

Lasken, R. S. and Stockwell, T. B. (2007) 'Mechanism of chimera formation during the Multiple Displacement Amplification reaction', *BMC Biotechnology*. BioMed Central, 7(1), p. 19.

Lazinski, D. W. and Camilli, A. (2013) 'Homopolymer tail-mediated ligation PCR: A streamlined and highly efficient method for DNA cloning and library construction', *BioTechniques*. NIH Public Access, 54(1), pp. 25–34.

Ledger, W. L. *et al.* (2006) 'The costs to the NHS of multiple births after IVF treatment in the UK', *BJOG: An International Journal of Obstetrics and Gynaecology*. Blackwell Science Ltd, 113(1), pp. 21–25.

Lee, A. and Kiessling, A. A. (2017) 'Early human embryos are naturally aneuploid???can that be corrected?', *Journal of Assisted Reproduction and Genetics*. Springer, 34(1), pp. 15–21.

Lee, J. *et al.* (2002) 'Erasing genomic imprinting memory in mouse clone embryos produced from day 11.5 primordial germ cells.', *Development (Cambridge, England)*, 129(8), pp. 1807–1817.

Lennerz, J. K. *et al.* (2010) 'Addition of H19 "loss of methylation testing" for Beckwith-Wiedemann syndrome (BWS) increases the diagnostic yield', *Journal of Molecular Diagnostics*, 12(5), pp. 576–588.

Li, E. (2002) 'Chromatin modification and epigenetic reprogramming in mammalian development', *Nature Reviews Genetics*. Nature Publishing Group, 3(9), pp. 662–673.

Li, Y. and Sasaki, H. (2011) 'Genomic imprinting in mammals: its life cycle, molecular mechanisms and reprogramming.', *Cell research*. Nature Publishing Group, 21(3), pp. 466–73.

Licznerski, G. and Lindsten, J. (2009) 'Trisomy 21 in man due to maternal non-disjunction during the first meiotic division', *Hereditas*. Blackwell Publishing Ltd, 70(1), pp. 153–154.

Liu, W. Q. *et al.* (2017) 'Non-invasive pre-implantation aneuploidy screening and diagnosis of beta thalassemia IVSII654 mutation using spent embryo culture medium', *Annals of Medicine*. Taylor & Francis, 49(4), pp. 319–328.

Lonergan, P. *et al.* (2000) 'Relationship between time of first cleavage and the expression of IGF-I growth factor, its receptor, and two housekeeping genes in bovine two-cell embryos and blastocysts produced in vitro', *Molecular Reproduction and Development*, 57(2), pp.

146–152.

Lonergan, P. *et al.* (2006) 'Effect of culture environment on gene expression and developmental characteristics in IVF-derived embryos', *Theriogenology*, 65(1), pp. 137–152.

Lorthongpanich, C. *et al.* (2013) 'Single-cell DNA-methylation analysis reveals epigenetic chimerism in preimplantation embryos', *Science*, 341(6150), pp. 1110–1112.

Lu, Y., Wang, N. and Jin, F. (2013) 'Long-term follow-up of children conceived through assisted reproductive technology', *Journal of Zhejiang University SCIENCE B*. Zhejiang University Press, 14(5), pp. 359–371.

Luna, M. *et al.* (2013) 'Validation of blastocoele fluid aspiration for preimplantation genetic screening using array comparative genomic hybridization (aCGH)', *Fertility and Sterility*. Elsevier, 100(3), p. S208.

Magli, M. C. *et al.* (2016) 'Preimplantation genetic testing: Polar bodies, blastomeres, trophectoderm cells, or blastocoelic fluid?', *Fertility and Sterility*, 105(3), p. 676–683e5.

Maher, E. R. *et al.* (2003) 'Beckwith-Wiedemann syndrome and assisted reproduction technology (ART)', *J Med Genet*, 40(1), pp. 62–64.

Manandhar, G., Schatten, H. and Sutovsky, P. (2005) 'Centrosome Reduction During Gametogenesis and Its Significance', *Biology of Reproduction*, 72(1), pp. 2–13.

Mann, M. R. W. (2004) 'Selective loss of imprinting in the placenta following preimplantation development in culture', *Development*, 131(15), pp. 3727–3735.

Mantikou, E. *et al.* (2012) 'Molecular origin of mitotic aneuploidies in preimplantation embryos', *Biochimica et Biophysica Acta - Molecular Basis of Disease*, 1822(12), pp. 1921–1930.

Mantikou, E. *et al.* (2013) 'Embryo culture media and IVF/ICSI success rates: a systematic review', *Human Reproduction Update*. Oxford University Press, 19(3), pp. 210–220.

Market-Velker, B. A. *et al.* (2009) 'Dual effects of superovulation: Loss of maternal and paternal imprinted methylation in a dose-dependent manner', *Human Molecular Genetics*, 19(1), pp. 36–51.

Mascarenhas, M. N. *et al.* (2012) 'National, Regional, and Global Trends in Infertility Prevalence Since 1990: A Systematic Analysis of 277 Health Surveys', *PLoS Medicine*. Edited by N. Low. Public Library of Science, 9(12), p. e1001356.

Mastenbroek, S. *et al.* (2007) 'In Vitro Fertilization with Preimplantation Genetic Screening', *New England Journal of Medicine*. Massachusetts Medical Society, 357(1), pp. 9–17.

Matzuk, M. M. and Lamb, D. J. (2008) 'The biology of infertility: research advances and clinical challenges', *Nat Med*. Nature Publishing Group, 14(11), pp. 1197–1213.

Mccord, B. R. *et al.* (2011) 'An Investigation of the Effect of DNA Degradation and Inhibition on PCR Amplification of Single Source and Mixed Forensic Samples', *Project 2006-DN-BX-K006. Final Report to the US Department of Justice*, pp. 1–66.

McCoy, R. C., Demko, Z., *et al.* (2015) 'Common variants spanning PLK4 are associated with

mitotic-origin aneuploidy in human embryos', *Science*, 348(6231), pp. 235–238.

McCoy, R. C., Demko, Z. P., *et al.* (2015) 'Evidence of Selection against Complex Mitotic-Origin Aneuploidy during Preimplantation Development', *PLoS Genetics*. Edited by N. Arnheim. CRC Press, 11(10), p. e1005601.

McCoy, R. C. (2017) 'Mosaicism in Preimplantation Human Embryos: When Chromosomal Abnormalities Are the Norm', *Trends in Genetics*, 33(7), pp. 448–463.

Mehta, A. and Haber, J. E. (2014) 'Sources of DNA double-strand breaks and models of recombinational DNA repair', *Cold Spring Harbor Perspectives in Biology*, 6(9), pp. a016428–a016428.

Menasha, J. *et al.* (2005) 'Incidence and spectrum of chromosome abnormalities in spontaneous abortions: New insights from a 12-year study', *Genetics in Medicine*, 7(4), pp. 251–263.

Moley, K. H., Chi, M. M. and Mueckler, M. M. (1998) 'Maternal hyperglycemia alters glucose transport and utilization in mouse preimplantation embryos.', *The American journal of physiology*, 275(1 Pt 1), pp. E38–E47.

Moore, C. M. and Best, R. G. (2001) 'Chromosomal Genetic Disease: Structural Aberrations', *Encylopedia of Life Sciences*. Chichester, UK: John Wiley & Sons, Ltd, 1, pp. 1–8.

Morales, C. *et al.* (2008) 'Cytogenetic study of spontaneous abortions using semi-direct analysis of chorionic villi samples detects the broadest spectrum of chromosome abnormalities', *American Journal of Medical Genetics Part A*, 146A(1), pp. 66–70.

Mouliere, F. and Rosenfeld, N. (2015) 'Circulating tumor-derived DNA is shorter than somatic DNA in plasma', *Proceedings of the National Academy of Sciences*, 112(11), pp. 3178–3179.

Mukaida, T. *et al.* (2006) 'Artificial shrinkage of blastocoeles using either a micro-needle or a laser pulse prior to the cooling steps of vitrification improves survival rate and pregnancy outcome of vitrified human blastocysts', *Human Reproduction*. Oxford University Press, 21(12), pp. 3246–3252.

Munné, S. *et al.* (1993) 'Diagnosis of major chromosome aneuploidies in human preimplantation embryos.', *Human reproduction (Oxford, England)*, 8(12), pp. 2185–2191.

Munné, S. *et al.* (1993a) 'Diagnosis of major chromosome aneuploidies in human preimplantation embryos.', *Human reproduction (Oxford, England)*. Oxford University Press, 8(12), pp. 2185–2191.

Munné, S. *et al.* (1993b) 'Fertilization and early embryology: Diagnosis of major chromosome aneuploidies in human preimplantation embryos', *Human Reproduction*. Oxford University Press, 8(12), pp. 2185–2191.

Munné, S. *et al.* (1994) 'Chromosome mosaicism in human embryos.', *Biology of reproduction*. Oxford University Press, 51(3), pp. 373–379.

Munné, S. *et al.* (1994) 'Chromosome mosaicism in human embryos.', *Biology of reproduction*, 51(3), pp. 373–379.

Munné, S. *et al.* (1995) 'Embryo morphology, developmental rates, and maternal age are correlated with chromosome abnormalities.', *Fertility and sterility*, 64(2), pp. 382–91.

Munné, S. *et al.* (1995) 'Embryo morphology, developmental rates, and maternal age are correlated with chromosome abnormalities**Presented at the 50th Annual Meeting of The American Fertility Society, San Antonio, Texas, November 4 to 9, 1994, where it was awarded the prize paper of the Society for Assisted Reproductive Technology.', *Fertility and Sterility*, 64(2), pp. 382–391.

Munné, S. *et al.* (2007) 'Maternal age, morphology, development and chromosome abnormalities in over 6000 cleavage-stage embryos.', *Reproductive biomedicine online*, 14(5), pp. 628–634.

Munné, S. *et al.* (2017) 'Detailed investigation into the cytogenetic constitution and pregnancy outcome of replacing mosaic blastocysts detected with the use of high-resolution next-generation sequencing', *Fertility and Sterility*, 108(1), p. 62–71.e8.

Munne, S. and Cohen, J. (1998) 'Chromosome abnormalities in human embryos', *Human Reproduction Update*. Oxford University Press, 4(1355–4786 (Print)), pp. 842–855.

Munné, S. and Wells, D. (2017) 'Detection of mosaicism at blastocyst stage with the use of high-resolution next-generation sequencing', *Fertility and Sterility*, pp. 1085–1091.

Nagaoka, S. I., Hassold, T. J. and Hunt, P. A. (2012a) 'Human aneuploidy: mechanisms and new insights into an age-old problem', *Nature Reviews Genetics*. NIH Public Access, 13(7), pp. 493–504.

Nagaoka, S. I., Hassold, T. J. and Hunt, P. A. (2012a) 'Human aneuploidy: mechanisms and new insights into an age-old problem', *Nat Rev Genet*. Nature Publishing Group, 13(7), pp. 493–504.

Nagaoka, S. I., Hassold, T. J. and Hunt, P. A. (2012b) 'Human aneuploidy: mechanisms and new insights into an age-old problem', *Nature Reviews Genetics*, 13(7), pp. 493–504.

Nagaoka, S. I., Hassold, T. J. and Hunt, P. A. (2012b) 'Human aneuploidy: mechanisms and new insights into an age-old problem', *Nat Rev Genet*. NIH Public Access, 13(7), pp. 493–504.

Nakanishi, M. O. *et al.* (2012) 'Trophoblast-specific dna methylation occurs after the segregation of the trophectoderm and inner cell mass in the mouse periimplantation embryo', *Epigenetics*. Taylor & Francis, 7(2), pp. 173–182.

Natesan, S. A. *et al.* (2014) 'Genome-wide karyomapping accurately identifies the inheritance of single-gene defects in human preimplantation embryos in vitro', *Genetics in Medicine*, 16(11), pp. 838–845.

Niakan, K. K. *et al.* (2012) 'Human pre-implantation embryo development', *Development*, 139(5), pp. 829–841.

Oehninger, S. and Hodgen, G. D. (1990) 'Induction of ovulation for assisted reproduction programmes.', *Bailliere's clinical obstetrics and gynaecology*, 4(3), pp. 541–73.

Owen, C. M. *et al.* (2016) 'Aneuploidy rates do not differ between blastocysts biopsied on

day 5 (D5) versus day 6 (D6)', *Fertility and Sterility*. Elsevier, 106(3), p. e148.

de Paepe, C. *et al.* (2014) 'Totipotency and lineage segregation in the human embryo', *Molecular Human Reproduction*, 20(7), pp. 599–618.

Paez, J. G. *et al.* (2004) 'Genome coverage and sequence fidelity of 29 polymerase-based multiple strand displacement whole genome amplification', *Nucleic Acids Research*. Oxford University Press, 32(9), pp. e71–e71.

Palermo, G. *et al.* (1992) 'Pregnancies after intracytoplasmic injection of single spermatozoon into an oocyte', *The Lancet*, 340(8810), pp. 17–18.

Palini, S. *et al.* (2013a) 'Genomic DNA in human blastocoele fluid', *Reproductive BioMedicine Online*, 26(6), pp. 603–610.

Palini, S. *et al.* (2013b) 'Genomic DNA in human blastocoele fluid', *Reproductive BioMedicine Online*, 26(6), pp. 603–610.

Pan, H. *et al.* (2005) 'Transcript profiling during mouse oocyte development and the effect of gonadotropin priming and development in vitro', *Developmental Biology*, 286(2), pp. 493–506.

Papanikolaou, E. G. *et al.* (2008) 'Live birth rates after transfer of equal number of blastocysts or cleavage-stage embryos in IVF. A systematic review and meta-analysis', *Human Reproduction*. Oxford University Press, 23(1), pp. 91–99.

Patel, O. V *et al.* (2007) 'Functional genomics studies of oocyte competence: Evidence that reduced trascript abundance for follistatin is associated with poor developmental competence of bovine oocytes', *Reproduction*, 133(1), pp. 95–106.

Paternot, G. *et al.* (2010) 'Early embryo development in a sequential versus single medium: a randomized study.', *Reproductive biology and endocrinology : RB&E*. BioMed Central, 8, p. 83.

Pellestor, F. *et al.* (2002) 'Mechanisms of non-disjunction in human female meiosis: the co-existence of two modes of malsegregation evidenced by the karyotyping of 1397 in-vitro unfertilized oocytes.', *Human reproduction (Oxford, England)*, 17(8), pp. 2134–2145.

Penzias, A. *et al.* (2017) 'Guidance on the limits to the number of embryos to transfer: a committee opinion', *Fertility and Sterility*, 107(4), pp. 901–903.

Petropoulos, S. *et al.* (2016) 'Single-Cell RNA-Seq Reveals Lineage and X Chromosome Dynamics in Human Preimplantation Embryos', *Cell*, 165(4), pp. 1012–1026.

Polanski, Z. (2013) 'Spindle assembly checkpoint regulation of chromosome segregation in mammalian oocytes', *Reproduction, Fertility and Development*, 25(3), pp. 472–483.

Poli, M. *et al.* (2013) 'The blastocoel fluid as a source of DNA for preimplantation genetic diagnosis and screening', *Fertility and Sterility*. Elsevier, 100(3), p. S37.

Poli, M. *et al.* (2015) 'Characterization and quantification of proteins secreted by single human embryos prior to implantation', *EMBO Molecular Medicine*. Wiley-Blackwell, 7(11), pp. 1–15.

Prevention, C. for D. C. and (2014) *2014 Assisted Reproductive Technology National Summary Report*.

Putkonen, M. T. *et al.* (2010) 'Factors affecting the STR amplification success in poorly preserved bone samples', *Investig Genet*. BioMed Central, 1(1), p. 9.

Rabinowitz, M. *et al.* (2012) 'Origins and rates of aneuploidy in human blastomeres', *Fertility and Sterility*, 97(2), pp. 395–401.

Ravichandran, K. *et al.* (2017) 'Mitochondrial DNA quantification as a tool for embryo viability assessment: retrospective analysis of data from single euploid blastocyst transfers', *Human Reproduction*. Oxford University Press, 32(6), pp. 1–11.

Reik, W. and Walter, J. (2001) 'Genomic imprinting: parental influence on the genome.', *Nature Reviews Genetics*, 2(1), pp. 21–32.

Richardson, C., Horikoshi, N. and Pandita, T. K. (2004) 'The role of the DNA double-strand break response network in meiosis', *DNA Repair*, 3(8–9), pp. 1149–1164.

Rinaudo, P. and Schultz, R. M. (2004) 'Effects of embryo culture on global pattern of gene expression in preimplantation mouse embryos.', *Reproduction (Cambridge, England)*. Society for Reproduction and Fertility, 128(3), pp. 301–11.

Roberts, S. A., Hann, M. and Brison, D. R. (2016) 'Factors affecting embryo viability and uterine receptivity: insights from an analysis of the UK registry data', *Reproductive BioMedicine Online*, 32(2), pp. 197–206.

Robinson, W. P. *et al.* (1997) 'Meiotic origin of trisomy in confined placental mosaicism is correlated with presence of fetal uniparental disomy, high levels of trisomy in trophoblast, and increased risk of fetal intrauterine growth restriction.', *American journal of human genetics*. Elsevier, 60(4), pp. 917–27.

Rodgaard, T., Heegaard, P. M. H. and Callesen, H. (2015) 'Non-invasive assessment of in-vitro embryo quality to improve transfer success', *Reproductive BioMedicine Online*. Elsevier, 31(5), pp. 585–592.

Romar, R. *et al.* (2011) 'Expression of Maternal Transcripts During Bovine Oocyte In Vitro Maturation is Affected by Donor Age', *Reproduction in Domestic Animals*, 46(1), pp. e23–e30.

Roque, M. *et al.* (2013) 'Fresh embryo transfer versus frozen embryo transfer in in vitro fertilization cycles: A systematic review and meta-analysis', *Fertility and Sterility*, 99(1), pp. 156–162.

Rossignol, S. *et al.* (2006) 'The epigenetic imprinting defect of patients with Beckwitn-Wiedemann syndrome born after assisted reproductive technology is not restricted to the 11p15 region', *Journal of Medical Genetics*. BMJ Publishing Group, 43(12), pp. 902–907.

Rubio, C. *et al.* (2003) 'Chromosomal abnormalities and embryo development in recurrent miscarriage couples', *Human Reproduction*. Oxford University Press, 18(1), pp. 182–188.

Saksouk, N., Simboeck, E. and Déjardin, J. (2015) 'Constitutive heterochromatin formation and transcription in mammals', *Epigenetics & Chromatin*. BioMed Central, 8(1), p. 3.

Sallam, H. N., Sallam, N. H. and Sallam, S. H. (2016) 'Non-invasive methods for embryo selection.', *Facts, views & vision in ObGyn*. Vlaamse Vereniging voor Obstetrie en Gynaecologie, 8(2), pp. 87–100.

Sandalinas, M. *et al.* (2000) 'Spectral Karyotyping of Unfertilized and Noninseminated Oocytes', *Fertility and Sterility*, 74(3), p. S2.

Sasaki, H. and Matsui, Y. (2008) 'Epigenetic events in mammalian germ-cell development: reprogramming and beyond', *Nature Reviews Genetics*, 9(2), pp. 129–140.

Scott, R. T. *et al.* (2012a) 'Comprehensive chromosome screening is highly predictive of the reproductive potential of human embryos: A prospective, blinded, nonselection study', *Fertility and Sterility*. Elsevier, 97(4), pp. 870–875.

Scott, R. T. *et al.* (2012b) 'Comprehensive chromosome screening is highly predictive of the reproductive potential of human embryos: A prospective, blinded, nonselection study', *Fertility and Sterility*, 97(4), pp. 870–875.

Seli, E., Robert, C. and Sirard, M. A. (2010) 'Omics in assisted reproduction: Possibilities and pitfalls', *Molecular Human Reproduction*, 16(8), pp. 513–530.

Sermon, K. *et al.* (2016) 'The why, the how and the when of PGS 2.0: current practices and expert opinions of fertility specialists, molecular biologists, and embryologists.', *Molecular human reproduction*, p. gaw034.

Shamonki, M. I. *et al.* (2016) 'Proof of concept: preimplantation genetic screening without embryo biopsy through analysis of cell-free DNA in spent embryo culture media', *Fertility and Sterility*. Elsevier, 106(6), pp. 1312–1318.

Shi, X. *et al.* (2014) 'Abnormal DNA Methylation of Imprinted Loci in Human Preimplantation Embryos', *Reproductive Sciences*, 21(8), pp. 978–983.

Shoaib, M. *et al.* (2008) 'Multiple displacement amplification for complex mixtures of DNA fragments', *BMC Genomics*. BioMed Central, 9(1), p. 415.

Smallwood, S. A. *et al.* (2011) 'Dynamic CpG island methylation landscape in oocytes and preimplantation embryos', *Nature Genetics*. Nature Publishing Group, 43(8), pp. 811–814.

Smith, Z. D. *et al.* (2014) 'DNA methylation dynamics of the human preimplantation embryo', *Nature*. Nature Publishing Group, 511(7511), pp. 611–615.

Spanos, S. *et al.* (2002) 'Caspase activity and expression of cell death genes during development of human preimplantation embryos', *Reproduction*, 124(3), pp. 353–363.

Staessen, C. *et al.* (2004) 'Comparison of blastocyst transfer with or without preimplantation genetic diagnosis for aneuploidy screening in couples with advanced maternal age: a prospective randomized controlled trial', *Human Reproduction*, 19(12), pp. 2849–2858.

Van Steirteghem, A. C., Nagy, Z., *et al.* (1993) 'High fertilization and implantation rates after intracytoplasmic sperm injection.', *Human reproduction (Oxford, England)*, 8(7), pp. 1061–6.

Van Steirteghem, A. C., Liu, J., *et al.* (1993) 'Higher success rate by intracytoplasmic sperm injection than by subzonal insemination. Report of a second series of 300 consecutive treatment cycles.', *Human reproduction (Oxford, England)*, 8(7), pp. 1055–60.

Steptoe, P. C. and Edwards, R. G. (1992a) 'Birth after the reimplantation of a human embryo', *Archives of Pathology and Laboratory Medicine*, p. 321.

Steptoe, P. C. and Edwards, R. G. (1992b) 'Birth after the reimplantation of a human embryo', *Archives of Pathology and Laboratory Medicine*, p. 321.

Stigliani, S. *et al.* (2013) 'Mitochondrial DNA content in embryo culture medium is significantly associated with human embryo fragmentation', *Human Reproduction*, 28(10), pp. 2652–2660.

Stigliani, S. *et al.* (2014) 'Mitochondrial DNA in Day 3 embryo culture medium is a novel, non-invasive biomarker of blastocyst potential and implantation outcome', *Molecular Human Reproduction*, 20(12), pp. 1238–1246.

Sullivan, A. E. *et al.* (2004) 'Recurrent Fetal Aneuploidy and Recurrent Miscarriage', *Obstetrics & Gynecology*, 104(4), pp. 784–788.

Sultan, M. *et al.* (2008) 'A Global View of Gene Activity and Alternative Splicing by Deep Sequencing of the Human Transcriptome', *Science*, 321(5891), pp. 956–960.

Summers, M. C. and Biggers, J. D. (2003) 'Chemically defined media and the culture of mammalian preimplantation embryos: Historical perspective and current issues', *Human Reproduction Update*, 9(6), pp. 557–582.

Sutcliffe, A. G. *et al.* (2006) 'Assisted reproductive therapies and imprinting disorders - A preliminary British survey', *Human Reproduction*, 21(4), pp. 1009–1011.

Suzuki, M. M. and Bird, A. (2008) 'DNA methylation landscapes: Provocative insights from epigenomics', *Nature Reviews Genetics*, 9(6), pp. 465–476.

Swain, J. E. (2010) 'Optimizing the culture environment in the IVF laboratory: Impact of pH and buffer capacity on gamete and embryo quality', *Reproductive BioMedicine Online*, pp. 6–16.

Tatone, C. *et al.* (2008) 'Cellular and molecular aspects of ovarian follicle ageing', *Human Reproduction Update*, 14(2), pp. 131–142.

Telford, N. A., Watson, A. J. and Schultz, G. A. (1990) 'Transition from maternal to embryonic control in early mammalian development: A comparison of several species', *Molecular Reproduction and Development*, pp. 90–100.

Templado, C., Bosch, M. and Benet, J. (2005) 'Frequency and distribution of chromosome abnormalities in human spermatozoa', *Cytogenetic and Genome Research*, 111(3–4), pp. 199–205.

Templado, C., Vidal, F. and Estop, A. (2011) 'Aneuploidy in human spermatozoa', *Cytogenetic and Genome Research*, 133(2–4), pp. 91–99.

Thornhill, A. R. *et al.* (2005) 'ESHRE PGD Consortium "Best practice guidelines for clinical preimplantation genetic diagnosis (PGD) and preimplantation genetic screening (PGS)"', *Human Reproduction*. Oxford University Press, 20(1), pp. 35–48.

Tobler, K. J. *et al.* (2015) 'Blastocoel fluid from differentiated blastocysts harbors embryonic genomic material capable of a whole-genome deoxyribonucleic acid amplification and

comprehensive chromosome microarray analysis', *Fertility and Sterility*, 104(2), pp. 418–425.

Tournaye, H. *et al.* (1992) 'Comparison of in-vitro fertilization in male and tubal infertility: a 3 year survey*', *Human Reproduction*. Oxford University Press, 7(2), pp. 218–222.

Tournaye, H. *et al.* (1994) 'Microsurgical epididymal sperm aspiration and intracytoplasmic sperm injection: a new effective approach to infertility as a result of congenital bilateral absence of the vas deferens.', *Fertility and sterility*, 61(6), pp. 1045–51.

Treff, N. R. *et al.* (2010) 'Accurate single cell 24 chromosome aneuploidy screening using whole genome amplification and single nucleotide polymorphism microarrays', *Fertility and Sterility*. Elsevier, 94(6), pp. 2017–2021.

Treff, N. R. *et al.* (2012) 'Development and validation of an accurate quantitative real-time polymerase chain reaction-based assay for human blastocyst comprehensive chromosomal aneuploidy screening', *Fertility and Sterility*, 97(4), p. 819–824.e2.

Treff, N. R. *et al.* (2017) 'Levels of trophectoderm mitochondrial DNA do not predict the reproductive potential of sibling embryos', *Human Reproduction*. Oxford University Press, 32(4), pp. 954–962.

Tu, J. *et al.* (2015) 'Systematic characteristic exploration of the chimeras generated in multiple displacement amplification through next generation sequencing data reanalysis', *PLoS ONE*. Edited by J. Wang. Public Library of Science, 10(10), p. e0139857.

Tur-Kaspa, I. and Jeelani, R. (2015) 'Clinical guidelines for IVF with PGD for HLA matching', *Reproductive BioMedicine Online*, pp. 115–119.

Uroz, L., Rajmil, O. and Templado, C. (2011) 'Meiotic chromosome abnormalities in fertile men: Are they increasing?', *Fertility and Sterility*, 95(1), pp. 141–146.

Uyar, A. and Seli, E. (2014) 'The impact of assisted reproductive technologies on genomic imprinting and imprinting disorders', *Curr Opin Obstet Gynecol*. NIH Public Access, 26(3), pp. 210–221.

Vanneste, E. *et al.* (2009a) 'Chromosome instability is common in human cleavage-stage embryos', *Nature Medicine*, 15(5), pp. 577–583.

Vanneste, E. *et al.* (2009b) 'Chromosome instability is common in human cleavage-stage embryos.', *Nature medicine*, 15(5), pp. 577–583.

Vera-Rodriguez, M. *et al.* (2015) 'Prediction model for aneuploidy in early human embryo development revealed by single-cell analysis', *Nature Communications*, 6(May), p. 7601.

Verlinsky, Y. *et al.* (1995) 'Pregnancies following pre-conception diagnosis of common aneuploidies by fluorescent in-situ hybridization', *Molecular Human Reproduction*, 1(5), pp. 265–269.

Vermeesch, J. R., Voet, T. and Devriendt, K. (2016) 'Prenatal and pre-implantation genetic diagnosis.', *Nature reviews. Genetics*, 17(10), pp. 643–56.

Vickers, A. D. (1969) 'Delayed fertilization and chromosomal anomalies in mouse embryos.', *Journal of reproduction and fertility*. Society for Reproduction and Fertility, 20(1), pp. 69–76.

Victor, A. R. *et al.* (2017) 'Accurate quantitation of mitochondrial DNA reveals uniform levels in human blastocysts irrespective of ploidy, age, or implantation potential', *Fertility and Sterility*, 107(1), p. 34–42.e3.

Voullaire, L. *et al.* (1999) *Detection of aneuploidy in single cells using comparative genomic hybridization.*, *Prenatal diagnosis*.

Voullaire, L. *et al.* (2000) 'Chromosome analysis of blastomeres from human embryos by using comparative genomic hybridization.', *Human genetics*, 106(2), pp. 210–217.

Vrooman, L. A. and Bartolomei, M. S. (2016) 'Can assisted reproductive technologies cause adult-onset disease? Evidence from human and mouse', *Reproductive Toxicology*.

de Waal, E. *et al.* (2014) 'In Vitro Culture Increases the Frequency of Stochastic Epigenetic Errors at Imprinted Genes in Placental Tissues from Mouse Concepti Produced Through Assisted Reproductive Technologies1', *Biology of Reproduction*, 90(2), p. 22.

Wale, P. L. and Gardner, D. K. (2016) 'The effects of chemical and physical factors on mammalian embryo culture and their importance for the practice of assisted human reproduction', *Human Reproduction Update*. Oxford University Press, 22(1), pp. 2–22.

Wallerstein, R. *et al.* (2000) 'Common trisomy mosaicism diagnosed in amniocytes involving chromosomes 13, 18, 20 and 21: Karyotype-phenotype correlations', *Prenatal Diagnosis*. John Wiley & Sons, Ltd., 20(2), pp. 103–122.

Wang, D. and Bodovitz, S. (2010) 'Single cell analysis: The new frontier in "omics"', *Trends in Biotechnology*, pp. 281–290.

Wang, Q. *et al.* (2009) 'Maternal diabetes causes mitochondrial dysfunction and meiotic defects in murine oocytes.', *Molecular endocrinology (Baltimore, Md.)*, 23(10), pp. 1603–12.

Wells, D. *et al.* (1999) 'Detailed chromosomal and molecular genetic analysis of single cells by whole genome amplification and comparative genomic hybridisation.', *Nucleic acids research*. Oxford University Press, 27(4), pp. 1214–8.

Wells, D. *et al.* (2014) 'Clinical utilisation of a rapid low-pass whole genome sequencing technique for the diagnosis of aneuploidy in human embryos prior to implantation', *Journal of Medical Genetics*. BMJ Publishing Group Ltd, 51(8), pp. 553–562.

Wells, D., Alfarawati, S. and Fragouli, E. (2008) 'Use of comprehensive chromosomal screening for embryo assessment: Microarrays and CGH', *Molecular Human Reproduction*. Oxford University Press, pp. 703–710.

Wells, D. and Delhanty, J. D. (2000) 'Comprehensive chromosomal analysis of human preimplantation embryos using whole genome amplification and single cell comparative genomic hybridization.', *Molecular human reproduction*, 6(11), pp. 1055–1062.

Wells, D. and Delhanty, J. D. (2001) 'Preimplantation genetic diagnosis: applications for molecular medicine.', *Trends in molecular medicine*. Elsevier, 7(1), pp. 23–30.

Wells, D. and Delhanty, J. D. A. (2000) 'Comprehensive chromosomal analysis of human preimplantation embryos using whole genome amplification and single cell comparative genomic hybridization', *Molecular Human Reproduction*. Oxford University Press, 6(11), pp.

1055–1062.

Werner, M. D. *et al.* (2016) ‘Sequential versus Monophasic Media Impact Trial (SuMMIT): A paired randomized controlled trial comparing a sequential media system to a monophasic medium’, *Fertility and Sterility*, 105(5), pp. 1215–1221.

White, C. R. *et al.* (2015) ‘High Frequency of Imprinted Methylation Errors in Human Preimplantation Embryos’, *Scientific Reports*. Nature Publishing Group, 5(1), p. 17311.

White, C. R. *et al.* (2015) ‘High Frequency of Imprinted Methylation Errors in Human Preimplantation Embryos.’, *Scientific reports*. Nature Publishing Group, 5, p. 17311.

Wilkins-Haug, L., Quade, B. and Morton, C. C. (2006) ‘Confined placental mosaicism as a risk factor among newborns with fetal growth restriction’, *Prenatal Diagnosis*. John Wiley & Sons, Ltd., 26(5), pp. 428–432.

Wilton, L. (2002a) ‘Preimplantation genetic diagnosis for aneuploidy screening in early human embryos: a review’, *Prenat. Diagn.*, 22(6), pp. 512–518.

Wilton, L. (2002b) ‘Preimplantation genetic diagnosis for aneuploidy screening in early human embryos: a review’, *Prenatal Diagnosis*. John Wiley & Sons, Ltd., 22(6), pp. 512–518.

Wolstenholme, J., Rooney, D. E. and Davison, E. V (1994) ‘Confined placental mosaicism, IUGR, and adverse pregnancy outcome: A controlled retrospective U.K. collaborative survey’, *Prenatal Diagnosis*, 14(5), pp. 345–361.

Wrenzycki, C. *et al.* (2005) ‘Messenger RNA expression patterns in bovine embryos derived from in vitro procedures and their implications for development’, *Reproduction, Fertility and Development*. CSIRO PUBLISHING, 17(2), pp. 23–35.

Xu, J. *et al.* (2016) ‘Noninvasive chromosome screening of human embryos by genome sequencing of embryo culture medium for in vitro fertilization’, *Proceedings of the National Academy of Sciences*. National Academy of Sciences, 113(42), pp. 11907–11912.

Yang, Y.-S. *et al.* (2015) ‘Preimplantation genetic screening of blastocysts by multiplex qPCR followed by fresh embryo transfer: validation and verification.’, *Molecular cytogenetics*. BioMed Central, 8, p. 49.

Zegers-Hochschild, F. *et al.* (2017) ‘The International Glossary on Infertility and Fertility Care, 2017’, *Fertility and Sterility*, 108(3), pp. 393–406.

Zegers-Hochschild, F. *et al.* (no date) ‘International Committee for Monitoring Assisted Reproductive Technology (ICMART) and the World Health Organization (WHO) revised glossary of ART terminology, 2009∗’, *Fertility and Sterility*, 92, pp. 1520–1524.

Zhang, C.-H. *et al.* (2013) ‘Maternal diabetes causes abnormal dynamic changes of endoplasmic reticulum during mouse oocyte maturation and early embryo development.’, *Reproductive biology and endocrinology : RB&E*. BioMed Central, 11, p. 31.

Zhang, Y. *et al.* (2016) ‘Molecular analysis of DNA in blastocoele fluid using next-generation sequencing’, *Journal of Assisted Reproduction and Genetics*. Springer, 33(5), pp. 637–645.

Zhou, B.-B. B. and Elledge, S. J. (2000) ‘The DNA damage response: putting checkpoints in perspective.’, *Nature*. Nature Publishing Group, 408(6811), pp. 433–9.

Appendices

Appendix A

Table 1. Segmental aneuploidy in cleavage stage embryos from 18 different IVF

IVF Clinic number	Avg Mat age (Egg donor age)	Tot embryos	Aneuploid	Normal	Partial aneuploids	Total partials rate (%)
1	30.1	181	34	134	6	3.31
2	32.1	157	44	101.00	7	4.46
3	31.6	84	13	65.00	4	4.76
4	30.6	84	22	48.00	4	4.76
6	31.1	263	52	192.00	14	5.32
7	31.8	123	38	72.00	7	5.69
8	29.1	1219	265	848.00	73	5.99
9	30.2	250	66	153.00	15	6.00
10	30.3	919	251	577.00	56	6.09
11	27.5	2866	576	1921.00	177	6.18
12	27	461	76	335.00	32	6.94
13	25.7	280	64	188.00	20	7.14
14	27.3	406	100	255.00	33	8.13
15	29.9	107	21	74.00	9	8.41
17	26.7	104	21	73.00	9	8.65
18	28.7	126	33	82.00	11	8.73
19	29.4	428	103	276.00	40	9.35
20	26.9	191	40	124.00	18	9.42

Table 2. Segmental aneuploidy in blastocysts from 22 different IVF clinics by NGS

Clinic number	Total embryos	Euploid embryos	Aneuploid embryos	Full segmental	Mosaic embryos	Mosaic segmental	%full segmental	%mosaic segmentals	Total segementals	Total partials rate	Total aneuploidy rate
1	110	28	47	3	28	4	2.73	3.64	7.00	6.36	42.73
2	124	47	37	5	30	5	4.03	4.03	10.00	8.06	29.84
3	299	105	112	8	53	17	2.68	5.69	25.00	8.36	37.46
4	288	58	149	8	55	17	2.78	5.90	25.00	8.68	51.74
5	188	77	57	4	36	13	2.13	6.91	17.00	9.04	30.32
6	457	148	204	12	53	32	2.63	7.00	44.00	9.63	44.64
7	83	33	28	1	13	7	1.20	8.43	8.00	9.64	33.73
8	460	237	102	14	76	31	3.04	6.74	45.00	9.78	22.17
9	858	346	337	41	85	45	4.78	5.24	86.00	10.02	39.28
10	4974	1445	2275	141	706	373	2.83	7.50	514.00	10.33	45.74
11	164	66	61	4	19	13	2.44	7.93	17.00	10.37	37.20
12	151	71	41	4	22	12	2.65	7.95	16.00	10.60	27.15
13	2504	1034	843	66	346	202	2.64	8.07	268.00	10.70	33.67
14	2015	745	811	91	219	127	4.52	6.30	218.00	10.82	40.25
15	681	266	239	21	92	57	3.08	8.37	78.00	11.45	35.10
16	210	59	86	7	34	21	3.33	10.00	28.00	13.33	40.95
17	502	136	182	19	103	48	3.78	9.56	67.00	13.35	36.25
18	502	136	182	19	103	48	3.78	9.56	67.00	13.35	36.25
19	307	106	102	7	54	34	2.28	11.07	41.00	13.36	33.22
20	101	22	43	1	19	14	0.99	13.86	15.00	14.85	42.57
21	390	190	95	13	45	46	3.33	11.79	59.00	15.13	24.36
22	390	190	95	13	45	46	3.33	11.79	59.00	15.13	24.36
23	504	163	159	20	96	58	3.97	11.51	78.00	15.48	31.55

Table 3. Culture media conditions for clinics with NGS dataset

Clinic number	Oxygen %	Carbon dioxide %	Temperature (°C)
1	5	6	37
2	5	8	36.4
3	6	6	37
4	5	5	37
5	6	6	37
6	5	6	37
7	6	7	37
8	5	6	37
9	5	6	37
10	6	6	37
11	5	6	36.8
12	5	6	37.1
13	5	6	37
14	5	6	37
15	5	6	37
16	6	6	37 C
17	5	7	37
18	5	7	37
19	5	7	37
20	5	7	36.8
21	5	7	37
22	5	7	37
23	5	7	36.8

Table 4. Culture media conditions for clinics with aCGH dataset

IVF clinic number	Oxygen %	Carbon dioxide %	Temperature(°C)
1	6	6	37
2	5	6	37
3	6	6	37
4	5	7	36.8
6	6	7	37.0
7	6	6	37 C
8	5	6	37
9	6	6	37
10	6	6	36.8
11	5	7	36.8
12	5	6	37
13	5	6	37
14	5	6	37
15	5	6	37.1
17	5	6	37
18	5	7	36.9
19	5	6	37
20	6	7	37

Appendix B

Table 5. Chimeras for experimental validation of ligation based MDA method

Sample	% single genomic site only	% genomic chimeras within chromosomes	% genomic chimeras between chromosomes	% genomic + linker	% linker + linker
A1-1	94.29	3.80	0.49	0.36	1.07
A1-2	94.56	3.52	0.56	0.37	0.99
B1-1	3.56	19.65	74.12	2.49	0.18
B1-2	4.32	15.97	76.86	2.66	0.20
B2-1	4.91	57.34	28.39	5.55	3.82
B2-2	6.06	52.22	30.91	6.22	4.59
B3-1	9.97	24.75	3.59	16.21	45.47
B3-2	10.73	20.37	3.68	17.11	48.10
B4-1	3.78	3.15	0.91	20.03	72.12
B4-2	4.05	2.26	0.90	21.82	70.97
B5-1	0.23	0.13	0.26	0.81	98.57
B5-2	0.19	0.07	0.18	0.98	98.58
C1-1	3.29	11.14	85.57	0.00	0.01
C1-2	4.14	8.79	87.07	0.00	0.01
C2-.1	3.33	27.58	69.07	0.00	0.01
C2-2	4.11	23.46	72.42	0.00	0.01
C3-1	1.61	30.84	67.55	0.00	0.01
C3-2	1.91	25.01	73.07	0.00	0.01

Table 6. Mapped reads for blastocoel fluid samples from fresh embryo cultures

Original Sample	Total Reads	Total Mapped Reads	% Total Mapped Reads
MM-1-1	1097262	539799	49.19509
MM-1-2	1097262	533566	48.62704
MM-2-1	1118001	756835	67.69538
MM-3-1	1807300	1299374	71.89587
MM-3-2	1807300	1271496	70.35334
MM-6-1	1234758	620793	50.27649
MM-6-2	1234758	610431	49.4373
MM-7-1	1447393	931376	64.34852
MM-7-2	1447393	917527	63.3917
MM-8-1	588248	413921	70.36505
MM-8-2	588248	408219	69.39573
MM-9-1	675396	254902	37.74112
MM-9-2	675396	241280	35.72423
MM-10-1	1112308	649007	58.34778
MM-10-2	1112307	646520	58.12424

Table 7. Chimeras for blastocoel fluid samples from fresh embryo cultures

Sample	% single genomic site only	% genomic chimeras within chromosomes	% genomic chimeras between chromosomes	% genomic + linker	% linker + linker
MM-1	73.13	25.06	1.61	0.15	0.05
MM-2	72.69	25.41	1.88	0.01	0.01
MM-3	81.35	17.19	1.39	0.06	0.01
MM-6	63.41	27.33	8.44	0.81	0.01
MM-7	78.41	19.62	1.83	0.14	0.00
MM-8	82.76	15.78	1.39	0.07	0.01
MM-9	33.88	61.79	4.15	0.04	0.14
MM-10	83.57	15.24	1.16	0.01	0.03

Table 8. Chimeras for blastocoel fluid samples from fresh embryos

Sample	% single genomic site only	% genomic chimeras within chromosomes	% genomic chimeras between chromosomes	% genomic + linker	% linker + linker
1B	9.28	4.99	76.64	0.55	8.55
2B	65.38	29.86	4.49	0.04	0.23
3B	9.58	4.93	74.76	0.71	10.02
4B	12.17	6.51	71.02	6.32	3.98
5B	61.54	20.18	15.84	0.44	2.00
6B	58.62	37.09	3.87	0.04	0.39
7B	22.70	21.75	46.03	2.85	6.67
8B	67.32	9.73	21.03	0.00	1.93
11B	28.80	14.41	47.23	1.12	8.44
12B	30.71	11.09	54.78	0.51	2.91
13B	79.20	14.31	6.06	0.24	0.20
16B	70.55	14.50	13.20	0.03	1.71
17B	88.06	5.60	5.96	0.04	0.34
18B	58.47	6.70	32.32	0.35	2.16
19B	75.57	11.47	9.78	0.15	3.02
21B	40.68	4.33	51.09	0.33	3.57

Table 9. Chimeras for spent media samples from fresh embryos

Sample	% single genomic site only	% genomic + linker	% linker + linker	% genomic chimeras within chromosomes	% genomic chimeras between chromosomes
1F	80.00	0.16	0.01	18.37	1.46
2F	89.54	0.04	0.01	9.64	0.78
3F	81.92	0.20	0.02	16.83	1.02
4F	83.87	0.05	0.04	15.01	1.03
5F	81.91	0.32	0.01	16.73	1.02
6F	86.56	0.23	0.13	12.30	0.78
7F	83.21	0.11	0.01	31.48	1.02
8F	84.08	0.13	0.01	15.76	0.87
9F	90.02	0.16	0.03	9.03	0.76
10F	80.38	0.31	0.02	18.88	1.02
11F	85.91	0.08	0.01	12.96	1.04
12F	89.87	0.04	0.04	8.78	1.26
13F	81.23	0.06	0.00	17.06	1.65
14F	89.34	0.07	0.02	9.58	0.99
15F	84.16	0.05	0.01	14.56	1.22

Table 10. Chimeras for spent media samples from frozen-thawed embryos

Sample	% single genomic site only	% genomic chimeras within chromosomes	% genomic chimeras between chromosomes	% genomic + linker	% linker + linker
1FT	78.32	19.98	1.63	0.03	0.04
2FT	84.39	14.72	0.84	0.01	0.04
3FT	57.09	39.66	2.91	0.03	0.30
4FT	62.55	34.97	2.41	0.05	0.02
5FT	47.74	48.32	3.84	0.07	0.02
6FT	74.34	24.01	1.62	0.01	0.02
7FT	80.78	17.73	1.44	0.01	0.04
8FT	89.90	9.49	0.60	0.00	0.01
9FT	54.97	42.01	2.94	0.07	0.01
10FT	40.11	56.03	3.81	0.04	0.02
11FT	79.47	19.28	1.22	0.01	0.02
12FT	70.48	27.65	1.83	0.01	0.04
13FT	82.53	16.44	1.01	0.00	0.02
14FT	91.88	6.42	1.67	0.00	0.03
15FT	79.36	19.02	1.47	0.01	0.15
16FT	80.52	18.27	1.19	0.00	0.02
17FT	85.40	13.78	0.78	0.00	0.04
18FT	72.12	25.91	1.93	0.01	0.04
19FT	86.10	12.71	1.16	0.00	0.03
20FT	91.54	7.88	0.56	0.00	0.01
21FT	84.61	14.19	1.06	0.14	0.01
22FT	68.72	28.46	2.61	0.20	0.01
23FT	84.61	13.35	1.91	0.12	0.01
24FT	90.35	8.76	0.82	0.07	0.01
25FT	87.98	11.11	0.75	0.14	0.02

Table 11. Concordance between blastocoel fluid samples and TE karyotypes from fresh embryo cultures

Sample	Spent media karyotype	TE karyotype
2MM	47,XX,+22	47,XY,+20
3MM	46, XX	46,XX
7MM	46, XX	46,XX

Table 12. Concordance between spent media samples and TE karyotypes from fresh embryo cultures

Sample	Spent media karyotype	TE karyotype
1F	46,XY	46,XY
2F	48,XY,+17,+20	47,XY,+20
3F	46,XX	46,XX
4F	46,XX	46,XX
5F	46,XX	46,XX
6F	46,XX	46,XX
7F	46,XY	45,XY,-4
8F	45, XX, -1	46XX
9F	46, XY	46 XY
10F	46, XY	46 XY

Table 13. Concordance between spent media samples and TE karyotypes from frozen thawed embryos

Sample	Spent media karyotype	TE karyotype
1S	48, XX, +16, +21	48, XX, +16, +21
2S	47, XX, +18	47, XX, +18, +11 (mosaic)
3S	47, XX, +15	47, XX, +15
4S	45, XO, -X/Y	45, XO, -X/Y
5S	47, XX, +21	47, XX, +21
6S	47, XX, +18	47, XX, +18
7S	46, XY, +16, -21	46, XY, +16, -21
8S	46, XX, +15, -20	46, XX, +15, -20
9S	45, XX, -12	45, XX,-12, XO (mosaic)
10S	47, XX, -9	47, XX, +18
11S	46, XX, +13, -22	46, XX, +13, -22
12S	44, XX, +2, -4,-6,+9, -10,-15	42, XX, -4,-6,-10,-15
13S	Complex	Complex
14S	45,XX,-16	45,XX,-16
15S	46,XY	46,XY,-15q (mosaic)
16S	45,XO,-X/Y	45,XO,-X/Y
17S	49,XX, +3, +19,+20	46, XX
18S	45,XY,-13	45,XY,-13
19S	45,XY,-16	45,XY,-16
20S	46,XX	46, XX
21S	46, XX	46, XX
22S	46, XX	46, XX
23S	46, XX	46, XX
24S	46, XX	46, XX
25S	46, XX	46, XX

Appendix C: Average methylation levels for ICM and TE samples across 23 DMRs

Gene name	100 G	100 M	TE1	ICM 1	TE2	ICM 2	TE3	ICM 3	TE4	ICM 4	TE5	ICM 5	TE6	ICM 6	TE7	ICM 7	TE8	ICM 8	TE9	ICM 9
DIRAS-3	44.00	3.11		13.00	67.67	36.22	22.33	29.22	47.11	20.00		44.33	18.33		54.00	62.44		58.11	58.78	51.33
ZDBF2	55.83	3.33	0.00	0.00	4.50	4.17	2.67	11.67	0.00	4.00	0.33	1.67	7.50	2.67	4.67	3.33	6.17	2.17	1.50	6.17
NAP1L	47.13	4.56	99.88	12.75	56.25	47.75	45.31	56.94	85.75	52.38	41.75	37.81	21.06	49.94	0.06	57.38	54.06	62.88	31.88	62.00
NAP1L5	38.36	3.79	0.21	0.00	26.64	22.36	40.36	26.14	76.14	0.14	41.14	26.00	41.79	61.57	54.71	4.07	28.43	15.64	21.50	19.43
PLAGL1	54.29	4.57	0.43	44.29	31.14	25.14	30.29	65.71	95.71	44.71	54.00	48.43	55.14	56.00	56.00	32.43	31.71	41.86	27.71	42.57
IGF2R	54.90	3.10	6.00	59.70	52.70	25.50	37.70	48.90	47.80	38.80	66.30	37.40	5.20	12.40	39.20	36.50	32.60	36.70	7.60	5.50
GRB10	43.03	6.00	87.41	41.31	57.91	47.41	64.16		54.94		24.59	46.78	3.44	37.66	20.16	58.97	1.09	47.91	29.69	32.88
PEG10	39.23	3.38	48.31	52.62	39.08	65.62	17.23	23.23	100	61.31	39.92	36.15	36.69	88.31	76.85	46.08	47.23	58.85	36.54	49.77
MEST	51.69	3.75			47.44	42.94	21.13	51.44	5.25	30.06	64.38	38.81	0.06	47.00	3.81	28.63	47.19	26.25	53.19	37.75
H19-1	57.33	3.33	51.08	91.33	26.58	51.17	39.00	5.33			35.67	46.58	81.50	46.92	27.00	38.92		35.50	48.42	48.33
H19-2	47.30	3.40	41.60	70.50	41.00	46.10	42.90	41.40	50.50	40.00	40.80	41.40	23.40	46.80	51.70	37.90	24.90	36.80	36.00	43.00
KCNQ1OT1	45.23	4.77		55.00	48.00	45.65	23.62	5.15	31.27	65.23	52.35	44.27		85.96	3.12	34.77	1.77	22.50	31.46	45.46
MEG3-1	70.88	3.63	61.38	7.88	45.50	35.63	25.13	13.50	65.25	36.75	32.63	32.50	12.25	12.00	29.75	39.50	75.63	12.63	22.63	29.13
MEG3-2	52.58	3.83	0.33	5.42	1.92	7.67	1.58	0.67	4.58	3.25	8.42	5.58	2.25	5.33	16.75	5.25	4.50	2.50	2.58	4.08
SNURF-1	50.43	3.14	57.14	43.71	15.71	51.00	34.71	59.43	57.14	18.57	50.86	44.43	67.71	18.71	82.00	28.00	59.86	70.14	25.71	37.43
SNURF-2	33.31	3.56	80.38	31.00	5.50	27.19	22.31	16.56	52.44	47.00	20.06	31.38	52.94	67.06	39.38	36.56	45.69	33.81	25.75	29.69
ZNF597-1	41.35	3.57		44.30	30.30	24.04	36.65	39.96	2.00	9.09	18.43	26.61	31.43	60.96	8.57	30.52	37.00	49.96	36.30	45.09
ZNF597-2	41.30	2.80	4.60	1.60	0.10	5.80	3.50	0.00	0.30	3.80	3.30	2.00	2.10	14.60	2.10	5.80	3.30	4.70	3.10	3.10
PEG3-1	44.55	3.00	69.00	70.82	47.27	30.82	80.36	42.09	40.64	0.09	21.09	41.27	0.55	14.18	51.55	30.36	20.36	44.45	47.27	41.82
PEG3-2	47.67	3.44	0.11	64.22	38.22	35.11	19.67	49.67	37.33	35.00	26.44	43.44	68.78	52.44	33.33	55.00	31.67	50.11	41.00	39.11
GNAS-NESP	41.72	3.44	0.39	3.28	5.50	8.44	4.83	1.72	11.11	6.33	3.17	3.39	7.00	1.50	5.50	10.61	2.94	8.89	22.28	2.17
GNAS-AS1	46.33	3.67	83.33	26.08	49.25	28.00	68.67	19.92	2.42	58.33	45.50	33.83	51.50	83.67	41.00	37.58	13.17	47.42	50.00	46.00
NNAT	56.00	14.00	16.83	18.83	34.83	23.33	22.17	9.33	66.83	18.00	44.67	36.33	25.17	32.50	30.50	40.50	44.83	55.83	26.00	36.33
average methylation:	**48.02**	**4.14**	**37.28**	**34.44**	**33.61**	**32.05**	**30.71**	**28.09**	**42.48**	**28.23**	**33.45**	**32.63**	**27.99**	**40.83**	**31.81**	**33.09**	**29.24**	**35.90**	**29.86**	**32.96**